UNIVERSIDADE FEDERAL DO RIO GRANDE DO SUL

CENTRO DE BIOTECNOLOGIA

PROGRAMA DE PÓS-GRADUAÇÃO EM BIOLOGIA CELULAR E MOLECULAR

“Efeitos da urease majoritária de *Canavalia ensiformis* sobre o sistema imunitário do hemíptero *Rhodnius prolixus*”

Marina Schumacher Defferrari

Tese submetida ao Programa de Pós-Graduação em Biologia Celular e Molecular da UFRGS, para a obtenção do título de Doutor em Ciências.

Orientação: Drª. Célia Regina Ribeiro da Silva Carlini

Co-orientação: Dr. Ian Orchard

Porto Alegre, março de 2014.

BANCA EXAMINADORA

Dra. Angela Lange
Universidade de Toronto, Canadá.

Dra. Maria Fátima Grossi de Sá
Embrapa Recursos Genéticos e Biotecnologia, Brasil.

Dra. Maria Elena de Lima Perez Garcia
Universidade Federal de Minas Gerais, Brasil.

Dra. Adriana Seixas
Universidade Federal de Ciências da Saúde de Porto Alegre, Brasil.
Revisora da tese e membro suplente da banca

Dr. Guido Lenz
Universidade Federal do Rio Grande do Sul, Brasil.
Membro suplente da banca

Este trabalho foi desenvolvido no Laboratório de Proteínas Tóxicas, Departamento de Biofísica e Centro de Biotecnologia da Universidade Federal do Rio Grande do Sul, sob orientação da Prof[a]. Dr[a]. Célia Regina Ribeiro da Silva Carlini, e no Laboratório de Neurofisiologia de Insetos, Departamento de Biologia da Universidade de Toronto em Mississauga (Canadá), sob orientação do Professor Ian Orchard, PhD, durante o período de doutorado sanduíche.

As agências financiadoras do trabalho foram o Conselho Nacional de Desenvolvimento Científico e Tecnológico (CNPq), responsável pela concessão da bolsa de doutorado no Brasil, a Fundação de Amparo à Pesquisa do Estado do Rio Grande do Sul (FAPERGS) e a Coordenação de Aperfeiçoamento de Pessoal de Nível Superior (CAPES), órgão responsável pela concessão da bolsa de doutorado sanduíche no Canadá, no programa Ciência Sem Fronteiras. No Canadá, o trabalho também teve suporte do órgão de fomento NSERC (Natural Sciences and Engineering Research Council of Canada). No Brasil, o trabalho experimental da tese foi financiado pela CAPES (Ed. Toxinologia), CNPq (Edital Universal 2011) e pela FAPERGS (Pronex).

AGRADECIMENTOS/ *ACKNOWLEDGEMENTS*

Agradeço a Célia pela paciência, pelo conhecimento transmitido e pela oportunidade de fazer parte da família Laprotox. As palavras *(muito) muito obrigada* não são suficientes para expressar o que sinto!

As agências brasileiras de financiamento, CAPES, CNPq, FAPERGS e FINEP por fazerem possível o desenvolvimento da ciência em nosso país e em nosso estado; e em especial ao CNPq, por me conceder a bolsa de doutorado no Brasil e a CAPES, por me conceder a bolsa de doutorado sanduíche no Canadá.

Aos colegas e amigos do Laboratório de Proteínas Tóxicas, muito obrigada pela convivência diária, pelo apoio nos momentos complicados e pela parceria nos momentos de festa.

Agradeço a minha família e aos meus pais pelo que mais valorizo: o amor incondicional e os genes que carrego.

I would like to thank Ian and Angela for the very constructive chats and for the guidance throughout my graduate years. At UTM I had the chance to learn about science, about life and about rock'n'roll!

And last, but surely not least, I would like to thank David for being on my side all the time, even when we had 12k kilometers between us. My PhD is also yours.

ÍNDICE

ANEXOS

Lista de Abreviaturas

AA: ácido araquidônico

PLA_2: fosfolipase A_2

DEX: dexametasona

COX: ciclooxigenase

LOX: lipoxigenase

PG: prostaglandina

JBU: urease de *Canavalia ensiformis*

CNTX: canatoxina

RNAi: ácido ribonucleico de interferência

PCR: reação em cadeia da polimerase

qPCR: reação em cadeia da polimerase quantitativa

PBS: tampão fosfato salina

PBST: tampão fosfato salina com triton

FBS: soro bovino fetal

FL/PL: fosfolipídios

LPC: lisofosfatidilcolina

Resumo

Ureases são enzimas que possuem atividades biológicas independentes de suas funções enzimáticas, como indução de exocitose e atividade inseticida. *Rhodnius prolixus* é um dos modelos de inseto sensíveis a essa toxicidade. Quando testada em tecidos isolados de *R. prolixus*, a urease de *Canavalia ensiformis* (JBU) causa diferentes efeitos deletérios modulados por eicosanóides. A via de biossíntese dos eicosanóides envolve fosfolipases A_2 (PLA_2), que são enzimas responsáveis pela liberação de ácido araquidônico (AA). Uma vez liberado, AA pode ser oxigenado na via da ciclooxigenase, a qual produz prostaglandinas (PGs). Em insetos, a resposta imune compreende as reações humoral e celular e é centralmente modulada por eicosanóides, principalmente PGs. Em busca de uma ligação entre o efeito tóxico de JBU e reações imunológicas em insetos, estudamos os efeitos desta toxina em hemócitos de *R. prolixus*. Descobrimos que JBU ativa a agregação de hemócitos, tanto após injeção na hemolinfa quanto em células *in vitro*. Em ensaios *in vitro*, observamos que os inibidores da síntese de eicosanóides, dexametasona e indometacina, inibem a agregação induzida por JBU, sugerindo que produtos da ciclooxigenase modulam a reação. Após hemócitos cultivados serem tratados com JBU, sítios imunorreativos anti-JBU, danos no citoesqueleto e agregação de núcleos foram observados nas células. Também identificamos e clonamos os transcritos de dois genes de PLA_2s de *R. prolixus*, *Rhopr-PLA2III* e *Rhopr-PLA2XII*. Analisamos os perfis de expressão de ambos os genes, e observamos que os transcritos são amplamente distribuídos em vários tecidos, porém em diferentes níveis. Utilizando a estratégia de RNAi, silenciamos a expressão de *Rhopr-PLA2XII* em ninfas de *R. prolixus* em uma média de 70% entre variados tecidos. Observamos que a toxicidade de JBU foi diminuída em mais de 50% em ninfas com a expressão de *Rhopr-PLA2XII* diminuída, indicando que o gene está ligado ao efeito tóxico de JBU nesse inseto. No presente estudo demonstramos pela primeira vez a capacidade de uma urease de induzir a agregação de hemócitos. Da mesma forma, os genes de PLA_2 aqui apresentados foram os primeiros a serem identificados e a terem seus transcritos clonados em um vetor da doença de Chagas. Nossos resultados estão de acordo com estudos anteriores que demonstraram que eicosanóides modulam a toxicidade de JBU, contribuindo para a compreensão dos mecanismos entomotóxicos de ação dessas proteínas multifuncionais.

Abstract

Ureases are multifunctional enzymes that display biological activities independent of their enzymatic function, including induction of exocytosis and insecticidal effects. *Rhodnius prolixus*, a major vector of Chagas' disease, is one of the known susceptible models of this toxicity. When tested in isolated tissues of *R. prolixus*, jack bean urease (JBU) causes different deleterious effects modulated by eicosanoids. The eicosanoid biosynthetic pathway involves phospholipase A_2 (PLA_2) enzymes that are responsible for releasing arachidonic acid (AA), along with other products. Once released, AA may enter different enzymatic oxygenation pathways, among which is the cyclooxygenase pathway, yielding products such as prostaglandins (PGs). In insects, the immune response comprises cellular and humoral reactions, and is centrally modulated by eicosanoids, mainly PGs. Searching for a link between JBU toxic effect and immune reactions in insects we have studied the effects of this toxin on *R. prolixus* hemocytes. We have found that JBU triggers aggregation of the hemocytes either after injection in the hemocoel as well as in isolated cells. *In vitro* assays in presence of the eicosanoid synthesis inhibitors dexamethasone and indomethacin counteracted JBU's effect, indicating eicosanoids, more specifically cyclooxygenase products, are likely to modulate the reaction. Cultured cells were treated with JBU and immune reactive sites were found in the cells along with damage to the cytoskeleton. The highest concentration of JBU used in the cultured cells also led to nuclei aggregation of adherent hemocytes. We have also identified two genes and cloned the transcripts with complete coding sequences of two PLA_2s from *R. prolixus, Rhopr-PLA2III* and *Rhopr-PLA2XII.* We have analyzed their expression profiles and found the transcripts to be distributed in various tissues, but at different levels. We have knocked down 70% of *Rhopr-PLA2XII* expression in 5^{th} instar *R. prolixus*, and JBU's toxicity was decreased by more than 50%, indicating that *Rhopr-PLA2XII* gene is linked to JBU's toxic effect in this insect. This was the first time effects of an urease on insect hemocytes were demonstrated. The PLA_2 genes here presented were also the first to be identified and to have their transcripts cloned in a Chagas' disease vector. Our findings support previous data demonstrating that eicosanoids modulate JBU's toxicity, and contribute to the understanding of the mechanisms of entomotoxic action of this multifunctional protein.

1. Introdução

1.1. Ureases

Ureases, enzimas níquel-dependentes que catalisam a hidrólise da ureia em amônia e dióxido de carbono, são amplamente distribuídas na natureza, sendo sintetizadas por plantas, fungos e bactérias (Mobley *et al*., 1995; Carter *et al*., 2009). De maneira independente da função enzimática, ureases apresentam atividades biológicas tais como ação inseticida e antifúngica, e efeito secretagogo em diferentes modelos celulares (Follmer *et al*., 2004; Follmer *et al*., 2001; Staniscuaski & Carlini, 2012). As sementes da leguminosa *Canavalia ensiformis*, popularmente chamada de feijão-de-porco (Jack bean), são fontes ricas de isoformas de urease, que contribuem em grande parte para a resistência da planta ao ataque de insetos. A urease majoritária de *C. ensiformis* (JBU) foi a primeira enzima a ser cristalizada e a primeira enzima níquel-dependente caracterizada (Dixon *et al*., 1975).

Carlini e Guimarães isolaram das sementes de *C. ensiformis* uma proteína indutora de convulsões chamada canatoxina (CNTX), que causa morte de camundongos e ratos quando injetada intraperitonealmente (DL_{50}= 0,5 a 2,0 mg/ kg) (Carlini & Guimaraes, 1981). A CNTX também é ativa por via intravenosa, intramuscular e subcutânea, porém não é capaz de induzir os efeitos letais se administrada por via oral, provavelmente devido à sua instabilidade em meio ácido (Carlini & Guimaraes, 1981; Carlini *et al*., 1984). Comparações de sequencias parciais indicaram alto grau de homologia (cerca de 85%) com a JBU, e estudos posteriores demonstraram que a CNTX é uma isoforma de urease, possuindo de 30 a 40% da atividade ureolítica da forma

majoritária da enzima na semente (Follmer *et al*., 2001). Estudos sobre o mecanismo de ação da CNTX mostraram que esta apresenta potente efeito secretagogo em vários tipos de células de mamíferos, ativando a produção de eicosanóides e as vias de lipoxigenases, e induzindo alterações dos níveis e fluxos intracelulares de Ca^{2+} (Carlini *et al*., 1985; Barja-Fidalgo *et al*., 1991a; Barja-Fidalgo *et al*., 1991b; Ghazaleh *et al*., 1992; Ghazaleh *et al*., 1997). A CNTX induz em ratos bradicardia, hipertensão e hipotermia, fatos que precedem o fenômeno convulsivo tônico-clônico, característico da ação tóxica (Carlini *et al*., 1984).

Com exceção da toxicidade intraperitoneal em camundongos, a JBU parece compartilhar todas as outras propriedades farmacológicas descritas para a CNTX (Follmer *et al*., 2001). A exemplo de outras toxinas (Eidels *et al*., 1983), JBU e CNTX se comportam como lectinas monovalentes ligando-se a glicoderivados complexos, como gangliosídeos e fetuína (Carlini & Guimaraes, 1991; Follmer *et al*., 2001). Ureases bacterianas também são capazes de ativar diferentes modelos celulares através da produção de eicosanóides, como por exemplo a urease de *Helicobacter pylori,* que induz a ativação de plaquetas e neutrófilos através de vias de eicosanóides (Wassermann *et al*., 2010; Uberti *et al*., 2013).

1.2. Atividades inseticida e entomotóxica das ureases

Quando administradas por via oral, ureases de *C. ensiformis* são tóxicas para insetos que possuem no trato digestório enzimas do tipo catepsinas, que atuam em pH acídicos (Carlini & Grossi-de-Sá, 2002). Como exemplos de insetos suscetíveis podemos citar os hemípteros *Rhodnius prolixus, Dysdercus*

peruvianus, e *Oncopeltus fasciatus* (Carlini *et al*., 1997; Staniscuaski *et al*., 2005; Defferrari *et al*., 2011). Por outro lado, insetos resistentes a esta ação tóxica possuem enzimas digestivas do tipo tripsinas, que atuam em pH básicos, como por exemplo os lepidópteros *Anticarsia gemmatalis* e *Spodoptera frugiperda* (Carlini *et al*., 1997; Terra & Ferreira, 1994). Essa dependência da toxicidade é, em grande parte, explicada pela maneira como as ureases são processadas no intestino dos insetos. As enzimas do tipo catepsinas B e D hidrolisam as moléculas de urease em sítios específicos para a liberação de peptídeos com atividade tóxica letal (Piovesan *et al*., 2008; Defferrari *et al*., 2011, Real-Guerra *et al.*, 2013).

A partir da hidrólise *in vitro* da isoforma CNTX por catepsinas digestivas do coleóptero *Callosobruchus maculatus*, foi isolado um peptídeo de 10 KDa altamente tóxico quando administrado por via oral a insetos de diferentes ordens (Ferreira-DaSilva *et al.*, 2000). Com base na sequência deste peptídeo, foi desenhado um peptídeo recombinante, chamado Jaburetox, que se mostrou tóxico quando administrado por via oral a insetos independente dos tipos de suas enzimas digestivas, demonstrando um grande potencial biotecnológico (Mulinari *et al*., 2007; Stanisçuaski *et al.,* 2005). Subsequentemente, observou-se que os mecanismos de ação do peptídeo Jaburetox são variados, como o efeito desestabilizador de membranas lipídicas (Barros *et al*., 2009) e a inibição da secreção induzida por serotonina em túbulos de Malpighi isolados de *R. prolixus* (Stanisçuaski *et al.,* 2009). A serotonina regula a formação de urina primária pelos túbulos de Malpighi (Maddrell *et al*., 1993) além de ter importantes funções no sistema nervoso dos insetos, atuando como neurotransmissor ou como modulador de funções integradas em órgãos

periféricos e em sistemas musculares (Settembrini & Villar, 2004). Utilizando-se como modelo a barata *Phoetalia pallida*, foi observada uma redução na força de contração muscular após tratamento com Jaburetox, reforçando a ideia de que o peptídeo pode interferir no sistema nervoso e neurolocomotor (Martinelli *et al*., 2014).

Demonstrou-se que horas após ninfas de *R. prolixus* serem alimentadas com uma solução contendo JBU, moléculas enzimaticamente ativas da proteína podem ser detectadas na hemolinfa (Staniscuaski *et al*., 2010). Quando ninfas do mesmo inseto são injetadas com JBU diretamente na hemocele, observa-se uma taxa de mortalidade próxima a 100% em apenas 24 horas após as injeções (Staniscuaski *et al*., 2010). A permeabilidade do epitélio intestinal à moléculas de urease já havia sido previamente observada no lepidóptero *Bombyx mori* (Hirayama *et al*., 2000; Kurahashi *et al*., 2005), mas ainda não existem dados referentes à ação da proteína quando diretamente injetada em insetos dessa mesma ordem. A presença de inibidores de atividade ureásica foi detectada na hemolinfa dos lepidópteros *S. frugiperda* e *Galleria melonella* e do hemíptero *D. peruvianus* (Marco-Salvadori *et al*., 2012). Porém, para um mesmo volume de hemolinfa, observamos que a inibição da urease causada pela hemolinfa dos lepidópteros é mais intensa do que a causada pela hemolinfa de *D. peruvianus* (dados não publicados). Considerando-se que lepidópteros são resistentes e hemípteros suscetíveis à ação por via oral da urease, poder-se-ia inferir que o(s) inibidor(s) presente(s) na hemolinfa poderia(m) ter um papel de proteção nos insetos, sugerindo que esta ação entomotóxica não é somente devido a fragmentos gerados na digestão, mas também à moléculas intactas da proteína que atravessam o

epitélio intestinal. De fato, quando testada em tecidos isolados de *R. prolixus*, a JBU interfere com rotas de sinalização moduladas por eicosanóides: nos intestinos, potenciando contrações musculares induzidas por serotonina e aumentando o conteúdo de prostaglandinas nos tecidos (Staniscuaski *et al*., 2010) e nos túbulos de Malpighi, inibindo a secreção de fluidos (Staniscuaski *et al*., 2009).

1.3. Eicosanóides

Eicosanóides são sintetizados através da oxigenação enzimática do ácido araquidônico (AA), ou de outros ácidos graxos poli-insaturados contendo 20 átomos de carbono. O termo *eicosanóide* foi primeiramente utilizado por Corey e colaboradores (1980) com base na palavra grega "eikosi" (= vinte), de forma que o termo é uma generalização para todos metabólitos biologicamente ativos do AA. A biossíntese de eicosanóides começa com a hidrólise do AA, a partir da posição *sn*-2 de fosfolipídios de membrana, catalisada por uma fosfolipase A_2 ('phospholipase A_2' - PLA_2) (Burke & Dennis, 2009b; Burke e Dennis, 2009a). Após a hidrólise, o AA pode seguir três diferentes rotas de oxigenação: da ciclooxigenase (COX; gera prostaglandinas e tromboxanos), da lipoxigenase (LOX; gera uma variada gama de produtos) (Fig. 1) ou do citocromo P-450 ‘epoxigenase’ (gera ácidos epoxieicosatrienóicos). A maioria dos trabalhos em modelos de insetos têm como foco as prostaglandinas (PGs), que além de outras funções na fisiologia dos insetos, são moduladoras centrais do sistema imunitário (Stanley *et al*., 2009). Os níveis de PGs na hemolinfa de *Pseudaletia unipuncta* e a atividade de PLA_2 nos hemócitos de *Manduca sexta* aumentam após a infecção destes lepidópteros com bactérias (Tunaz *et al*.,

2003; Jurenka *et al*., 1999). Em *R. prolixus*, a atividade de PLA_2s e a presença de PGs foram detectadas na hemolinfa e nos hemócitos, aparentemente participando na resposta imune celular (Figueiredo *et al*., 2008b; Figueiredo *et al*., 2008a). Enquanto pelo menos duas formas de COX (COX-1, expressa de forma constitutiva, e COX-2, induzível) são conhecidas em mamíferos, ainda não sabemos quantas formas de COX são expressas em insetos, principalmente porque os genes responsáveis por codificar as enzimas COX e COX-like são ainda desconhecidos. O gene *Pxt* de *Drosophila* é provavelmente um gene COX-like, estando envolvido na produção de PGs durante a maturação de folículos e produção de ovos (Tootle *et al*., 2011).

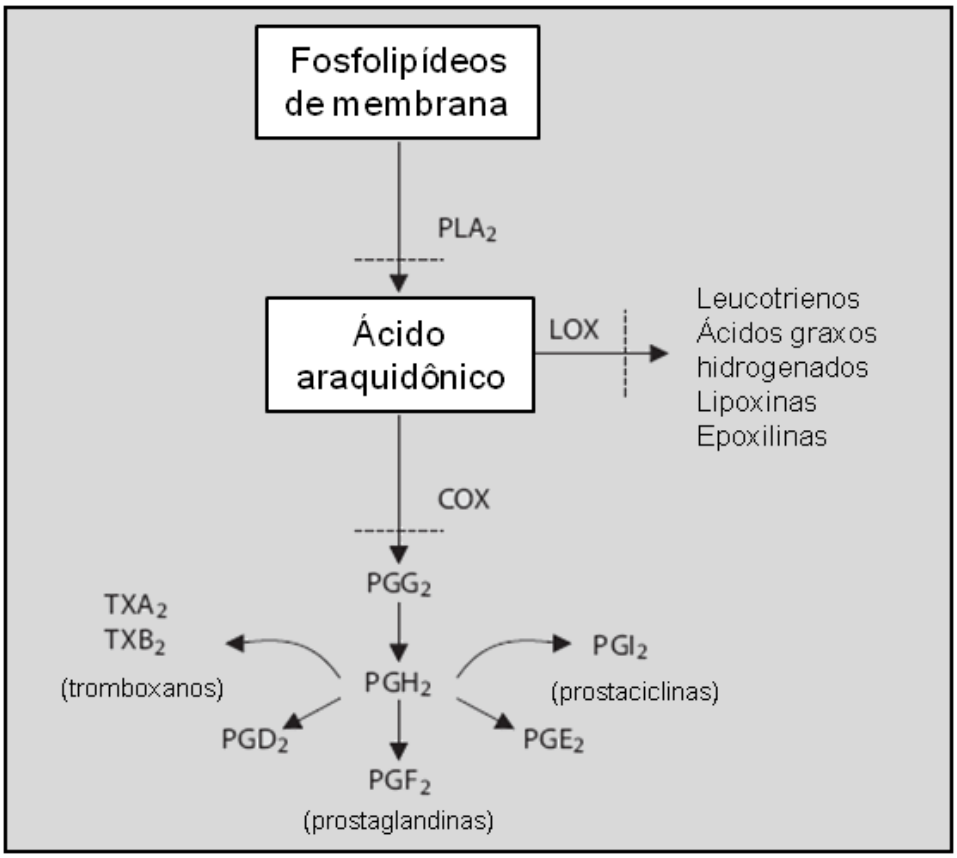

Figura 1. Esquema representando parte da cascata enzimática de produção de eicosanóides (adaptado de Stanley *et al*., 2009).

1.4. O sistema imunitário em insetos

De um modo geral, animais, assim como humanos, defendem-se de organismos infecciosos através de dois sistemas conhecidos como imunidade inata e imunidade adquirida. A imunidade inata depende de fatores de proteção codificados desde o nascimento de um indivíduo, enquanto a adquirida envolve a produção de moléculas efetoras que reconhecem antígenos específicos, e o desenvolvimento da memória imunológica (Fearon, 1997). Insetos possuem uma resposta imunológica inata bem desenvolvida, porém não possuem um sistema imunitário adquirido. O sistema imunitário inato dos insetos pode ser majoritariamente dividido em três etapas (Fig. 2). A primeira etapa são as barreiras físicas, que são a superfície externa do corpo, composta por uma camada celular basal simples e pela cutícula, e a membrana peritrófica, que reveste o intestino da maioria dos insetos. Uma vez que as células do intestino ou a hemocele forem invadidas, a resposta celular, a segunda etapa ou barreira, é então ativada. Essa resposta envolve interações diretas entre os hemócitos circulantes e os organismos invasores, incluindo as funções de agregação, fagocitose, nodulação e encapsulamento (Strand, 2008). A terceira etapa, a imunidade humoral, envolve a indução da expressão de peptídeos antimicrobianos e da enzima lisozima e a ativação do sistema da profenoloxidase (Kanost *et al*., 2004). A resposta celular é desencadeada imediatamente após uma invasão, enquanto que a maioria das respostas humorais aparecem somente após algumas horas. Juntas, as defesas física, celular e humoral conferem uma proteção efetiva aos insetos. Toda essa rede, finamente organizada, é principalmente coordenada e mediada por

eicosanóides, particularmente as respostas que envolvem as reações celulares (Stanley *et al*., 2009).

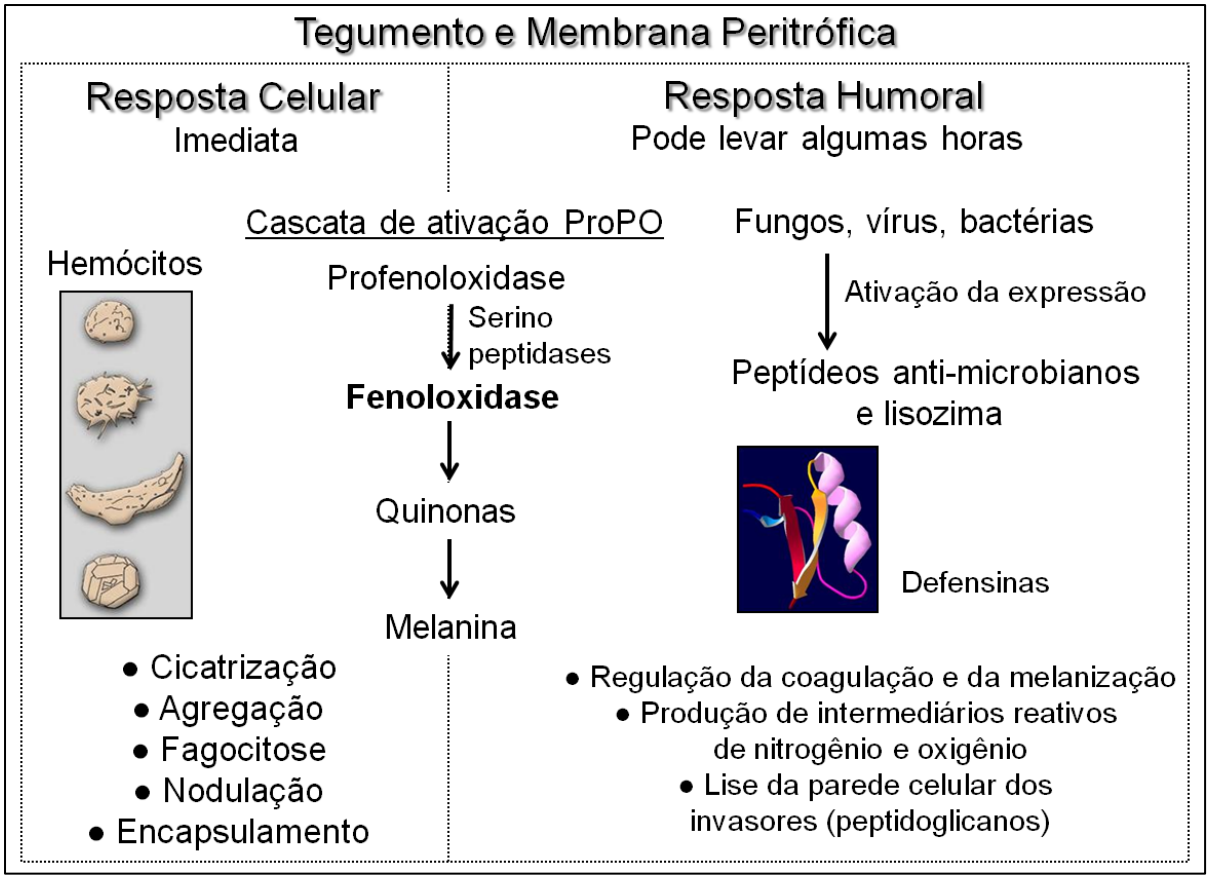

Figura 2. Esquema representando a dinâmica do sistema imunitário em insetos.

1.5. *Rhodnius prolixus*

O triatomínio *Rhodnius prolixus* (Fig. 3) é um dos principais vetores da doença de Chagas, uma parasitose crônica causada pelo protozoário *Trypanosoma cruzi*. Em países latino-americanos aproximadamente 100 milhões de pessoas estão sob risco e, estima-se, outras 16 milhões já estão infectadas (Dias *et al*., 2002; Coura *et al*., 2002). *Rhodnius prolixus* se alimenta exclusivamente de sangue de vertebrados, podendo ingerir de uma só vez o

equivalente a 10 vezes sua massa corporal. Imediatamente após a alimentação, o inseto elimina grandes volumes de sais e água, em forma de urina e fezes, na pele do hospedeiro, transmitindo assim o parasita *T. cruzi* (Orchard & Paluzzi, 2009; Andrade & Andrews, 2005). Estudos anteriores do nosso grupo demonstraram que o *R. prolixus* é sensível à ação tóxica das ureases de *C. ensiformis*, tanto quando a toxina é administrada por via oral ou por injeção na hemolinfa, bem como *ex vivo*, em preparações com tecidos isolados (Carlini *et al*., 1997; Ferreira-Dasilva *et al*., 2000; Staniscuaski *et al*., 2009; Staniscuaski *et al*., 2010). Como citado anteriormente, o sistema imunitário de insetos é centralmente mediado por eicosanóides, sendo um interessante alvo para o estudo e compreensão do mecanismo de ação entomotóxica da JBU em *R. prolixus*.

Figura 3. Ninfa de quinto instar de *R. prolixus*. (Foto: Gutemberg Brito, Fundação Oswaldo Cruz)

2. Objetivo

Considerando-se os efeitos causados pelas ureases em diferentes eventos coordenados por eicosanóides, tanto em modelos mamíferos quanto no hemíptero *Rhodnius prolixus*, o objetivo deste trabalho foi estudar a atividade da urease majoritária de *Canavalia ensiformis* (JBU) sobre o sistema imunitário deste inseto.

2.2. Objetivos específicos

a. Isolar hemócitos de ninfas de *R. prolixus* a partir da coleta de hemolinfa, identificando e quantificando o número de células e agregados;

b. Testar a ação de JBU após injeção na hemolinfa, e em células isoladas, sobre a agregação de hemócitos de ninfas de *R. prolixus*;

c. Testar *in vitro* a ação de JBU sobre a agregação de hemócitos de ninfas de *R. prolixus* em presença de inibidores das vias de eicosanóides;

d. Estabelecer um protocolo de cultura de células para hemócitos de ninfas de *R. prolixus* e localizar JBU, por imunocitoquímica, após tratamento *in vitro* das células em cultura;

e. Identificar, clonar e caracterizar o gene e o transcrito de uma ou mais PLA_2s em ninfas de *R. prolixus*;

f. Caracterizar o perfil de expressão de genes de PLA_2 nos diferentes tecidos de ninfas de *R. prolixus*;

g. Avaliar alterações na expressão gênica de PLA_2s em ninfas de *R. prolixus* após tratamento com JBU;

h. Avaliar o envolvimento de genes de PLA_2 na modulação da toxicidade de JBU em ninfas de *R. prolixus,* através de silenciamento da expressão.

3. Resultados - Capítulo I

3.1. Artigo publicado

Defferrari, M.S., da Silva, R., Orchard, I., Carlini, C.R. Jack bean (*Canavalia ensiformis*) urease induces eicosanoid-modulated hemocyte aggregation in the Chagas' disease vector *Rhodnius prolixus*. *Toxicon,* 82(C), 18-25. 2014.

Resumo

Ureases são proteínas multifuncionais que possuem atividades biológicas independentes de suas funções enzimáticas, tais como a indução da exocitose e efeitos inseticidas. *Rhodnius prolixus*, um dos principais vetores da doença de Chagas, é um modelo para estudos sobre a entomotoxicidade da urease de *Canavalia ensiformis* (JBU). Previamente demonstramos que JBU induz a produção de eicosanóides em tecidos isolados de *Rhodnius prolixus*. Em insetos, a resposta imune compreende as reações humoral e celular, e é centralmente modulada por eicosanóides. Produtos da ciclooxigenase sinalizam a imunidade em insetos, principalmente reações celulares como a agregação de hemócitos . Em busca de uma ligação entre os efeitos tóxicos de JBU e reações imunológicas em insetos, estudamos os efeitos desta toxina em hemócitos de *R. prolixus*. JBU induz a agregação de hemócitos após injeção na hemolinfa, bem como quando administrada a células isoladas. Em ensaios *in vitro*, inibidores da síntese de eicosanóides dexametasona (inibidor indireto de fosfolipase A2) e indometacina (inibidor de ciclooxigenase) neutralizaram o efeito de JBU, indicando que eicosanóides, mais especificamente produtos da ciclooxigenase, são prováveis moduladores desta resposta de agregação. De forma oposta, os inibidores esculetina e baicaleína não afetaram a reação, indicando que produtos de lipoxigenase não estão envolvidos no efeito de JBU. O cálcio extracelular também se mostrou necessário ao efeito de JBU, de acordo com o que foi visto em outros modelos de células sensíveis a urease. Observou-se um escurecimento progressivo do meio de hemócitos tratados com JBU, sugerindo também a ativação da resposta humoral. Após tratamento de células em cultura com JBU, observou-se sítios imunorreativos e danos no

citoesqueleto. A concentração mais elevada de JBU testada na cultura de células também desencadeou a agregação de núcleos de hemócitos aderentes. Esta é a primeira vez que se demonstra o efeito de uma urease sobre hemócitos de insetos, contribuindo para a compreensão dos mecanismos de ação entomotóxica dessa proteína.

Toxicon 82 (2014) 18–25

Contents lists available at ScienceDirect

Toxicon

journal homepage: www.elsevier.com/locate/toxicon

Jack bean (*Canavalia ensiformis*) urease induces eicosanoid-modulated hemocyte aggregation in the Chagas' disease vector *Rhodnius prolixus*

M.S. Defferrari [a,*], R. da Silva [b], I. Orchard [c,2], C.R. Carlini [a,d,1,3]

[a] *Graduate Program in Cellular and Molecular Biology, Center of Biotechnology, Institute of Biosciences, Universidade Federal do Rio Grande do Sul, Porto Alegre, RS, Brazil*
[b] *Department of Biology, McMaster University, Hamilton, ON, Canada*
[c] *Department of Biology, University of Toronto Mississauga, Mississauga, ON, Canada*
[d] *Instituto do Cérebro – InsCer, Pontificia Universidade Católica do Rio Grande do Sul, and Department of Biophysics, Biosciences Institute, Universidade Federal do Rio Grande do Sul, Porto Alegre, RS, Brazil*

ARTICLE INFO

Article history:
Received 16 November 2013
Received in revised form 29 January 2014
Accepted 4 February 2014
Available online 18 February 2014

Keywords:
Insect
Immune system
Eicosanoids
Toxicity
Cyclooxygenase
Immunocytochemistry

ABSTRACT

Ureases are multifunctional proteins that display biological activities independently of their enzymatic function, such as induction of exocytosis and insecticidal effects. *Rhodnius prolixus*, a major vector of Chagas' disease, is a model for studies on the entomotoxicity of jack bean urease (JBU). We have previously shown that JBU induces the production of eicosanoids in isolated tissues of *R. prolixus*. In insects, the immune response comprises cellular and humoral reactions, and is centrally modulated by eicosanoids. Cyclooxygenase products signal immunity in insects, mainly cellular reactions, such as hemocyte aggregation. In searching for a link between JBU's toxic effects and immune reactions in insects, we have studied the effects of this toxin on *R. prolixus* hemocytes. JBU triggers aggregation of hemocytes after injection into the hemocoel and when applied to isolated cells. On *in vitro* assays, the eicosanoid synthesis inhibitors dexamethasone (phospholipase A_2 indirect inhibitor) and indomethacin (cyclooxygenase inhibitor) counteracted JBU's effect, indicating that eicosanoids, more specifically cyclooxygenase products, are likely to mediate the aggregation response. Contrarily, the inhibitors esculetin and baicalein were inactive, suggesting that lipoxygenase products are not involved in JBU's effect. Extracellular calcium was also necessary for JBU's effect, in agreement to other cell models responsive to ureases. A progressive darkening of the medium of JBU-treated hemocytes was observed, suggestive of a humoral response. JBU was immunolocalized in the cultured cells upon treatment along with cytoskeleton damage. The highest concentration of JBU tested on cultured cells also led to nuclei aggregation of adherent hemocytes. This is the first time urease has been shown to affect insect hemocytes, contributing to our understanding of the entomotoxic mechanisms of action of this protein.

* Corresponding author. Av. Bento Gonçalves, 9500 Building 43.431, Rooms 209/214, Porto Alegre 91501-970, RS, Brazil. Tel.: +55 51 3308 7606; fax: +55 51 3308 7600.
E-mail addresses: marina.defferrari@ufrgs.br (M.S. Defferrari), rosa.dasilva@mcmaster.ca (R. da Silva), ian.orchard@utoronto.ca (I. Orchard), celia.carlini@pucrs.br, ccarlini@ufrgs.br (C.R. Carlini).
[1] PI at home institution.
[2] PI in Canada.
[3] http://www.ufrgs.br/laprotox.

http://dx.doi.org/10.1016/j.toxicon.2014.02.006
0041-0101/

1. Introduction

Seeds of the legume *Canavalia ensiformis* (jack bean) are rich sources of proteins with biotechnological interest. These proteins include enzymes such as ureases (Carlini and Polacco, 2008), which catalyze the hydrolysis of urea into ammonia and carbon dioxide (Dixon et al., 1975). Ureases display biological activities such as entomotoxicity and exocytosis induction, which are independent of their catalytic function (Follmer et al., 2001; Follmer et al., 2004; Staniscuaski and Carlini, 2012). *C. ensiformis* urease isoforms display insecticidal effects mainly due to the digestive processing of ingested urease molecules and subsequent release of derived peptides within the lumen of the insect digestive tract (Carlini et al., 1997; Defferrari et al., 2011; Ferreira-Dasilva et al., 2000; Piovesan et al., 2008). Susceptible insects such as the hemipterans *Rhodnius prolixus*, *Oncopeltus fasciatus* and *Dysdercus peruvianus*, rely on cathepsin-like digestive enzymes, which cleave urease molecules on specific sites for the release of entomotoxic peptides (Carlini et al., 1997; Defferrari et al., 2011; Piovesan et al., 2008; Real-Guerra et al., 2013). Additionally, it has been found that hours after feeding on a solution containing *C. ensiformis* urease, intact protein molecules can be detected in the hemolymph of *R. prolixus* (Staniscuaski et al., 2010) and that urease is insecticidal even when injected directly into the insect's hemolymph, indicating that the entomotoxic activity is also due to actions of the whole molecule (Defferrari et al., 2013; Staniscuaski et al., 2010). When tested *ex vivo* on different *R. prolixus* tissues, urease interferes with cell signaling pathways modulated by eicosanoids, specifically cyclooxygenase products (Staniscuaski et al., 2009; Staniscuaski et al., 2010). Also modulated by eicosanoids, plant and bacterial ureases are capable of inducing inflammation and activating several mammalian cell types such as platelets and neutrophils. However, in contrast to what has been seen for *R. prolixus*, ureases act through lipoxygenase products in mammalian models (Barja-Fidalgo et al., 1991b; Carlini et al., 1985; Olivera-Severo et al., 2006; Uberti et al., 2013; Wassermann et al., 2010). Eicosanoids are synthesized from fatty acids, mainly arachidonic acid (AA), released from membrane phospholipids upon cell stimulation, via activation of a phospholipase A_2 (Harizi et al., 2008). Arachidonic acid then follows different enzymatic oxygenation pathways involving cyclooxygenases (COX) to yield prostaglandins (PGs) and thromboxanes, and lipoxygenases (LOX) producing, among other compounds, lipoxins and leukotrienes (Lone and Tasken, 2013). Most of the work done with insects focused on the PGs, which serve, among other functions, as central mediators of the immune response (Stanley, 2006; Stanley et al., 2009). The insect immune system encompasses broadly two types of defense reactions, the immediate cellular responses and, subsequently, the humoral responses (Marmaras and Lampropoulou, 2009). It has been shown in *R. prolixus* that hemocyte functions, including aggregation and phagocytosis, are modulated by eicosanoids (Figueiredo et al., 2008; Garcia et al., 2004a; Garcia et al., 2004b). Insect's humoral responses tend to appear a few hours after challenge and infection, and result in the activation of the prophenoloxidase (PPO) cascade (Kanost et al., 2004). The active form of PPO, phenoloxidase (PO), is required for melanization of nodules and capsules formed upon the cellular response. Melanin is also necessary for protection against toxic compounds after an invasion or damage to the cuticle (Cerenius and Soderhall, 2011). Here, based on previously reported data on eicosanoid-modulated effects of ureases on insects and on diverse mammalian cell models, we studied the effects of the *C. ensiformis* major urease (JBU) on hemocytes and immune responses of the Chagas' disease vector *R. prolixus*.

2. Materials and methods

2.1. Insects

Fifth instars *R. prolixus* Stål (1859) were used throughout this study. The colony was reared at 25 °C under 60% humidity, and maintained by feeding once each instar on defibrinated rabbit blood (Cedarlane Laboratories, Burlington, ON, Canada).

2.2. Rhodnius prolixus *saline and jack bean urease*

Rhodnius prolixus saline was prepared as follows: NaCl 150 mM, KCl 8.6 mM, $CaCl_2$ 2.0 mM, $MgCl_2$ 8.5 mM, NaHCO3 4.0 mM, glucose 34.0 mM, HEPES 5.0 mM, pH 7.0 (Lane et al., 1975). Crystalline Jack bean urease (JBU) was obtained from Sigma–Aldrich (Mississauga, ON, Canada) and diluted in *R. prolixus* saline to the appropriate concentrations.

2.3. In vivo *hemocyte aggregation assays*

Unfed insects (mean weight 50 mg) were injected into the hemocoel with solutions of JBU diluted in *R. prolixus* saline to a final dose of 6 μg per insect and control insects were injected solely with saline. Six hours after injections, the insects had their surface sterilized by immersion in 70% ethanol and hemolymph was collected from a cut in one of the legs. Hemolymph samples were immediately diluted in cold anticoagulant solution (EDTA 10 mM, glucose 100 mM, NaCl 62 mM, sodium citrate 30 mM, citric acid 26 mM, pH 4.6) at a ratio of 1:5 (anticoagulant: hemolymph), as described by Azambuja et al. (Azambuja et al., 1991). hemocyte viability was assessed by the Trypan Blue dye (Sigma–Aldrich, Mississauga, ON, Canada) exclusion method (Boyes et al., 1964). Briefly, 0.1% Trypan Blue diluted in *R. prolixus* saline was added directly to the tubes containing the suspension of hemolymph for 10 min at room temperature. The number of cells and aggregates (defined as a cluster of nine or more cells) was then determined for each sample by counting in a hemocytometer with phase-contrast optical microcopy, according to Miller and Stanley (Miller and Stanley, 2001).

2.4. In vitro *hemocyte aggregation assays*

Unfed insects had their surface sterilized by immersion in 70% ethanol for 5 min and the hemolymph was collected

from a cut in one of the legs. Hemolymph samples were immediately added to cold, sterile, *R. prolixus* saline at a ratio of 1:1 in sterile tubes. In other sterile tubes 100 μM EGTA (ethylene glycol tetraacetic acid) and eicosanoid synthesis inhibitors at different final concentrations were diluted in saline. The final concentrations were 50 and 100 μM for dexamethasone and indomethacin, 100 and 300 μM for esculetin and baicalein The inhibitors of the eicosanoid pathway synthesis, namely dexamethasone, indomethacin, baicalein and esculetin were obtained from Sigma–Aldrich (Mississauga, ON, Canada) and the stock solutions were prepared in 95% ethanol. The diluted hemolymph was mixed with solutions of EGTA plus inhibitors, or equivalent volumes of saline, and the tubes were incubated at room temperature for 30 min under gentle shaking. Subsequently, JBU was added in different concentrations to the tubes containing hemolymph and EGTA plus inhibitors or saline, followed by incubation at room temperature with gentle shaking, for 1 h. The final ethanol concentration in the experiments was 0.5%–1% v/v (ethanol:hemocytes suspension). As controls in each experiment, hemolymph samples were incubated in the same conditions without JBU. Hemocyte viability was again assessed by the Trypan Blue dye exclusion method as described above.

2.5. Hemocytes culture

To establish hemocyte cultures, 5th instars (5 days after feeding) had their surface sterilized by immersion in 70% ethanol for 5 min and then hemolymph was collected from a cut in one of the legs under aseptic conditions using a laminar flow cabinet. Hemolymph samples were immediately added to Schneider's insect medium (Sigma–Aldrich, Mississauga, ON, Canada) with supplements at a ratio of 1:1 in sterile tubes. The hemolymph/medium suspension was placed in 9-well plates containing glass cover slips inside each well, and allowed to settle for 30 min. Subsequently, 1 mL of the supplemented culture medium was slowly added to the wells such that the glass cover slips were fully immersed, and the plates were kept inside an incubator at 23 °C. The supplemented Schneider's insect medium was prepared as follows: 2 mg/mL tryptose phosphate, 10% inactivated fetal bovine serum (FBS), 0.5 mg/mL glucose, 30 mg/mL L-glutamine, 1× insect medium supplement (low protein), 0.04 mg/mL tetracycline, 0.05 μg/mL amphotericin B and 0.05 mg/mL gentamicin, pH 7.0 (all reagents from Sigma–Aldrich, Mississauga, ON, Canada).

2.6. Immunocytochemistry

One day after being collected, cultured insect cells were exposed to JBU at different concentrations for 24 h. Controls cells were treated solely with saline. The glass cover slips with the attached cells were removed from the culture plates and the monolayers were fixed with 4% paraformaldehyde for 20 min, room temperature (RT), followed by 3 washes, 5 min each, with phosphate buffered saline – PBS (Na_2HPO_4 10 mM, NaCl 150 mM, pH 7.2). After the washes, the cells were permeabilized with 0.1% Triton and 100 mM glycine in PBS for 20 min, RT, and washed with PBS as described. Subsequently, cells were blocked with 5% FBS in PBS for 1 h, RT, and, without washing, the blocking solution was replaced by 1% FBS plus the primary antibodies, anti-α-tubulin and anti-JBU (1:10,000 dilution each), in PBS. The incubation with primary antibodies was carried out for 1 h, RT, and cells were again washed 3 times with PBS. As secondary antibodies, anti-mouse IgG-Cy5 and anti-rabbit IgG-Cy3 conjugates (Jackson Immuno, West Grove, PA, USA, and Invitrogen-Life Technologies, Burlington, ON, Canada, respectively), were diluted (1:1000) in 1% FBS in PBS and incubated for 1 h, RT. DAPI (4′,6-diamidino-2-phenylindole, Invitrogen-Life Technologies, Burlington, ON, Canada) was added during the last 10 min of secondary antibody incubation for nuclear staining. Finally, cells were washed 3 times with PBS, 5 min each wash, and twice with double distilled water, 2 min each wash. The cells were mounted with glycerol/*n*-propyl gallate mounting medium (glycerol 90% and 0.5% *n*-propyl gallate in 1 M TRIS-HCl, pH 8.0) for observation under a laser scanning confocal microscope with LSM image browser software (Zeiss, Jena, Germany).

2.7. Statistical analysis

Results are expressed as mean ± standard error. Significance of differences between means was determined using one-way ANOVA followed by Holm–Sidack method (SigmaPlot software), and results were considered statistically different when $P < 0.05$.

3. Results

3.1. *JBU induces hemocyte aggregation* in vivo

Rhodnius prolixus 5th instars show nearly 100% mortality rate 24 h after injections of approximately 12 μg of JBU per insect (Staniscuaski et al., 2010). To be able to observe JBU's effects upon hemolymph cells, we used lower doses and shorter periods in the following experiments. The insects were injected with 6 μg of JBU each, or saline in the case of controls. Formation of cell aggregates in the hemolymph was analyzed 6 h after injection. This time interval allowed sealing of the wound caused by the needle on injection thereby facilitating hemolymph extraction. The number of free non-aggregated cells was very similar in both JBU and saline injected insects (Fig. 1A). In contrast JBU injections triggered hemocyte aggregation (Figs. 1B and 2) while saline injections had not such effect (Fig. 1B).

3.2. *JBU induces hemocyte aggregation* in vitro

After 1 h of *in vitro* incubation, JBU (200 nM or 500 nM) induced a decrease in the number of freely suspended cells along with induction of hemocyte aggregation (Fig. 3A and B). Control hemocytes, which were collected and kept in the same conditions but in the absence of JBU, did not show any significant formation of aggregates (Fig. 3B). In addition to aggregate formation, a darkening of the hemolymph in response to JBU treatment was observed (Fig. 3C).

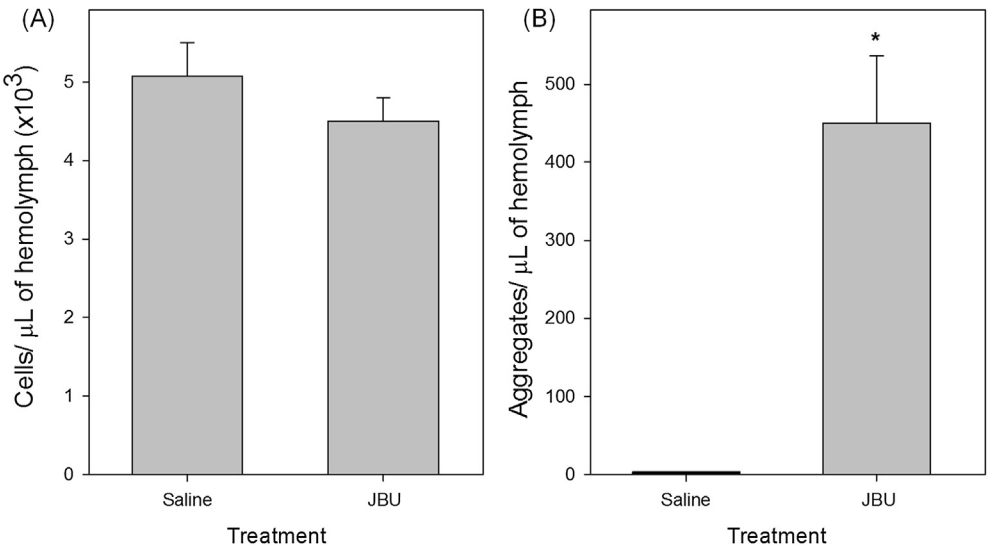

Fig. 1. *In vivo* hemocyte aggregation induced by JBU. Unfed 5th instars (mean weight 50 mg) were injected with 6 µg of JBU per insect or solely with saline for the control insects and 6 h after injections hemolymph was collected in anticoagulant solution. In order to verify cell viability, 0.1% Trypan Blue was added to the solution 10 min prior to counting. Hemocytes and aggregates were counted under phase-contrast optical microscopy with a hemocytometer. (A) Number of cells per µL of hemolymph, (B) Number of aggregates per µL of hemolymph. Results are shown as means of 3 biological replicates with standard error. "*" indicates statistically significant difference from saline controls.

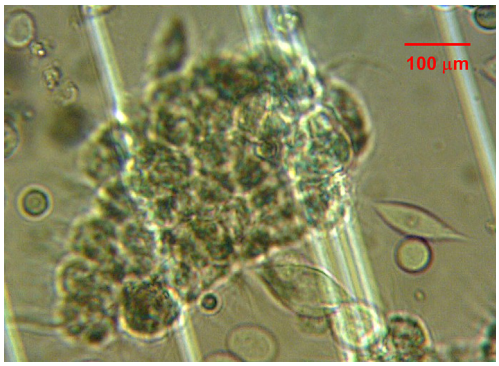

Fig. 2. Hemocyte aggregation induced by JBU *in vivo*. Unfed 5th instars (mean weight 50 mg) were injected with 6 µg of JBU and hemolymph was collected in anticoagulant solution 6 h after injections. The aggregates were observed under phase-contrast optical microscopy with a hemocytometer. Typical result. 20×/0.5 magnification.

3.3. Effect of EGTA and inhibitors of eicosanoid synthesis on JBU-induced hemocytes aggregation

JBU-induced aggregation was tested in the presence of the eicosanoid synthesis inhibitors, dexamethasone (inhibits PLA_2 activity) (Herbert et al., 2007), indomethacin (inhibits COX-1 and COX-2) (Rainsford, 2004), baicalein (inhibits 12-LOX) (Donald et al., 2012) and esculetin (inhibits 5-LOX and 12-LOX) (Buyukguzel et al., 2010), as well as EGTA, a calcium ion chelating agent. EGTA (Fig. 3B), as well as dexamethasone and indomethacin (Fig. 4A and B), inhibited JBU-induced hemocyte aggregation besides increasing the number of cells counted in the suspension. These results suggest that JBU's effect on hemocytes are mediated by COX-derived eicosanoids products and are dependent on extracellular calcium. The LOX inhibitors, baicalein and esculetin, did not alter JBU-induced effects (Fig. 5B), indicating that products of LOX have no roles in hemocyte aggregation. From the controls of each treatment, it was found that hemocytes did not aggregate when tested only with the inhibitors, with EGTA or with ethanol in the absence of JBU (data not shown). The number of non-aggregated cells in the presence of JBU preceded by dexamethasone or indomethacin (Fig. 4A), or EGTA (Fig. 3A) pre-treatments reverted to values similar to those in the control groups. On the other hand the decreased number of non-aggregated cells in presence of JBU was not prevented by baicalein or esculetin pre-treatments (Fig. 5A). When the aggregation reactions were inhibited by dexamethasone and indomethacin the darkening of the hemolymph caused by JBU also diminished (data not shown), in contrast to the effect of EGTA which inhibited aggregation but not the darkening of the medium (Fig. 3C).

3.4. Immunolocalization of JBU in cultured cells

Cell cultures treated with 50 nM JBU appeared to internalize the protein into vesicles, accompanied by slight damage to the cytoskeleton (as shown by some α-tubulin immunoreactivity spreading onto the cover slip around the cells, Fig. 6); however in cells incubated with 100 nM JBU severe structural damage could be seen, with intense α-tubulin immunoreactive sites around aggregated nuclei (Fig. 6). The pattern of JBU immunoreactivity was different between the two tested concentrations and nuclei aggregation was observed only at the higher JBU dose. While at the lower concentration JBU appears to be present inside cell vesicles, at 100 nM JBU appears also associated to α-tubulin found outside cells (Fig. 6).

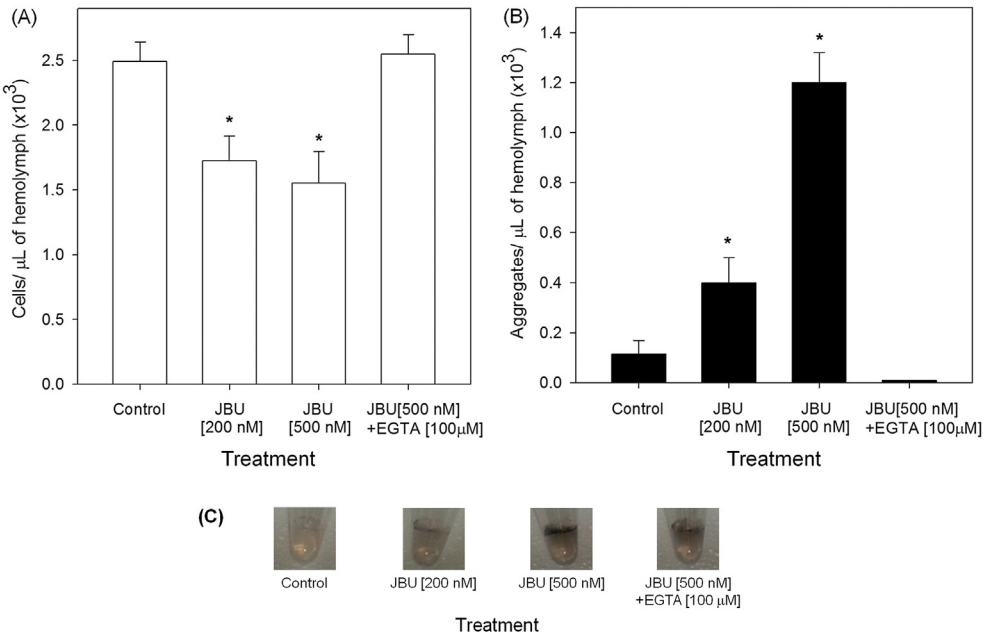

Fig. 3. *In vitro* hemocyte aggregation induced by JBU. Hemolymph was collected from unfed 5th instars in *R. prolixus* saline and incubated at room temperature for one hour in the presence of JBU at 200 and 500 nM. Controls were incubated in saline alone. EGTA (100 μM) was added to the cells 30 min prior to JBU addition. In order to verify cell viability, 0.1% Trypan Blue was added to the solution 10 min prior to counting. Hemocytes and aggregates were counted under phase-contrast optical microscopy with a hemocytometer. (A) Number of cells per μL of hemolymph, (B) Number of aggregates per μL of hemolymph, (C) Reaction tubes containing hemolymph and saline after the incubation period. Results are shown as means of 3 biological replicates with standard error. "*" indicates statistically significant difference from saline controls.

4. Discussion

Here we demonstrated that *C. ensiformis* urease (JBU) triggers the immune system of the hemipteran model *R. prolixus*, activating the insect's hemocytes both *in vivo* and *in vitro*. Based on previous evidences we aimed to evaluate if eicosanoid metabolites could be involved in the response triggered by JBU. Pretreatment with inhibitors of eicosanoid synthesis, dexamethasone and indomethacin, blocked the *in vitro* JBU-induced hemocyte aggregation also reducing the concomitant darkening of the medium, suggestive of activation of the PPO cascade. We have already shown the involvement of a PLA_2 gene in JBU's lethal effect on *R. prolixus*, with the toxicity being significantly reduced

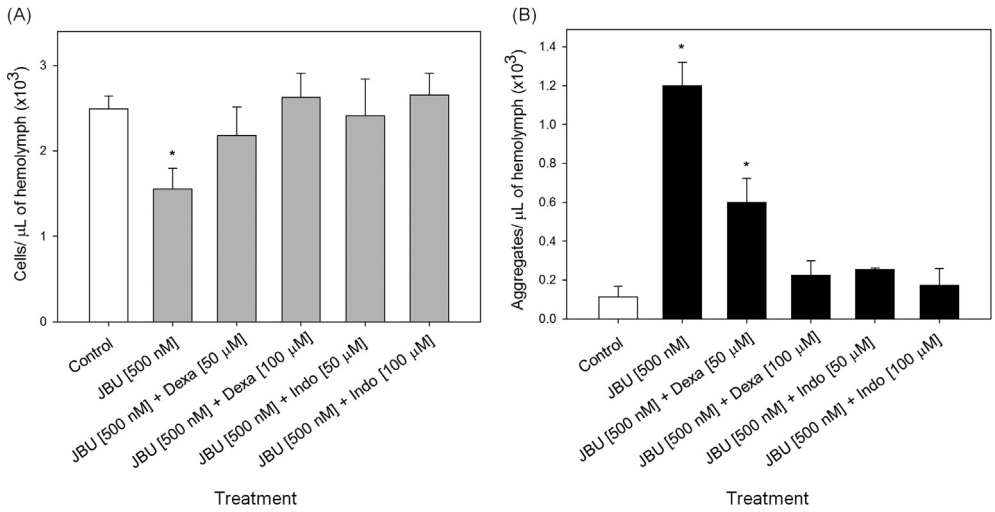

Fig. 4. Inhibition of JBU-induced *in vitro* hemocyte aggregation. Hemolymph was collected from unfed 5th instars in *R. prolixus* saline and incubated at room temperature for one hour in the presence of JBU at 500 nM. Controls were incubated with saline only. Dexamethasone and indomethacin were added to the cells 30 min prior to JBU addition. In order to verify cell viability, 0.1% Trypan Blue was added to the solution 10 min prior to counting. Hemocytes and aggregates were counted under phase-contrast optical microscopy with a hemocytometer. (A) Number of cells per μL of hemolymph, (B) Number of aggregates per μL of hemolymph. Results are shown as means of 3 biological replicates with standard error. "*" indicates statistically significant difference from saline controls.

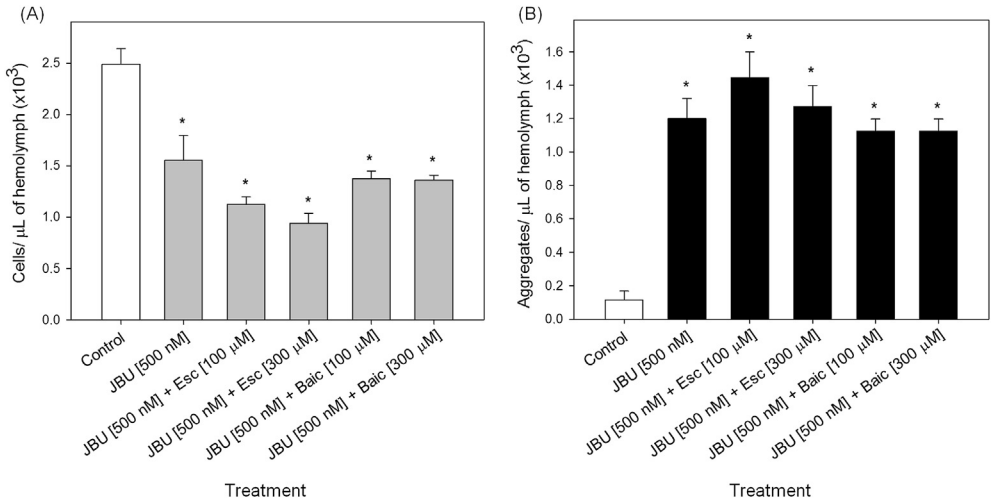

Fig. 5. Effect of lipoxygenase inhibitors on *in vitro* hemocyte aggregation induced by JBU. Hemolymph was collected from unfed 5th instars in *R. prolixus* saline and incubated at room temperature for one hour in the presence of JBU at 500 nM. Controls were incubated in saline only. Esculetin and baicalein were added to the cells 30 min prior to JBU addition. In order to verify cell viability, 0.1% Trypan Blue was added to the solution 10 min prior to counting. Hemocytes and aggregates were counted under phase-contrast optical microscopy with a hemocytometer. (A) Number of cells per µL of hemolymph, (B) Number of aggregates per µL of hemolymph. Results are shown as means of 3 biological replicates with standard error. "*" indicates statistically significant difference from saline controls.

after knocking down the expression of this PLA_2 gene (Defferrari et al., 2013). The glucocorticoid dexamethasone acts by increasing the expression of annexin A1, a protein that binds to PLA_2 and blocks its activity, therefore inhibiting eicosanoids production at the beginning of the cascade (Herbert et al., 2007). Indomethacin directly inhibits cyclooxygenase (COX) activity and subsequent release of prostaglandins (PGs) (Rainsford, 2004). Although

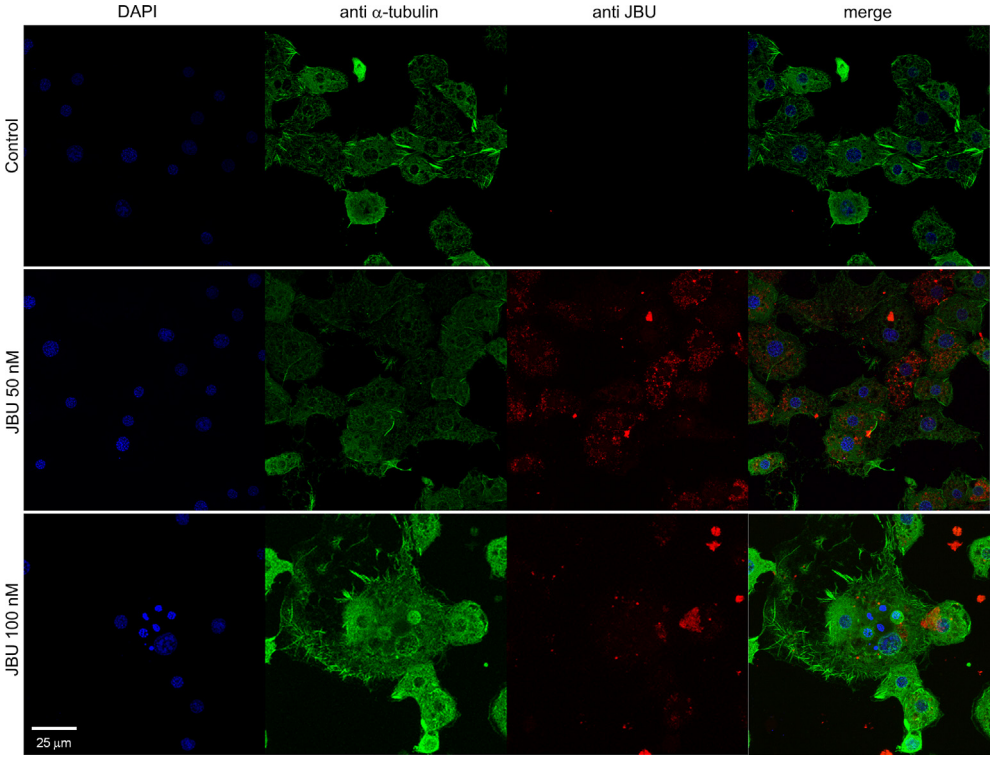

Fig. 6. JBU and α-tubulin immunoreactivity in cultured hemocytes. Hemolymph was collected from 5th instars 5 days after feeding and placed into supplemented Schneider's insect medium. Cells were kept inside incubators at 23 °C for 24 h and then JBU was added (50 and 100 nM) to the medium. After JBU addition, the cells were incubated in the same conditions for another 24 h. Confocal microscopy images of JBU immunoreactivity (red) and α-tubulin immunoreactivity (green). The nuclei of the cells were stained with DAPI (blue). (For interpretation of the references to color in this figure legend, the reader is referred to the web version of this article.)

it has been shown that LOX products can modulate some cellular responses in *Spodoptera exigua* (Shrestha and Kim, 2009), COX products, particularly PGs, are known to mediate cellular reactions in insects infected with fungi, bacteria and other pathogens (Dean et al., 2002; Downer et al., 1997; Jurenka et al., 1999; Lord et al., 2002; Stanley, 1997; Stanley-Samuelson et al., 1997; Stanley-Samuelson et al., 1991). COX-derived eicosanoids have also been shown to signal PPO release and activation in *S. exigua* (Shrestha and Kim, 2008), *Galleria mellonella* (Downer et al., 1997) and *R. prolixus* (Garcia et al., 2004a), leading to PO, the active form of PPO, which initiates the melanization process (Cerenius and Soderhall, 2004). Further studies are needed to evaluate the production of melanin by JBU-treated hemocytes, and to determine if the toxin could also be triggering a humoral response.

The involvement of COX-derived eicosanoids in JBU-induced hemocyte aggregation contrasts to what has been observed in mammalian cells activated by different ureases, which require LOX-derived products, as reported in platelets (Carlini et al., 1985; Olivera-Severo et al., 2006; Wassermann et al., 2010), pancreatic β-cells (Barja-Fidalgo et al., 1991a), rat brain synaptosomes (Barja-Fidalgo et al., 1991b) and neutrophils (Uberti et al., 2013). On the other hand, activation of murine macrophages by canatoxin, an isoform of JBU, does not seem to require LOX products (Ghazaleh, 1992). It has been shown that insect hemocytes are very similar to mammalian phagocytic cells such as neutrophils, despite the facts that the insect cells are larger, show a higher density of granules and do not have a multilobed nucleus (Browne et al., 2013). EGTA also inhibited the *in vitro* aggregation response, suggesting that extracellular calcium is necessary for the reaction. The dependence of calcium ions in most biological activities of JBU has been reported in previous studies, such as JBU-induced inhibition of diuresis in *R. prolixus* Malpighian tubules (Staniscuaski et al., 2009) and platelet activation (Ghazaleh et al., 1997; Wassermann et al., 2010).

To examine the fate of JBU and its cytotoxic effect in a more controlled manner, we used cultured cells and developed 24 h long experiments. Cultured cells were considerably more sensitive and vulnerable than fresh isolated hemocytes, thus lower doses of JBU had to be used. JBU appeared to be internalized in vesicles into the hemocytes, causing mild to severe damage to the cytoskeleton and nuclei aggregation. Programmed cell death of hemocytes is one of the mechanisms to control infections. For example, *Drosophila melanogaster* cells fight bacterial infections by triggering cytoplasmatic autophagy (Yano et al., 2008). Apoptosis mechanisms are especially important in insects during viral infections, reducing viral replication and the consequent spreading within the host (Clem, 2005). The damage we observed in insect cells treated with JBU could possibly be part of programmed cell death. It has been shown that canatoxin, a JBU isoform, induces damage and cytolytic effect in cultures of various types of mammalian cell in doses ranging from 50 to 500 nM (Campos et al., 1991). Interestingly, *Helicobacter pylori* urease has been reported to increase survival of human neutrophils by affecting their apoptosis pathways (Uberti et al., 2013).

Altogether we conclude that in *R. prolixus* JBU activates cellular responses through modulation by COX metabolites, similar to what has been observed in previous studies for the activation of the insect immune system by pathogens. These reactions might contribute to the overall entomotoxicity of JBU, acting synergistically with the effects of urease-derived peptides released in the insect's digestive tract. We have shown for the first time that a urease directly affects hemocytes and hemolymph in an insect, contributing to the overall understanding of the mechanism of action of these toxins.

Authors contributions

M.S.D. conceived the study, conducted all the experiments and wrote the manuscript, R.S. helped with cell cultures and imaging, C.R.C. and I.O. conceived the study, revised the manuscript and supervised all the work.

Ethical statement

The authors declare that: a) the material has not been published in whole or in part elsewhere, except in the form of an abstract or part of academic thesis; b) the work is not currently being considered for publication elsewhere; c) all authors have agreed upon the content and form of the manuscript; d) all relevant ethical safeguards have been met regarding animal experimentation.

Acknowledgments

This research was funded by the Brazilian agency CAPES-MEC (Coordenação de Aperfeiçoamento de Pessoal de Nível Superior), which provided Marina S. Defferrari a scholarship at the University of Toronto Mississauga, through the Sciences Without Borders Program; by the Natural Sciences and Engineering Research Council of Canada grants to Dr. Ian Orchard; and by grants from the Brazilian agencies CAPES-MEC, CNPq-MCT (Conselho Nacional de Desenvolvimento Científico e Tecnológico) and FAPERGS (Fundação de Amparo a Pesquisa do Estado do Rio Grande do Sul) to Dr. Celia R. Carlini. Thanks to Dr. Angela B. Lange for the support at University of Toronto Mississauga, and to Nikki Sarkar for maintaining the *R. prolixus* colony used in all experiments.

Conflict of interest

The authors declare that there are no conflicts of interest.

Transparency document

Transparency document related to this article can be found online at http://dx.doi.org/10.1016/j.toxicon.2014.02.006.

References

Azambuja, P., Garcia, E.S., Ratcliffe, N.A., 1991. Aspects of classification of Hemiptera hemocytes from six triatomine species. Mem. Inst. Oswaldo Cruz 86, 1–10.

Barja-Fidalgo, C., Guimaraes, J.A., Carlini, C.R., 1991a. Canatoxin, a plant protein, induces insulin release from isolated pancreatic islets. Endocrinology 128, 675–679.
Barja-Fidalgo, C., Guimaraes, J.A., Carlini, C.R., 1991b. Lipoxygenase-mediated secretory effect of canatoxin the toxic protein from *Canavalia ensiformis seeds*. Toxicon 29, 453–459.
Boyes, E.A., ld, L.J., Haroulikov, J., 1964. Cytotoxic test for demonstration of antibodies. Methods Med. Res. 10, 39–51.
Browne, N., Heelan, M., Kavanagh, K., 2013. An analysis of the structural and functional similarities of insect hemocytes and mammalian phagocytes. Virulence 4, 597–603.
Buyukguzel, E., Hyrsl, P., Buyukguzel, K., 2010. Eicosanoids mediate hemolymph oxidative and antioxidative response in larvae of *Galleria mellonella* L. Comp. Biochem. Physiol. A Mol. Integr. Physiol. 156, 176–183.
Campos, M.M., Carlini, C.R., Guimaraes, J.A., Marques-Silva, V.M., Rumjanek, V.M., 1991. Effect of canatoxin on cell cultures. Cell Biol. Int. Rep. 15, 581–594.
Carlini, C.R., Guimaraes, J.A., Ribeiro, J.M., 1985. Platelet release reaction and aggregation induced by canatoxin, a convulsant protein: evidence for the involvement of the platelet lipoxygenase pathway. Br. J. Pharmacol. 84, 551–560.
Carlini, C.R., Oliveira, A.E., Azambuja, P., Xavier-Filho, J., Wells, M.A., 1997. Biological effects of canatoxin in different insect models: evidence for a proteolytic activation of the toxin by insect cathepsin like enzymes. J. Econ. Entomol. 90, 340–348.
Carlini, C.R., Polacco, J.C., 2008. Toxic properties of urease. Crop Sci. 45, 1665–1672.
Cerenius, L., Soderhall, K., 2004. The prophenoloxidase-activating system in invertebrates. Immunol. Rev. 198, 116–126.
Cerenius, L., Soderhall, K., 2011. Coagulation in invertebrates. J. Innate Immun. 3, 3–8.
Clem, R.J., 2005. The role of apoptosis in defense against baculovirus infection in insects. Curr. Top. Microbiol. Immunol. 289, 113–129.
Dean, P., Gadsden, J.C., Richards, E.H., Edwards, J.P., Keith, C.A., et al., 2002. Modulation by eicosanoid biosynthesis inhibitors of immune responses by the insect *Manduca sexta* to the pathogenic fungus *Metarhizium anisopliae*. J. Invertebr. Pathol. 79, 93–101.
Defferrari, M.S., Demartini, D.R., Marcelino, T.B., Pinto, P.M., Carlini, C.R., 2011. Insecticidal effect of *Canavalia ensiformis* major urease on nymphs of the milkweed bug *Oncopeltus fasciatus* and characterization of digestive peptidases. Insect Biochem. Mol. Biol. 41, 388–399.
Defferrari, M.S., Lee, D.H., Fernandes, C.L., Orchard, I., Carlini, C.R., 2013. A phospholipase A2 gene is linked to Jack bean urease toxicity in the Chagas' disease vector *Rhodnius prolixus*. Biochim. Biophys. Acta 1840, 396–405.
Dixon, N.E., Gazzola, T.C., blakeley, R.L., Zermer, B., 1975. Letter: Jack bean urease (EC 3.5.1.5). A metalloenzyme. A simple biological role for nickel? J. Am. Chem. Soc. 97, 4131–4133.
Donald, G., Hertzer, K., Eibl, G., 2012. Baicalein–an intriguing therapeutic phytochemical in pancreatic cancer. Curr. Drug Targets 13, 1772–1776.
Downer, R.G., Moore, S.J., Diehl-Jones, L., Mandato, C.A., 1997. The effects of eicosanoid biosynthesis inhibitors on prophenoloxidase activation, phagocytosis and cell spreading in *Galleria mellonella*. J. Insect Physiol. 43, 1–8.
Ferreira-Dasilva, C.T., Gombarovits, M.E., Masuda, H., Oliveira, C.M., Carlini, C.R., 2000. Proteolytic activation of canatoxin, a plant toxic protein, by insect cathepsin-like enzymes. Arch. Insect Biochem. Physiol. 44, 162–171.
Figueiredo, M.B., Garcia, E.S., Azambuja, P., 2008. Blockades of phospholipase A(2) and platelet-activating factor receptors reduce the hemocyte phagocytosis in Rhodnius prolixus: *in vitro* experiments. J. Insect Physiol. 54, 344–350.
Follmer, C., Barcellos, G.B., Zingali, R.B., Machado, O.L., Alves, E.W., et al., 2001. Canatoxin, a toxic protein from jack beans (*Canavalia ensiformis*), is a variant form of urease (EC 3.5.1.5): biological effects of urease independent of its ureolytic activity. Biochem. J. 360, 217–224.
Follmer, C., Real-Guerra, R., Wasserman, G.E., Olivera-Severo, D., Carlini, C.R., 2004. Jackbean, soybean and *Bacillus pasteurii* ureases: biological effects unrelated to ureolytic activity. Eur. J. Biochem. 271, 1357–1363.
Garcia, E.S., Machado, E.M., Azambuja, P., 2004a. Effects of eicosanoid biosynthesis inhibitors on the prophenoloxidase-activating system and microaggregation reactions in the hemolymph of *Rhodnius prolixus* infected with *Trypanosoma rangeli*. J. Insect Physiol. 50, 157–165.
Garcia, E.S., Machado, E.M., Azambuja, P., 2004b. Inhibition of hemocyte microaggregation reactions in *Rhodnius prolixus* larvae orally infected with *Trypanosoma rangeli*. Exp. Parasitol. 107, 31–38.
Ghazaleh, F.A., 1992. Canatoxina: Efeito Secretor e Quimiotaxia em Macrófagos Peritoneais de Camundongos.
Ghazaleh, F.A., Francischetti, I.M., Gombarovits, M.E., Carlini, C.R., 1997. Stimulation of calcium influx and platelet activation by canatoxin: methoxyverapamil inhibition and downregulation by cGMP. Arch. Biochem. Biophys. 339, 362–367.
Harizi, H., Corcuff, J.B., Gualde, N., 2008. Arachidonic-acid-derived eicosanoids: roles in biology and immunopathology. Trends Mol. Med. 14, 461–469.
Herbert, S.P., Odell, A.F., Ponnambalam, S., Walker, J.H., 2007. The confluence-dependent interaction of cytosolic phospholipase A2-alpha with annexin A1 regulates endothelial cell prostaglandin E2 generation. J. Biol. Chem. 282, 34468–34478.
Jurenka, R.A., Pedibhotla, V.K., Stanley, D.W., 1999. Prostaglandin production in response to a bacterial infection in true armyworm larvae. Arch. Insect Biochem. Physiol. 41, 225–232.
Kanost, M.R., Jiang, H., Yu, X.Q., 2004. Innate immune responses of a lepidopteran insect, *Manduca sexta*. Immunol. Rev. 198, 97–105.
Lane, N.J., Leslie, R.A., Swales, L.S., 1975. Insect peripheral nerves: accessibility of neurohaemal regions to lanthanum. J. Cell Sci. 18, 179–197.
Lone, A.M., Tasken, K., 2013. Proinflammatory and immunoregulatory roles of eicosanoids in T cells. Front. Immunol. 4, 130.
Lord, J.C., Anderson, S., Stanley, D.W., 2002. Eicosanoids mediate *Manduca sexta* cellular response to the fungal pathogen *Beauveria bassiana*: a role for the lipoxygenase pathway. Arch. Insect Biochem. Physiol. 51, 46–54.
Marmaras, V.J., Lampropoulou, M., 2009. Regulators and signalling in insect haemocyte immunity. Cell Signal 21, 186–195.
Miller, J.S., Stanley, D.W., 2001. Eicosanoids mediate microaggregation reactions to bacterial challenge in isolated insect hemocyte preparations. J. Insect Physiol. 47, 1409–1417.
Olivera-Severo, D., Wassermann, G.E., Carlini, C.R., 2006. *Bacillus pasteurii* urease shares with plant ureases the ability to induce aggregation of blood platelets. Arch. Biochem. Biophys. 452, 149–155.
Piovesan, A.R., Staniscuaski, F., Marco-Salvadori, J., Real-Guerra, R., Defferrari, M.S., et al., 2008. Stage-specific gut proteinases of the cotton stainer bug *Dysdercus peruvianus*: role in the release of entomotoxic peptides from *Canavalia ensiformis* urease. Insect Biochem. Mol. Biol. 38, 1023–1032.
Rainsford, K.D., 2004. Inhibitors of Eicosanoids, pp. 189–210.
Real-Guerra, R., Carlini, C.R., Staniscuaski, F., 2013. Role of lysine and acidic amino acid residues on the insecticidal activity of Jackbean urease. Toxicon 71, 76–83.
Shrestha, S., Kim, Y., 2008. Eicosanoids mediate prophenoloxidase release from oenocytoids in the beet armyworm *Spodoptera exigua*. Insect Biochem. Mol. Biol. 38, 99–112.
Shrestha, S., Kim, Y., 2009. Various eicosanoids modulate the cellular and humoral immune responses of the beet armyworm, *Spodoptera exigua*. Biosci. Biotechnol. Biochem. 73, 2077–2084.
Staniscuaski, F., Carlini, C.R., 2012. Plant ureases and related peptides: understanding their entomotoxic properties. Toxins (Basel) 4, 55–67.
Staniscuaski, F., TeBrugge, V., Carlini, C.R., Orchard, I., 2010. Jack bean urease alters serotonin-induced effects on *Rhodnius prolixus* anterior midgut. J. Insect Physiol. 56, 1078–1086.
Staniscuaski, F., TeBrugge, V., Carlini, C.R., Orchard, I., 2009. Invitro effect of *Canavalia ensiformis* urease and the derived peptide Jaburetox-2Ec on *Rhodnius prolixus* Malpighian tubules. J. Insect Physiol. 55, 255–263.
Stanley, D., 2006. Prostaglandins and other eicosanoids in insects: biological significance. Annu. Rev. Entomol. 51, 25–44.
Stanley, D., Miller, J., Tunaz, H., 2009. Eicosanoid actions in insect immunity. J. Innate Immun. 1, 282–290.
Stanley, D.W., 1997. Eicosanoids mediate insect cellular immune reactions to bacterial infections. Adv. Exp. Med. Biol. 433, 359–362.
Stanley-Samuelson, D., Rana, R.L., Pedibhotla, V.K., Miller, J.S., Jurenka, R.A., 1997. Eicosanoids mediate microaggregation and nodulation responses to bacterial infections in black cutworms, *Agrotis ipsilon*, and true armyworms, *Pseudaletia unipuncta*. J. Insect Physiol. 43, 125–133.
Stanley-Samuelson, D.W., Jensen, E., Nickerson, K.W., Tiebel, K., Ogg, C.L., et al., 1991. Insect immune response to bacterial infection is mediated by eicosanoids. Proc. Natl. Acad. Sci. U. S. A. 88, 1064–1068.
Uberti, A.F., Olivera-Severo, D., Wassermann, G.E., Scopel-Guerra, A., Moraes, J.A., et al., 2013. Pro-inflammatory properties and neutrophil activation by *Helicobacter pylori* urease. Toxicon 69, 240–249.
Wassermann, G.E., Olivera-Severo, D., Uberti, A.F., Carlini, C.R., 2010. *Helicobacter pylori* urease activates blood platelets through a lipoxygenase-mediated pathway. J. Cell Mol. Med. 14, 2025–2034.
Yano, T., Mita, S., Ohmori, H., Oshima, Y., Fujimoto, Y., et al., 2008. Autophagic control of listeria through intracellular innate immune recognition in drosophila. Nat. Immunol. 9, 908–916.

3.2. Experimentos complementares

3.2.1. Imunoreatividade anti-ciclooxigenase-2 em amostras de hemolinfa

Ninfas de quinto instar foram injetadas com 6 μg de JBU (por inseto) e a hemolinfa foi coletada após 6 horas, como descrito no Capítulo I, item 2.3 do artigo "Jack bean (*Canavalia ensiformis*) urease induces eicosanoid-modulated hemocyte aggregation in the Chagas' disease vector *Rhodnius prolixus*". Insetos injetados somente com solução salina foram utilizados como controle. A suspensão de hemócitos foi equilibrada com tampão TRIS 20 mM, Tween 0.2%, pH 8.0, e agitada em vórtex por 15 segundos. Em seguida a suspensão foi centrifugada a 8000 *g*, por 4 min a 4°C, o sobrenadante coletado e mantido em banho de gelo até o momento do uso. O conteúdo proteico das amostras foi estimado pelo método de Layne (1957) utilizando-se um espectrofotômetro Spectra Max M3 (Molecular Devices, Sunnyvale, CA, USA) e calculando-se a razão dos valores obtidos nos comprimentos de onda de 280 e 260 nm.

Alíquotas contendo 50 μg de proteína do lisado de hemócitos foram aplicadas em membranas de nitrocelulose. Após secarem naturalmente, as membranas foram bloqueadas com 1% de caseína em PBST (PBS contendo 0.2% de Tween) por 1 hora, a 37°C, sob agitação constante. Após o bloqueio as membranas foram incubadas com os anticorpos primários diluídos em PBST contendo 1% de caseína, por 2 horas, a 37°C, sob agitação constante. Em seguida as membranas foram lavadas 3 vezes com PBST, por 10 min cada lavagem. Após as lavagens as membranas foram incubadas com os anticorpos secundários diluídos em PBST contendo 1% de caseína, por 2 horas, a 37°C, sob agitação constante. As membranas foram novamente lavadas 3 vezes com

PBST, por 10 min cada lavagem. Foi feita uma última lavagem em PBS por 5 min, repetida duas vezes. Os anticorpos primários (anti-COX-2 e anti-α-tubulina) foram utilizados em diluições de 1:10.000, e os anticorpos secundários conjugados a peroxidase foram utilizados em diluições de 1:5.000. Subsequentemente as membranas foram incubadas em um substrato luminescente para peroxidase, Luminata Forte (Merck Millipore, Darmstadt, Germany), por 5 min. Após, as membranas foram expostas a filmes radiográficos para a revelação do resultado. O experimento foi repetido duas vezes.

Observamos um aumento da imunoreatividade anti-COX-2 em amostras de hemolinfa coletadas de insetos tratados com JBU, quando comparadas a imunoreatividade em amostras de insetos controle (Fig. 4). Esse incremento visual pode ser devido a um aumento na expressão de COX-2, mais uma vez sugerindo que o efeito causado por JBU é modulado pela atividade desta enzima. Em estudos anteriores com *R. prolixus,* um aumento no conteúdo de prostaglandinas E_2 (PGE_2) foi detectado em órgãos isolados após o tratamento com JBU (Stanisçuaski *et al*., 2010). Estes metabólitos são produtos de oxigenação por COX-2, que, em outros animais, tem sua expressão induzida de acordo com a demanda (Smith *et al*., 2000). Contudo, este resultado ainda necessita de validação posterior, com ensaios quantitativos e que demonstrem essa possível diferença de forma conclusiva. Ainda existem limitações na comprovação de diferenças na expressão gênica de COX-2 em insetos, já que, até o momento, nenhum gene que codifique qualquer ciclooxigenase foi encontrado (Tootle *et al*., 2011).

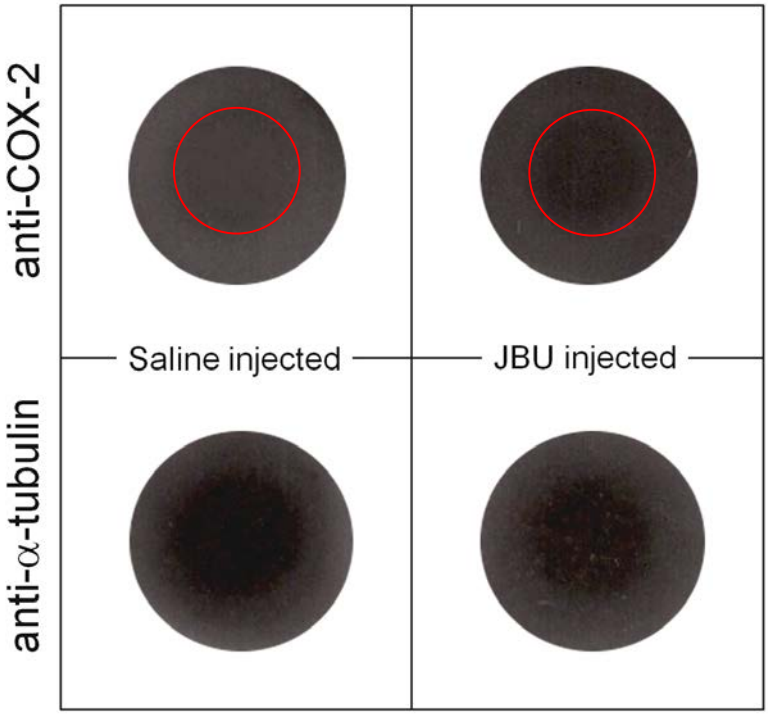

Figura 4. Imunoreatividade anti-ciclooxigenase-2 em amostras de hemolinfa. Amostras de hemolinfa de insetos injetados com JBU (6 μg por inseto) e de insetos controle foram aplicadas em membranas de nitrocelulose e incubadas com anticorpos anti-COX-2 e anti-α-tubulina. Após incubação com os anticorpos secundários conjugados a peroxidase, as membranas foram incubadas com um substrato luminescente para peroxidase e expostas a filmes radiográficos. O experimento foi repetido duas vezes. A soma dos pixels na área circulada é 1.7 vezes maior no grupo tratado com JBU em relação ao controle.

3.2.2. Cultura de hemócitos

O protocolo de cultura de células proposto no Capítulo I, item 2.5, como parte do artigo "Jack bean (*Canavalia ensiformis*) urease induces eicosanoid-modulated hemocyte aggregation in the Chagas' disease vector *Rhodnius prolixus"*, foi adaptado com a adição de fator de crescimento epidermal de camundongo para que fosse possível a manutenção das células por períodos de tempo estendidos. Da mesma forma como descrito anteriormente, ninfas de quinto instar, 5 dias após serem alimentadas, foram esterilizadas por imersão em etanol 70%, por 5 minutos, e a hemolinfa foi coletada a partir de um corte em uma das patas do inseto, em ambiente estéril de um fluxo laminar. As amostras de hemolinfa foram imediatamente adicionadas ao meio de cultivo Schneider para células de inseto (Sigma-Aldrich, Mississauga, ON, Canadá), com suplementos, em tubos estéreis em uma proporção de 1:1. A suspensão hemolinfa:meio de cultura foi colocada sobre lamínulas de vidro dentro de poços de placas de cultura. Após 30 minutos, 1 mL do meio de cultura com suplementos foi adicionado lentamente a cada poço, para evitar agitação do meio, até que o fundo ficasse totalmente coberto. As placas foram mantidas em incubadoras a 23°C e o meio foi trocado a cada cinco dias. O meio de cultivo de Schneider foi suplementado da seguinte maneira: 2 mg/mL triptose fosfato, 10% soro bovino fetal inativado (FBS), 0.5 mg/mL glicose, 30 mg/mL L-glutamina, 1x suplemento para meio de cultura de inseto (baixa concentração proteica), 0.04 mg/mL tetraciclina, 0.05 μg/mL anfotericina B e 0.05 mg/mL gentamicina, reagentes adquiridos da Sigma-Aldrich (Mississauga, ON, Canada), 10 μg/mL fator de crescimento epidermal de camundongo, reagente

adquirido da Reprokine (Valley Cottage, NY, EUA), e a solução foi ajustada a pH 7.0.

3.2.3. Imuncitoquímica e PCR quantitativo em hemócitos cultivados

Para a validação do protocolo de cultura de células foram utilizadas as técnicas de imunocitoquímica e de PCR quantitativo. Na primeira técnica foi utilizado um anticorpo anti-α-tubulina, isto porque a tubulina é uma das principais proteínas componentes do citoesqueleto, e a integridade do citoesqueleto indica a condição saudável das células (Luduena, 2013). Na segunda técnica foi monitorada a expressão de três genes de referência validados para *R. prolixus*, sendo eles os genes de proteína ribossomal 49 (rp49), de β-actina e de α-tubulina (Paluzzi & O'Donnell, 2012). A manutenção dos níveis de expressão dos genes de referência também é um indicativo das condições em que as células se encontram. As metodologias foram descritas no Capítulo I desta tese, item 2.6, para a imunocitoquímica, e no Capítulo II, item 2.7 de materiais e metodologias, para o PCR quantitativo.

Com ambas técnicas observamos que houve a manutenção da viabilidade das células com até 4 semanas de cultivo após a extração da hemolinfa e estabelecimento das culturas, o que indicou a eficiência do protocolo de cultura de células proposto. Com a imunocitoquímica (Fig. 5) observamos (1) que a porção do citoesqueleto composta por α-tubulina nos hemócitos cultivados encontrou-se íntegra, e (2) que processos de divisão celular potencialmente estavam ocorrendo. Com o PCR quantitativo (Tabela 1) observamos a manutenção dos níveis de expressão dos genes de referência em relação a expressão em hemócitos coletados diretamente de insetos vivos.

Tabela 1. Análise da expressão de genes de referência em hemócitos cultivados por 4 semanas a partir de ninfas de quinto instar de *R. prolixus*. A expressão foi quantificada em relação a expressão em hemócitos recém coletados de insetos vivos.

	Gene de referência		
	rp49	β-actina	α-tubulina
% da expressão gênica em relação ao controle (hemócitos recém coletados)	100%	100%	98%

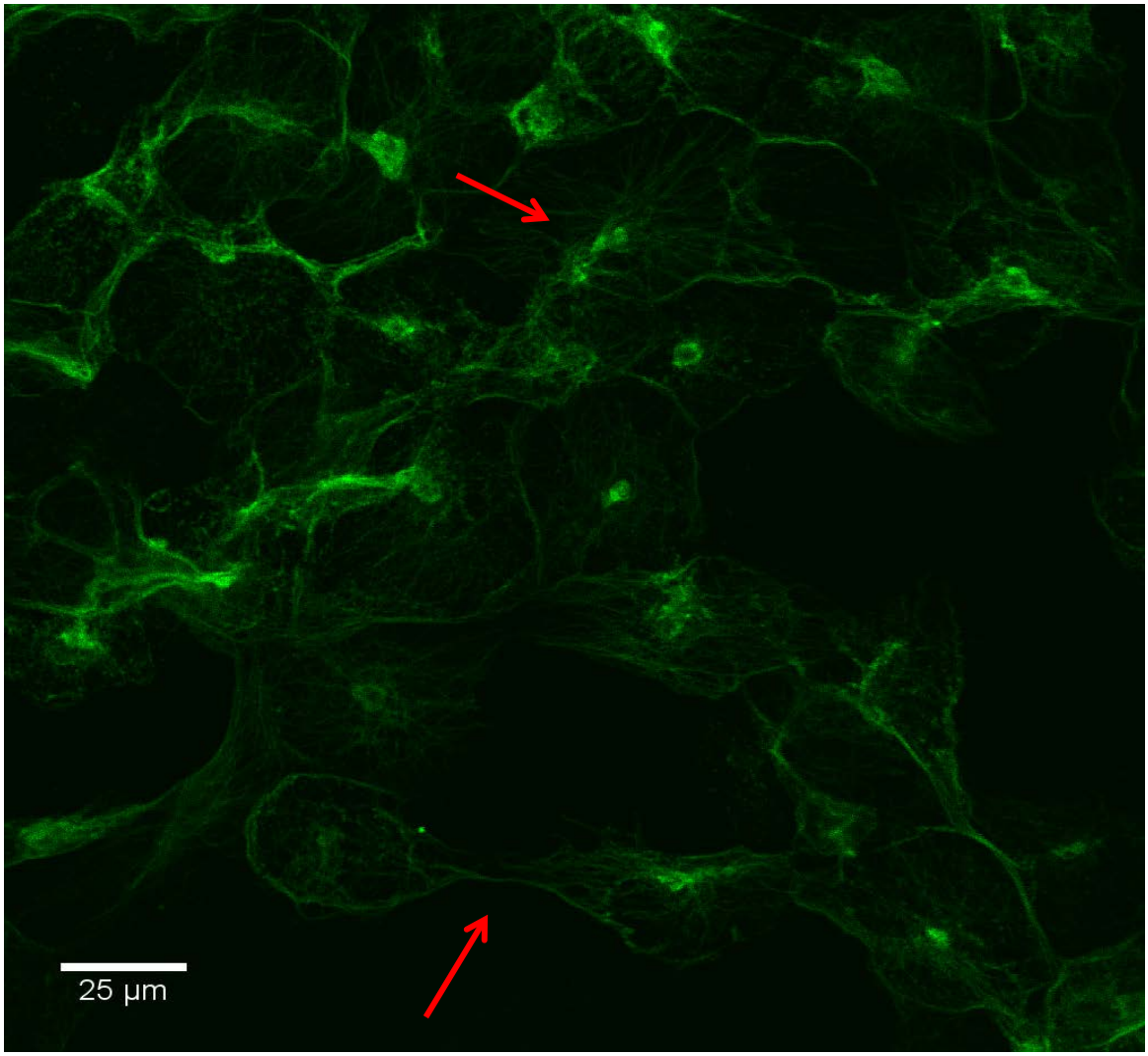

Figura 5. Microscopia confocal de hemócitos em cultura. A hemolinfa foi coletada de ninfas de quinto instar de *R. prolixus*, e adicionada ao meio de cultura. As células foram mantidas a 23°C por 4 semanas, fixadas com paraformaldeído 4%, incubadas com anticorpo primário anti-α-tubulina e anticorpo secundário conjugado com Cy5 (verde). As setas vermelhas indicam possíveis sítios de divisão celular.

4. Resultados - Capítulo II

4.1. Artigo publicado

Defferrari, M.S., Lee, D.H., Fernandes, C.L., Orchard, I., Carlini, C.R. A phospholipase A2 gene is linked to jack bean urease toxicity in the Chagas' disease vector *Rhodnius prolixus*. *Biochimica et Biophysica Acta - General Subjects.* 1840(1): 396-405. 2014.

Resumo

Introdução: Ureases são enzimas multifuncionais que exibem atividades biológicas independentes da função enzimática, incluindo a indução de exocitose e o efeito inseticida. O hemíptero *Rhodnius prolixus* é um modelo sensível a esta toxicidade. Foi demonstrado que a urease de *Canavalia ensiformis* (JBU) tem efeitos prejudiciais sobre *Rhodnius prolixus*, e estes efeitos são modulados por eicosanóides, os quais são sintetizados em uma cascata envolvendo enzimas fosfolipase A_2 (PLA_2) .

Métodos: O genoma de *R. prolixus* foi analisado e transcritos putativos de PLA_2s foram clonados. As sequências de aminoácidos deduzidas foram analisadas e a expressão dos transcritos em variados tecidos foi determinada por qPCR. Foram utilizadas técnicas de RNAi e ensaios de toxicidade de JBU foram subsequentemente realizados.

Resultados: Dois genes de PLA_2s foram identificados, *Rhopr-PLA2III* e *Rhopr-PLA2XII*. Os transcritos são amplamente distribuídos nos tecidos, porém em diferentes níveis. As análises enquadram as proteínas putativas nos grupos III e XII de PLA_2s secretórias. Após o silenciamento de 70% da expressão de *Rhopr-PLA2XII*, a toxicidade do JBU foi reduzida em mais de 50% em ninfas de quinto instar de *R. prolixus*.

Conclusão: O gene *Rhopr-PLA2XII* é ligado ao efeito tóxico de JBU em *R. prolixus* e nossas descobertas reiteram estudos anteriores que demonstraram a modulação desta toxicidade por eicosanóides.

Significância geral: Além de identificarmos e caracterizarmos pela primeira vez genes de PLA_2 em um inseto vetor da doença de Chagas demonstramos que a toxicidade de JBU, esta potente toxina, está ligada a um destes genes. Nossos resultados contribuem para a compreensão geral dos mecanismos de ação de ureases em insetos, e, potencialmente, para estudos sobre o controle da transmissão do parasita causador da doença de Chagas.

Biochimica et Biophysica Acta 1840 (2014) 396–405

Contents lists available at ScienceDirect

Biochimica et Biophysica Acta

journal homepage: www.elsevier.com/locate/bbagen

A phospholipase A_2 gene is linked to Jack bean urease toxicity in the Chagas' disease vector *Rhodnius prolixus*

M.S. Defferrari [a,*], D.H. Lee [b], C.L. Fernandes [a], I. Orchard [b,1], C.R. Carlini [c,2,3]

[a] Graduate Program in Cellular and Molecular Biology, Center of Biotechnology, Institute of Biosciences, Universidade Federal do Rio Grande do Sul, Porto Alegre, RS, Brazil
[b] Department of Biology, University of Toronto Mississauga, Mississauga, ON, Canada
[c] Department of Biophysics & Center of Biotechnology, Universidade Federal do Rio Grande do Sul, Porto Alegre, RS, Brazil and Graduate Program in Cellular and Molecular Biology Applied to Health, Universidade Luterana do Brasil, Canoas, RS, Brazil, Present address: Instituto do Cérebro-InsCer, Pontificia Universidade Católica do Rio Grande do Sul, Porto Alegre, RS, Brazil

ARTICLE INFO

Article history:
Received 12 May 2013
Received in revised form 26 July 2013
Accepted 11 September 2013
Available online 18 September 2013

Keywords:
Insect
Eicosanoid
qPCR
Transcript cloning
RNAi
Gene knockdown

ABSTRACT

Background: Ureases are multifunctional enzymes that display biological activities independent of their enzymatic function, including exocytosis induction and insecticidal effects. The hemipteran *Rhodnius prolixus* is one of the known susceptible models for this toxicity. It has been shown that Jack bean urease (JBU) has deleterious effects on *R. prolixus*, and these effects are modulated by eicosanoids, which are synthesized in a cascade involving phospholipase A_2 (PLA_2) enzymes.
Methods: R. prolixus genome was screened for putative PLA_2s and matching transcripts were cloned. Predicted amino acid sequences were analyzed and transcript distribution among tissues was determined by qPCR. RNAi techniques were used and subsequent JBU toxicity assays were performed.
Results: Two PLA_2 genes were identified, *Rhopr-PLA2III* and *Rhopr-PLA2XII*. The transcripts are widely distributed in the tissues but at different levels. The analyses fit the putative proteins into groups III and XII of secretory PLA_2s. After 70% of *Rhopr-PLA2XII* expression was knocked down, JBU's toxicity was decreased by more than 50% on 5th instars *R. prolixus*.
Conclusions: Rhopr-PLA2XII gene is linked to JBU's toxic effect in *R. prolixus* and our findings support previous studies demonstrating that eicosanoids modulate this toxicity.
General significance: Besides identifying and characterizing two PLA_2 genes in the major Chagas' disease vector *R. prolixus*, we have shown that the potent toxicity of JBU is linked to one of these genes. Our results contribute to the general comprehension of urease's mechanisms of action in insects, and, potentially, to studies on the control of the Chagas' disease parasite transmission.

1. Introduction

Ureases are metallo enzymes that catalyze urea hydrolysis and are synthesized by plants, fungi and bacteria [12,28]. These enzymes have other biological properties that are independent from their catalytic function, such as entomotoxic activity and exocytosis induction [18,19,44]. Urease isoforms isolated from the seeds of the legume *Canavalia ensiformis* display strong insecticidal effects, partly due to the processing of urease and release of internal peptides inside the insects' gut. Nymphs of the hemipterans *Rhodnius prolixus*, *Dysdercus peruvianus* and *Oncopeltus fasciatus* are examples of susceptible insects [11,14,38]. It was recently demonstrated in nymphs of *R. prolixus* that within hours after feeding on a urease solution, intact molecules are detected in the hemolymph, and when urease is directly injected into the hemolymph it displays insecticidal effects [46]. These findings indicate that` urease's entomotoxic activity is also due to actions of the intact molecule. When tested *ex vivo* on individual *R. prolixus* tissues, urease interferes with different cell signaling pathways and these effects are modulated by eicosanoids [45,46]. The same happens in different mammalian models, where plant and bacterial ureases induce exocytosis modulated by eicosanoids [3,21,40,52,53].

Phospholipases A_2 (PLA_2s; EC 3.1.1.4) are enzymes on the beginning of the eicosanoid biosynthetic pathway, where they catalyze the hydrolysis of the fatty acid ester at the *sn*−2 position of glycerophospholipids, releasing both unsaturated fatty acids and lysophospholipids [7,8]. These enzymes are remarkably diverse and are found in viruses, bacteria, plants and animals. They are classified into 18 different groups and several subgroups based on their sequence homology and biochemical characteristics [7,8]. Arachidonic acid, like other polyunsaturated fatty acids with 20 carbon chains, is released by PLA_2 hydrolysis reaction and it can be subsequently oxygenated by three different enzymes:

* Corresponding author at: Av. Bento Gonçalves, 9500 Building 43.431 Rooms 110/114 Porto Alegre, RS 91501-970, Brazil. Tel.: +55 51 3308 7606; fax: +55 51 3308 7600.
E-mail addresses: marina.defferrari@ufrgs.br (M.S. Defferrari), dohee.lee@utoronto.ca (D.H. Lee), claudia.lemelle@gmail.com (C.L. Fernandes), ian.orchard@utoronto.ca (I. Orchard), carlini@ufrgs.br, celia.carlini@pq.cnpq.br (C.R. Carlini).
[1] PI in Canada.
[2] PI at home institution.
[3] http://www.ufrgs.br/laprotox.

0304-4165/$ – see front matter © 2013 Elsevier B.V. All rights reserved.
http://dx.doi.org/10.1016/j.bbagen.2013.09.016

cyclooxygenase (yielding prostaglandins), lipoxygenase, or cytochrome P 450 — 'epoxygenase'. Most work on insect systems has focused on the prostaglandins, which act as central mediators of the insects' immune response, particularly in cellular reactions [48]. In insects PLA_2s also act in digestion, reproduction and general metabolism [47]. Previous studies characterized the genes encoding PLA_2s in *Drosophila melanogaster* [41], in the bumblebee *Bombus ignitus* [54] and in *Tribolium castaneum* [43].

Rhodnius prolixus is a major vector of human Chagas' disease, a chronic parasitic disease caused by the protozoan *Trypanosoma cruzi*. It is endemic in all Latin American countries, where approximately 100 million people are at risk and 16 million people are estimated to be infected [13,15]. *Rhodnius prolixus* feeds exclusively on vertebrate blood, ingesting up to ten times its own body mass per meal. After ingestion, it must rapidly eliminate large volumes of salts and water, defecating on the host's skin and thereby transmitting the parasite [2,34]. Phospholipids and lysophospholipids (products of PLA_2 hydrolysis) have been shown to be present in the saliva of *R. prolixus*, where lysophosphatidylcholine acts as an antihemostatic molecule facilitating the feeding process [20]. The activity of PLA_2s has also been detected in *R. prolixus* hemolymph and hemocytes, where PLA_2s play roles in cellular immune reactions [16,17]. More recently, it was demonstrated that the lysophosphatidylcholine present in saliva modulates the transmission and infection of *T. cruzi*, along with being present in the feces of *R. prolixus* [27].

Although urease toxicity is modulated by eicosanoids both in insects and in mammals, the oxygenation pathway of arachidonic acid seems to be different in each case. In *R. prolixus* the effect is modulated by prostaglandins, products of cyclooxygenase [46], while in different mammal models the effects are modulated by lipoxygenase products [3,53]. Considering that the common step for both cases is the release of arachidonic acid by PLA_2s, we have investigated the connection between urease toxicity and a PLA_2 gene in the well known model *R. prolixus*.

Here we have identified two PLA_2 genes from *R. prolixus* and cloned the complete coding sequence of the two transcripts. After isolating and identifying the transcripts we have analyzed their expression profiles in different tissues by real time qPCR. We have phylogenetically compared the two *R. prolixus* PLA_2 sequences with other PLA_2 sequences from vertebrates and invertebrates available through GenBank. Also, we have inferred some of the properties of the proteins, which suggest that they are both secretory PLA_2s but possibly with distinct functions. Based on function predictions for the two PLA_2s and their distribution among tissues, we have chosen to knockdown the *Rhopr-PLA2XII* transcript in order to study effects on urease toxicity. We have tested urease on knockdown insects and observed a significant decrease in mortality when compared to control insects, suggesting that in *R. prolixus* urease toxicity is linked to *Rhopr-PLA2XII* gene.

2. Methods

2.1. Screening of the predicted peptidome and the transcriptome of R. prolixus for the identification of putative PLA_2s

In order to identify putative PLA_2s present in *R. prolixus*, the predicted peptidome (available at rprolixus.vectorbase.org/GetData/Downloads/) was screened using the search tool in the program Geneious Basic [25]. The PLA_2 conserved pattern present in all known functional PLA_2s, and characterized by the sequence C-C-{P}-x-H-{LGY}-x-C (accordingly to the online tool PROSITE, prosite.expasy.org, x means any residue, {} means any residue but the ones indicated and the histidine indicates the active site), was used as a reference for the search. After the identification of putative amino acid sequences, the relative mRNA sequences were used to design primers and clone the transcripts.

2.2. Identification of PLA_2 cDNA sequences from 5th instar R. prolixus CNS cDNA library

For the identification of the previously predicted PLA_2 cDNA sequences, a cDNA library from the CNS of 5th instar *R. prolixus* [36] was screened using a modified amplification of cDNA ends (RACE) PCR as outlined below. Gene-specific primers (GSPs) were designed based on two predicted PLA_2 mRNA sequences (Table S1). For the 3′ RACE PCR, GSPs were used successively combined with the cDNA library plasmid reverse primers (Table S1) in a semi-nested PCR approach, which was used to increase the specificity of the amplified products. Next, 5′ RACE GSPs (Table S1) were used successively combined with the cDNA library plasmid forward primers (Table S1), also in a semi-nested approach. After the first round of PCRs was completed, the products were column purified (Biobasic, Markham, ON, Canada) and used as a template for the second semi-nested PCRs. The conditions of all reactions were 3 min initial denaturation at 94 °C, 35 cycles of denaturation for 30 s at 94 °C, annealing for 30 s at 59–60 °C, extension for 1 min at 72 °C, and a final extension for 10 min at 72 °C. The final amplified PCR products were run on 1.5% agarose gels stained with ethidium bromide, and the desired bands were extracted. The amplified fragments extracted from the gels were column purified and cloned using the pGEM-T Easy Vector system, according to the manufacturer instructions (Promega, Madison, WI, USA). The clones expressing the desired products were submitted to column purification and the PLA_2 nucleotide sequences were determined at the Centre for Applied Genomics, at the Hospital for Sick Children in Toronto (MaRS Centre, Toronto, ON, Canada). Sequences were confirmed from at least three independent clones to ensure base accuracy.

2.3. Isolation of the complete PLA_2 ORF nucleotide sequences from 5th instar R. prolixus CNS cDNA library

In order to isolate the complete PLA_2 open reading frame (ORF) nucleotide sequences, the cDNA library from the CNS of 5th instar *R. prolixus* [36] was used as template for PCRs with GSPs (Table S2) designed from the sequences obtained with RACE PCRs. The conditions of all reactions were 3 min initial denaturation at 94 °C, 35 cycles of denaturation for 30 s at 94 °C, annealing for 30 s at 60–61 °C, extension for 1 min at 72 °C, and a final extension for 10 min at 72 °C. The final amplified PCR products were run on 1.5% agarose gels, stained with ethidium bromide, and the desired bands were extracted. The amplified fragments extracted from the gels were column purified and cloned using the pGEM-T Easy Vector system, according to the manufacturer instructions (Promega, Madison, WI, USA). The clones expressing the desired products were submitted to column purification and the PLA_2 nucleotide sequences were determined at the Centre for Applied Genomics, at the Hospital for Sick Children in Toronto (MaRS Centre, Toronto, ON, Canada). Sequences were confirmed from at least three independent clones to ensure base accuracy.

2.4. Prediction of PLA_2 gene structure and sequence analyses

The predictions of location and size of introns in the identified PLA_2 genes were performed using the nucleotide sequences in a local BLASTN search against the *R. prolixus* genome assembly database with Geneious Basic [25]. After selecting the high scoring hits, the PLA_2 cDNA sequences were compared to the assembled genomic sequences to predict the location and size of exons/introns. The sequences were analyzed for potential signal peptides using the SignalP 4.0 server (www.cbs.dtu.dk/services/SignalP) and TargetP 1.1 server (www.cbs.dtu.dk/services/TargetP), and the membrane topologies were predicted using the TMHMM Server v. 2.0 189 (http://www.cbs.dtu.dk/services/TMHMM/).

2.5. Phylogenetic analysis of PLA_2 proteins

The predicted protein sequences of Rhopr-PLA2III (JQ670894) and Rhopr-PLA2XII (KC896626), along with other arthropod and chordate PLA_2s (*Triatoma matogrossensis*, gi|307095164; *Anasa tristis*, gi|391226623; *T. castaneum*, gi|225543488; *Acyrthosiphon pisum*, gi|326368257; *Phlebotomus arabicus*, gi|242554316; *Drosophila virilis*, gi|195396407; *Drosophila erecta*, gi|194895667; *D. melanogaster*, gi|24641677; *Megachile rotundata*, gi|383849880; *Bombus impatiens*, gi|350406620; *Bombus terrestris*, gi|340721396; *B. terrestris*, gi|340725190; *Bombus lucorum*, gi|229890780; *Harpegnathos saltator*, gi|307198397; *Acromyrmex echinatior*, gi|332029748; *Glossina morsitans*, gi|289742203; *Camponotus floridanus*, gi|307187781; *A. echinatior*, gi|332031357; *Apis mellifera*, gi|328786047; *M. rotundata*, gi|383848342; *Apis florea*, gi|380021879; *Nasonia vitripennis*, gi|156542901; *Pediculus humanus corporis*, gi|242020505; *Branchiostoma belcheri*, gi|374675332; *Gallus gallus*, gi|50749318; *Salmo salar*, gi|209737974; *Sus scrofa*, gi|343183417; *Xenopus* (*Silurana*) *tropicalis*, gi|56118646; *Mus musculus*, gi|148680280; *Anolis carolinensis*, gi|327274146), were aligned using ClustalW [50], and the regions with conserved residues were used to construct the phylogenetic tree. In order to select the best-fit model of amino acid substitution for the data set, the Molecular Evolutionary Genetics Analysis 5 (MEGA5) [49] evaluation tool was employed, suggesting that the most appropriate model would be WAG + G. Two different phylogenetic trees were constructed with the WAG + G model, a maximum likelihood (ML) and a Bayesian inference. The ML trees were generated by MEGA5 with phylogeny test by bootstrap method with 1000 replications to calculate the consensus tree. In order to construct the Bayesian inference, the analyses were carried out with MrBayes [24] for 100,000 generations, sampling every 10 generations with a 'burn-in' of 25%. The obtained topologies were used to calculate the consensus tree, with the percentage of samples recovering any particular clade representing that clade's posterior probability.

2.6. Insects

Fifth instars *R. prolixus* were maintained at high relative humidity in incubators at 25 °C and were fed on defibrinated rabbit blood (Cedarlane Laboratories Inc., Burlington, ON, Canada). Tissues were dissected under nuclease-free phosphate-buffered saline (PBS) (Sigma-Aldrich, Oakville, ON, Canada) and stored at −20 °C in RNAlater™ RNA stabilization reagent (Qiagen Inc., Mississauga, ON, Canada) until use for RNA isolation. Hemolymph samples were carefully collected from a cut leg with a 10 μl micropipette and immediately added to RNA extraction TRIzol Reagent (Invitrogen, Burlington, ON, Canada).

2.7. Quantitative tissue-specific expression analysis by real time qPCR

Quantitative expression profiles were conducted with starved fifth instars (3–4 weeks after feeding as fourth instars). Tissues were dissected as described above and pooled into eleven different groups: (1) central nervous system — CNS, (2) salivary glands, (3) foregut, (4) anterior midgut, (5) posterior midgut, (6) hindgut, (7) Malpighian tubules, (8) fat bodies and trachea, (9) immature testes, (10) immature ovaries and (11) hemocytes. Total RNA was isolated from the tissues with TRIzol Reagent (Invitrogen, Burlington, ON, Canada), according to the manufacturer's protocol, and quantified using a NanoDrop System (ND-1000, Thermo Scientific). cDNA was synthesized with 100 ng of RNA from each tissue using the cDNA iScript Reverse Transcription Supermix (Bio-Rad, Mississauga, ON, Canada) following the manufacturer recommendations. The cDNA synthesis reactions were diluted to the appropriate concentrations with nuclease-free water and 5 ng of cDNA per well was used as template for real time qPCR reactions. Primers for the amplification of *Rhopr-PLA2III* and *Rhopr-PLA2XII* (Table S2) were optimized to amplify target fragments of similar size across all experimental and reference genes (rp49, β-actin and α-tubulin) [35]. All qPCR reactions were carried out on a CFX384 Touch™ Real-Time PCR Detection System (Bio-Rad, Mississauga, ON, Canada) with reaction parameters as follows: initial denaturation at 95 °C for 30 s, followed by 40 cycles of denaturation for 5 s at 95 °C, annealing for 5 s at 59.5 °C, and extension for 5 s at 72 °C, with data acquisition during the extension step. To validate the specificity of the SYBR Green detected products, melting curve analyses along with gel electrophoresis were performed. The expression levels were quantified using the ΔΔCt method [37] and quantities were normalized to the reference genes. Experiments were repeated for a total of three biological replicates with three technical replicates each.

2.8. Rhopr-PLA2XII double-stranded RNA synthesis

Two fragments, of 653 and 589 nucleotides, from different but overlapping regions in the *Rhopr-PLA2XII* transcript were amplified by PCR from the *R. prolixus* CNS cDNA library [36] using gene specific primers (Table S3). The amplification of two distinct fragments from the same transcript was performed in order to use one of the fragments as a positive control for the gene expression knockdown. As previously validated in the lab, a fragment of the ampicillin resistance gene (ARG) from the pGEM-T Easy Vector system (Promega, Madison, WI, USA) was amplified by PCR with specific primers (Table S3) and used as a negative control throughout the experiment. After the first PCR amplification round, each reaction product was used as template for a PCR with gene specific primers conjugated with the T7 RNA polymerase promoter at the 5′ end (5′-TAATACGACTCACTATAGGGAGA-3′) (Table S3). All PCR amplification conditions were as follow: initial denaturation for 5 min at 94 °C, 35 cycles of 30 s at 94 °C, 30 s at 58 °C and 60 s at 72 °C, and final extension for 10 min at 72 °C. The resulting products of the second round of PCRs were used as templates for the double-stranded RNA (dsRNA) synthesis using the T7 Ribomax Express RNAi System (Promega, Madison, WI, USA). After synthesis the dsRNAs were precipitated with isopropanol and resuspended in nuclease-free water. Subsequently, the dsRNAs were quantified by a 260 nm wavelength using a NanoDrop System (ND-1000, Thermo Scientific) and the quality of products was verified by 1% agarose gel electrophoresis. The dsRNA products were stored at −80 °C in aliquots, which were independently thawed and diluted with nuclease-free water, to a 1 μg/μl concentration, immediately before use.

2.9. Injections of Rhopr-PLA2XII double-stranded RNA into unfed 5th instar R. prolixus and gene expression knockdown quantification

Injections of the two different *Rhopr-PLA2XII* dsRNAs and the ARG dsRNA were performed using a 10 μl volume capacity Hamilton Syringe (Hamilton Company, Reno, NV, USA) into the hemocoel of starved fifth instars (3–4 weeks after feeding as fourth instars) *R. prolixus*, where 1 μl of nuclease-free water containing 1 μg of dsRNA was injected per bug. The bugs were divided into 3 groups of 20 to 30 individuals each after injections: (1) dsRhopr-PLA2XII injected, (2) positive control dsRhopr-PLA2XII injected and (3) negative control dsARG injected. In order to quantify *Rhopr-PLA2XII* gene expression knockdown, different tissues of bugs from each of the three groups were dissected every day, from day 1 to day 5 after injections. Tissue dissection, RNA extraction and quantitative qPCR were performed as described above, using gene specific primers for *Rhopr-PLA2XII* (Table S2) and reference genes for normalizing expression (rp49, β-actin and α-tubulin) [35]. The *Rhopr-PLA2XII* transcript expression knockdown in dsRhopr-PLA2XII injected bugs, and in positive control dsRhopr-PLA2XII injected bugs, was quantified relatively to the expression of the transcript in dsARG

injected bugs. The expression knockdown screening was repeated to a total of three biological replicates.

2.10. Rhodnius prolixus saline and Jack bean urease

Rhodnius prolixus saline was prepared as follows: NaCl 150 mM, KCl 8.6 mM, $CaCl_2$ 2.0 mM, $MgCl_2$ 8.5 mM, $NaHCO_3$ 4.0 mM, glucose 34.0 mM, HEPES 5.0 mM, and pH 7.0 [26]. Crystalline Jack bean urease type III (JBU) was obtained from Sigma-Aldrich (Mississauga, ON, Canada) and diluted into *R. prolixus* saline to the appropriate concentrations.

2.11. Injections of JBU into Rhopr-PLA2XII knockdown 5th instars R. prolixus

Two days after the injections of 5th instars *R. prolixus* with dsRhopr-PLA2XII and dsARG, 20 to 25 bugs from each group were injected into the hemocoel with JBU diluted in *R. prolixus* saline to a final dose of 0.14 μg per mg of insect. Experiments were repeated for a total of three biological replicates. A negative control group was injected solely with saline along with each toxicity experiment to ensure that the injections were not killing the insects.

2.12. Statistical analysis

Results are expressed as mean ± standard error. Significance of differences between means was determined using one-way ANOVA followed by Holm–Sidack method (SigmaPlot software), and results were considered statistically different when $P < 0.001$.

3. Results

3.1. Identification, cloning and characterization of two PLA_2 transcripts from 5th instars R. prolixus

Based on predicted features of the two identified PLA_2 transcripts, we have named the genes *Rhopr-PLA2III* and *Rhopr-PLA2XII*, because they match with secretory PLA_2s from groups III and XII, respectively. We have cloned and sequenced 862 base pairs of *Rhopr-PLA2III* cDNA, where the coding sequence starts at base 55 and ends at base 768, yielding a protein of 238 amino acids (Fig. 1A). When comparing the cloned cDNA sequence with the genome assembly of *R. prolixus*, using a local BLASTN search on Geneious Basic [25], the corresponding gene exhibited 4 exons and 3 introns, ranging at least 12 kb of the whole

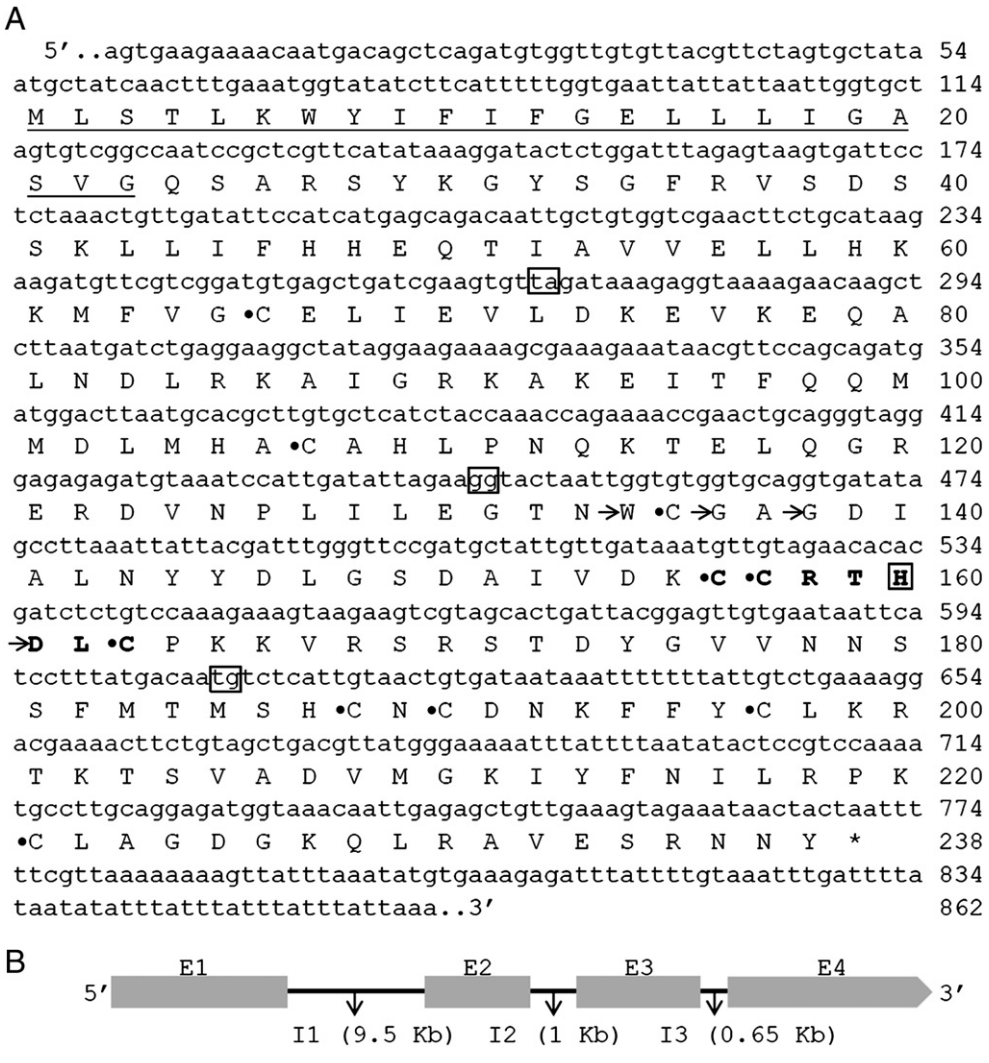

Fig. 1. Nucleotide sequence and predicted structure of *Rhopr-PLA2III* gene in *R. prolixus*. (A) Nucleotide sequence of *Rhopr-PLA2III* and deduced amino acid sequence of the protein. The numbering for each sequence is shown at right. The underlined region from residues 1 to 23 indicates the signal peptide. The characters highlighted in bold indicate the PLA_2 consensus pattern with the histidine residue on the active site inside the box. The dots indicate 10 cysteine residues that form 5 disulfide bonds and the arrows indicate the Ca^{2+} binding loop residues, both characteristic features to the group III sPLA_2s in arthropods. The nucleotides in squares indicate exon–exon boundaries. (B) Schematic diagram of predicted structure of the *Rhopr-PLA2III* gene, with exons and introns represented as boxes and lines, respectively.

genome (Fig. 1B). The putative protein has a signal peptide predicted with the cleavage site between residues 23 and 24, according to SignalP v4.1. The online tool TargetP 1.1 also predicted a signal peptide for the sequence, along with indicating that the protein is secreted to the extracellular environment. According to TMHMM Server v. 2.0, residues 1 to 6 stay inside the cell, residues 7 to 26 comprise a transmembrane helix and residues 27 to 238 are outside the cell, reaffirming the presence of a signal peptide in the N-terminal region of the protein. The putative Rhopr-PLA2III protein has the conserved catalytic histidine residue inside the PLA_2 signature, defined by the residues 156–163 (C-C-R-T-**H**-D-L-C). As specific features for the group III of $sPLA_2$s, Rhopr-PLA2III has 10 cysteine residues that are likely to form 5 disulfide bonds in the mature enzyme, and the conserved Ca^{2+}-binding loop with tryptophan, glycine and aspartic acid residues, respectively, in positions 134, 136, 138 and 161 [32] (Fig. 1A).

For *Rhopr-PLA2XII* we have cloned and sequenced a length of 1016 base pairs of the cDNA, with the coding sequence ranging from base 114 to base 716 and resulting in a 201 amino acid protein (Fig. 2A). After performing a local BLASTN search with the sequenced transcript on Geneious Basic [25], against the genome assembly of *R. prolixus*, it was demonstrated that the correspondent gene has an estimated size of at least 1.2 kb and is composed of 4 exons and 3 introns (Fig. 2B). According to the online tool SignalP v4.1, the putative protein does not have a signal peptide; however, the online tool TargetP 1.1 predicts a signal peptide with a very low score, suggesting that the protein could be secreted. The TMHMM Server v. 2.0 predicts that residues 1 to 6 remain inside the cell, residues 7 to 29 comprise a transmembrane helix and residues 30 to 201 are outside the cell, along with suggesting that there is the possibility of a signal peptide in the N-terminal region of the protein. Again though, this prediction has low scores. The putative Rhopr-PLA2XII protein shows the consensus sequence present in the invertebrate group XII PLA_2 functional domain, with conserved cysteines, asparagine, histidine and aspartic acid in the histidine-catalytic site, denoted by residues 114–121 (**C**-**C**-**N**-E-**H**-**D**-I-**C**). For the Ca^{2+} binding site, Rhopr-PLA2XII has the conserved glycine (residue 95) and the aspartic acid residue in the HD dyad inside the catalytic site, like other invertebrate group XII PLA_2s [31]. Also, as another conserved feature of group XII PLA_2s, the protein has 14 cysteine residues that will form 7 disulfide bonds [7] (Fig. 2A).

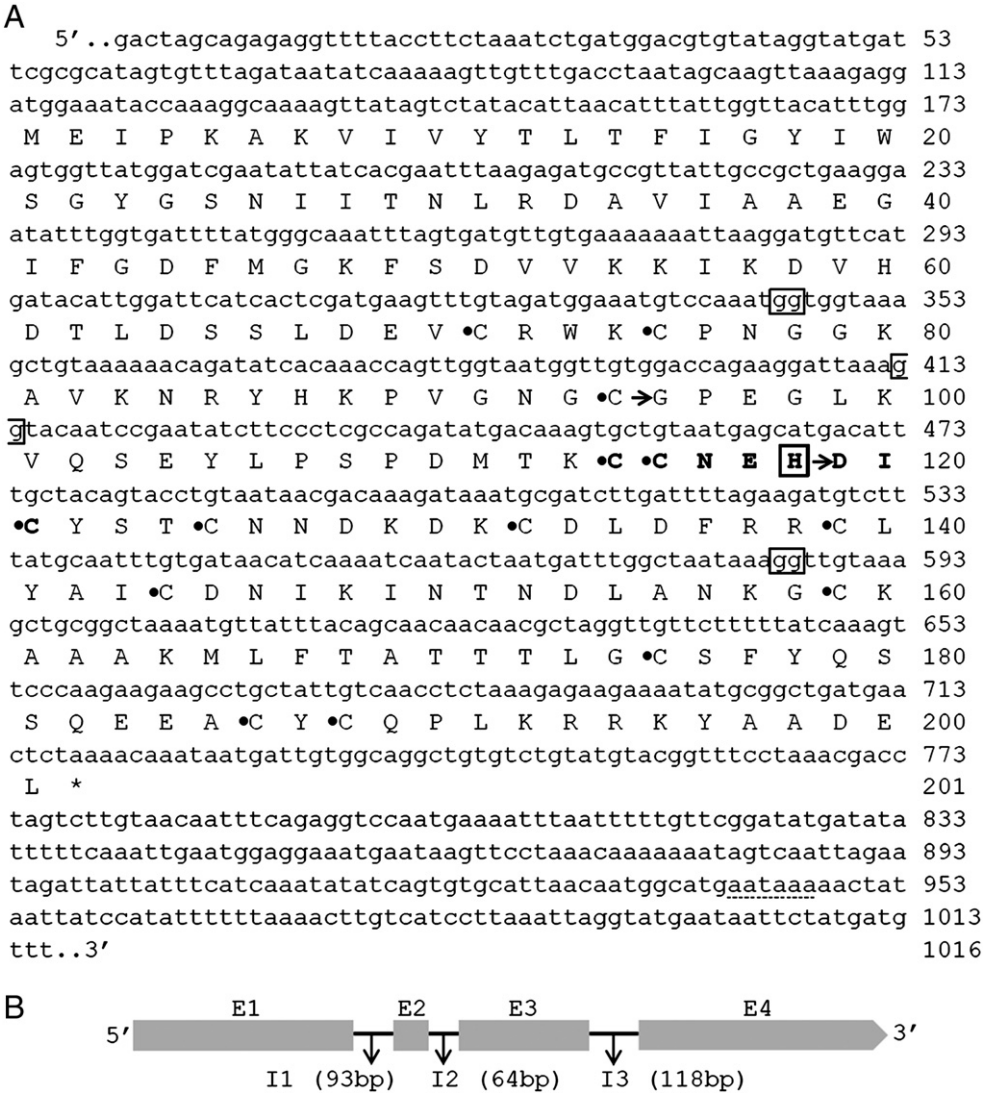

Fig. 2. Nucleotide sequence and predicted structure of *Rhopr-PLA2XII* gene in *R. prolixus*. (A) Nucleotide sequence of *Rhopr-PLA2XII* and deduced amino acid sequence of the protein. The numbering for each sequence is shown at right. The characters highlighted in bold indicate the PLA_2 consensus pattern with the histidine residue on the active site inside the box. The dots indicate 14 cysteine residues forming 7 disulfide bonds and the arrows indicate the Ca^{2+} binding loop residues that are conserved in group XII $sPLA_2$s. The nucleotides in squares indicate exon–exon boundaries. (B) Schematic diagram of predicted structure of the *Rhopr-PLA2XII* gene, with exons and introns represented as boxes and lines, respectively.

3.2. Characterization of Rhopr-PLA2III and Rhopr-PLA2XII expression profiles in unfed 5th instars

The spatial distribution pattern of *Rhopr-PLA2III* and *Rhopr-PLA2XII* was investigated using qPCR. *Rhopr-PLA2III* transcript is observed in most tissues with relatively low expression levels, except for the CNS, the salivary glands and the hindgut where it is highly expressed (Fig. 3). *Rhopr-PLA2XII* transcript is expressed in all tissues examined with similar abundant levels. The highest expression, observed in the salivary glands and in the immature testis, is only 3 fold higher than the lowest, observed in the anterior midgut and in the hemocytes (Fig. 4). In order to compare the expression of both transcripts, we quantified *Rhopr-PLA2XII* relative to *Rhopr-PLA2III*, where we observed that in all tissues scanned, except for the hindgut, *Rhopr-PLA2XII* has a higher expression rate. The anterior midgut has the biggest difference between the two transcripts, with *Rhopr-PLA2XII* being expressed almost 120 fold higher than *Rhopr-PLA2III* (Fig. 5).

3.3. Phylogenetic analyses of PLA_2s

The alignments of the PLA_2 sequences were performed with ClustalW and the conservative region around the active site was used to construct the phylogenies (Fig. 6). Two types of phylogenetic trees were constructed, a Bayesian inference and a maximum likelihood (ML). The Bayesian inference was used to generate trees and measure nodal support for the relationship among sampled sequences. The analyses were carried out with MrBayes for 1,000,000 generations, sampling every 10 generations, with a 'burn-in' of 25%. The obtained topologies were used to calculate the consensus tree, with the percentage of samples recovering any particular clade representing that clade's posterior probability (Fig. 7). The ML trees were generated with MEGA5 using phylogeny test by bootstrap method and 1000 replications to calculated the consensus tree (Fig. S1). The two PLA_2s from *R. prolixus* group separately into two distinct branches. As expected, Rhopr-PLA2XII grouped with other arthropod's group XII PLA_2s, while Rhopr-PLA2III grouped with a different set of sequences, where some of them have already been identified as possible group III $sPLA_2$s, like *T. castaneum* PLA_2 [43] and *H. saltator* PLA_2 [5].

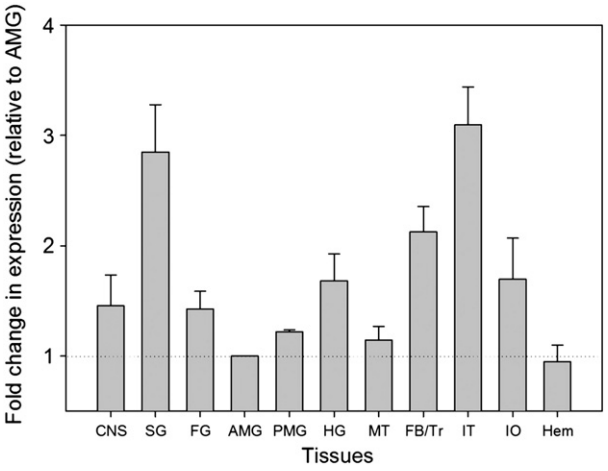

Fig. 4. Expression pattern of *Rhopr-PLA2XII* in various tissues of 5th instar *R. prolixus*. Tissues were dissected from at least 10 insects and pooled together into different categories: CNS — central nervous system, SG — salivary glands, FG — foregut, AMG — anterior midgut, PMG — posterior midgut, HG — hindgut, MT — Malpighian tubules, FB/Tr — fat body and trachea, IT — immature testes, IO — immature ovaries and Hem — hemocytes. The expression was quantified by qPCR and fold difference is relative to the anterior midgut (AMG), which is the tissue with lowest expression levels for *Rhopr-PLA2XII* transcript. Results are shown as means of 3 biological replicates with standard error.

3.4. Knockdown of Rhopr-PLA2XII expression in 5th instars and influence on urease toxicity

Based on what is known about urease toxic activity in *R. prolixus* [45,46] and the observed characteristics and distribution of both PLA_2 transcripts described here, we decided to investigate the involvement of the toxin with *Rhopr-PLA2XII* gene. We have tested the influence of Jack bean urease (JBU) on the expression of the transcript, where we observed that it does not alter transcript expression following injection with JBU (data not shown). In order to further investigate the connection of JBU toxicity with *Rhopr-PLA2XII* we used RNA interference to silence the expression. *Rhopr-PLA2XII* transcript in the knockdowns was always quantified relative to the expression of the transcript in the bugs injected with ARG dsRNA. We quantified

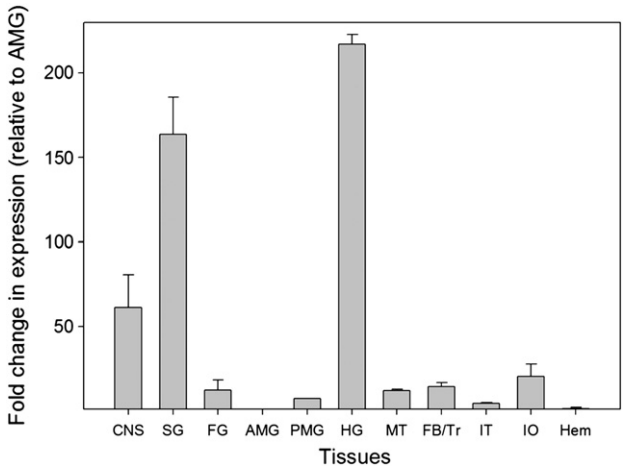

Fig. 3. Expression pattern of *Rhopr-PLA2III* in various tissues of 5th instar *R. prolixus*. Tissues were dissected from at least 10 insects and pooled together into different categories: CNS — central nervous system, SG — salivary glands, FG — foregut, AMG — anterior midgut, PMG — posterior midgut, HG — hindgut, MT — Malpighian tubules, FB/Tr — fat body and trachea, IT — immature testes, IO — immature ovaries and Hem — hemocytes. The expression was quantified by qPCR and fold difference is relative to the anterior midgut (AMG), which is the tissue with lowest expression levels for *Rhopr-PLA2III* transcript. Results are shown as means of 3 biological replicates with standard error.

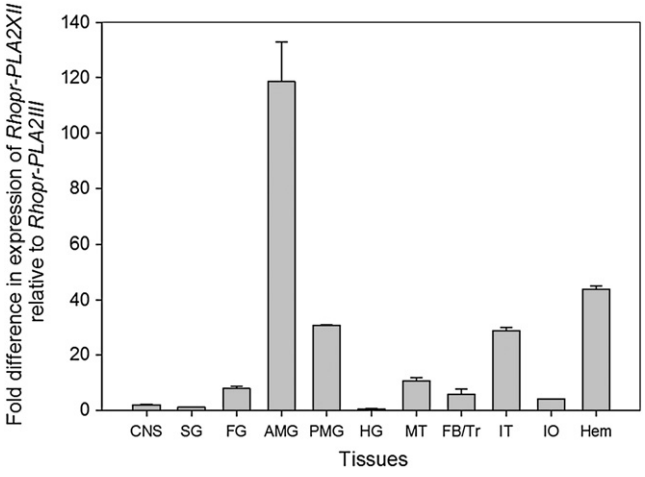

Fig. 5. Expression pattern of *Rhopr-PLA2XII* relative to *Rhopr-PLA2III* in various tissues of 5th instar *R. prolixus*. Tissues were dissected from at least 10 insects and pooled together into different categories: CNS — central nervous system, SG — salivary glands, FG — foregut, AMG — anterior midgut, PMG — posterior midgut, HG — hindgut, MT — Malpighian tubules, FB/Tr — fat body and trachea, IT — immature testes, IO — immature ovaries and Hem — hemocytes. The expression was quantified by qPCR and fold difference in *Rhopr-PLA2XII* transcript expression is relative to the expression *Rhopr-PLA2III* in the indicated tissues. Results are shown as means of 3 biological replicates with standard error.

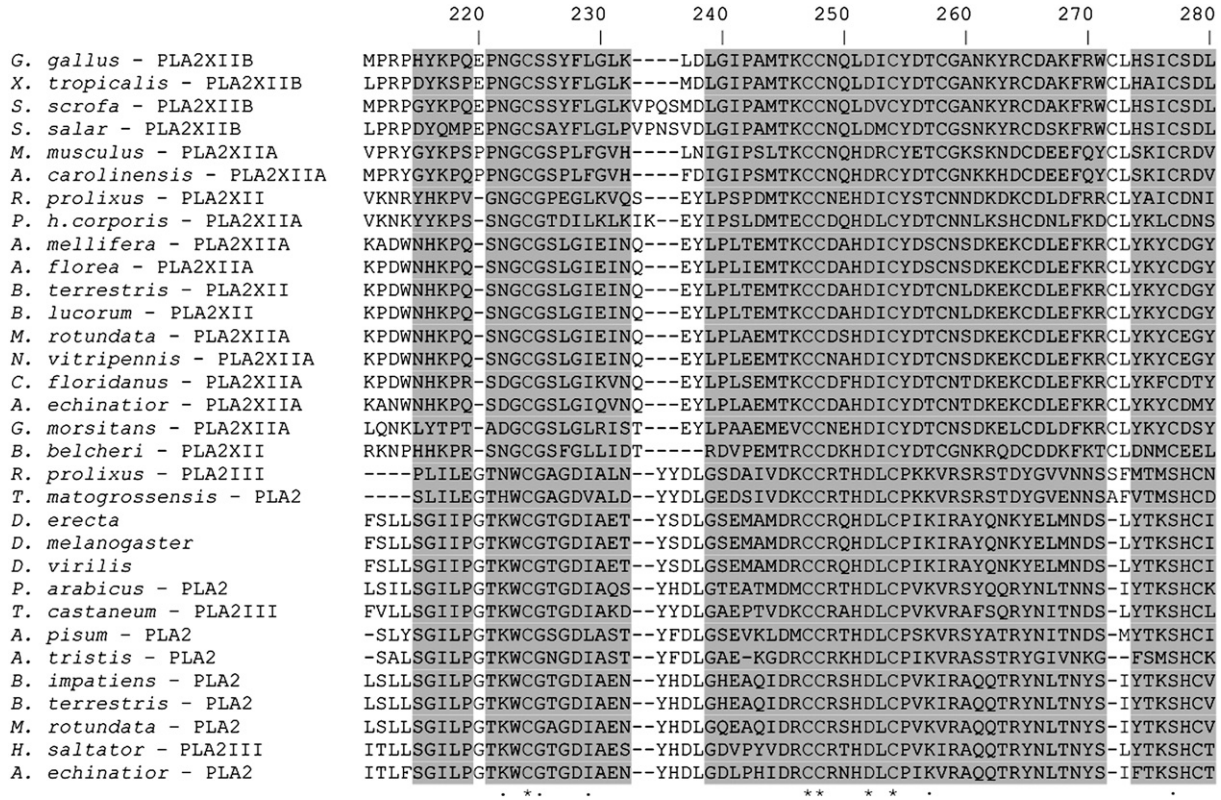

Fig. 6. Alignment of different PLA_2 sequences from arthropods and chordates. ClustalW alignment of the sequences was used to construct the trees. The gray shadows represent the conservative region around the active site. "*" indicates highly conserved residues and "." indicates residues with similarity.

the knockdown of *Rhopr-PLA2XII* expression from 24 h up to 5 days after injection, and we observed an average reduction of 70% among tissues that was persistent throughout this period, with exception of the hemocytes, where we did not observe any reduction in expression. JBU toxicity was significantly reduced in *Rhopr-PLA2XII* knockdown insects when compared to insects that have normal expression of the transcript. 72 h after JBU injections, 90% of negative control bugs (ARG dsRNA injected) had died, in contrast to only 40% mortality in the *Rhopr-PLA2XII* knockdown group (Fig. 8).

4. Discussion

In the present work we have identified two genes encoding PLA_2s in *R. prolixus*, *Rhopr-PLA2III* and *Rhopr-PLA2XII*. We have cloned the two respective transcripts and inferred characteristics of the putative proteins, which, according to the predictions, are both secretory PLA_2s, but from different groups. The first gene, *Rhopr-PLA2III*, encodes a protein of 238 amino acids with several conserved features of group III PLA_2s, while the second gene, *Rhopr-PLA2XII*, encodes a 201 residue protein with characteristics of group XII PLA_2s. When phylogenetically compared to other PLA_2s, including representatives of groups III and XII, the sequences from *R. prolixus* group separately in the respective branches of each group, supporting the classification based on structural predictions. *Rhopr-PLA2III* is expressed in most tissues of 5th instars *R. prolixus* in relatively low levels, with exception of the central nervous system, the salivary glands and the hindgut, where expression is relatively high. On the other hand, the *Rhopr-PLA2XII* transcript is more highly expressed, and in similar levels, in all tissues scanned. When comparing the expression of the two transcripts we observed that in all tissues, except for the hindgut, *Rhopr-PLA2XII* has the highest levels, especially in the anterior midgut and in the hemocytes. The presence of PLA_2s was reported in the saliva and salivary glands of arthropods, including the caterpillar *Manduca sexta* [51] and the tick *Amblyomma americanum* [6], where they are involved in digestive processes. Also, PLA_2 transcripts were identified in the salivary glands of the sand fly *P. arabicus* [23], the mosquito *Anopheles funestus* [9] and the dipteran 'Tsetse' *G. morsitans* [1]. Rhopr-PLA2III has a strongly predicted signal peptide, suggesting that the mature enzyme could act in digestion of phospholipids outside the cell, such as inside the salivary glands. It was demonstrated that group III secretory PLA_2s efficiently hydrolyse high density phospholipids releasing lysophosphatidylcholine (lysoPC) [42]. Phospholipids and lysophospholipids are present in *R. prolixus* saliva, where they play antihemostatic roles during the feeding process [20]. LysoPC is one of the lysophospholipids present in *R. prolixus* saliva, acting as a modulator of *T. cruzi* infection to the vertebrate host [27]. The prominent presence of *Rhopr-PLA2III* transcript in the hindgut, along with cell signaling, could be related to the digestion of the remaining phospholipids in the blood meal, and once the parasite is transmitted with the feces, the parasite could be taking advantage of the availability of these products for the infection process. In the CNS, *Rhopr-PLA2III* is probably linked to the breakdown of phospholipids from cell membranes and to cell signaling, as already observed for $sPLA_2$s in vertebrate models [8,30].

In contrast to Rhopr-PLA2III, Rhopr-PLA2XII does not have a signal peptide predicted by the online tool SignalP; however other tools suggest, with a low score, that there could be a signal peptide present in the N-terminal region of the protein. Rhopr-PLA2XII could be associated with cell membranes, or even with organelle membranes as shown for a murine group XII PLA_2 that is associated with Golgi/endoplasmic reticulum membranes. It was suggested that this same group XII PLA_2 provides arachidonic acid to cyclooxygenase 2 for the generation of prostaglandins in cells of the immune system of murines [22]. The biosynthesis of eicosanoids seems to be dependent on the cellular location of the enzymes involved in the process, which apparently occurs in perinuclear locations [4]. Since there is considerable conservation within the group XII PLA_2 catalytic functional domains across evolution from

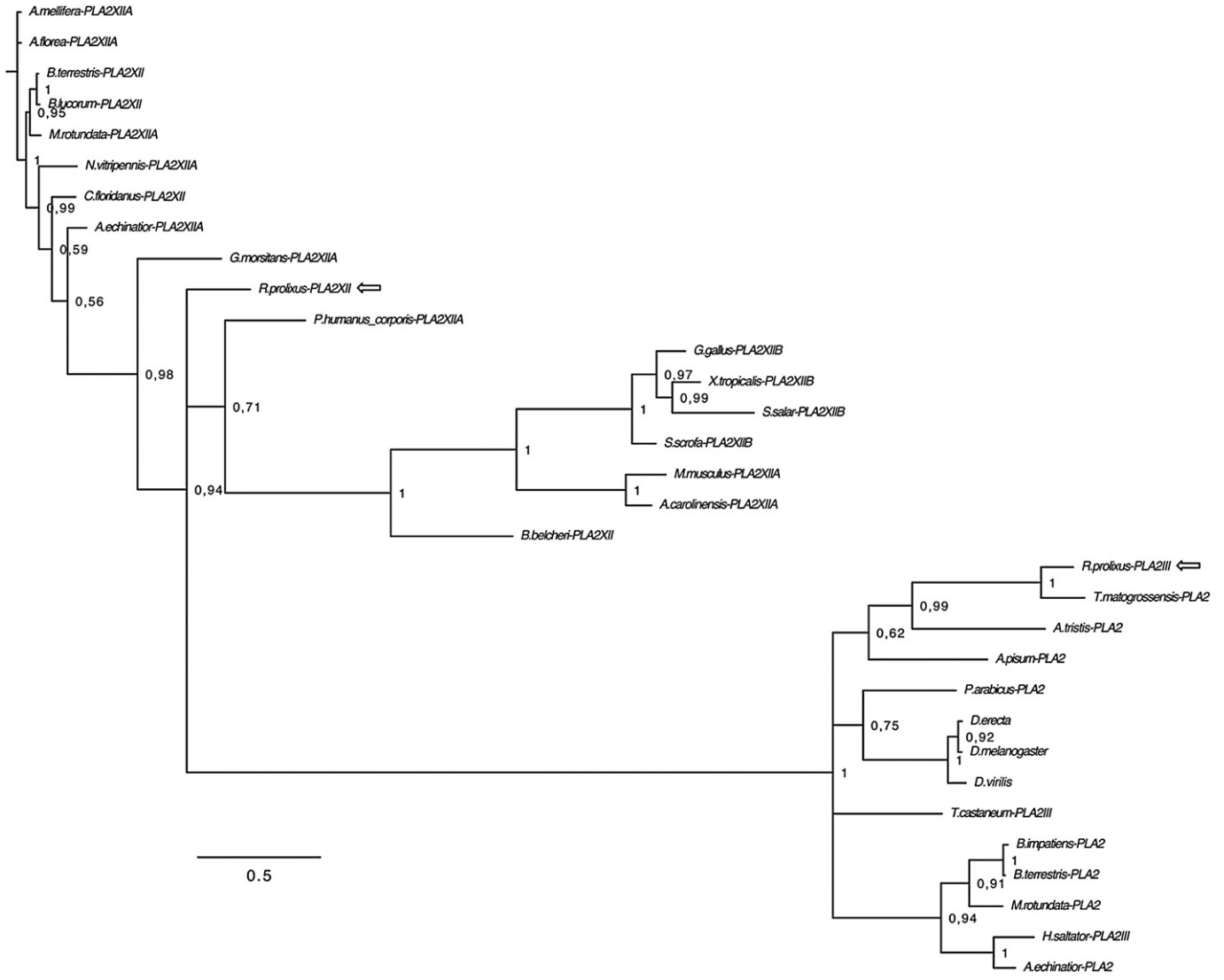

Fig. 7. Bayesian inference for phylogenetic analysis of different PLA_2 sequences from arthropods and chordates. Phylogenetic tree illustrating the relationships among 30 PLA_2s, Rhopr-PLA2III and Rhopr-PLA2XII, generated by the Bayesian inference using the WAG + G model. The analyses were carried out for 100,000 generations, sampling every 10 generations with a 'burn-in' of 25%. Rhopr-PLA2XII and Rhopr-PLA2III are indicated by arrows.

vertebrates to invertebrates [31], Rhopr-PLA2XII could also be an enzyme releasing arachidonic acid inside the cells for subsequent oxygenation and production of prostaglandins. The activity of PLA_2s, sometimes also along with presence of prostaglandins, has been detected in *R. prolixus* hemolymph and hemocytes, where they apparently play roles in cellular immune reactions. This activity has been identified in living insects as well as in isolated hemocytes [16,17], suggesting that the eicosanoid signaling for hemocyte functions can be locally produced in those cells. When Jack bean urease (JBU) was tested in preparations *ex vivo* on *R. prolixus* anterior midgut [46] and Malpighian tubules [45], it caused disturbing effects modulated by eicosanoids, indicating that these molecules can also be locally produced in those tissues.

Because of the relatively very low expression of *Rhopr-PLA2III* in the anterior midgut and other tissues, we have tested the influence of a JBU treatment on the expression of the gene, in order to check for a possible up-regulation after exposure to the toxin. 1, 6 and 18–20 h after injecting 5th instars *R. prolixus* with JBU, neither *Rhopr-PLA2III* nor *Rhopr-PLA2XII* expression levels changed in any tissues. These findings suggest that it is unlikely that *Rhopr-PLA2III* is linked to JBU's toxic activity, since the transcript is not significantly present in the anterior midgut (where JBU has a strong eicosanoid mediated effect), even when the insects are challenged with the toxin. The fact that *Rhopr-PLA2XII* does not have its expression altered is not enough to discard any linkage with JBU's toxicity, since the connection could be downstream with PLA_2 products.

To further investigate a possible interaction between *Rhopr-PLA2XII* presence and JBU's toxicity, we used RNA interference to knockdown the expression. The *Rhopr-PLA2XII* transcript was reduced by an average of 70% in the tissues throughout the 5 days of quantification. Subsequently we tested JBU on knockdown insects. Interestingly, JBU's toxicity was significantly decreased in knockdown insects, with more than 50% reduction in mortality when compared to those normally expressing the transcript. When 5th instars *R. prolixus* are injected into the hemolymph with 0.25 μg of JBU per mg of insect, a 96% mortality is observed 24 h after injection [46], but whether this lethal action was mediated by eicosanoids, as in isolated tissues, was unclear. With our results we can conclude that normal expression levels of *Rhopr-PLA2XII* are necessary for JBU's toxicity in living insects, and *Rhopr-PLA2XII* is likely to be responsible for the release of eicosanoids modulating this toxicity. We are not excluding the existence and involvement of more PLA_2s in the eicosanoid biosynthesis pathway in *R. prolixus*, and also we are not excluding the possibility that *Rhopr-PLA2III* produces

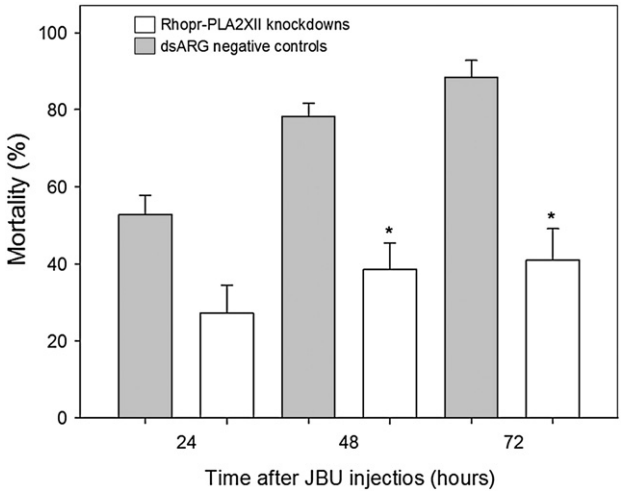

Fig. 8. Mortality of *Rhopr-PLA2XII* knockdown in 5th instar *R. prolixus* after JBU injections. Insects were injected into the hemocoel with 1 μl of nuclease-free water containing 1 μg of dsRhopr-PLA2XII or 1 μg of dsARG. 48 h after the dsRNA treatment, the same insects were injected with JBU to a final dose of 0.14 μg per mg of insect. Mortality was monitored for 72 h after JBU injections. Results are shown as means of 3 biological replicates with standard error. "*" indicates statistically significant difference.

eicosanoids in this insect. The fact that JBU's toxicity was not totally inhibited suggests that the cells that are still expressing *Rhopr-PLA2XII* could be sufficient to signal deleterious effects in *R. prolixus*. It is interesting to note that in the hemocytes we did not observe any reduction in expression, which could mean that those cells play a significant role in JBU's toxicity signaling. In order to better understand the interactions between *Rhopr-PLA2XII* and JBU, future experiments focusing on the PLA_2 protein and at the physiological level are necessary.

For the past 30 years ureases have been studied as potent toxins that display a variety of effects in different models, including fungi, insects and mammals [10,14,18,33,39]. Throughout the years many advances have been made in elucidating ureases' effects, such as the discovery of urease's internal insecticidal peptides, which led to the design of a recombinant peptide with high potential for biotechnological applications [29]. Other advances have been made in the fields of medically important organisms, as for example the bacterial urease from *Helicobacter pylori* that induces inflammation and exocytosis in different cell models modulated by eicosanoids [52,53]. The recent findings on the eicosanoid modulated toxic effects of JBU in *R. prolixus* opened the door for the present study, where, for the first time, an insect gene linked to urease's toxic effect was identified and characterized. Also, *Rhopr-PLA2III* and *Rhopr-PLA2XII* are the first phospholipase A2 genes to be identified and to have their transcripts cloned in a Chagas' disease vector, which may be helpful for future studies on the control of the transmission of the parasite *T. cruzi*.

Supplementary data to this article can be found online at http://dx.doi.org/10.1016/j.bbagen.2013.09.016.

Acknowledgements

This research was funded by the Brazilian agency CAPES-MEC (Coordenação de Aperfeiçoamento de Pessoal de Nível Superior), through the Edital de Toxinologia program and providing Marina S. Defferrari the scholarship for the interchange program to University of Toronto Mississauga, in the Sciences Without Borders program; by a Natural Sciences and Engineering Research Council of Canada grant to Dr. Ian Orchard; and by grants from the Brazilian agencies CNPq-MCT (Conselho Nacional de Desenvolvimento Científico e Tecnológico) and FAPERGS (Fundação de Amparo a Pesquisa do Estado do Rio Grande do Sul) to Dr. Celia R. Carlini. Thanks to Dr. Angela B. Lange for the support at University of Toronto Mississauga, and to Nikki Sarkar for maintaining the *R. prolixus* colony used in all experiments presented here.

References

[1] J. Alves-Silva, J.M. Ribeiro, J. Van Den Abbeele, G. Attardo, Z. Hao, L.R. Haines, M.B. Soares, M. Berriman, S. Aksoy, M.J. Lehane, An insight into the sialome of *Glossina morsitans morsitans*, BMC Genomics 11 (2010) 213.
[2] L.O. Andrade, N.W. Andrews, The *Trypanosoma cruzi*-host-cell interplay: location, invasion, retention, Nat. Rev. Microbiol. 3 (2005) 819–823.
[3] C. Barja-Fidalgo, J.A. Guimaraes, C.R. Carlini, Lipoxygenase-mediated secretory effect of canatoxin the toxic protein from *Canavalia ensiformis* seeds, Toxicon 29 (1991) 453–459.
[4] C.O. Bingham III, K.F. Austen, Phospholipase A_2 enzymes in eicosanoid generation, Proc. Assoc. Am. Physicians 111 (1999) 516–524.
[5] R. Bonasio, G. Zhang, C. Ye, N.S. Mutti, X. Fang, N. Qin, G. Donahue, P. Yang, Q. Li, C. Li, P. Zhang, Z. Huang, S.L. Berger, D. Reinberg, J. Wang, J. Liebig, Genomic comparison of the ants *Camponotus floridanus* and *Harpegnathos saltator*, Science 329 (2010) 1068–1071.
[6] A.S. Bowman, C.L. Gengler, M.R. Surdick, K. Zhu, R.C. Essenberg, J.R. Sauer, J.W. Dillwith, A novel phospholipase A_2 activity in saliva of the lone star tick, *Amblyomma americanum* (L.), Exp. Parasitol. 87 (1997) 121–132.
[7] J.E. Burke, E.A. Dennis, Phospholipase A_2 biochemistry, Cardiovasc. Drugs Ther. 23 (2009) 49–59.
[8] J.E. Burke, E.A. Dennis, Phospholipase A_2 structure/function, mechanism, and signaling, J. Lipid Res. 50 (2009) S237–S242(Suppl.).
[9] E. Calvo, A. Dao, V.M. Pham, J.M. Ribeiro, An insight into the sialome of *Anopheles funestus* reveals an emerging pattern in anopheline salivary protein families, Insect Biochem. Mol. Biol. 37 (2007) 164–175.
[10] C.R. Carlini, J.A. Guimaraes, Isolation and characterization of a toxic protein from *Canavalia ensiformis* (jack bean) seeds, distinct from concanavalin A, Toxicon 19 (1981) 667–675.
[11] C.R. Carlini, A.E. Oliveira, P. Azambuja, J. Xavier-Filho, M.A. Wells, Biological effects of canatoxin in different insect models: evidence for a proteolytic activation of the toxin by insect cathepsinlike enzymes, J. Econ. Entomol. 90 (1997) 340–348.
[12] E.L. Carter, N. Flugga, J.L. Boer, S.B. Mulrooney, R.P. Hausinger, Interplay of metal ions and urease, Metallomics 1 (2009) 207–221.
[13] J.R. Coura, A.C. Junqueira, M.N. Boia, O. Fernandes, C. Bonfante, J.E. Campos, L. Santos, R. Devera, Chagas disease in the Brazilian Amazon: IV. A new cross-sectional study, Rev. Inst. Med. Trop. Sao Paulo 44 (2002) 159–165.
[14] M.S. Defferrari, D.R. Demartini, T.B. Marcelino, P.M. Pinto, C.R. Carlini, Insecticidal effect of *Canavalia ensiformis* major urease on nymphs of the milkweed bug *Oncopeltus fasciatus* and characterization of digestive peptidases, Insect Biochem. Mol. Biol. 41 (2011) 388–399.
[15] J.C. Dias, A.C. Silveira, C.J. Schofield, The impact of Chagas disease control in Latin America: a review, Mem. Inst. Oswaldo Cruz 97 (2002) 603–612.
[16] M.B. Figueiredo, E.S. Garcia, P. Azambuja, Blockades of phospholipase A_2 and platelet-activating factor receptors reduce the hemocyte phagocytosis in *Rhodnius prolixus*: in vitro experiments, J. Insect Physiol. 54 (2008) 344–350.
[17] M.B. Figueiredo, F.A. Genta, E.S. Garcia, P. Azambuja, Lipid mediators and vector infection: *Trypanosoma rangeli* inhibits *Rhodnius prolixus* hemocyte phagocytosis by modulation of phospholipase A2 and PAF-acetylhydrolase activities, J. Insect Physiol. 54 (2008) 1528–1537.
[18] C. Follmer, G.B. Barcellos, R.B. Zingali, O.L. Machado, E.W. Alves, C. Barja-Fidalgo, J.A. Guimaraes, C.R. Carlini, Canatoxin, a toxic protein from jack beans (*Canavalia ensiformis*), is a variant form of urease (EC 3.5.1.5): biological effects of urease independent of its ureolytic activity, Biochem. J. 360 (2001) 217–224.
[19] C. Follmer, R. Real-Guerra, G.E. Wasserman, D. Olivera-Severo, C.R. Carlini, Jackbean, soybean and *Bacillus pasteurii* ureases: biological effects unrelated to ureolytic activity, Eur. J. Biochem. 271 (2004) 1357–1363.
[20] D.M. Golodne, R.Q. Monteiro, A.V. Graca-Souza, M.A. Silva-Neto, G.C. Atella, Lysophosphatidylcholine acts as an anti-hemostatic molecule in the saliva of the blood-sucking bug *Rhodnius prolixus*, J. Biol. Chem. 278 (2003) 27766–27771.
[21] D.M. Grassi-Kassisse, G. Ribeiro-DaSilva, Canatoxin triggers histamine secretion from rat peritoneal mast cells, Agents Actions 37 (1992) 204–209.
[22] I.C. Ho, J.P. Arm, C.O. Bingham III, A. Choi, K.F. Austen, L.H. Glimcher, A novel group of phospholipase A_2s preferentially expressed in type 2 helper T cells, J. Biol. Chem. 276 (2001) 18321–18326.
[23] J. Hostomska, V. Volfova, J. Mu, M. Garfield, I. Rohousova, P. Volf, J.G. Valenzuela, R.C. Jochim, Analysis of salivary transcripts and antigens of the sand fly *Phlebotomus arabicus*, BMC Genomics 10 (2009) 282.
[24] J.P. Huelsenbeck, F. Ronquist, MRBAYES: Bayesian inference of phylogenetic trees, Bioinformatics 17 (2001) 754–755.
[25] M. Kearse, R. Moir, A. Wilson, S. Stones-Havas, M. Cheung, S. Sturrock, S. Buxton, A. Cooper, S. Markowitz, C. Duran, T. Thierer, B. Ashton, P. Meintjes, A. Drummond, Geneious Basic: an integrated and extendable desktop software platform for the organization and analysis of sequence data, Bioinformatics 28 (2012) 1647–1649.
[26] N.J. Lane, R.A. Leslie, L.S. Swales, Insect peripheral nerves: accessibility of neurohemal regions to lanthanum, J. Cell Sci. 18 (1975) 179–197.
[27] R.D. Mesquita, A.B. Carneiro, A. Bafica, F. Gazos-Lopes, C.M. Takiya, T. Souto-Padron, D.P. Vieira, A. Ferreira-Pereira, I.C. Almeida, R.T. Figueiredo, B.N. Porto, M.T. Bozza, A.V. Graca-Souza, A.H. Lopes, G.C. Atella, M.A. Silva-Neto, *Trypanosoma cruzi*

infection is enhanced by vector saliva through immunosuppressant mechanisms mediated by lysophosphatidylcholine, Infect. Immun. 76 (2008) 5543–5552.
[28] H.L. Mobley, M.D. Island, R.P. Hausinger, Molecular biology of microbial ureases, Microbiol. Rev. 59 (1995) 451–480.
[29] F. Mulinari, F. Staniscuaski, L.R. Bertholdo-Vargas, M. Postal, O.B. Oliveira-Neto, D.J. Rigden, M.F. Grossi-de-Sa, C.R. Carlini, Jaburetox-2Ec: an insecticidal peptide derived from an isoform of urease from the plant *Canavalia ensiformis*, Peptides 28 (2007) 2042–2050.
[30] M. Murakami, Y. Taketomi, C. Girard, K. Yamamoto, G. Lambeau, Emerging roles of secreted phospholipase A2 enzymes: lessons from transgenic and knockout mice, Biochimie 92 (2010) 561–582.
[31] T.J. Nevalainen, J.C. Cardoso, Conservation of group XII phospholipase A_2 from bacteria to human, Comp. Biochem. Physiol. D Genomics Proteomics 7 (2012) 340–350.
[32] T.J. Nevalainen, J.C. Cardoso, P.T. Riikonen, Conserved domains and evolution of secreted phospholipases A_2, FEBS J. 279 (2012) 636–649.
[33] D. Olivera-Severo, G.E. Wassermann, C.R. Carlini, *Bacillus pasteurii* urease shares with plant ureases the ability to induce aggregation of blood platelets, Arch. Biochem. Biophys. 452 (2006) 149–155.
[34] I. Orchard, J.P. Paluzzi, Diuretic and antidiuretic hormones in the blood-gorging bug *Rhodnius prolixus*, Ann. N. Y. Acad. Sci. 1163 (2009) 501–503.
[35] J.P. Paluzzi, M.J. O'Donnell, Identification, spatial expression analysis and functional characterization of a pyrokinin-1 receptor in the Chagas' disease vector, *Rhodnius prolixus*, Mol. Cell. Endocrinol. 363 (2012) 36–45.
[36] J.P. Paluzzi, W.K. Russell, R.J. Nachman, I. Orchard, Isolation, cloning, and expression mapping of a gene encoding an antidiuretic hormone and other CAPA-related peptides in the disease vector, *Rhodnius prolixus*, Endocrinology 149 (2008) 4638–4646.
[37] M.W. Pfaffl, A new mathematical model for relative quantification in real-time RT-PCR, Nucleic Acids Res. 29 (2001) e45.
[38] A.R. Piovesan, F. Staniscuaski, J. Marco-Salvadori, R. Real-Guerra, M.S. Defferrari, C.R. Carlini, Stage-specific gut proteinases of the cotton stainer bug *Dysdercus peruvianus*: role in the release of entomotoxic peptides from *Canavalia ensiformis* urease, Insect Biochem. Mol. Biol. 38 (2008) 1023–1032.
[39] M. Postal, A.H. Martinelli, A.B. Becker-Ritt, R. Ligabue-Braun, D.R. Demartini, S.F. Ribeiro, G. Pasquali, V.M. Gomes, C.R. Carlini, Antifungal properties of *Canavalia ensiformis* urease and derived peptides, Peptides 38 (2012) 22–32.
[40] G. Ribeiro-DaSilva, J.F. Prado, Increased insulin circulating levels induced by canatoxin in rats, Toxicon 31 (1993) 1131–1136.
[41] Y. Ryu, Y. Oh, J. Yoon, W. Cho, K. Baek, Molecular characterization of a gene encoding the *Drosophila melanogaster* phospholipase A_2, Biochim. Biophys. Acta 1628 (2003) 206–210.
[42] H. Sato, R. Kato, Y. Isogai, G. Saka, M. Ohtsuki, Y. Taketomi, K. Yamamoto, K. Tsutsumi, J. Yamada, S. Masuda, Y. Ishikawa, T. Ishii, T. Kobayashi, K. Ikeda, R. Taguchi, S. Hatakeyama, S. Hara, I. Kudo, H. Itabe, M. Murakami, Analyses of group III secreted phospholipase A_2 transgenic mice reveal potential participation of this enzyme in plasma lipoprotein modification, macrophage foam cell formation, and atherosclerosis, J. Biol. Chem. 283 (2008) 33483–33497.
[43] S. Shrestha, Y. Park, D. Stanley, Y. Kim, Genes encoding phospholipases A_2 mediate insect nodulation reactions to bacterial challenge, J. Insect Physiol. 56 (2010) 324–332.
[44] F. Staniscuaski, C.R. Carlini, Plant ureases and related peptides: understanding their entomotoxic properties, Toxins (Basel) 4 (2012) 55–67.
[45] F. Staniscuaski, V. Te Brugge, C.R. Carlini, I. Orchard, Invitro effect of *Canavalia ensiformis* urease and the derived peptide Jaburetox-2Ec on *Rhodnius prolixus* Malpighian tubules, J. Insect Physiol. 55 (2009) 255–263.
[46] F. Staniscuaski, V Te Brugge, C.R. Carlini, I. Orchard, Jack bean urease alters serotonin-induced effects on *Rhodnius prolixus* anterior midgut, J. Insect Physiol. 56 (2010) 1078–1086.
[47] D. Stanley, The non-venom insect phospholipases A_2, Biochim. Biophys. Acta 1761 (2006) 1383–1390.
[48] D. Stanley, J. Miller, H. Tunaz, Eicosanoid actions in insect immunity, J. Innate Immun. 1 (2009) 282–290.
[49] K. Tamura, D. Peterson, N. Peterson, G. Stecher, M. Nei, S. Kumar, MEGA5: molecular evolutionary genetics analysis using maximum likelihood, evolutionary distance, and maximum parsimony methods, Mol. Biol. Evol. 28 (2011) 2731–2739.
[50] J.D. Thompson, D.G. Higgins, T.J. Gibson, CLUSTAL W: improving the sensitivity of progressive multiple sequence alignment through sequence weighting, position-specific gap penalties and weight matrix choice, Nucleic Acids Res. 22 (1994) 4673–4680.
[51] H. Tunaz, D.W. Stanley, Phospholipase A_2 in salivary glands isolated from tobacco hornworms, *Manduca sexta*, Comp. Biochem. Physiol. B Biochem. Mol. Biol. 139 (2004) 27–33.
[52] A.F. Uberti, D. Olivera-Severo, G.E. Wassermann, A. Scopel-Guerra, J.A. Moraes, P. Barcellos-de-Souza, C. Barja-Fidalgo, C.R. Carlini, Pro-inflammatory properties and neutrophil activation by *Helicobacter pylori* urease, Toxicon 69 (2013) 240–249.
[53] G.E. Wassermann, D. Olivera-Severo, A.F. Uberti, C.R. Carlini, *Helicobacter pylori* urease activates blood platelets through a lipoxygenase-mediated pathway, J. Cell Mol. Med. 14 (2010) 2025–2034.
[54] Y. Xin, Y.M. Choo, Z. Hu, K.S. Lee, H.J. Yoon, Z. Cui, H.D. Sohn, B.R. Jin, Molecular cloning and characterization of a venom phospholipase A_2 from the bumblebee *Bombus ignitus*, Comp. Biochem. Physiol. B Biochem. Mol. Biol. 154 (2009) 195–202.

Supplementary data

Table S1. Gene specific primers and cDNA library plasmid primers used for performing RACE PCR of both 5' and 3' of *Rhopr-PLA2III* and *Rhopr-PLA2XII.*

	Primer name	**Sequence (5' – 3')**
3'RACE GSP	Rhopr-PLA2IIIRACE Fw1	CGATTTGGGTTCCGATGCTA
	Rhopr-PLA2IIIRACE Fw2	GAACACACGATCTCTGTCCAAAG
	Rhopr-PLA2XIIRACE Fw1	AGGTTGTAAAGCTGCGGC
	Rhopr-PLA2XIIRACE Fw2	CTAAAGAGAAGAAAATATGCGGC
5' RACE GSP	Rhopr-PLA2IIIRACE Rv1	CGTAACACAACCACATCTGAGC
	Rhopr-PLA2IIIRACE Rv2	GGATTGGCCGACACTAGCA
	Rhopr-PLA2XIIRACE Rv1	TCAGCGGCAATAACGG
	Rhopr-PLA2XIIRACE Rv2	TAATATTCGATCCATAACCACTCC
3'RACE *plasmid primers*	pDNR-LIB 3 -55 Rv	GACCATGTTCACTTACCTACTGG
	pDNR-LIB 3 -25 Rv	*GCCAAACGAATGGTCTAGAAAG*
5' RACE *plasmid primers*	DNR-LIB Fw1	GTGGATAACCGTATTACCGCC
	DNR-LIB Fw2	*ACGGTACCGGACATATGCC*

Table S2. Gene specific primers designed for amplification of *Rhopr-PLA2III* and *Rhopr-PLA2XII* complete open reading frame sequences and for the real time quantitative PCR.

	Primer name	**Sequence (5' – 3')**
Rhopr-PLA2III ORF	Rhopr-PLA2III Fw	CTCAGATGTGGTTGTGTTACG
	Rhopr-PLA2III Rv	CCTTGCTATGAAATGGAATGATT
Rhopr-PLA2III qPCR	qRhopr-PLA2III Fw	GAGCTGATCGAAGTGTTAGATAA AGAGG
	qRhopr-PLA2III Rv	CCTGCACCACACCAATTAGTACC
Rhopr-PLA2XII ORF	Rhopr-PLA2XII Fw	GCGATAACTATGAATCAGTCACC
	Rhopr-PLA2XII Rv	AGAATTATTCATACCTAATTTAAG GATGAC
Rhopr-PLA2XII qPCR	qRhopr-PLA2XII Fw	CACTCGATGAAGTTTGTAGATGG
	qRhopr-PLA2XII Rv	AGGGAAGATATTCGGATTGTACC

Table S3. Gene specific primers designed for the production of *Rhopr-PLA2XII* dsRNA and ARG dsRNA templates.

	Primer name	**Sequence (5' – 3')**
Rhopr-PLA2XII	iRhopr-PLA2XIIFw	GGACGTGTATAGGTATGATTCGC
	iRhopr-PLA2XIIRev	TTAGAGGTTGACAATAGCAGGC
Rhopr-PLA2XII positive control	pciRhopr-PLA2XIIFw	CGTTATTGCCGCTGAAGG
	pciRhopr-PLA2XIIRev	CATTGGACCTCTGAAATTGTTAC
Rhopr-PLA2XII T7	T7iRhopr-PLA2XIIFw	TAATACGACTCA CTATAGGGAGAGGA CGTGTATAGGTATGATTCGC
	T7iRhopr-PLA2XIIRev	TAATACGACTCACTATAGGGAGA TTAGAG GTTGACAATAGCAGG C
Rhopr-PLA2XII T7 positive control	T7pciRhopr-PLA2XIIFw	TAATACGACTCACTATAGGGAGA CGTTAT TGCCGCTGAAGG
	T7pciRhopr-PLA2XIIRev	TAATACGACTCACTATAGGGAGA CATTGG ACCTCTGAAATTGTTAC
ARG	ARG Fw	ATGAGTATTCAACATTTCCGTGTC
	ARG Rev	AATAGTTTGCGCAACGTTG
ARG T7	T7 ARG Fw	TAATACGACTCACTATAGGGAGA ATGAGTATTCAACATTTCCGTGTC
	T7 ARG Rev	TAATACGACTCACTATAGGGAGA AATAGTTTGCGCAACGTTG

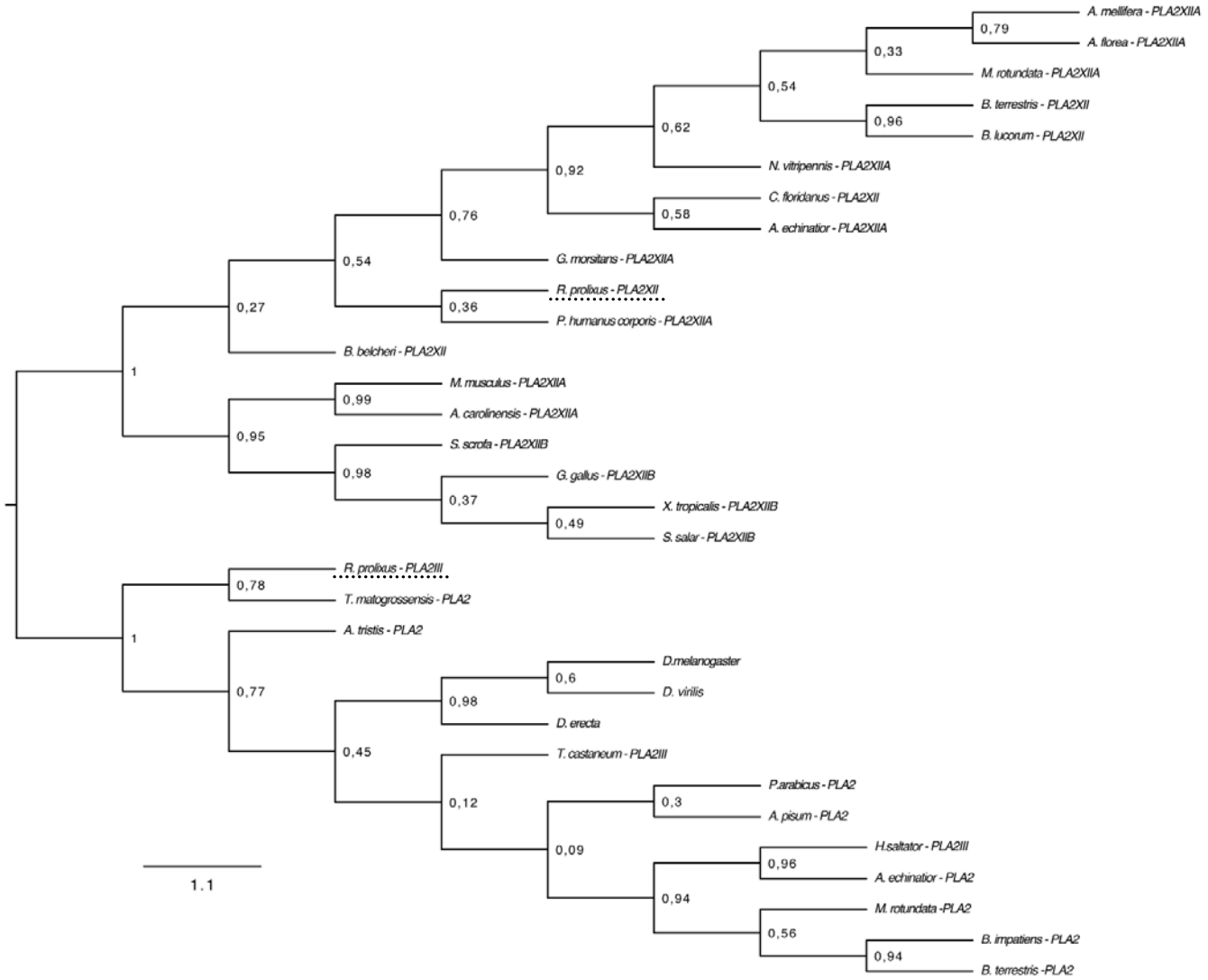

Figure S1. Maximum likelihood phylogenetic analysis of different PLA_2 sequences from arthropods and chordates. Phylogenetic tree illustrating the relationships among 30 PLA_2s, Rhopr-PLA2III and Rhopr-PLA2XII, generated by maximum likelihood method (ML), using the WAG + G model. The ML trees were generated with MEGA5 using phylogeny test by bootstrap method and 1,000 replications to calculate the consensus tree.

4.2. Experimento complementar

4.2.1. Análise da expressão de Rhopr-PLA2III em ninfas de quinto instar após alimentação

A expressão de *Rhopr-PLA2III* em ninfas de quinto instar foi analisada por PCR quantitativo, após alimentação em sangue de coelho, nos tecidos onde se observou níveis mais altos de expressão. A metodologia utilizada foi descrita no Capítulo II desta tese, item 2.7 de materiais e metodologias.

Os resultados obtidos indicam que há um aumento na expressão do gene no intestino posterior (hindgut), chegando, em 24 horas após a alimentação, a valores 8 vezes maiores em relação a expressão em insetos em jejum (Fig. 6). De acordo com as análises da sequência de aminoácidos predita para Rhopr-PLA2III, e apresentadas no capítulo 2 desta tese, a enzima possivelmente participa do processamento de fosfolipídios (FL) para a geração de lisofosfolipídios, como a lisofosfatidilcolina (LPC).

Mesquita e colaboradores (Mesquita *et al*., 2008) demonstraram que LPC presente na saliva de *R. prolixus* é moduladora da transmissão do parasita da doença de Chagas, *T. cruzi*, ao hospedeiro vertebrado. De acordo com os autores, a LPC injetada juntamente com a saliva facilita a invasão e a infecção do hospedeiro pelo parasita, que é depois excretado sobre a pele, juntamente com urina e fezes próximo ao local da picada. Além disso, LPC também está presente nas fezes e, segundo os autores, poderia participar do processo juntamente com a LPC originária da saliva. O aumento na expressão de *Rhopr-PLA2III* que observamos neste trabalho poderia estar relacionado com a utilização de FLs remanescentes da dieta para a produção de LPC. Talvez o

conteúdo de LPC presente nas fezes seja mais importante para a infecção do hospedeiro do que foi proposto por Mesquita e colaboradores.

Estudos futuros acerca da função exata de *Rhopr-PLA2III*, incluindo a expressão heteróloga da proteína para sua caracterização, e, possivelmente, o silenciamento do gene, poderiam responder de forma pertinente se este gene participa de alguma forma da transmissão da doença de Chagas.

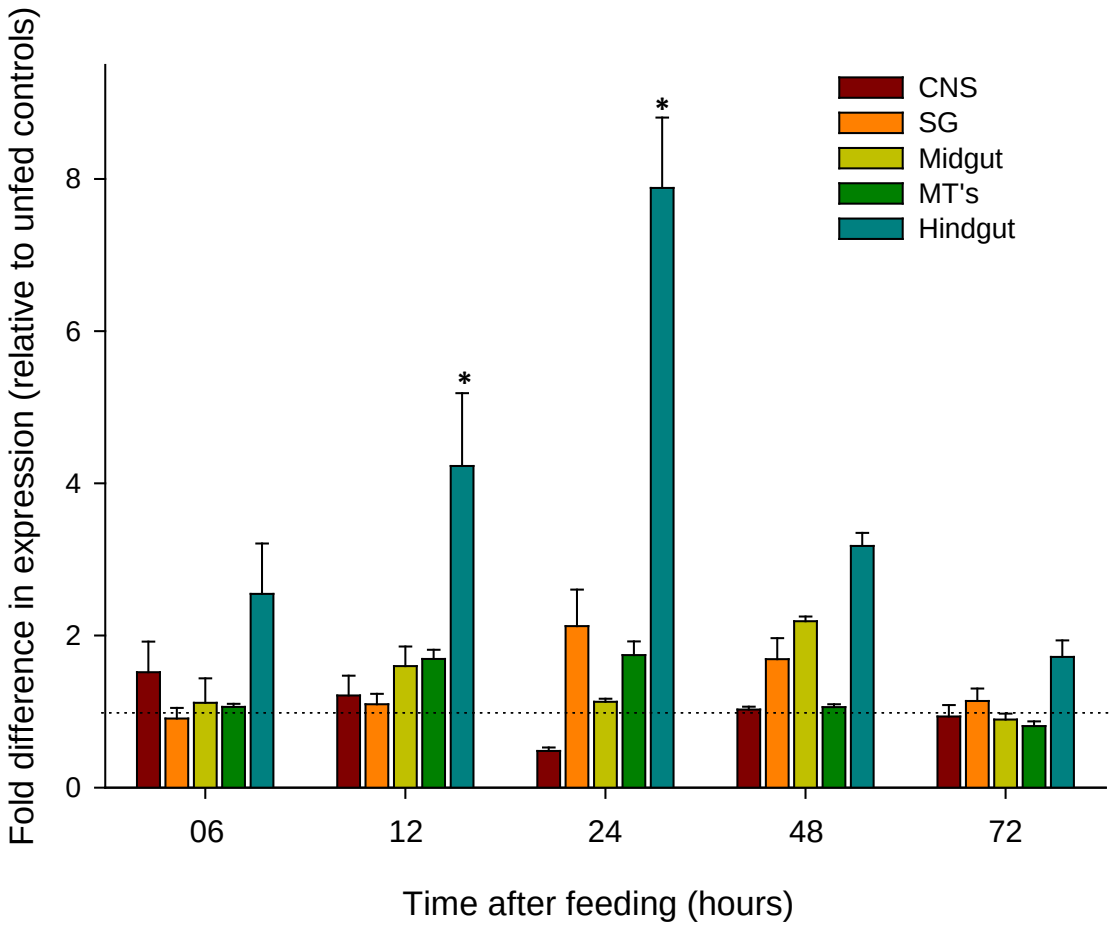

Figura 6. Análise da expressão de *Rhopr-PLA2III* em ninfas de quinto instar após alimentação em sangue de coelho. Em diferentes momentos após a alimentação os tecidos foram dissecados de pelo menos 5 insetos e organizados em 5 diferentes categorias: CNS - sistema nervoso central, SG - glândulas salivares, Midgut - intestino médio, MT's - túbulos de Malpighi, Hindgut - intestino posterior. A expressão foi quantificada por qPCR em relação a insetos não alimentados. Os resultados estão expressos como média de três replicatas biológicas com erro padrão. "*" indica diferença estatisticamente significativa em relação ao controle.

5. Discussão geral e perspectivas

Este trabalho deu continuidade ao estudo do mecanismo de ação entomotóxica das ureases, respondendo parte das questões abordadas e propondo novas hipóteses. Exploramos tópicos relativos a fisiologia de *R. prolixus*, estabelecendo novos procedimentos e técnicas de estudo do inseto, bem como contribuindo com conhecimentos básicos, tais como novas sequências gênicas.

Após isolarmos hemócitos de ninfas de quinto instar de *R. prolixus* analisamos parte do perfil da atividade tóxica da JBU sobre essas células. Observamos que a agregação de hemócitos induzida pela toxina é, muito provavelmente, modulada por produtos de COX, da mesma forma como estudos anteriores já haviam demonstrado a indução de exocitose em outros tecidos (Stanisçuaski *et al.*, 2009; Stanisçuaski *et al.*, 2010). Também após o tratamento de ninfas de *R. prolixus* com JBU por injeção na hemolinfa, observamos um aparente aumento na expressão de COX-2, utilizando-se anticorpos específicos para esta enzima. Esse possível aumento foi observado através de experimentos de dot-blot e deverá ser complementado com técnicas mais refinadas, como ELISAs, imunohistoquímica e PCRs quantitativos - neste último caso, uma vez que se tenha o(s) gene(s) de COX identificado(s).

Desenvolvemos um protocolo eficaz de cultura primária de hemócitos, o que possibilitou a incubação de JBU com as células por períodos mais longos que nos ensaios *in vitro*. Desta forma pudemos analisar o comportamento da proteína ao interagir com as células por microscopia confocal. Nossos resultados indicam que JBU de fato causa danos as células, induzindo

agregação dos núcleos e aparente morte celular. Daremos sequência aos experimentos de toxicidade de JBU em culturas de células, buscando compreender os mecanismos pelos quais a toxina causa danos aos hemócitos. Também com o protocolo de cultura de hemócitos será possível explorar isoladamente rotas de sinalização celular envolvidas no sistema imunitário de *R. prolixus*, bem como será possível adaptá-lo a outros tipos celulares deste e de outros insetos.

Identificamos dois genes de PLA_2s em ninfas de *R. prolixus*, e, de acordo com as análises das proteínas putativas, ambos são codificadores de PLA_2s secretórias. Os genes foram chamados de *Rhopr-PLA2III* e *Rhopr-PLA2XII*, seguindo as características bioquímicas e estruturais dos grupos de PLA_2s secretórias III e XII, respectivamente. Após silenciarmos a expressão de *Rhopr-PLA2XII* observamos uma diminuição na toxicidade de JBU sobre os insetos que não expressavam o gene em níveis constitutivos. Por outro lado, de acordo com nossos resultados e nossas inferências, *Rhopr-PLA2III* não tem envolvimento com a toxicidade de JBU, mas pode ter influência na transmissão do parasita causador da doença de Chagas, o protozoário *Trypanosoma cruzi*. Porém, como discutido anteriormente nesta tese, ao que tudo indica *Rhopr-PLA2III* poderia gerar lisofosfolipídeos como a lisofosfatidilcolina, que é essencial para a transmissão do parasita ao hospedeiro vertebrado. Desta forma, este gene seria um alvo interessante para o aprofundamento da questão. De um modo geral, os genes de PLA_2s identificados em *R. prolixus* poderão ser utilizados em estudos relativos ao metabolismo de fosfolipídios, incluindo eventos mediados por eicosanóides e por lisofosfolipídeos.

Perspectivas de sequência a essa tese incluem: a) obter a expressão heteróloga de *Rhopr-PLA2XII* e a produção de anticorpos contra essa isoenzima, visando compreender melhor o envolvimento do gene na toxicidade de JBU; b) explorar outras etapas da produção de eicosanóides, buscando outros genes provavelmente envolvidos na toxicidade da JBU, como por exemplo, genes de COX-2; c) dosar metabólitos de eicosanóides em insetos com a expressão de *Rhopr-PLA2XII* diminuída e tratados com JBU, buscando diferenças com os insetos controles; d) tratar insetos com a expressão de *Rhopr-PLA2XII* diminuída com eicosanóides, como prostaglandinas e tromboxanos, para testar uma possível reversão da resistência a toxicidade de JBU; e) identificar tecidos/células de insetos alvos de eicosanóide (s) que desencadeiam o efeito inseticida da urease; entre outras.

Em resumo, considerando-se que as ureases são proteínas multifuncionais de grande potencial de uso biotecnológico, o estudo do modo de ação destas toxinas no sistema imunitário de insetos poderá revelar novas estratégias e ferramentas para o combate de insetos pragas e vetores de doenças.

6. Conclusões

✓ A urease majoritária de *Canavalia ensiformis* induz a agregação de hemócitos em *Rhodnius prolixus* em doses nanomolares, tanto *in vivo,* após injeção na hemolinfa, quanto *in vitro*, em hemócitos isolados.

✓ A agregação induzida *in vitro* por JBU em hemócitos de *R. prolixus* é modulada por eicosanóides, e, ao que tudo indica, por produtos de ciclooxigenase.

✓ O tratamento com JBU por injeção direta na hemolinfa de ninfas de quinto instar de *R. prolixus* causa, aparentemente, um aumento na expressão/ativação da enzima ciclooxigenase-2.

✓ Considerando-se o efeito de agregação modulado por eicosanóides que a JBU desencadeia em hemócitos *R. prolixus*, sugere-se que a toxina ativa a resposta imune do inseto, da mesma forma como esta proteína promove ativação de outros modelos celulares.

✓ Hemócitos de ninfas de *R. prolixus* podem ser cultivados e mantidos em cultura por, pelo menos, quatro semanas.

✓ Sítios imunorreativos anti-JBU podem ser observados em hemócitos em cultura de *R. prolixus* tratados com JBU, sugerindo uma interação direta da toxina com as células.

✓ Danos ao citoesqueleto e agregação de núcleos são observados em hemócitos cultivados após o tratamento com JBU.

✓ Ninfas de *R. prolixus* expressam pelos menos 2 genes de PLA_2 secretórias, sendo que um deles provavelmente codifica uma proteína com

características do grupo III, e o outro provavelmente codifica uma proteína com características do grupo XII.

✓ Os dois genes de PLA_2 identificados foram clonados, caracterizados e chamados *Rhopr-PLA2III* e *Rhopr-PLA2XII*. O tratamento com JBU, por injeção na hemolinfa, não altera a expressão de nenhum dos transcritos em ninfas de quinto instar de *R. prolixus*.

✓ *Rhopr-PLA2XII* teve sua expressão diminuída, em média, em 70% nos variados tecidos de ninfas de quinto instar de *R. prolixus*. O silenciamento persiste por pelo menos 5 dias e não é observada mortalidade entre os insetos tratados com o RNA de interferência.

✓ Após silenciar o transcrito de *Rhopr-PLA2XII* em ninfas de quinto instar de *R. prolixus,* foi observada uma redução na toxicidade de JBU, o que indica que produtos do gene em questão participam da modulação da atividade inseticida da proteína.

✓ Os dados obtidos reforçam a ideia de que o efeito tóxico da JBU em insetos não é somente devido aos peptídeos resultantes da clivagem proteolítica por enzimas digestivas - possivelmente há contribuição da molécula intacta no processo, o que aumenta o leque de questões a serem investigados futuramente sobre o modo de ação entomotóxica das ureases.

7. Referências bibliográficas

Andrade,L.O. & Andrews,N.W. The *Trypanosoma cruzi*-host-cell interplay: location, invasion, retention. *Nat. Rev. Microbiol*. 3: 819-823. 2005.

Barja-Fidalgo,C., Guimaraes,J.A., & Carlini,C.R. Canatoxin, a plant protein, induces insulin release from isolated pancreatic islets. *Endocrinology.* 128: 675-679. 1991a.

Barja-Fidalgo,C., Guimaraes,J.A., & Carlini,C.R. Lipoxygenase-mediated secretory effect of canatoxin the toxic protein from *Canavalia ensiformis seeds*. *Toxicon.* 29: 453-459. 1991b.

Barros,P.R., Stassen,H., Freitas,M.S., Carlini,C.R., Nascimento,M.A., & Follmer,C. Membrane-disruptive properties of the bioinsecticide Jaburetox-2Ec: implications to the mechanism of the action of insecticidal peptides derived from ureases. *Biochim. Biophys. Acta.* 1794: 1848-1854. 2009.

Burke,J.E. & Dennis,E.A. Phospholipase A2 biochemistry. *Cardiovasc. Drugs Ther.* 23: 49-59. 2009a.

Burke,J.E. & Dennis,E.A. Phospholipase A2 structure/function, mechanism, and signaling. *J. Lipid Res.* 50(Suppl): S237-S242. 2009b.

Carlini,C.R., Gomes,C., Guimaraes,J.A., Markus,R.P., Sato,H., & Trolin,G. Central nervous effects of the convulsant protein canatoxin*. Acta Pharmacol. Toxicol. (Copenh).* 54: 161-166. 1984.

Carlini,C.R. & Grossi-de-Sa,M.F. Plant toxic proteins with insecticidal properties. A review on their potentialities as bioinsecticides. *Toxicon*. 40: 1515-1539. 2002.

Carlini,C.R. & Guimaraes,J.A. Isolation and characterization of a toxic protein from *Canavalia ensiformis* (jack bean) seeds, distinct from concanavalin A. *Toxicon*. 19: 667-675. 1981.

Carlini,C.R. & Guimaraes,J.A. Plant and microbial toxic proteins as hemilectins: emphasis on canatoxin. *Toxicon*. 29: 791-806. 1991.

Carlini,C.R., Guimaraes,J.A., & Ribeiro,J.M. Platelet release reaction and aggregation induced by canatoxin, a convulsant protein: evidence for the involvement of the platelet lipoxygenase pathway. *Br. J. Pharmacol*. 84: 551-560. 1985.

Carlini,C.R., Oliveira,A.E., Azambuja,P., Xavier-Filho,J., & Wells,M.A. Biological effects of canatoxin in different insect models: evidence for a proteolytic activation of the toxin by insect cathepsin like enzymes. *J. Econ. Entomol.* 90: 340-348. 1997.

Carter,E.L., Flugga,N., Boer,J.L., Mulrooney,S.B., & Hausinger,R.P. Interplay of metal ions and urease. *Metallomics.* 1: 207-221. 2009.

Coura,J.R., Junqueira,A.C., Boia,M.N., Fernandes,O., Bonfante,C., Campos,J.E., Santos,L., & Devera,R. Chagas disease in the Brazilian Amazon: IV. a new cross-sectional study. *Rev. Inst. Med. Trop. Sao Paulo.* 44: 159-165. 2002.

Corey,E.J., Albright,J.O., Barton,A. E., & Hashimoto,S. Chemical and enzymic synthesis of 5- HPETE, a key biological precursor of slow-reacting substance of anaphylaxis (SRS) and 5-HETE. *J. Am. Chem.Soc.* 102: 1435–1436. 1980.

Defferrari,M.S., Demartini,D.R., Marcelino,T.B., Pinto,P.M., & Carlini,C.R. Insecticidal effect of *Canavalia ensiformis* major urease on nymphs of the milkweed bug *Oncopeltus fasciatus* and characterization of digestive peptidases. *Insect Biochem. Mol. Biol.* 41: 388-399. 2011.

Dias,J.C., Silveira,A.C., & Schofield,C.J. The impact of Chagas disease control in Latin America: a review. *Mem. Inst. Oswaldo Cruz.* 97: 603-612. 2002.

Dixon,N.E., Gazzola,C., Watters,J.J., Blakely,R.L., & Zerner,B. Inhibition of Jack Bean urease (EC 3.5.1.5) by acetohydroxamic acid and by phosphoramidate. An equivalent weight for urease. *J. Am. Chem. Soc.* 97: 4130-4131. 1975.

Eidels,L., Proia,R.L., & Hart,D.A. Membrane receptors for bacterial toxins. *Microbiol. Rev.* 47: 596-620. 1983.

Fearon, D.T. Seeking wisdom in innate immunity. *Nature.* 388: 323-324. 1997.

Ferreira-Dasilva,C.T., Gombarovits,M.E., Masuda,H., Oliveira,C.M., & Carlini,C.R. Proteolytic activation of canatoxin, a plant toxic protein, by insect cathepsin-like enzymes. *Arch. Insect Biochem. Physiol*. 44: 162-171. 2000.

Figueiredo,M.B., Garcia,E.S., & Azambuja,P. Blockades of phospholipase A(2) and platelet-activating factor receptors reduce the hemocyte phagocytosis in Rhodnius prolixus: in vitro experiments. *J. Insect Physiol.* 54: 344-350. 2008a.

Figueiredo,M.B., Genta,F.A., Garcia,E.S., & Azambuja,P. Lipid mediators and vector infection: Trypanosoma rangeli inhibits Rhodnius prolixus hemocyte phagocytosis by modulation of phospholipase A2 and PAF-acetylhydrolase activities. *J. Insect Physiol.* 54: 1528-1537. 2008b.

Follmer,C., Barcellos,G.B., Zingali,R.B., Machado,O.L., Alves,E.W., Barja-Fidalgo,C., Guimaraes,J.A., & Carlini,C.R. Canatoxin, a toxic protein from jack beans (*Canavalia ensiformis*), is a variant form of urease (EC 3.5.1.5): biological effects of urease independent of its ureolytic activity. *Biochem. J.* 360: 217-224. 2001.

Follmer,C., Real-Guerra,R., Wasserman,G.E., Olivera-Severo,D., & Carlini,C.R. Jackbean, soybean and *Bacillus pasteurii* ureases: biological effects unrelated to ureolytic activity. *Eur. J. Biochem*. 271: 1357-1363. 2004.

Ghazaleh,F.A., Araujo,C.F., Barja-Fidalgo,C., & Carlini,C.R. Canatoxin induces activation on mice peritoneal macrophages. *Braz. J. Med. Biol. Res*. 25: 1033-1035.

Ghazaleh,F.A., Francischetti,I.M., Gombarovits,M.E., & Carlini,C.R. Stimulation of calcium influx and platelet activation by canatoxin: methoxyverapamil inhibition and downregulation by cGMP. *Arch. Biochem. Biophys*. 339: 362-367. 1997.

Hirayama,C., Sugimura,M., Saito,H., & Nakamura,M. Host plant urease in the hemolymph of the silkworm, *Bombyx mori*. *J. Insect Physiol.* 46: 1415-1421. 2000.

Jurenka,R.A., Pedibhotla,V.K., & Stanley,D.W. Prostaglandin production in response to a bacterial infection in true armyworm larvae. *Arch. Insect Biochem. Physiol.* 41: 225-232. 1999.

Kanost,M.R., Jiang,H., & Yu,X.Q. Innate immune responses of a lepidopteran insect, *Manduca sexta. Immunol. Rev.* 198: 97-105. 2004.

Kurahashi,H., Atiwetin,P., Nagaoka,S., Miyata,S., Kitajima,S., & Sugimura,Y. Absorption of mulberry root urease to the hemolymph of the silkworm, *Bombyx mori*. *J. Insect Physiol.* 51: 1055-1061. 2005.

Layne, E. Spectrophotometric and turbidimetric methods for measuring proteins. *Methods Enzimol.* 3: 447-454. 1957.

Luduena,R.F. A hypothesis on the origin and evolution of tubulin. *Int. Rev. Cell Mol. Biol.* 302: 41-185. 2013.

Maddrell,S.H., O'Donnell,M.J., & Caffrey,R. The regulation of haemolymph potassium activity during initiation and maintenance of diuresis in fed *Rhodnius prolixus*. *J. Exp. Biol.* 177: 273-285. 1993.

Martinelli, A.H., Kappaun, K., Ligabue-Braun, R., Defferrari, M.S., Piovesan, A.R., Stanisçuaski, F., Demartini, R.D., Verli, H., Dal Belo, C.A., Almeida, C.G., Follmer, C., Carlini, C.R., & Pasquali, G. Structure-function studies on Jaburetox, a recombinant insecticidal and antifungal peptide derived from jack bean (*Canavalia ensiformis*) urease. *BBA Gen. Subjects.* 1840: 935-944. 2014.

Mesquita,R.D., Carneiro,A.B., Bafica,A., Gazos-Lopes,F., Takiya,C.M., Souto-Padron,T., Vieira,D.P., Ferreira-Pereira,A., Almeida,I.C., Figueiredo,R.T., Porto,B.N., Bozza,M.T., Graca-Souza,A.V., Lopes,A.H., Atella,G.C., & Silva-Neto,M.A. Trypanosoma cruzi infection is enhanced by vector saliva through

immunosuppressant mechanisms mediated by lysophosphatidylcholine. *Infect. Immun.* 76: 5543-5552. 2008.

Mobley,H.L., Island,M.D., & Hausinger,R.P. Molecular biology of microbial ureases. Microbiol. Rev. 59: 451-480. 1995.

Mulinari,F., Staniscuaski,F., Bertholdo-Vargas,L.R., Postal,M., Oliveira-Neto,O.B., Rigden,D.J., Grossi-de-Sa,M.F., & Carlini,C.R. Jaburetox-2Ec: an insecticidal peptide derived from an isoform of urease from the plant *Canavalia ensiformis*. *Peptides*. 28: 2042-2050. 2007.

Orchard,I. & Paluzzi,J.P. Diuretic and antidiuretic hormones in the blood-gorging bug Rhodnius prolixus. *Ann. N. Y. Acad. Sci*. 1163: 501-503. 2009.

Paluzzi,J.P. & O'Donnell,M.J. Identification, spatial expression analysis and functional characterization of a pyrokinin-1 receptor in the Chagas' disease vector, *Rhodnius prolixus*. *Mol. Cell Endocrinol*. 363: 36-45. 2012.

Piovesan,A.R., Staniscuaski,F., Marco-Salvadori,J., Real-Guerra,R., Defferrari,M.S., & Carlini,C.R. Stage-specific gut proteinases of the cotton stainer bug *Dysdercus peruvianus*: role in the release of entomotoxic peptides from *Canavalia ensiformis* urease. *Insect Biochem. Mol. Biol.* 38: 1023-1032. 2008.

Real-Guerra, R., Carlini, C. R., & Staniscuaski, F. Role of lysine and acidic amino acid residues on the insecticidal activity of Jackbean urease. *Toxicon*. 71: 76-83. 2013.

Settembrini,B.P. & Villar,M.J. Distribution of serotonin in the central nervous system of the blood-feeding heteropteran, *Triatoma infestans* (Heteroptera: Reduviidae). *J. Morphol*. 260: 21-32. 2004.

Smith, W.L., DeWitt, D.L., & Garavito, R.M. Cyclooxygenases: structural, cellular, and molecular biology. *Annu Rev Biochem.* 69: 145-82. 2000.

Staniscuaski,F. & Carlini,C.R. Plant ureases and related peptides: understanding their entomotoxic properties. *Toxins. (Basel).* 4: 55-67. 2012.

Staniscuaski,F., Ferreira-Dasilva,C.T., Mulinari,F., Pires-Alves,M., & Carlini,C.R. Insecticidal effects of canatoxin on the cotton stainer bug *Dysdercus peruvianus* (Hemiptera: Pyrrhocoridae). *Toxicon*. 45: 753-760. 2005.

Staniscuaski,F., TeBrugge,V., Carlini,C.R., & Orchard,I. Jack bean urease alters serotonin-induced effects on *Rhodnius prolixus* anterior midgut. *J. Insect Physiol.* 56: 1078-1086. 2010.

Staniscuaski,F., TeBrugge,V., Carlini,C.R., & Orchard,I. In vitro effect of *Canavalia ensiformis* urease and the derived peptide Jaburetox-2Ec on *Rhodnius prolixus* Malpighian tubules. *J. Insect Physiol.* 55: 255-263. 2009.

Stanley,D., Miller,J., & Tunaz,H. Eicosanoid actions in insect immunity. *J. Innate Immun.* 1: 282-290. 2009.

Strand,M.R. Insect hemocytes and their role in immunity. In Insect Immunology, N.E.Beckage, ed. (Amsterdam: Elsevier), pp. 25-47. 2008.

Terra,W.R. & Ferreira,C. Insect digestive enzymes: properties, compartmentalization and function. *Comp. Biochem. Physiol*. 109B: 1-62. 1994.

Tootle,T.L., Williams,D., Hubb,A., Frederick,R., & Spradling,A. Drosophila eggshell production: identification of new genes and coordination by Pxt. *PLoS One.* 6: e19943. 2011.

Tunaz,H., Park,Y., Buyukguzel,K., Bedick,J.C., Nor Aliza,A.R., & Stanley,D.W. Eicosanoids in insect immunity: bacterial infection stimulates hemocytic phospholipase A2 activity in tobacco hornworms. *Arch. Insect Biochem. Physiol.* 52: 1-6. 2003.

Uberti,A.F., Olivera-Severo,D., Wassermann,G.E., Scopel-Guerra,A., Moraes,J.A., Barcellos-de-Souza,P., Barja-Fidalgo,C., & Carlini,C.R. Pro-inflammatory properties and neutrophil activation by *Helicobacter pylori* urease. *Toxicon*. 69: 240-249. 2013.

Wassermann,G.E., Olivera-Severo,D., Uberti,A.F., & Carlini,C.R. *Helicobacter pylori* urease activates blood platelets through a lipoxygenase-mediated pathway. *J. Cell Mol. Med.* 14: 2025-2034. 2010.

ANEXOS

I. Artigo Publicado

Defferrari *et al.*, 2011

● Trabalho desenvolvido e escrito a partir de experimentos da dissertação de mestrado ao longo do primeiro ano do doutorado.

Insect Biochemistry and Molecular Biology 41 (2011) 388–399

Contents lists available at ScienceDirect

Insect Biochemistry and Molecular Biology

journal homepage: www.elsevier.com/locate/ibmb

Insecticidal effect of *Canavalia ensiformis* major urease on nymphs of the milkweed bug *Oncopeltus fasciatus* and characterization of digestive peptidases

Marina S. Defferrari [a,1], Diogo R. Demartini [a,1], Thiago B. Marcelino [b], Paulo M. Pinto [b,c], Celia R. Carlini [a,b,*]

[a] Graduate Program in Cellular and Molecular Biology, Center of Biotechnology, Universidade Federal do Rio Grande do Sul, Av. Bento Gonçalves 9500, CEP 91501-970 Porto Alegre, Rio Grande do Sul, Brazil
[b] Center of Biotechnology and Department of Biophysics, IB, Universidade Federal do Rio Grande do Sul, Av. Bento Gonçalves 9500, CEP 91501-970 Porto Alegre, Rio Grande do Sul, Brazil
[c] Universidade Federal do Pampa, Campus de São Gabriel, São Gabriel, Rio Grande do Sul, Brazil

ARTICLE INFO

Article history:
Received 4 June 2010
Received in revised form
29 January 2011
Accepted 24 February 2011

Keywords:
Cysteine endopeptidase
Cathepsin L
Canavalia ensiformis
Purification
Insecticide
Insect digestion

ABSTRACT

Jackbean (*Canavalia ensiformis*) ureases are entomotoxic upon the release of internal peptides by insect's digestive enzymes. Here we studied the digestive peptidases of *Oncopeltus fasciatus* (milkweed bug) and its susceptibility to jackbean urease (JBU). *O. fasciatus* nymphs fed urease showed a mortality rate higher than 80% after two weeks. Homogenates of midguts dissected from fourth instars were used to perform proteolytic activity assays. The homogenates hydrolyzed JBU *in vitro*, yielding a fragment similar in size to known entomotoxic peptides. The major proteolytic activity at pH 4.0 upon protein substrates was blocked by specific inhibitors of aspartic and cysteine peptidases, but not significantly affected by inhibitors of metallopeptidases or serine peptidases. The optimal activity upon N-Cbz-Phe-Arg-MCA was at pH 5.0, with complete blockage by E-64 in all pH tested. Optimal activity upon Abz–AIAFFSRQ–EDDnp (a substrate for aspartic peptidases) was detected at pH 5.0, with partial inhibition by Pepstatin A in the pH range 2–8. Fluorogenic substrates corresponding to the N- and C-terminal regions flanking a known entomotoxic peptide within urease sequence were also tested. While the midgut homogenate did not hydrolyze the N-terminal peptide, it cleaved the C-terminal peptide maximally at pH 4.0–5.0, and this activity was inhibited by E-64 (10 μM). The midgut homogenate was submitted to ion-exchange chromatography followed by gel filtration. A 22 kDa active fraction was obtained, resolved in SDS-PAGE (12%), the corresponding band was *in-gel* digested by trypsin, the peptides were analyzed by mass spectrometry, retrieving a cathepsin L protein. The purified cathepsin L was shown to have at least two possible cleavage sites within the urease sequence, and might be able to release a known insecticidal peptide in a single or cascade event. The results suggest that susceptibility of *O. fasciatus* nymphs to jackbean urease is, like in other insect models, due mostly to limited proteolysis of ingested protein and subsequent release of entomotoxic peptide(s) by cathepsin-like digestive enzymes.

1. Introduction

Plants have diverse physicochemical defense mechanisms to resist insect attack, among which are insecticidal proteins such as lectins, arcelins, ribosome inactivating proteins, peptidase- and amylase inhibitors, thiaminases, chitinases, modified storage proteins (Bolter and Jongsma, 1997; Felton, 1996; Koiwa et al., 1997; Ryan, 1990; Stotz et al., 1999). More recently ureases were characterized as part of the arsenal of plant entomotoxic proteins (Carlini and Grossi-de-Sá, 2002; Carlini and Polacco, 2008; Follmer et al., 2004a; Polacco and Holland, 1993).

Ureases (urea amidohydrolase; EC 3.5.1.5) are nickel-dependent enzymes that catalyze urea hydrolysis into ammonia and carbon dioxide, and are synthesized by plants, fungi and bacteria (Follmer, 2008; Mobley et al., 1995). In plants, ureases are homotrimers or hexamers of 90 kDa subunits and contribute to the use of urea as nitrogen source (Follmer, 2008; Polacco and Holland, 1993; Sirko and Brodzik, 2000). Canatoxin is a less abundant urease isoform

Abbreviations: aa, amino acid; Abz, *ortho*-aminobenzoic acid; EDDnp, ethylenediamine 2,4-dinitrophenyl; JBU, jackbean major urease isoform; MH, midgut homogenate.

* Corresponding author. Center of Biotechnology and Department of Biophysics, IB, Universidade Federal do Rio Grande do Sul, CEP 91501-970 Porto Alegre, Brazil. Tel.: +55 51 3308 7606; fax: +55 51 3308 7003.
E-mail addresses: ccarlini@ufrgs.br, celia.carlini@pq.cnpq.br (C.R. Carlini).

[1] These authors contributed equally to the present work.

0965-1748/$ – see front matter © 2011 Elsevier Ltd. All rights reserved.
doi:10.1016/j.ibmb.2011.02.008

isolated from *Canavalia ensiformis* seeds (Carlini and Guimarães, 1981; Follmer et al., 2001) and similar to the seed's major urease, both proteins display insecticidal properties (Carlini et al., 1997) independent of ureolytic activity (Follmer et al., 2004a,b; Stanisçuaski et al., 2005). This toxicity is mostly due to the release of urease's internal peptides by the insect's digestive enzymes; insects with cathepsin-like peptidases are susceptible to this effect, while insects with trypsin-like enzymes are not (Carlini et al., 1997; Ferreira-DaSilva et al., 2000; Piovesan et al., 2008).

Nymphs of the hematophagous kissing bug, *Rhodnius prolixus* (Hemiptera: Reduviidae), larvae of the cowpea weevil, *Callosobruchus maculatus* (Coleoptera: Bruchidae), and nymphs of the cotton stainer bug, *Dysdercus peruvianus* (Hemiptera: Pyrrochoridae) are examples of susceptible insects, all relying on cathepsin-like digestive enzymes (Ferreira-DaSilva et al., 2000; Stanisçuaski et al., 2005). Acidic metallopeptidases were also shown to be involved in urease breakdown in *D. peruvianus* nymphs (Piovesan et al., 2008). A 10 kDa entomotoxic peptide named pepcanatox was obtained from canatoxin hydrolysis by *C. maculatus* digestive enzymes (Ferreira-DaSilva et al., 2000). Jaburetox-2Ec, a recombinant peptide equivalent to pepcanatox (Mulinari et al., 2004, 2007), is a potent insecticide but does not affect mice or neonate rats when administered by oral or intraperitoneal routes (Mulinari et al., 2007). This recombinant peptide also kills insects that are resistant to intact ureases, such as *Spodoptera frugiperda* (Mulinari et al., 2007) or *Triatoma infestans* adults (Tomazzeto et al., 2007).

Digestive peptidases play critical roles in insect physiology: breaking down proteins into essential amino acids for growth and development, and inactivating ingested protein toxins (Terra et al., 1996). There are six groups of endopeptidases according to the amino acid residue, or metal ion, present in the active site, involved in peptide bond hydrolysis (Barret et al., 1998): serine, cysteine, aspartic, glutamic, threonine and metallopeptidases. Insects that have neutral to alkaline digestive tracts usually use serine peptidases for digestion, while insects with acidic midguts generally have cysteine and aspartic peptidases (Howe and Jander, 2008; Terra and Ferreira, 1994).

The large milkweed bug, *Oncopeltus fasciatus* (Hemiptera: Lygaeidae), is found east of the Rocky Mountains in Canada and the United States, feeding on milkweed seeds, *Asclepias syriaca*, but occasionally they suck juices from other plants. *O. fasciatus* has been used in physiological studies as an insect model for developmental studies, being easy to rear and presenting a short life cycle (egg to adult in approximately 50 days) (Feir, 1974; Te Brugge and Orchard, 2007). Acidic pH values for the digestive tract of *O. fasciatus* were previously reported (Bongers, 1970), as well as the presence of cysteine peptidases and the absence of the serine peptidases trypsin and chymotrypsin (Woodring et al., 2007). In this study, we aimed to investigate urease toxicity and processing by nymphs of *O. fasciatus* and to characterize the profile of their digestive enzymes. Because the release of entomotoxic peptides could be due to concerted or sequential action of more than one enzyme, we decided to study the enzymatic activity profile of whole midguts' homogenates. We have also isolated one cysteine peptidase able to perform *in vitro* hydrolysis of urease and of urease-mimetic synthetic peptides.

2. Material and methods

2.1. Reagents

Azocasein, bovine hemoglobin, trans-epoxysuccinyl-L-leucylamido(4-guanidino)-butane (E-64), Pepstatin A, ethylenediamine tetraacetic acid (EDTA), phenylmethylsulfonyl fluoride (PMSF), methylcoumarin amide (MCA)-coupled peptide substrates, anti-rabbit IgG conjugated with alkaline phosphatase, nitro-blue tetrazolium (NBT), 5-bromo-4-chloro-3-indolyl phosphate (BCIP), Jackbean urease and Protein-A Agarose were from Sigma Chemical Company (Saint Louis, USA). *o*-phenantrolin was from ProAnalysis, Merck (Darmstadt, Germany). Hybond-P membrane (Polyvinylidene Fluoride - PVDF, 0.22 μm) was from Amersham Biosciences (Little Chalfont, England). CM-Sepharose Fast Flow and Sephadex G-50 were from GE Healthcare, Amersham Biosciences (Little Chalfont, England). Centriprep and Amicon devices with YM-3 and YM-30 membranes were from Amicon Inc. (Beverly, MA, USA). Dialysis membranes were from SpectraPor (California, USA). Fluorogenic peptide substrates coupled to *ortho*-aminobenzoic acid (Abz) and ethylenediamine 2,4-dinitrophenyl (EDDnp) were supplied by Dr. Luis Juliano Neto and Dr. Maria Aparecida Juliano (Dept. Biophysics, Universidade Federal de São Paulo, São Paulo, Brazil). The recombinant peptide Jaburetox-2Ec and anti-Jaburetox-2Ec polyclonal antibodies raised in rabbits were prepared as described previously (Mulinari et al., 2007; Tomazzeto et al., 2007). Chemicals and reagents used for high performance liquid chromatographics (HPLC) and nano-liquid tandem mass spectrometry (LC-MS/MS) analyses were HPLC or sequencing grade.

2.2. Insects

A colony of *O. fasciatus* was established in our laboratory from individuals initially supplied by Dr. Patrícia Azambuja Penna (Fundação Oswaldo Cruz, Rio de Janeiro) and by Dr. Denise Feder (Universidade Federal Fluminense, Rio de Janeiro). The colony was kept under controlled temperature (22 °C ± 2 °C) and humidity (70% ± 5%) and a 14/10 h photoperiod (light/dark), according to Milano et al. (1999). The insects were fed on sunflower (*Helianthus annuus*) and cotton (*Gossipium hirsutum*) seeds and had free access to water, developing from eggs to adults in about 30–35 days.

2.3. Bioassay of urease insecticidal activity

The bioassay was carried out essentially as described by Stanisçuaski et al. (2005). Groups of 14 nymphs (third instar) of *O. fasciatus* were fed on artificial cotton seeds, consisting of gelatin capsules (size 2, Elli Lilly Co.) containing cotton seed flour mixed with 0.01% or 0.2% (w/w) freeze-dried urease. Survival rates and molting were recorded daily until day 15.

2.4. Midgut homogenates

Homogenates of *O. fasciatus* whole midguts were used for determination of soluble proteolytic activities. Non-starved fourth instars were anaesthetized in ice, whole midguts were removed and stored at −20 °C in 0.02 M sodium phosphate buffer (NaPB) pH 7.0 with 0.02% sodium azide, in a proportion of 50 intestines per mL. To prepare the midgut homogenates (MH), the material was thawed, homogenized with an ice-cold hand-held Potter pestle, centrifuged at 4 °C at 8000 × *g* for 5 min, the supernatants were collected and then centrifuged at 8000 × *g* for 30 min. The final supernatants were filtered through a 0.22 μm membrane, dialyzed against 2 L of NaPB and kept frozen at −20 °C until use.

2.5. Protein determination

Protein concentration was determined by the method of Layne (1957), using a spectrophotometer (UV/Vis Spectrophotometer Hitachi, California, USA) at 280/260 nm absorbances.

2.6. Enzyme assays

For the enzyme assays the buffers used were sodium phosphate for pH 2.0, 6.0 and 7.0, sodium acetate for pH 4.0 and 5.0, ammonium formate for pH 3.0, TRIS·Cl for pH 8.0 and 9.0, and sodium carbonate for pH 10.0.

2.6.1. Macromolecular substrates

For determination of proteolytic activity upon protein substrates, MH aliquots (50 μg of protein) were incubated with 0.2% azocasein or 0.2% hemoglobin in a 300 μL volume buffered (final concentration 0.1 M) at different pHs varying from 2.0 to 10.0, at 37 °C. When present, inhibitors were incubated for 30 min with MH prior addition of the substrate. After 1 h, 250 μL of 10% trichloroacetic acid was added, followed by centrifugation (20 min, 8000 × *g*). To 450 μL of the supernatant 250 μL NaOH (2 M) was added, mixed and then absorbance was read at 420 nm (azocasein) or 280 nm (hemoglobin). One activity unit was defined as the amount of enzyme releasing 1 A_{420} or 1 A_{280} of trichloroacetic acid-soluble peptides, per hour at 37 °C.

2.6.2. Fluorogenic substrates

Different fluorogenic substrates were employed to characterize the enzymatic activities in the midgut extracts.

In fluorescence resonance energy transfer substrates, the fluorescence of *ortho*-aminobenzioc acid (Abz) is quenched by the ethylenediamine 2,4-dinitrophenyl (EDDnp) portion (Korkmaz et al., 2008). The amino acid sequence (aa) is within these two portions of the substrate (Abz–aa–EDDnp). In the absence of hydrolysis, only a basal fluorescence is seen. When hydrolysis happens at any point separating the two portions of the substrate it results in an abrupt increase of fluorescence, sometimes reaching several orders of magnitude (Korkmaz et al., 2008).

Two sets of fluorogenic substrates were used. The first set was used to follow up the purification process or characterize the purified enzyme (Abz–AIAFFSRQ–EDDnp, 20 μM final and N-Cbz-Phe-Arg-MCA, 2 μM final, - N-Cbz: carboxybenzoyl; MCA: methylcoumarin). The second set of substrates (Abz–NAIADGPVQ–EDDnp and Abz–KVIRDGMGQ–EDDnp) was used to determine the cleavage point of jackbean urease by the purified enzyme. This experiment is detailed in Section 2.10.

Aliquots of MH containing 10 μg of protein were individually incubated in dark opaque microplates, at 37 °C, in 100 μL final volume. The pH was adjusted from 2.0 to 8.0 with the buffers already indicated and reaction was carried out for 30 min. For Abz substrates, wavelengths used for excitation/emission were 320/430 nm and for MCA substrates, 370/460 nm, respectively. Results are shown as relative fluorescence units (RFU) per hour per mg of MH, taken the highest activity as 100%.

2.7. Purification of a cysteine peptidase from midgut homogenates

All purification steps were analyzed using the fluorogenic substrate 2 μM N-Cbz-Phe-Arg-MCA, in 100 μL final volume, pH 5.0, at 37 °C, 30 min, as described above.

2.7.1. Cation-exchange chromatography

For cation-exchange chromatography, a column packed with 10 mL of CM-Sepharose Fast-Flow resin was equilibrated in 20 mM sodium acetate buffer pH 5.0 (buffer A). After sample application (91.8 A_{280}), the column was washed with buffer A to remove non-retained proteins and then stepwise eluted with buffer A containing 0.1, 0.3, 0.5 and 1 M NaCl. Non-retained and eluted materials were collected in 10 mL fractions. Enzymatically active fractions were pooled, dialyzed against buffer A in a 3.5 kDa cut-off membrane, and concentrated using a Centriprep™ ultrafiltration device, 3 kDa cut-off.

2.7.2. Size exclusion chromatography

Gel filtration was performed using a Sephadex G-50™ column (1.2 × 30 cm) equilibrated in buffer A. Active pools (total 7.84 A_{280}) from cation-exchange chromatography were applied to the column. Protein peaks, monitored at 280 nm, were individually collected in 0.5 mL fractions and assayed for enzymatic activity. For molecular mass determination, the column was previously calibrated with protein markers from a gel filtration LMW Calibration Kit (GE Healthcare, Amersham Biosciences, Little Chalfont, England).

2.8. Sodium dodecyl sulfate-polyacrylamide gel electrophoresis (SDS-PAGE)

Sodium dodecyl sulfate-polyacrylamide gel electrophoresis (SDS-PAGE) was performed as described by Laemmli (1970). Samples were mixed 4:1 (v/v) with the SDS-PAGE sample buffer and loaded on 5%-stacking/12%-separating gels. After the run, gels were stained with Coomassie brilliant blue R-250, and destained with 10% acetic acid, or stained with silver nitrate. Molecular mass markers used were Bench Mark Protein Ladder (Invitrogen Life Technologies, California, United States).

2.9. Urease in vitro hydrolysis

Urease digestion by *O. fasciatus* peptidases was performed as described in Ferreira-DaSilva et al. (2000) with minor modifications, under two different conditions, 1.5 mU and 2 mU of MH azocaseinolytic activity per microgram of urease, in 0.05 M ammonium formate, pH 5.6, at 37 °C, under continuous stirring for 24 h. The reaction was stopped by freeze-drying the samples.

2.10. Western blot

Urease hydrolysis was followed by Western blot (Towbin et al., 1979) after SDS-PAGE in 12% polyacrylamide gels. Protein bands were transferred to 0.22 μm PVDF membranes, followed by overnight incubation with anti-Jaburetox-2Ec antibodies (1:25,000) and with anti-rabbit IgG coupled to alkaline phosphatase (1:50,000). The color reaction was developed with NBT and BCIP in buffer containing $MgCl_2$, pH 9.6.

2.11. Immunoprecipitation with anti-Jaburetox-2Ec antibodies

Fragments generated by *in vitro* hydrolysis of urease with *O. fasciatus* enzyme were recovered using an Amicon ultrafiltration device, 30 kDa cut-off. The flow-through fractions (fragments smaller than 30 kDa) were then immunoprecipitated with anti-Jaburetox-2Ec antibodies. For that, aliquots (in triplicates) of the flow-through fractions were mixed with 50 μL of Protein-A Agarose slurry buffered with 0.02 M sodium phosphate, 0.15 M sodium chloride, pH 7.5, in a total volume of 1 mL. Incubations were carried out for 2 h at room temperature, under gentle agitation, to control for non-specific binding to Protein-A Agarose. After this incubation, the mixtures were centrifuged 2 min, 12,000 × *g*, and the supernatants were placed into new microcentrifuge tubes. Fifteen microliters of anti-Jaburetox-2Ec antibodies were added to supernatants, incubated overnight at 4 °C, then 50 μL of Protein-A slurry was added and let incubate overnight at 4 °C, to allow anti-Jaburetox-2Ec to bind to Protein-A Agarose. Finally, Protein-A slurry containing the antibody complexed to interacting polypeptides was washed with 0.02 M sodium phosphate, 0.15 M sodium chloride,

pH 7.5 (5 times, 0.5 mL each). Regular SDS-PAGE sample buffer containing 0.01 M dithiothreitol was added to each tube (50 μL), and interacting proteins were disrupted from anti-Jaburetox by heating at 96 °C for 5 min. Samples were resolved in 12% SDS-PAGE and transferred to a 0.45 μm PVDF membrane, stained with Coomassie brilliant blue R-250, and destained with 20% methanol (v/v).

2.12. In-gel trypsin digestion and mass spectrometry analysis

Protein bands were manually excised from Coomassie stained gels and *in-gel* digested with trypsin. Gel slices were completely destained using wash solution (0.1 M ammonium bicarbonate and 40% acetonitrile), followed by a dehydration step (100% acetonitrile) and freeze-dried. The dry gel slices were reduced with 0.01 M dithiothreitol in 0.1 M ammonium bicarbonate (56 °C for 30 min), and alkylated using 0.1 M iodoacetamide in 0.1 M ammonium bicarbonate, in the dark at room temperature. After alkylation, gel slices were washed three times with 180 μL of 50% acetonitrile and 50 mM ammonium bicarbonate for 15 min, followed by one washing step with 180 μL of acetonitrile. After the washing procedures, gel plugs were dried by vacuum centrifugation and digestion was performed for 18 h at 37 °C using 12 μL of 10 μg per mL modified porcine trypsin (sequencing grade modified trypsin, Promega Corporation, Wisconsin, USA) diluted in 0.05 M ammonium bicarbonate. After tryptic digestion, peptides were extracted in two washing steps with 50 μL of 50% acetonitrile and 5% trifluoroacetic acid for 1 h. Extracted peptides were dried and resuspended in 10 μL of 0.1% formic acid prior to MS analyses. Regular bovine serum albumin (one lane loaded with 1 μg) was processed concomitantly (from SDS-PAGE up to mass spectrometry analyses) as a control for mass spectrometry analyzes.

To identify proteins, a liquid chromatography (LC) separation (reversed-phase HPLC) coupled with tandem mass spectrometry (MS/MS) strategy was used. Tandem mass spectrometry analyses were performed in an electrospray ionization (ESI) quadrupole time-of-flight (Q-TOF) Q-TOF Micro™ mass spectrometer (Micromass, Waters, Milford, United States) coupled to a nanoAcquity Ultra Performance LC® (UPLC®, Waters, Milford, United States). A nanoflow ESI source was used with a lockspray source for lockmass measurement during all the chromatographic runs. The samples were separated in a Nanoease C18 (75 μm ID) capillary column eluted with a water/acetonitrile 0.1% formic acid gradient. Data were acquired in data-dependent mode (DDA), and multiple charged peptide ions (+2, +3 and +4) were automatically mass selected and dissociated in MS/MS experiments. Typical LC and ESI conditions were: flow of 600 nL/min, nanoflow capillary voltage of 3.5 kV, block temperature of 100 °C, and cone voltage of 100 V.

The MS/MS spectra were processed using Proteinlynx v. 2.0 software (Waters, Milford, US) and the generated PKL files were used to perform database searches using MASCOT software v. 2.2 (Matrix Science, London, UK). Two databases were used for analyses: the non-redundant NCBI database (9,868,855 sequences and 3,366,351,629 residues, as per Oct. 15, 2009) and the Peptidase Full-length Sequences Database (peptidase.lib), from MEROPS Peptidase Database (http://merops.sanger.ac.uk/index.htm; release 8.3), which contains both peptidases and peptidase inhibitors full-length sequences (Rawlings et al., 2010). Search parameters allowed a maximum of one missed cleavage, the carbamidomethylation of cysteine, the possible oxidation of methionine, peptide tolerance of 0.6 Da, and MS/MS tolerance of 0.6 Da. The significance threshold was set at $p < 0.05$, and identification required that each protein contained at least one peptide with an expected value <0.05. A minimum of two unique non-overlapping peptides were adopted as criteria for a protein match. Data were manually checked for validation.

2.13. Determination of cleavage site of Abz substrates

Peptide substrates corresponding to the N- and C-terminal regions flanking the entomotoxic peptide Jaburetox-2Ec, within urease sequence (Mulinari et al., 2007; Piovesan et al., 2008), were also tested. The reaction products were separated HPLC and their masses analyzed by matrix-assisted laser desorption/ionization time-of-flight spectrometry (MALDI-TOF).

The substrates were Abz–NAIADGPVQ–EDDnp (equivalent to the N-terminal region) and Abz–KVIRDGMGQ–EDDnp (equivalent to the C-terminal region). Aliquots of 1 μg of the purified cathepsin L were individually incubated in dark opaque microplates, at 37 °C, pH 5.0, with 20 μM of Abz–NAIADGPVQ–EDDnp and Abz–KVIRDGMGQ–EDDnp hydrolysis followed on a fluorescence plate reader (Spectra Max M2^e, Molecular Devices Inc. Downingtown, USA).

The reaction products in the plate wells were recovered with a pipette and applied into a ZitTip™ (Millipore, USA), and eluted according to the manufacturer instructions. Eluted Abz–aa (aa: amino acid) and aa–EDDnp reaction products were dried and fractionated by reverse phase chromatography in a HPLC system, using a 5 mL C-18 column (Shimadzu, Inc., Kyoto, Japan), equilibrated with 5% acetonitrile - 0.1% trifluoroacetic acid. After washing the column, elution was performed ramping from 5% acetonitrile up to 80% acetonitrile - 0.1% trifluoroacetic acid. Released Abz fluorescence was monitored by a RF10AXL Spectrofluorometer detector. Absorbance at 214 nm was monitored in a SPD-20A Spectrophotometer (both Shimadzu, Inc., Kyoto, Japan). Eluted peptides were collected and their masses were measured by MALDI-TOF. Theoretical masses were calculated using the Accelrys Draw 4.0™ (academic license available at http://accelrys.com/products), considering the possible modifications and adducts presents in the analyses.

3. Results

3.1. Urease insecticidal effect

In order to evaluate the insecticidal effect of *C. ensiformis* urease, third instar *O. fasciatus* nymphs were fed with the freeze-dried protein mixed with cotton flour in artificial seeds. Fig. 1 shows that

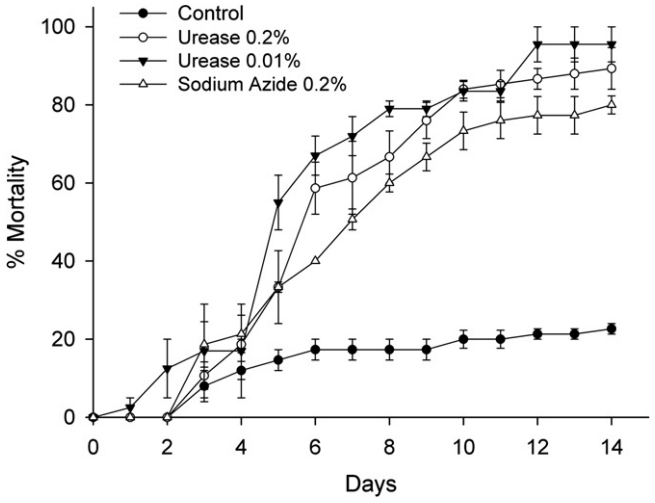

Fig. 1. Insecticidal urease effect on third instar *Oncopeltus fasciatus*. Groups of 14 insects were fed on artificial seeds containing jackbean urease in two different concentrations, 0.01 and 0.2% (w/w) and the mortality rate was followed daily up to two weeks. Results are expressed as means of triplicates.

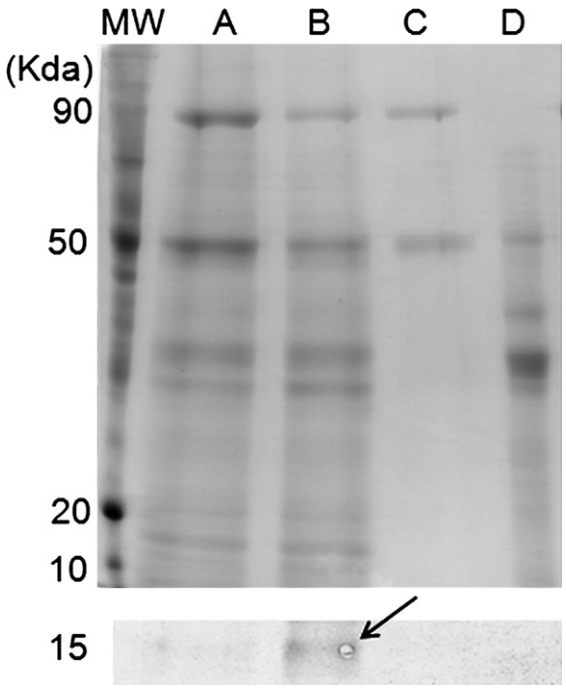

Fig. 2. Urease *in vitro* hydrolysis by *O. fasciatus* midgut homogenates. Up: 12% SDS-PAGE. Lane A: urease reaction with MH (1.5 mU of MH azocaseinolytic activity per microgram of urease); lane B: urease reaction with MH (2.0 mU of MH azocaseinolytic activity per microgram of urease); lane C: urease control; lane D: MH control. Molecular masses of standard proteins (kDa) are indicated. Bottom: Western blot analysis developed with anti-Jaburetox-2Ec antibodies. Black arrow indicates the fragment recognized by anti-Jaburetox antibodies.

a mortality rate of 90% is reached after 14 days for the two tested concentrations (0.01 and 0.2% w/w). These results are similar to previous observations for both isoforms of urease of *C. ensiformis* seeds, canatoxin and JBU, in *D. peruvianus* nymphs (Follmer et al., 2004b; Stanisçuaski et al., 2005).

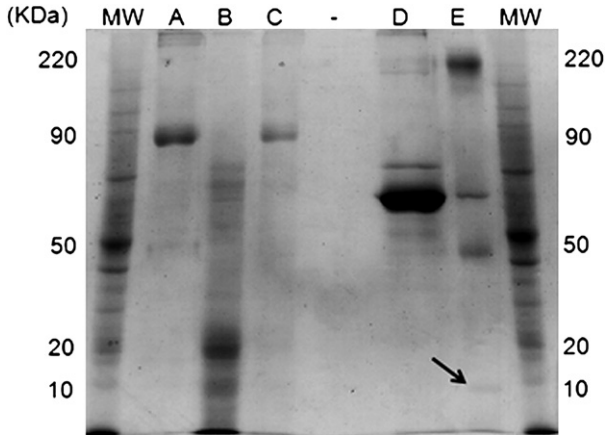

Fig. 3. *In vitro* hydrolysis of urease analyzed by immunoprecipitation. Midgut homogenates were incubated with jackbean urease (1.5 mU of MH azocaseinolytic activity per microgram of urease) for 24 h at 37 °C and reaction products were processed as described in Methods section. The figure presents a 12% SDS-PAGE. Lanes MW: molecular weight markers; lane A: urease control; lane B: urease-derived products smaller than 30 kDa; lane C: control urease incubated for 24 h at 37 °C and pH 5.6. Products from lane B were submitted to immunoprecipitation. Lane D: non-bound fraction from the immunoprecipitation assay, which contains excess of unbound IgG. Lane E: fraction eluted from Protein-A agarose, containing the polypeptides interacting with anti-Jaburetox antibodies. The arrow points to a ca.10 kDa band.

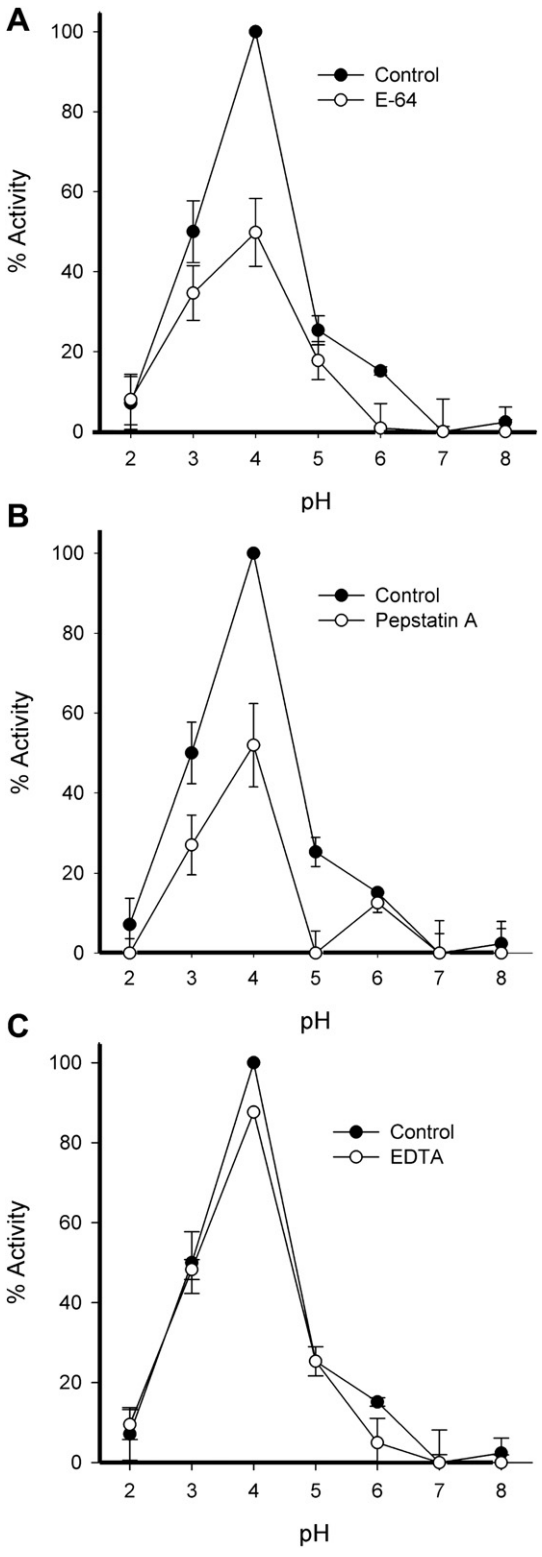

Fig . 4. Effect of inhibitors on hemoglobin hydrolysis by MH (50 μg of protein per tube). Activities were assayed in different pHs, at 37 °C for 1 h, in presence of 10 μM E-64 (A), 10 μM pepstatin A (B) and 1 mM EDTA, with a 0.2% final substrate concentration. Results are expressed as means of triplicates.

3.2. Urease in vitro hydrolysis

As previously shown for *D. peruvianus* (Piovesan et al., 2008), the release of the entomotoxic peptide(s) from urease could be due to the concerted or sequential action of more than one enzyme. Because of that, here we decided to analyze homogenates of whole midguts. After 24 h incubation at 37 °C, pH 5.6, urease was hydrolyzed by MH enzymes accompanied by the release of a fragment between 10 and 15 kDa (more visible with 2 mU of MH azocaseinolytic activity per microgram of urease), recognized by anti-Jaburetox-2Ec antibodies (Figs. 2 and 3). Unfortunately the low yield of this peptide recovered after immunoprecipitation with anti-Jaburetox-2EC was not enough to produce a reliable sequence by mass spectrometry analysis. However, by size and antigenicity criteria this peptide is similar to the entomotoxic peptide characterized by Ferreira-DaSilva et al. (2000).

3.3. Characterization of MH proteolytic activities

Aiming to characterize the major digestive proteinases present in *O. fasciatus* nymphs, several substrates and class-specific inhibitors were tested with the midgut homogenates.

3.3.1. Protein substrates

Hemoglobin is a non-specific protein substrate. The activity of MH upon this substrate (Fig. 4) was seen in pH ranging from pH 3.0 to 6.0, peaking at pH 4.0, with a strong inhibition by E-64

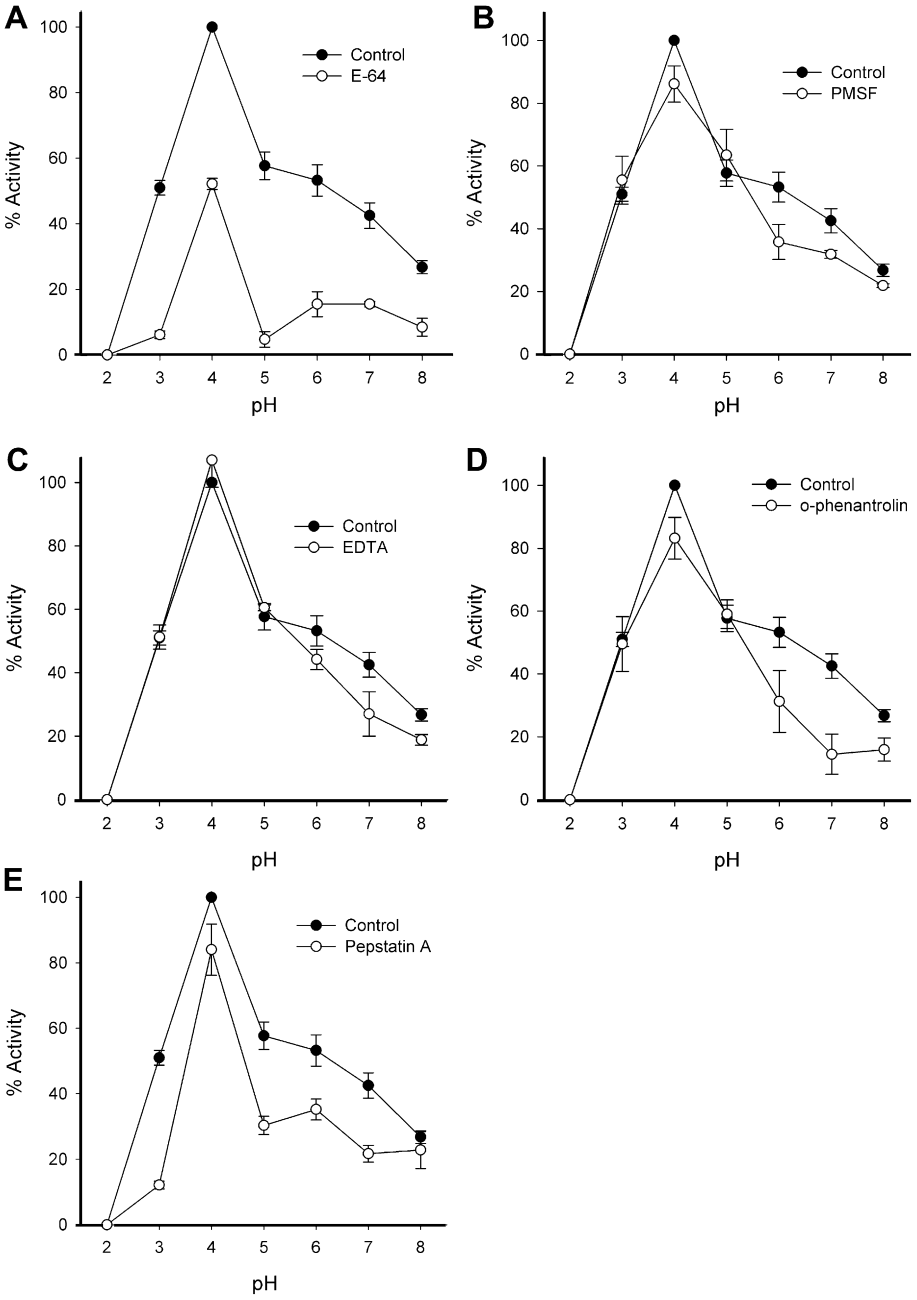

Fig. 5. Effect of inhibitors on azocasein hydrolysis by MH (50 μg of protein per tube). Activities were assayed in different pHs at 37 °C for 1 h, in presence of 10 μM E-64 (A), 1 mM PMSF (B), 1 mM EDTA (C), 1 mM *o*-phenantrolin (D) or 10 μM pepstatin A (D), with a 0.2% final substrate concentration. Results are expressed as means of triplicates.

(a cysteine peptidase inhibitor) (Fig. 4A) and by pepstatin A (an aspartic peptidase inhibitor, Fig. 4B), in the same pH range.

Azocasein is another non-specific protein substrate, being preferentially cleaved by cysteine peptidases (Barret et al., 1998). Fig. 5 shows that MH cleaved this substrate in pH ranging from pH 3.0 to 8.0, peaking at pH 4.0, being strongly inhibited by E-64 (Fig. 5A) and less inhibited by pepstatin A (Fig. 5E) in all pH values tested.

No significant inhibition by EDTA, a metallopeptidases inhibitor, of MH activity upon hemoglobin or azocasein was detected in any of the pH tested (Figs. 4C and 5C). PMSF and *o*-phenantrolin, respectively serine and metallopeptidases inhibitors, also did not significantly inhibited MH azocaseinolytic activity in any of the tested pH (Figs. 4D and 5B).

3.3.2. Synthetic substrates

Four synthetic substrates were used to characterize the peptidases present in the midgut homogenates. N-Cbz-Phe-Arg-MCA is a substrate suitable for the cysteine peptidases cathepsins B and L (Estrela et al., 2007; Renard et al., 2000). MH showed a major activity peak at pH 5.0 upon this substrate. While E-64 completely abolished this proteolytic activity in all pH values (Fig. 6A), pepstatin A inhibited only 20% of the activity detected at pH 5.0 (Fig. 6B).

The substrate Abz–AIAFFSRQ–EDDnp was developed for cathepsin-D like aspartic peptidases (Sorgine et al., 2000). Upon this substrate, MH showed an optimal activity at pH 4.0–5.0 (Fig. 7), strongly inhibited by pepstatin A in the pH 3.0–6.0 range (Fig. 7B). On the other hand, inhibition by E-64 was less proeminent, in all pH values tested (Fig. 7A).

MH peptidase activity was assayed upon synthetic substrates corresponding to N- and C-terminal regions flanking the entomotoxic peptide within urease to gain further insights into the processing of urease within the gut. MH efficiently cleaved (optimal pH 4.0–5.0) the C-terminal substrate, Abz–KVIRDGMGQ–EDDnp. The activity was blocked by E-64 (Fig. 8A) while pepstatin A did not affect it at all (Fig. 8B). The substrate Abz–NAIADGPVQ–EDDnp (equivalent to the N-terminal region) was not significantly hydrolyzed by the midgut homogenate (Fig. 9).

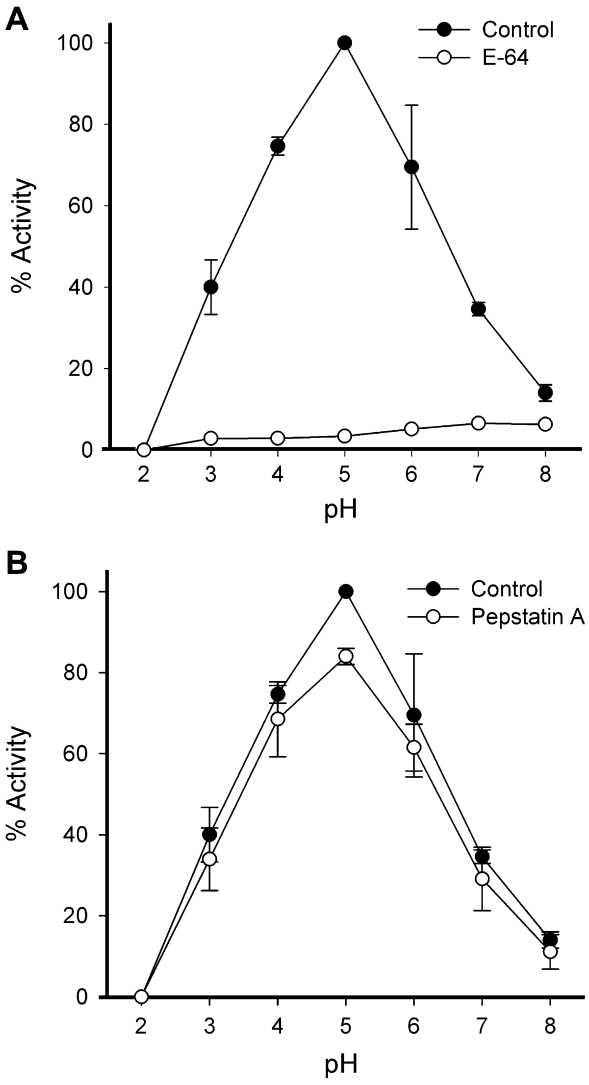

Fig. 6. Effect of inhibitors on the hydrolysis of N-Cbz-Phe-Arg-MCA by MH (10 μg of protein per well). Activities were assayed in different pHs, at 37 °C for 30 min, at 2 μM final substrate concentration, in presence of 10 μM E-64 (A) or 10 μM pepstatin A (B). Results are expressed as means of triplicates.

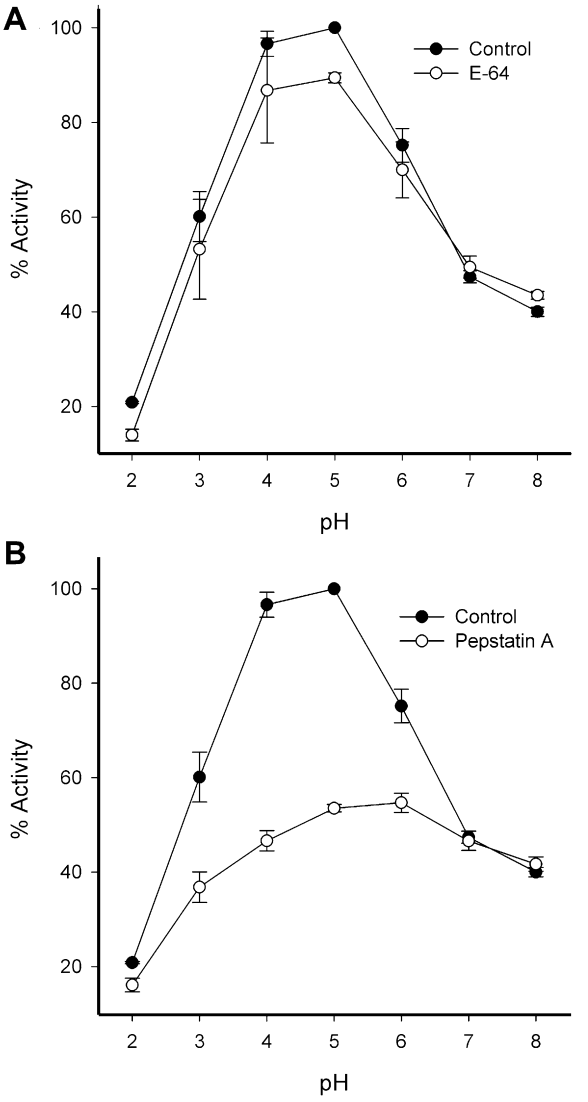

Fig. 7. Effect of inhibitors on the hydrolysis of Abz–AIAFFSRQ–EDDnp by MH (10 μg of protein per well). Activities were assayed in different pHs, 37 °C for 30 min, at 20 μM final substrate concentration, in presence of 10 μM E-64 (A) or 10 μM pepstatin A (B). Results are expressed as means of triplicates.

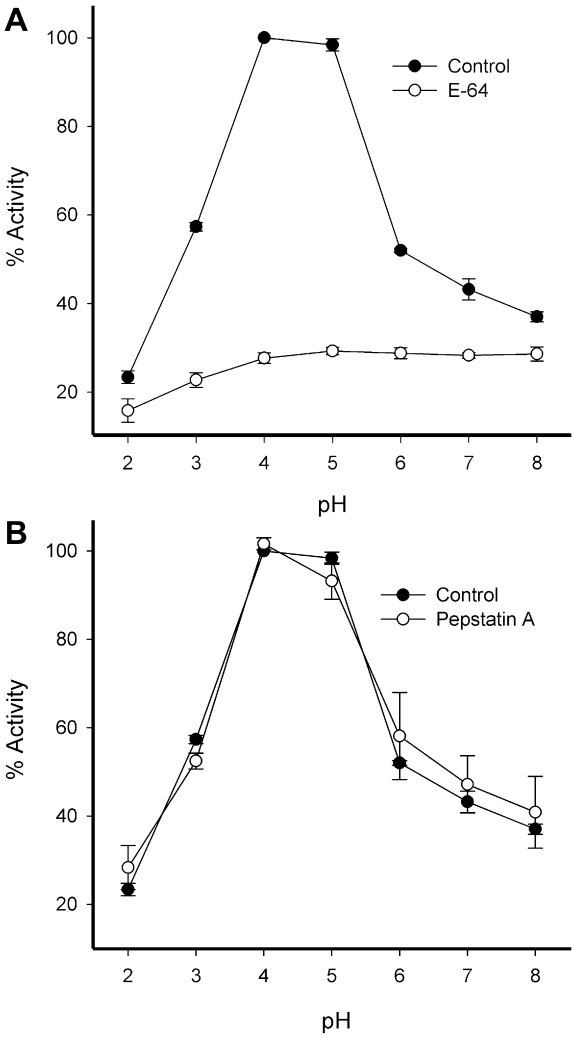

Fig. 8. Effect of inhibitors on the hydrolysis of Abz–KVIRDGMGQ–EDDnp by MH (10 μg of protein per well). Activities were assayed in different pHs, at 37 °C for 30 min, at 20 μM final substrate concentration, in presence of 10 μM E-64 (A) or 10 μM pepstatin A (B). Results are expressed as means of triplicates.

3.4. Purification and identification of a cathepsin L from midguts of *O. fasciatus* nymphs

Purification of a peptidase was accomplished by a combination of ion-exchange chromatography and gel filtration. As shown in Fig. 10, three major peaks were detected in the homogenates submitted to ion-exchange chromatography, with a cysteine peptidase activity concentrating in the first elution peak (0.1 M NaCl). The active fractions were pooled, concentrated and then applied into a Sephadex G-50 column. A major cysteine peptidase activity eluted between 13 and 15 mL, peaking at 14 mL (Fig. 11). A molecular mass of 22 kDa of this peptidase was calculated from its elution volume in the size exclusion column and further confirmed by SDS-PAGE (Fig. 11 inset). Table 1 summarizes the purification data of this protein. The cleavage of fluorogenic substrates by the purified enzyme is shown in Fig.12.

The corresponding 22 kDa band in the SDS-PAGE was excised from the gel, digested with trypsin and the peptides were analyzed by an ESI-Q-ToF mass spectrometer. Two independent samples from different purification batches gave the same set of results when searched against the MEROPS database. In all searches, a cathepsin L (zymogen or active) was retrieved, matching proteins from the nematode *Brugia malayi*, the mammal *Felis catus* and the plant *Arabidopsis thaliana* (Table 2). NCBI database was used for a BLAST (Basic Local Alignment Search Tool; Altschul et al., 1990) search to retrieve annotation, since at the time of this search, the retrieved enzymes of *A. thaliana* and *B. malayi* were not clearly annotated.

3.5. Determination of cleavage site of Abz–aa–EDDnp substrates

The cleavage sites of the urease-mimetic substrates Abz–NAIADGPVQ–EDDnp and Abz–KVIRDGMGQ–EDDnp by the purified cathepsin L were studied. The substrate Abz–NAIAD GPVQ–EDDnp was not significantly hydrolyzed, as presented in Fig. 9, and no further studies with this substrate were carried out. On the other hand, Abz–KVIRDGMGQ–EDDnp was hydrolyzed between I and R residues, as demonstrated by an 855.0376 *m/z* peak corresponding to the –RDGMGQ–EDDnp portion (considering one oxygen loss from one of the nitro groups present in the EDDnp quencher). The Abz–aa portion of the hydrolyzed substrate was not detected in these assays.

4. Discussion

Proteolytic enzymes present in digestive system of insects include aminopeptidases, carboxypeptidases and cysteine, aspartic, serine and metallo- endopeptidases (Bown et al., 1997; Ferry et al., 2004; Girard and Jouanin, 1999; Murdock and Shade, 2002; Patankar et al., 2001; Terra and Ferreira, 1994). This wide diversity implies multiple functions of insect enzymes, including involvement in developmental processes besides interactions with food components.

Hemipteran proteolytic enzymes are predominantly acidic, belonging to aspartic and cysteine peptidases classes (Houseman, 1978; Houseman and Downe, 1981, 1982a,b, 1983). The role played by these enzymes, usually located intracellularly, in extracellular protein digestion in insects (Cristofoletti et al., 2003; Houseman et al., 1984; Terra and Ferreira, 1994) is probably due to evolution and adaptation (Cristofoletti et al., 2003; Houseman et al., 1985). Terra et al. (1996) suggested that ancestral seed-feeding bugs modified lysosomal cathepsins to digest dietary proteins instead of using serine peptidases trypsin and chymotrypsin because seeds are, very often, rich sources of trypsin inhibitors.

In this work we investigated the digestive peptidase profile of the phytophagous hemipteran *O. fasciatus*, and tested the susceptibility of young forms of this insect to jackbean (*C. ensiformis*) major urease. We also isolated from midgut homogenates one cathepsin L-like digestive enzyme by a two-step purification procedure and demonstrated is ability to hydrolyze urease *in vitro*.

Third instars *O. fasciatus* were highly susceptible to ingestion of low doses of urease (0.01% w/w) - the deaths began 72 h after feeding and reached almost 100% mortality two weeks later. Ferreira-DaSilva et al. (2000) confirmed the proteolytic activation of canatoxin, an isoform of JBU, by enzymes from *C. maculatus* larvae, resulting in the release of pepcanatox, a 10 kDa toxic peptide. Here we showed that *C. ensiformis* major urease is hydrolyzed *in vitro* by *O. fasciatus* midgut homogenates releasing peptide(s) recognized by antibodies raised against Jaburetox-2Ec, a recombinant version of pepcanatox. Although intact urease also contributes to the entomotoxic effect (Stanisçuaski et al., 2009, 2010), the release of peptides equivalent to Jaburetox-2Ec from urease is enough to kill the insect (Mulinari et al., 2007).

Because the release of entomotoxic peptides could be due to a concerted or sequential action of more than one enzyme (Piovesan et al., 2008), studies of *in vitro* urease hydrolysis and

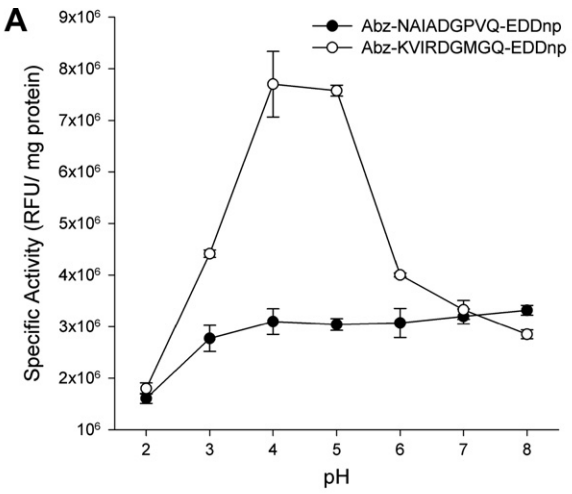

B

```
1   MKLSPREVEK LGLHNAGYLA QKRLARGVRL NYTEAVALIA SQIMEYARDG EKTVAQLMCL   60
61  GQHLLGRRQV LPAVPHLLNA VQVEATFPDG TKLVTVHDPI SRENGELQEA LFGSLLPVPS  120
121 LDKFAETKED NRIPGEILCE DECLTLNIGR KAVILKVTSK GDRPIQVGSH YHFIEVNPYL  180
181 TFDRRKAYGM RLNIAAGTAV RFEPGDCKSV TLVSIEGNKV IRGGNAIADG PVNETNLEAA  240
241 MHAVRSKGFG HEEEKDASEG FTKEDPNCPF NTFIHRKEYA NKYGPTTGDK IRLGDTNLLA  300
301 EIEKDYALYG DECVFGGGKV IRDGMGQSCG HPPAISLDTV ITNAVIIDYT GIIKADIGIK  360
361 DGLIASIGKA GNPDIMNGVF SNMIIGANTE VIAGEGLIVT AGAIDCHVHY ICPQLVYEAI  420
421 SSGITTLVGG GTGPAAGTRA TTCTPSPTQM RLMLQSTDYL PLNFGFTGKG SSSKPDELHE  480
481 IIKAGAMGLK LHEDWGSTPA AIDNCLTIAE HHDIQINIHT DTLNEAGFVE HSIAAFKGRT  540
541 IHTYHSEGAG GGHAPDIIKV CGIKNVLPSS TNPTRPLTSN TIDEHLDMLM VCHHLDREIP  600
601 EDLAFAHSRI RKKTIAAEDV LNDIGAISII SSDSQAMGRV GEVISRTWQT ADPMKAQTGP  660
661 LKCDSSDNDN FRIRRYIAKY TINPAIANGF SQYVGSVEVG KLADLVMWKP SFFGTKPEMV  720
721 IKGGMVAWAD IGDPNASIPT PEPVKMRPMY GTLGKAGGAL SIAFVSKAAL DQRVNVLYGL  780
781 NKRVEAVSNV RKLTKLDMKL NDALPEITVD PESYTVKADG KLLCVSEATT VPLSRNYFLF  840
```

Fig. 9. Hydrolysis by MH of urease-mimetic fluorogenic substrates Abz–NAIADGPVQ–EDDnp and Abz–KVIRDGMGQ–EDDnp. Panel A) Activities were assayed at 37 °C for 30 min, at 20 μM final substrate concentration. Results are expressed as means of triplicates. Panel B) Location of synthetic peptides within jackbean urease sequence (accession GenBank: AAA83831.1), represented by the underlined amino acids. The experimentally determined cleavage points (IR, using Abz–KVIRDGMGQ–EDDnp) are represented in bold/italic/gray.

enzymatic assays to characterize the presence of proteinases were done using whole midgut homogenates. Intestinal homogenates of *O. fasciatus* nymphs contain a major predominance of cysteine and aspartic cathepsin-like enzymes, demonstrated by using different substrates and specific inhibitors. The maximal activities in acidic pH values reported in the present work confirmed previous studies with this species (Bongers, 1970; Woodring et al., 2007), and many other heteropterans, including the cotton stainer bug *D. peruvianus* (Piovesan et al., 2008; Silva and Terra, 1994). As reported by Woodring et al. (2007), we also did not find proeminent serine or metallopeptidases, with a much lower proteolytic activity being detected at neutral to alkaline pH for some of the tested substrates. While no inhibition of MH activities at pH 5.0 or lower was seen for EDTA, *o*-phenantrolin, or PMSF, these compounds blocked partially the low activity detected in neutral to alkaline media, suggesting metallo- and serino-peptidase(s) as minor components of digestive proteinase profile in *O. fasciatus* nymphs. In previous study we demonstrated the presence of acidic metallopeptidase(s) in

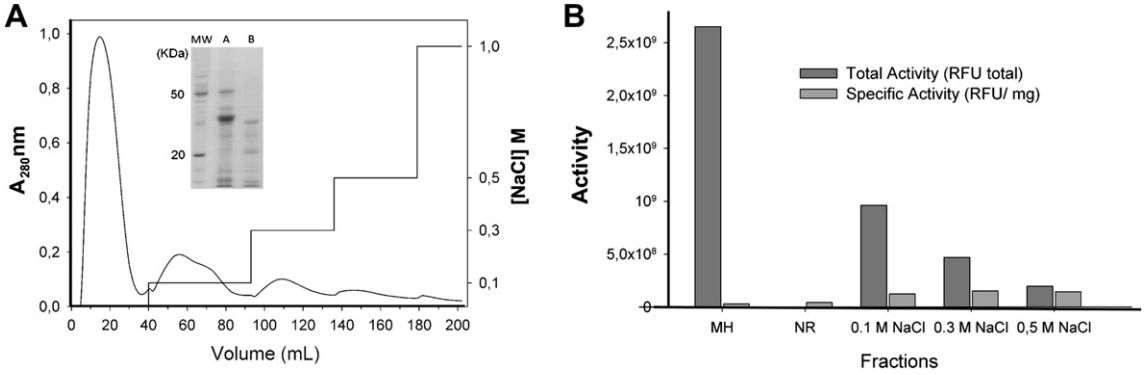

Fig. 10. Cation-exchange chromatography of MH on CM-Sepharose equilibrated with 20 mM Sodium Acetate pH 5.0. (A) Chromatogram shows 280 nm absorbance as a continuous line, and NaCl gradient as a stepwise line. Inset: 12% SDS-PAGE; lane A, MH; lane B, fraction eluted with 100 mM NaCl. Molecular masses of standard protein (kDa) are indicated. (B) Total and specific activity of fractions upon N-Cbz-Phe-Arg-MCA assayed at 37 °C for 30 min, in 20 mM sodium acetate pH 5.0.

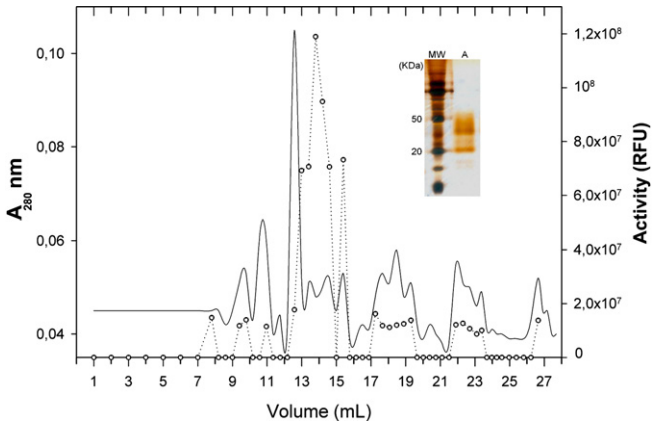

Fig. 11. Gel-filtration chromatography on Sephadex G-50 equilibrated with 20 mM Sodium Acetate pH 5.0 of the active pool from the CM-Sepharose column. Absorbance at 280 nm showed as a continuous line and activity of fractions upon N-Cbz-Phe-Arg-MCA as a dotted line. Protein peaks were assayed at 37 °C for 30 min, in 20 mM Sodium Acetate pH 5.0. The major peak of enzymatic activity corresponds to 22 kDa. Inset: SDS-PAGE of eluted fractions (silver stained); lane A, fraction eluted at 14 mL.

nymphs and serine peptidase(s) in adults of *D. peruvianus* (Piovesan et al., 2008).

While the protein substrates azocasein and hemoglobin were both inespecifically cleaved by cysteine and aspartic peptidases, the fluorogenic substrates N-Cbz-Phe-Arg-MCA, preferential for cysteine peptidases, and Abz–AIAFFSRQ–EDDnp, designed for aspartic peptidases, combined with the class-specific inhibitor E-64 and pepstatin A, respectively, demonstrated the presence of the cognate enzymes, with optimal activity at pH 5.0 (Fig. 12).

We have previously shown that *in vitro* hydrolysis of canatoxin by digestive enzymes from *C. maculatus* larvae produced a family of entomotoxic peptides, being pepcanatox the most toxic one (Ferreira-DaSilva et al., 2000). The N-terminal sequence GPVQ– of pepcanatox was determined by Edman degradation and based on its molecular mass, its C-terminal was deduced to be –KVIRD (Mulinari et al., 2007; Piovesan et al., 2008). *O. fasciatus* midgut homogenates did not cleave the substrate containing the N-terminal flanking sequence. In contrast, midgut homogenates of *D. peruvianus* nymphs hydrolyzed this substrate at pH 4.0, being strongly inhibited by EDTA, suggesting that a metallopeptidase activity could be responsible for cleavage of this specific sequence (Piovesan et al., 2008).

As no metallopeptidase activity was detected in *O. fasciatus* homogenates, this may imply that the N-terminal cleavage site of urease by *O. fasciatus* nymphs that results in the release of entomotoxic peptide(s)is different from that reported for *D. peruvianus*. The C-terminal substrate Abz–KVIRDGMGQ–EDDnp cleavage peaked at pH 4.0, with complete inhibition by E-64 in all tested pH.

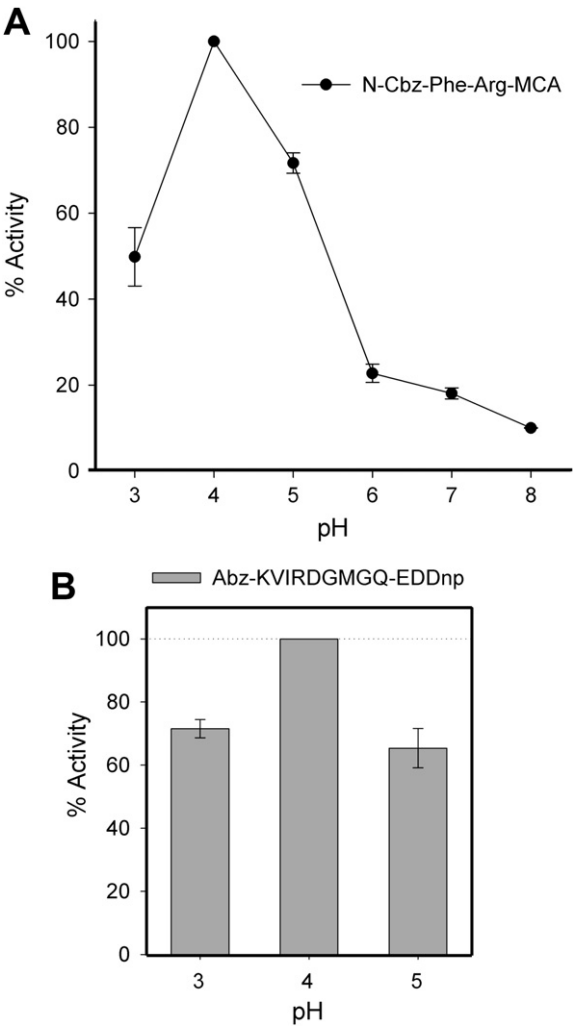

Fig. 12. Hydrolysis of the fluorogenic substrates N-Cbz-Phe-Arg-MCA (A) and Abz–KVIRDGMGQ–EDDnp (B) by the isolated cathepsin L (1 μg of protein per well; 2 μM and 20 μM of substrate, respectively). Activities were assayed in different pHs, at 37 °C for 30 min in (A) and until hydrolysis reached a maximal plateau (B).

The cleavage point of the substrate by the purified cathepsin-L was determined by combining HPLC (to separate the hydrolysis products) and MALDI-TOF (to identify the fragments by their *m/z*). Using this strategy, we were able to show that Abz–KVIRDGMGQ–EDDnp was hydrolyzed between the isoleucine and the arginine (IR) residues, contrasting with cleavage site of the same substrate by *D. peruvianus* digestive enzymes, that occurred between arginine and aspartic acid residues (RD) (Piovesan et al., 2008). In the case of

Table 1
Protein identification by LC-MS/MS.

Accession in MEROPS database	Annotation	Organism	MASCOT score[a]	pI/MW	Peptides detected[c]
MER014565	Cathepsin L-like cysteine proteinase[b]	*Brugia malayi*	76	9.03/44,699 Da	180-R.LPSSVDWR.K.K-192 (4)
MER005594	Cysteine proteinases superfamily protein[b]	*Arabidopsis thaliana*	60	5.99/40,371 Da	127-K.LPSSVDWR.K.K-139 (3)
MER101798	Cathepsin L[c]	*Felis catus*	57	6.00/37,175 Da	113-K.IPSSVDWRE.K -126 (4)

[a] MASCOT score is $-10 \times \log(P)$, where P is the probability that the observed match is a random event.
[b] Annotation retrieved after a BLAST search against NCBI NR-protein database. One hundred percent identity obtained.
[c] An isobaric change is observed (highlighted in gray); the number in parenthesis displays the abundance of the peptide. The position of the peptides within the sequences is presented.

Table 2
Purification of a cathepsin L-like digestive enzyme from *O. fasciatus* nymphs.

Sample	Volume (mL)	Protein (mg/mL)	Total protein (mg)	Activity (RFU/mL)	Specific activity (RFU/mg)	Total activity (RFU)	Yield (%)	Fold purified
Midgut homogenate	9	10.2	91.8	295×10^6	28×10^4	2651×10^6	100	1
CM-Sepharose	17.5	0.448	7.84	55×10^6	122×10^6	9625×10^5	36.3	424.97
Sephadex G-50	3	0.053	0.159	11×10^6	207×10^6	3300×10^4	1.24	718.44

Enzymatic activity of samples was assayed upon 2 μM N-Cbz-Phe-Arg-MCA at 37 °C for 30 min, in 20 mM sodium acetate pH 5.0 and shown as Relative Fluorescence Units. Midgut homogenate of *O. fasciatus*; CM-Sepharose (fraction eluted at 100 mM NaCl); Sephadex G-50 (fraction eluted at 14 mL).

D. peruvianus, the activity of midgut homogenates to cleave this substrate was significantly inhibited only by E-64 (Piovesan et al., 2008). Cathepsin L-like cysteine peptidases act as endopeptidases and the cleavage of RD bonds by human cathepsin L was previously described (Dahl et al., 2001). Although less efficient, these enzymes are also able to hydrolyze the bond between isoleucine and arginine (Puzer et al., 2004), as reported in our work. Considering that a motif KVIR is found twice within the urease chain (aa 219–222 and 319–322) encompassing the entomotoxic sequence (aa 222–314), the *O. fasciatus* cathepsin L alone could potentially cleave these two points and release an insecticidal peptide.

Our previous studies showed that simultaneous administration of canatoxin with either E-64 or pepstatin A to *R. prolixus* led to significant reduction in the mortality rate, suggesting that cysteine and aspartic peptidases are hydrolyzing the protein in this insect (Carlini et al., 1997). On the other hand, in *D. peruvianus* the presence of metallopeptidases seems to be very important for the release of the toxic peptide (Piovesan et al., 2008), while in *O. fasciatus* this class of enzymes appears not relevant for urease toxicity.

Altogether, the data show that the cleavage sites within urease releasing toxic peptides may differ among susceptible insects, generating slightly different sequences, without interfering in the entomotoxicity. Going along with this view, Barros et al. (2009) showed that the recombinant toxic peptide Jaburetox-2Ec displays membrane-disruptive properties and might adopt a well-defined β-hairpin conformation in its C-terminal half, similar to those found in some neurotoxic and antimicrobial pore-forming peptides. This information is consistent with the idea that the N-terminal portion of the insecticidal peptide(s) is less important for toxicity than its C-terminal half.

Previous studies by other groups have shown that acidic digestive enzymes are present in the midgut of *O. fasciatus* (Bongers, 1970), more specifically cysteine peptidases (Woodring et al., 2007). Here we demonstrate that besides cysteine peptidases, aspartic peptidases are also present. Furthermore, a cathepsin L from *O. fasciatus* midguts was isolated by a two-step purification protocol. The purified enzyme was identified by mass spectrometry, matching a 45 kDa cathepsin L-like cysteine peptidase precursor from the nematode *B. malayi* (considering the highest score in MASCOT searches). The abundance of the detected peptides, located in a conserved region of cathepsin L enzymes (Table 1), ensures that the *O. fasciatus* purified protease is a cathepsin L-like cysteine protease. The low coverage obtained probably reflects the very low amount of this enzyme present in the insect digestive system. The active form of this zymogen has 23 kDa (Guiliano et al., 2004), which is very similar to 22 kDa we observed for *O. fasciatus* enzyme in the gel-filtration chromatography and polyacrylamide gel electrophoresis. We also detected a band close to 40 kDa in the 14 mL fraction, which could be due to dimerization after the gel filtration, once the enzyme has cysteine residues in the active site that could be forming disulfide bonds.

In summary, data presented here aggregate information to our present knowledge on urease processing by insects digestive enzymes, and emphasize the need of a better comprehension of insect digestive physiology and how insecticidal proteins affect them, looking forward to develop biotechnological strategies to protect crops against pests.

Acknowledgments

This project was supported by CAPES (Coordenação de Aperfeiçoamento de Pessoal de Nível Superior, Brazil), by CNPq (Conselho Nacional de Desenvolvimento Científico e Tecnológico, Brazil) and by FAPERGS (Fundação de Amparo à Pesquisa do Estado do Rio Grande do Sul). M.S.D is a recipient of a CNPq fellowship; D.R.D. is recipient of a CAPES-PNPD fellowship. The authors declare no conflicts of interest.

References

Altschul, S.F., Gish, W., Miller, W., Myers, E.W., Lipman, D.J., 1990. Basic local alignment search tool. J. Mol. Biol. 215, 403–410.
Barret, A.J., Rawlings, N.D., Woessner, J.F., 1998. Handbook of Proteolytic Enzymes. Academic Press, San Diego. 1666 p.
Barros, P.R., Stassen, H., Freitas, M.S., Carlini, C.R., Nascimento, M.A.C., Follmer, C., 2009. Membrane-disruptive properties of the bioinsecticide Jaburetox-2Ec: implications to the mechanism of the action of insecticidal peptides derived from ureases. Biochim. Biophys. Acta 1794, 1848–1854.
Bolter, C., Jongsma, M.A., 1997. The adaptation of insects to plant peptidase inhibitors. J. Insect Physiol. 43 (10), 885–895.
Bongers, J., 1970. Die Carbohydrasen und Esterasen in Speicheldrüsen und Mitteldarm von *Oncopeltus fasciatus* (Lygaeidae). Zeitschrift für Vergleichende Physiologie 70, 382–400.
Bown, D.P., Wikinson, H.S., Gatehouse, J.A., 1997. Differentially regulated inhibitor-sensitive and insensitive peptidases genes from the phytophagous insect pest, *Helicoverpa armigera*, are member of complex multigene families. Insect Biochem. Mol. Biol. 27 (7), 625–638.
Carlini, C.R., Guimarães, J.A., 1981. Isolation and characterization of a toxic protein from *Canavalia ensiformis* ('Jackbean') seeds, distinct from concanavalin A. Toxicon 19, 667–676.
Carlini, C.R., Oliveira, A.E., Azambuja, P., Xavier-Filho, J., Wells, M.A., 1997. Biological effects of canatoxin in different insect models. Evidence for a proteolytic activation of the toxin by insect cathepsin-like enzymes. J. Econ. Entomol. 90, 340–348.
Carlini, C.R., Grossi-de-Sá, M.F., 2002. Plant toxic proteins with insecticidal properties. A review on their potentialities as bioinsecticides. Toxicon 40 (11), 1515–1539.
Carlini, C.R., Polacco, J.C., 2008. Toxic properties of urease. Crop Sci. 48, 1665–1672.
Cristofoletti, P.T., Ribeiro, A.F., Deraison, C., Rahbe, Y., Terra, W.R., 2003. Midgut adaptation and digestive enzyme distribution in a phloem feeding insect, the pea aphid *Acyrthosiphon pisum*. J. Insect Physiol. 49, 11–24.
Dahl, S.W., Halkier, T., Lauritzen, C., Dolenc, I., Pedersen, J., Turk, V., Turk, B., 2001. Human recombinant pro-dipeptidyl peptidase I (cathepsin C) can be activated by cathepsins L and S but not by autocatalytic processing. Biochemistry 40, 1671–1678.
Estrela, A., Seixas, A., Termignoni, C., 2007. A cysteine endopeptidase from tick (*Rhipicephalus (Boophilus) microplus*) larvae with vitellin digestion activity. Comp. Biochem. Physiol. 148B, 410–416.
Feir, D., 1974. *Oncopeltus fasciatus*: a research animal. Annu. Rev. Entomol. 19, 81–96.
Felton, G.W., 1996. Nutritive quality of plant protein: sources of variation and insect herbivore responses. Arch. Insect Biochem. Physiol. 32 (1), 107–130.
Ferreira-DaSilva, C.T., Gombarovits, M.E., Masuda, H., Oliveira, C.M., Carlini, C.R., 2000. Proteolytic activation of canatoxin, a plant toxic protein, by insect cathepsin-like enzymes. Arch. Insect Biochem. Physiol. 44, 162–171.
Ferry, N., Edwards, M.G., Gatehouse, J.A., 2004. Plant-insect interactions: molecular approaches to insect resistance. Curr. Opin. Biotechnol. 15 (2), 155–161.
Follmer, C., Barcellos, G.B.S., Zingali, R.B., Machado, O.L.T., Alves, E.W., Barja-Fidalgo, C., Guimarães, J.A., Carlini, C.R., 2001. Canatoxin, a toxic protein from 'Jackbean' (*Canavalia ensiformis*), is a variant form of urease (EC. 3.5.1.5): biological effects of urease independent of its ureolytic activity. Biochem. J. 360, 217–224.

Follmer, C., Real-Guerra, R., Wassermann, G.E., Olivera-Severo, D., Carlini, C.R., 2004a. 'Jackbean', soybean and *Bacillus pasteurii* ureases: biological effects unrelated to ureolytic activity. Eur. J. Biochem. 271, 1357–1363.

Follmer, C., Wassermann, G.E., Carlini, C.R., 2004b. Separation of 'Jackbean' (*Canavalia ensiformis*) urease isoforms by immobilized metal affinity chromatography and characterization of insecticidal properties unrelated to ureolytic activity. Plant Sci. 167, 241–246.

Follmer, C., 2008. Insights into the role and structure of plant ureases. Phytochemistry 69, 18–28.

Girard, C., Jouanin, L., 1999. Molecular cloning of cDNAs encoding a range of digestive enzymes from a phytophagous beetle, *Phaedon cochleariae*. Insect Biochem. Mol. Biol. 29 (12), 1129–1142.

Guiliano, D.B., Hong, X., McKerrow, J.H., Blaxter, M.L., Oksov, Yelena, Liu, Jing, Ghedin, Elodie, Lustigman, Sara, 2004. A gene family of cathepsin L-like peptidases of filarial nematodes is associated with larval molting and cuticle and eggshell remodeling. Mol. Biochem. Parasitol. 136 (2), 227–242.

Houseman, J., 1978. A thiol-activated digestive peptidase from adults of *Rhodinus prolixus* Stal (Hemiptera: Reduviidae). Can. J. Zool. 56 (5), 1140–1143.

Houseman, J.G., Downe, A.E.R., 1981. Identification and partial characterization of digestive peptidases from *Triatoma phyllosoma pallidipennis* (Hemiptera: Reduviidae). Comp. Biochem. Physiol. 70B (4), 713–717.

Houseman, J.G., Downe, A.E.R., 1982a. Identification and partial characterization of digestive peptidases from two species of bedbug (Hemiptera: Cimicidae). Can. J. Zool. 60 (8), 1837–1840.

Houseman, J.G., Downe, A.E.R., 1982b. Characterization of acidic peptidases from the posterior midgut of *Rhodnius prolixus* Stal (Hemiptera: Reduviidae). Insect Biochem. 12 (6), 651–655.

Houseman, J.G., Downe, A.E.R., 1983. Cathespin D-like activity in the posterior midgut of hemipteran insects. Comp. Biochem. Physiol. 75B (3), 509–512.

Houseman, J.G., Macnaughton, W.K., Downe, A.E.R., 1984. Cathepsin B and aminopeptidase in the posterior midgut of *Euschistis euschistoides* (Hemiptera: Pentatomidae). Can. J. Entomol. 116 (10), 1393–1396.

Houseman, J.G., Morrison, P.E., Downe, A.E.R., 1985. Cathepsin B and aminopeptidase in the posterior midgut of *Phymata wolffii* Stal (Hemiptera: Phymatidae). Can. J. Zool. 63 (6), 1288–1291.

Howe, G.A., Jander, G., 2008. Plant immunity to insect herbivores. Annu. Rev. Plant Biol. 59, 41–66.

Koiwa, H., Kato, H., Nakatsu, T., Oda, J., Yamada, Y., Sato, F., 1997. Purification and characterization of tobacco pathogenesis-related protein PR-5d, an antifungal thaumatin-like protein. Plant Cell Physiol. 38 (7), 783–791.

Korkmaz, B., Attucci, S., Juliano, M.A., Kalupov, T., Jourdan, M.L., Juliano, L., Gauthier, F., 2008. Measuring elastase, proteinase 3 and cathepsin G activities at the surface of human neutrophils with fluorescence resonance energy transfer substrates. Nat. Protoc. 3 (6), 991–1000.

Laemmli, U.K., 1970. Cleavage of structural proteins during assembly of the bacteriophage T4. Nature 227, 680–685.

Layne, E., 1957. Spectrophotometric and turbidimetric methods for measuring proteins. Methods Enzimol. 3, 447–454.

Milano, P., Cônsoli, F.L., Zério, N.G., Parra, J.R.P., 1999. Exigências térmicas de *Dysdercus peruvianus* Guérin-Méneville (Heteroptera: Pyrrhocoridae), o percevejo manchador do algodoeiro. Anais da Sociedade Entomológica do Brasil 28 (2), 233–238.

Mobley, H.L., Island, M.D., Hausinger, R.P., 1995. Molecular biology of microbial ureases. Microbiol. Rev. 59, 451–480.

Mulinari, F., Freitas-Silva, M.A., Grossi-De-Sa, M.F., Moraes, M.G., Kurtenbach, E., Carlini, C.R., 2004. Toxina Praguicida, Construção Gênica e Método de Controle de Pragas. National Institute for Intellectual Property (INPI), Brazil. 08/04/2004 [protocol BRPI0403435A].

Mulinari, F., Staniscuaski, F., Bertholdo-Vargas, L.R., Postal, M., Oliveira-Neto, O.B., Ridgen, D.J., Grossi-de-Sa, M.F., Carlini, C.R., 2007. Jaburetox-2Ec: an insecticidal peptide derived from an isoform of urease from the plant *Canavalia ensiformis*. Peptides 28, 2042–2050.

Murdock, L.L., Shade, R.E., 2002. Lectins and peptidase inhibitors as plant defenses against insects. J. Agric. Food Chem. 50 (22), 6605–6611.

Patankar, A.G., Giri, A.P., Harsulkar, A.M., Sainani, M.N., Deshpande, V.V., Ranjekar, P.K., Gupta, V.S., 2001. Complexity in specificities and expression of *Helicoverpa armigera* gut peptidases explains polyphagous nature of the insect pest. Insect Biochem. Mol. Biol. 31 (4–5), 453–464.

Piovesan, A.R., Staniscuaski, F., Marco-Salvadori, J., Real-Guerra, R., Defferrari, M.S., Carlini, C.R., 2008. Stage-specific gut peptidases of the cotton stainer bug *Dysdercus peruvianus*: role in the release of entomotoxic peptides from *Canavalia ensiformis* urease. Insect Biochem. Mol. Biol. 38, 1023–1032.

Polacco, J.C., Holland, M.A., 1993. Roles of urease in plant cells. Int. Rev. Cytol. 145, 65–103.

Puzer, L., Cotrin, S.S., Alves, M.F., Egborge, T., Araujo, M.S., Juliano, M.A., Juliano, L., Bromme, D., Carmona, A.K., 2004. Comparative substrate specificity analysis of recombinant human cathepsin V and cathepsin L. Arch. Biochem. Biophys. 430, 274–283.

Rawlings, N.D., Barrett, A.J., Bateman, A., 2010. MEROPS: the peptidase database. Nucleic Acids Res. 38, D227–D233.

Renard, G., Garcia, J.F., Cardoso, F.C., Richter, M.F., Sakanari, J.A., Ozaki, L.S., Termignoni, C., Masuda, A., 2000. Cloning and functional expression of a *Boophilus microplus* cathepsin L-like enzyme. Insect Biochem. Mol. Biol. 30, 1017–1026.

Ryan, C.A., 1990. Peptidase inhibitors in plants: genes for improving defenses against insects and pathogens. Annu. Rev. Phytopathol. 28, 425–449.

Silva, C.P., Terra, W.R., 1994. Digestive and absorptive sites along the midgut of the cotton seed sucker bug *Dysdercus peruvianus* (Hemiptera: Pyrrhocoridae). Insect Biochem. Mol. Biol. 24, 493–505.

Sirko, A., Brodzik, R., 2000. Plant ureases: role and regulation. Acta Biochim. Pol. 47, 1189–1195.

Sorgine, M.H., Logullo, C., Zingali, R.B., Paiva-Silva, G.O., Juliano, L., Oliveira, P.L., 2000. A heme-binding aspartic peptidase from the eggs of the hard tick *Boophilus microplus*. J. Biol. Chem. 275, 28659–28665.

Staniscuaski, F., Ferreira-Dasilva, C.T., Mulinari, F., Pires-Alves, M., Carlini, C.R., 2005. Insecticidal effects of canatoxin on the cotton stainer bug *Dysdercus peruvianus* (Hemiptera: Pyrrhocoridae). Toxicon 45, 753–760.

Staniscuaski, F., TeBrugge, V., Carlini, C.R., Orchard, I., 2009. In vitro effect of Canavalia ensiformis urease and the derived peptide Jaburetox-2Ec on Rhodnius prolixus malpighian tubules. J. Insect Physiol 55, 255–263.

Staniscuaski, F., TeBrugge, V., Carlini, C.R., Orchard, I., 2010. Jack bean urease alters serotonin-induced effects on Rhodnius prolixus anterior midgut. J. Insect Physiol 56, 1078–1086.

Stotz, H.U., Kroymann, J., Mitchell-Olds, T., 1999. Plant-insect interactions. Curr. Opin. Plant Biol. 2 (4), 268–272.

Te Brugge, V.A., Orchard, I., 2007. Distribution and activity of a Dippu DH31-like peptide in the large milkweed bug *Oncopeltus fasciatus*. Peptides 29, 206–213.

Terra, W.R., Ferreira, C., 1994. Insect digestive enzymes: properties, compartmentalization and function. Comp. Biochem. Physiol. 109, 1–62.

Terra, W.R., Ferreira, C., 2005. Biochemistry of digestion. In: Gilbert, L.I., Iatrov, K., Gill, S. (Org.). Comprehensive Molecular Insect Science, vol. 4. Oxford, pp. 171–224.

Terra, W.R., Ferreira, C., Jordão, B.P., Dillon, R.J., 1996. Digestive enzymes. In: Biology of the Insect Midgut. Chapman and Hall, London, pp. 153–194.

Tomazzeto, G., Mulinari, F., Staniscuaski, F., Settembrini, B.P., Carlini, C.R., Ayub, M.A.Z., 2007. Expression kinetics and plasmid stability of recombinant *E. coli* encoding urease-derived peptide with bioinsecticide activity. Enzyme Microb. Technol. 41, 821–827.

Towbin, H., Staehelin, T., Gordon, J., 1979. Electrophoretic transfer of proteins from polyacrylamide gels to nitrocellulose sheets: procedure and some applications. Proc. Natl. Acad. Sci. U.S.A. 76, 4350–4354.

Woodring, J., Hoffman, K.H., Lorenz, M.W., 2007. Feeding, nutrient flow, and digestive enzyme release in the giant milkweed bug, *Oncopeltus fasciatus*. Physiol. Entomol. 32, 328–335.

II. Artigo Publicado

Martinelli *et al.*, 2014

● Participação no desenho e na execução dos experimentos de toxicidade de Jaburetox e suas formas mutantes sobre o hemíptero *Rhodnius prolixus*, tanto por via oral quanto por injeção na hemolinfa. Item 3.4 (Fig. 5).

Biochimica et Biophysica Acta 1840 (2014) 935–944

Contents lists available at ScienceDirect

Biochimica et Biophysica Acta

journal homepage: www.elsevier.com/locate/bbagen

Structure–function studies on jaburetox, a recombinant insecticidal peptide derived from jack bean (*Canavalia ensiformis*) urease

Anne H.S. Martinelli [a,b], Karine Kappaun [a], Rodrigo Ligabue-Braun [a], Marina S. Defferrari [a], Angela R. Piovesan [a], Fernanda Stanisçuaski [a,c], Diogo R. Demartini [a], Chariston A. Dal Belo [d], Carlos G.M. Almeida [d], Cristian Follmer [e], Hugo Verli [a,c], Celia R. Carlini [a,b,f,*,1], Giancarlo Pasquali [a,c,**,1]

[a] Graduate Program in Cellular and Molecular Biology, Center of Biotechnology, Universidade Federal do Rio Grande do Sul (UFRGS), Porto Alegre, RS, Brazil
[b] Department of Biophysics, Institute of Biosciences, UFRGS, Brazil
[c] Department of Molecular Biology and Biotechnology, UFRGS, Porto Alegre, RS, Brazil
[d] Interdisciplinary Centre of Biotechnological Research, Universidade Federal do Pampa, UNIPAMPA, São Gabriel, RS, Brazil
[e] Department Physical Chemistry, Institute of Chemistry, Universidade Federal do Rio de Janeiro, RJ, Brazil
[f] Instituto do Cérebro (InsCer), Pontifícia Universidade Católica do Rio Grande do Sul, Porto Alegre, RS, Brazil

ARTICLE INFO

Article history:
Received 12 May 2013
Received in revised form 2 November 2013
Accepted 6 November 2013
Available online 14 November 2013

Keywords:
Site-directed mutagenesis
β-hairpin
Urease-derived peptide
Molecular modeling
Membrane-disturbing
Insect

ABSTRACT

Background: Ureases are metalloenzymes involved in defense mechanisms in plants. The insecticidal activity of *Canavalia ensiformis* (jack bean) ureases relies partially on an internal 10 kDa peptide generated by enzymatic hydrolysis of the protein within susceptible insects. A recombinant version of this peptide, jaburetox, exhibits insecticidal, antifungal and membrane-disruptive properties. Molecular modeling of jaburetox revealed a prominent β-hairpin motif consistent with either neurotoxicity or pore formation.
Methods: Aiming to identify structural motifs involved in its effects, mutated versions of jaburetox were built: 1) a peptide lacking the β-hairpin motif (residues 61–74), JbtxΔ-β; 2) a peptide corresponding the N-terminal half (residues 1–44), Jbtx N-ter, and 3) a peptide corresponding the C-terminal half (residues 45–93), Jbtx C-ter.
Results: 1) JbtxΔ-β disrupts liposomes, and exhibited entomotoxic effects similar to the whole peptide, suggesting that the β-hairpin motif is not a determinant of these biological activities; 2) both Jbtx C-ter and Jbtx N-ter disrupted liposomes, the C-terminal peptide being the most active; and 3) while Jbtx N-ter persisted to be biologically active, Jbtx C-ter was less active when tested on different insect preparations. Molecular modeling and dynamics were applied to the urease-derived peptides to complement the structure–function analysis.
Major conclusions: The N-terminal portion of the Jbtx carries the most important entomotoxic domain which is fully active in the absence of the β-hairpin motif. Although the β-hairpin contributes to some extent, probably by interaction with insect membranes, it is not essential for the entomotoxic properties of Jbtx.
General significance: Jbtx represents a new type of insecticidal and membrane-active peptide.

1. Introduction

Ureases (EC 3.5.1.5, urea amidohydrolase), are nickel dependent enzymes that catalyze urea hydrolysis into ammonia and carbon dioxide. Evolutionarily conserved [1], these proteins have been isolated from a wide variety of organisms including plants, fungi and bacteria. In plants, ureases contribute to the bioavailability of nitrogen and in defense mechanisms [2,3]. Ureases represent an unexplored group of plant proteins with potential use for insect control [3,4] and as antifungal agents [5]. Studies have shown that ureases from *Canavalia ensiformis* (jack bean) and *Glycine max* (soybean) display insecticidal activity (reviewed in [6]) and antifungal properties, inhibiting growth and affecting membrane integrity of filamentous fungi [7] as well as of yeasts [8] in the 10^{-7} M range. The urease from pigeon pea (*Cajanus cajan*) was recently described to exhibit insecticidal and antifungal properties at similar dose ranges [9].

The molecular basis of the insecticidal mechanism of action of plant ureases is not yet completely understood [6]. It has been demonstrated that the entomotoxic effect of canatoxin [10], an isoform of *C. ensiformis* (jack bean) urease [11], is partially due to an internal 10 kDa peptide

Abbreviations: Jbtx, jaburetox; JbtxΔ-β, β-hairpin deleted version of Jbtx; Jbtx N-ter, N-terminal domain of Jbtx; Jbtx C-ter, C-terminal domain of Jbtx; Jbtx-2Ec, a version of Jbtx containing a V5 epitope; LUV, large unilamellar vesicle; MD, molecular dynamics; RMSD, root mean square deviation; CD, circular dichroism

* Correspondence to: C. R. Carlini, Center of Biotechnology and Department of Biophysics, Universidade Federal do Rio Grande do Sul, Av. Bento Gonçalves, 9500, Predio 43.431, Porto Alegre, RS, CEP 91501-970, Brazil. Tel.: +55 51 3308 7606.
** Correspondence to: G. Pasquali, Department of Molecular Biology and Biotechnology, Universidade Federal do Rio Grande do Sul, Av. Bento Gonçalves, 9500, Predio 43.432, Porto Alegre, RS, CEP 91501-970, Brazil.
E-mail addresses: ccarlini@ufrgs.br, celia.carlini@pq.cnpq.br (C.R. Carlini), pasquali@cbiot.ufrgs.br (G. Pasquali).
[1] These authors share senior authorship.

0304-4165/$ – see front matter © 2013 Elsevier B.V. All rights reserved.
http://dx.doi.org/10.1016/j.bbagen.2013.11.010

(pepcanatox), that is released from the protein upon hydrolysis by insect cathepsin-like digestive enzymes [12–16]. Jaburetox-2Ec (Jbtx-2Ec), a recombinant peptide analog to pepcanatox, exhibited a potent insecticidal effect on two economically important crop pests: *Spodoptera frugiperda* (fall armyworm) and *Dysdercus peruvianus* (cotton stainer bug) [17,18]. Jbtx-2Ec was also shown to both permeabilize large unilamellar liposomes (LUVs) [19] and to affect transmembrane potential of insect Malpighian tubules, causing inhibition of diuresis [20]. A β-hairpin motif in the modeled structure of Jbtx-2Ec has been proposed [17,19] and its presence has been confirmed in the crystallographic structures of jack bean [21] and pigeon pea [9] ureases. This motif is present also in one class of pore-forming peptides and neurotoxic peptides [22] such as charybdotoxin, which affect ion channels [23]. A variant form of Jbtx-2Ec lacking the fused V5-antigen, here called simply Jbtx, also exhibited antifungal activity [8].

Aiming to identify motifs possibly involved in the different biological activities of Jbtx, here we described the cloning and expression of mutated versions of the Jbtx-encoding cDNA. Truncated versions of the peptide, with deletions of the regions of the β-hairpin motif, the N-terminal or the C-terminal halves of the molecule, were tested on LUV permeabilization, for insecticidal and other entomotoxic effects. Structural analyses of the truncated peptides were also carried out.

2. Materials and methods

2.1. Jbtx cDNA constructs

Jaburetox-2Ec, the first version of the recombinant urease-derived peptide cloned in [17], harbored a V5-antigen with 18 amino acids derived from the pET101/D-TOPO plasmid. In order to eliminate this foreign sequence, the jack bean urease truncated cDNA encoding 93 amino acids, called simply jaburetox (Jbtx), was cloned and expressed in *Escherichia coli* via pET-23a vector (Novagen), as described in [8]. This sequence was used as template for site-directed mutagenesis and PCR amplifications of the mutant forms as described below.

2.2. Jbtx lacking the internal β-hairpin (JbtxΔ-β)

In order to delete the β-hairpin motif (residues 61–74) of the Jbtx peptide, site-directed mutagenesis was performed using the QuickChange Site-directed Mutagenesis Kit (Stratagene). As this method is often used to generate a few nucleotide deletions, some modifications in the primers' design were made, as described by [24]. Pairs of complementary primers were designed (Table 1), and site-directed mutagenesis was performed according to the kit manufacturer's instructions. The deleted gene version was confirmed by sequencing on an ABI Prism 3100 automated sequencer (Applied Biosystems) platform (ACTGene Ltd, Center of Biotechnology, UFRGS). Sequence comparisons were performed using the BLASTx software [25], available at (http://www.ncbi.nlm.nih.gov). The resulting peptide was called JbtxΔ-β.

Table 1
Primers used in this study.

Primer	Size	Sequence
5′ Del_β-hairpin	40-Mer	AGTATGGTCCGACTATTGGTGAAAAGGATTTTGCCCT TTA
3′ Del_ β-hairpin	40-Mer	TAAAGGGCAAAATCCTTTTCACCAATAGTCGGACCAT ACT
5′ Del_ α-helix	40-Mer	CTTTCACCAAAGCCATTCCTTATGGTCCGACTATTGGTGA
3′ Del_ α-helix	40-Mer	TCACCAATAGTCGGACCATAAGGAATGGCTTTGGTGA AAG
5′ N-terminal	25-Mer	CCAACATATGGGTCCAGTTAAATGA
3′ N-terminal	25-Mer	CCCCCTCGAGGGTGAAAGGACAATC
5′ C-terminal	25-Mer	CCAACATATGAAAGCCATTCCTCGT
3′ C-terminal	25-Mer	CCCCCTCGAGTATAACTTTTCCACC

2.3. Jbtx N-terminal (Jbtx N-ter) and C-terminal (Jbtx C-ter) domain versions

The Jbtx gene regions corresponding to the N-terminal (residues 1–44) and C-terminal (residues 45–93) halves of the peptide were amplified by PCR with specifically designed primers (Table 1) and products were cloned into pET23a (Novagen). PCRs were performed in a final volume of 50 μL containing 50 ng of the template plasmid DNA, 200 ng of each primer, 200 μM each dNTPs, 2.5 U *Pfu* taq DNA polymerase (Fermentas) and 1× *Pfu* reaction buffer. Amplification was carried out under the following conditions: denaturation at 95 °C for 3 min, annealing at 55 °C for 30 s and elongation at 72 °C for 2 min. After a total of 35 cycles, the final products were digested with *Nde*I and *Xho*I (Fermentas), dephosphorylated with thermosensitive alkaline phosphatase (Promega) and ligated into the expression vector pET23a (Novagen). The inserts of the recombinant plasmids were fully sequenced in order to confirm their sequences essentially as described above. The resulting peptides were called Jbtx N-terminal (Jbtx N-ter) and Jbtx C-terminal (Jbtx C-ter). A schematic representation of all Jbtx-related peptides is shown in Fig. 1.

2.4. Expression and purification of Jbtx recombinant peptides

Recombinant pET23a plasmids were transformed into *E. coli* BL21-CodonPlus (DE3)-RIL cells (Stratagene) for Jbtx gene expressions following the provider's instructions. For the purification of the original Jbtx peptide and its mutated forms, 200 mL of Luria Bertani medium containing 100 μg/mL ampicillin and 40 μg/mL chloramphenicol were separately inoculated with 2 mL overnight cultures of each *E. coli* strain. Cells were grown for approximately 2 h at 37 °C under shaking until an optical density of 0.7 was reached. At this point, IPTG was added to cultures to a final concentration of 0.5 mM. After 3 h of additional culture, cells were harvested by centrifugation and suspended in 10 mL of lysis buffer (50 mM Tris buffer, pH 7.5, 500 mM NaCl, 5 mM imidazole), sonicated and centrifuged (14,000 *g*, 30 min). The supernatant was loaded onto a Ni^{+2} loaded Chelating Sepharose (GE Healthcare) column, previously equilibrated with the lysis buffer. After 30 min, the column was washed with 50 mL of the same buffer containing 50 mM imidazole. Bound protein was eluted with 200 mM imidazole in the lysis buffer. Samples were then dialyzed against buffer A (50 mM phosphate buffer, pH 7.5, 1 mM EDTA, 5 mM β-mercaptoethanol) in order to remove the imidazole. Protein concentration was measured by Bradford assay [26]. Predicted molecular mass of the peptides was obtained by submitting the deduced sequences to the ProtScale tool [27] available at the Expasy site (http://web.expasy.org/protscale).

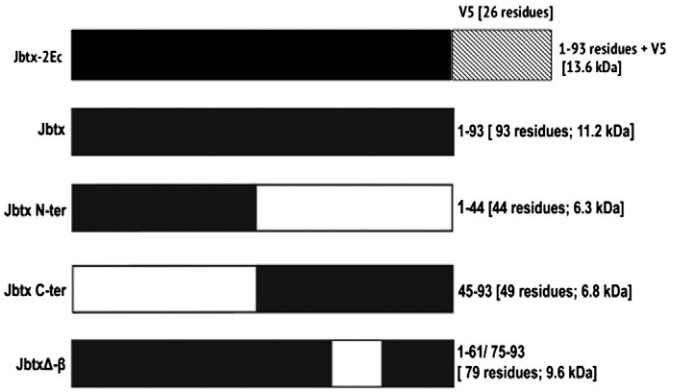

Fig. 1. Schematic representation of the sequences of jaburetox and mutants. The number of amino acid residues of each molecule (shown in black) is indicated on the right side.

Molar concentrations of peptides were calculated assuming a monomeric form in solution. Hydropathicity analysis of the peptides was carried out according to [28].

2.5. Tandem mass spectrometry (MS/MS)

In gel digestion of Jbtx peptides was performed for all samples analyzed, except for the positive control (C+), which was submitted to in solution digestion. For in gel digestion the protocol in [29] was followed, using 50 mM ammonium bicarbonate (AB) unless otherwise explained. Briefly, the bands on the gel were distained with 50 mM AB in 40% acetonitrile (ACN). Following, gel pieces were dehydrated with 100% ACN and lyophilized. Reduction was performed with 50 mM dithiothreitol (DTT) in 50 mM AB, for 30 min at 56 °C, in the dark, followed by the alkylation performed with 50 mM iodoacetamide (IAA) in 50 mM AB for 30 min, at room temperature, also in the dark. The gel pieces were washed with 50 mM AB + 40% ACN for 15 min, and a second dehydration step was done. Proteins in the gel were digested for 3 h (Jbtx N-ter and Jbtx C-ter) or 16 h (Jbtx and JbtxΔ-β) in 500 μL of 100 mM AB solution containing 100 ng of sequencing grade trypsin (Promega) at 37 °C. After digestion, supernatants were transferred to microcentrifuge tubes and gel pieces were washed with 1% formic acid in 60% ACN, and the supernatants were combined accordingly. Digested peptides were lyophilized and submitted to tandem mass spectrometry analyses. In the case of in solution digestion, sample of Jbtx peptide (30 μg in 20 mM sodium phosphate, 5 mM β-mercaptoethanol, 1 mM EDTA, pH 7.5) was reduced with 50 mM DTT and alkylated with 50 mM IAA (30 min each, at room temperature). Then, DTT to a final concentration of 10 mM was added for 15 min at room temperature. Digestion was performed in this case with 0.6 mg of trypsin (Promega) for 3 h at 37 °C. After the digestion process, the samples were desalted with ZipTip™ (Millipore®) according to the manufacturer's instructions. The eluted peptides were lyophilized and analyzed by tandem mass spectrometry.

The lyophilized digested peptides were suspended in 0.1% formic acid (10 μL) and 5 μL of each solution was subjected to reversed phase chromatography (NanoAcquity UltraPerformance LC-UPLC® chromatograph (Waters) using a Nanoease C18, 75 μm ID at 35 °C. The column was equilibrated with 0.1% trifluoroacetic acid (TFA) and the peptides were eluted in a 20 min gradient, ramping from 0 to 60% acetonitrile in 0.1% TFA at 0.6 nL/min constant flow. Eluted peptides were subjected to electrospray ionization and analyzed by mass spectrometry using a Q-TOF Micro™ spectrometer (Micromass). The voltage applied to the cone for the ionization step was 35 V. The three most intense ions in the range of m/z 200–2000 and +2 or +3 charges were selected for fragmentation. The acquired MS/MS spectra were processed using the Proteinlynx v.2.0 software (Waters) and the generated .mgf files were used to perform database searches using the MASCOT software version 2.4.00 (Matrix Science) against the NCBI database, and taxid was restricted to Viridiplantae (taxid:33090). Results were analyzed manually.

2.6. Electrophoresis

The peptide fractions of Jbtx and its mutant forms were visualized in SDS-Tricine gels [30]. The gels were stained with colloidal Coomassie G-250 (Sigma Chem. Co) according to [31].

2.7. Western blot

Western blots were performed according to [32]. Briefly, peptides were electrophoresed, transferred to PVDF membranes (Millipore) and immersed in a blocking buffer consisting of 5% nonfat dry milk in phosphate-buffered saline (PBS, 137 mM NaCl, 2.7 mM KCl and 4.3 mM $Na_2HPO_4 \cdot 7H_2O$, pH 7.3). After washing, the membrane was incubated with rabbit anti-jaburetox-2Ec polyclonal antibodies (1:7500 dilution) for 2 h at room temperature, followed by a 2 h incubation with anti-rabbit IgG (1:20,000 dilution) alkaline phosphatase conjugate (Sigma Chem. Co.). Colorimetric detection was carried out using 5-bromo-4-chloro-3-indolyl-phosphate p-toluidine salt and nitro-blue tetrazolium chloride.

2.8. Leakage experiment

Large unilamellar vesicles (LUVs) were produced and the leakage experiment was conducted as described previously [19]. LUVs were prepared using 10 mg of L-α-phosphatidic acid (egg chicken, Avant Polar Lipids), at a concentration of 20 mg/mL. The leakage promoted by Jbtx and its mutated forms at a final concentration of 5 μg/mL in 25 mM Tris, pH 7.0, was evaluated by the carboxyfluorescein release assay [19]. The concentration of LUVs in the experiment was estimated based on the absorbance of the fluorescent probe at 490 nm, and adjusted to a value of 0.1. In the leakage assays, fluorescence intensity of the reaction mixture (LUVs plus peptide or buffer) was recorded as a function of time. The samples were excited at 490 nm and the fluorescence was acquired at 518 nm. It was assumed that the absence of leakage (0%) corresponded to the fluorescence of the vesicles at time zero; 100% leakage was taken as the value of fluorescence intensity obtained after the addition of 1% (v/v) Triton X-100. All measurements were carried out in a Cary Eclipse fluorescence spectrophotometer (Varian).

2.9. Insecticidal activity

Fifth-instar *Rhodnius prolixus* were kindly provided by Dr. Hatisaburo Masuda and Dr. Pedro L. Oliveira (Institute of Medical Biochemistry, Universidade Federal do Rio de Janeiro, RJ, Brazil) and by Dr. Denise Feder (Universidade Federal Fluminense, RJ, Brazil). The phytophagous milkweed bugs (*Oncopeltus fasciatus*) were reared in our laboratory as previously described [15].

2.9.1. Injection assays

Fifth instars of *O. fasciatus* or *R. prolixus* were injected into the hemocoel using a Hamilton Microliter 900 series syringe (Hamilton). Group of 10 insects (*O. fasciatus*) or 5 insects (*R. prolixus*) were injected with 20 mM sodium phosphate buffer (pH 7.5) containing peptides at a final dose of 0.015 μg (*O. fasciatus*) or 0.05 μg (*R. prolixus*) per mg of insect body weight. Control insects received injections of buffer alone. Mortality rate within each group was recorded after 48 or 96 h. Two independent bioassays were carried out for each peptide on each insect model. Results shown are means ± standard errors.

2.9.2. Feeding assays

Fifth instars *R. prolixus* were fed on *R. prolixus* saline solution (150 mM NaCl, 8.6 mM KCl, 2.0 mM $CaCl_2$, 8.5 mM $MgCl_2$, 4.0 mM $NaHCO_3$, 34.0 mM glucose, 5.0 mM HEPES, pH 7.0) containing 1 mM ATP and enough peptide (tested individually) to give final doses of 0.1 μg per mg of body weight. Groups of 5 insects for each peptide were fed for approximately 30 min, at 37 °C, by placing their mouth apparatus inside glass capillaries containing the test solutions. Control insects fed solely on *R. prolixus* saline solution containing 1 mM ATP, under the same conditions. Mortality rate within each group was recorded after 24 h. One triplicated bioassay was carried out for each peptide. The results shown are means and standard errors.

2.10. Measurement of fluid secretion by Rhodnius prolixus Malpighian tubules

The assay was performed essentially as described in [20], using *R. prolixus* serotonin-stimulated Malpighian tubules. Secretion rate was expressed as the percentage of fluid secretion measured after the addition of Jbtx or mutated peptides as compared to serotonin (2.5×10^{-8} M) alone (control). For each peptide and dose, 5–6 replicates were done. The results shown are means ± standard error.

2.11. In vivo cockroach metathoracic coxal-adductor nerve–muscle preparation

The *in vivo* cockroach metathoracic coxal-adductor muscle preparation was used [33] to characterize further the entomotoxic activity of Jbtx and its mutated versions. Male adult *Phoetalia pallida* (3–4 months after molting) were reared in our laboratory at controlled temperature (22–25 °C) on a 12 h:12 h light:dark cycle. Animals were immobilized by chilling and mounted, ventral side up, in a Lucite holder covered with 1 cm soft rubber that restrained the body and provided a platform to which the metathoracic coxae could be firmly attached using entomologic needles. The left leg was then tied at the medial joint with a dentistry suture line connected to a 1 g force transducer (AVS Instruments, São Carlos, SP, Brazil). The transducer was mounted in a micromanipulator to allow adjustment of muscle length. The exoskeleton was removed from over the appropriated thoracic ganglion. Nerve 5, which includes the motor axon to the muscle, was exposed and a bipolar electrode was inserted to provide electrical stimulation. The nerve was covered with mineral oil to prevent dryness and stimulated at 0.5 Hz, 5 ms, with twice the threshold, during 120 min. Twitch tension was digitalized, recorded and retrieved using a computer based software AQCAD (AVS Instruments, São Carlos, SP, Brazil). Data were further analyzed using the software ANCAD (AVS Instruments, São Carlos, SP, Brazil). Jbtx and peptides were dissolved in insect physiological solution (214 mM NaCl, 3.1 mM KCl, 9 mM $CaCl_2$, 0.1 mM $MgSO_4$, and 5 mM HEPES, pH 7.2 [34]). The test solutions were prepared daily and 20 μL were injected into the insect's third abdominal segment using a Hamilton syringe.

2.12. Molecular modeling and simulation

The three-dimensional model for Jbtx was built by comparative modeling with MODELLER9v10 [35] employing the structure of the *C. ensiformis* major urease isoform (PDB ID: 3LA4), [21] as template. Ten models were built, stereochemically evaluated and theoretically validated for their three-dimensional profiles with PROCHECK [36] and Verify3D [37], respectively. The best scored model was then selected. The amino-terminal Met residue and the carboxy-terminal LEHHHHHH segment were added with SwissPDBviewer [38]. The Jbtx peptide was then subjected to molecular dynamics (MD) simulations with GROMACS 4.5 suite [39] using GROMOS96 53a6 force field [40] for 500 ns. The systems were solvated in triclinic boxes using periodic boundary conditions and SPC water models [41]. Counterions (Na^+) were added to neutralize the systems. The Lincs method [42] was applied to constrain covalent bond lengths, allowing an integration step of 2 fs after an initial energy minimization using Steepest Descents algorithm. Electrostatic interactions were calculated with Particle Mesh Ewald method [43]. Temperature and pressure were kept constant by coupling proteins, ions, and solvent to external temperature and pressure baths with coupling constants of $\tau = 0.1$ and 0.5 ps [44], respectively. The dielectric constant was treated as $\varepsilon = 1$, and the reference temperature was adjusted to 300 K. The system was slowly heated from 50 to 300 K, in steps of 5 ps, each step increasing the reference temperature by 50 K, allowing a progressive thermalization of the molecular system. The simulation was performed to 500 ns, with no restraint, considering a reference value of 3.5 Å between heavy atoms for a hydrogen-bond, and a cutoff angle of 30° between hydrogen-donor–acceptor [39].

2.13. Statistical analysis

Data were evaluated by ANOVA followed by the Bonferroni's or Student *t* test using GraphPad Prism software (Version 5.0 for Windows). See legends to figures for more details. A $p < 0.05$ was considered statistically significant.

3. Results

3.1. MD simulation of Jbtx

It has been previously suggested that a prominent β-hairpin in the predicted model of the urease-derived peptide Jbtx could be responsible at least in part for its membrane-disturbing activity and some of its biological properties [17,19]. The presence of this β-hairpin was confirmed by x-ray crystallographic data of jack bean urease [21], and short simulations of the crystal-derived peptide were performed [45].

In order to establish if this β-hairpin would still be present in the peptide once it has been released from the urease molecule, a 3D-model of Jbtx was constructed using the crystal structure of jack bean urease as template and subjected to molecular dynamics for 500 ns (Fig. 2, panels A and B). The MD simulation indicated that Jbtx becomes more globular when in aqueous solution (Fig. 2, panel B), changing its conformation along the simulation with an increase of RMSD, as compared to the initial crystal-derived structure (Supplementary Fig. 1). The secondary structure of Jbtx changed in solution, with loss of many helix turns and formation of a minute beta sheet. The β-hairpin at Jbtx's C-terminal half was conserved despite the increase in coil content (Fig. 2, panels B and D).

3.2. Expression of recombinant jaburetox (Jbtx) and mutated forms

Aiming to identify motifs probably involved in the biological activities of Jbtx, mutated forms of the peptide lacking the internal β-hairpin (JbtxΔ-β), the N-terminal half (Jbtx C-ter) or the C-terminal half (Jbtx N-ter) domains were constructed. A schematic representation of these peptides is shown in Fig. 1.

All the His-tagged peptides were purified and analyzed by SDS-PAGE (Fig. 3A and B). The predicted molecular masses of the peptides based on their deduced amino acid sequences are 11,193 Da for Jbtx, 9625.6 Da for JbtxΔ-β, 6325.8 Da for Jbtx N-ter and 6772.5 Da for Jbtx C-ter. As it can be observed from the SDS-PAGE results, all the recombinant peptides showed the expected mass, except for the Jbtx N-ter peptide which behaved as a dimer with an estimated molecular mass of approximately 12 kDa (Fig. 3B).

Anti-Jbtx-2Ec polyclonal antibodies recognized equally Jbtx-2Ec, Jbtx and JbtxΔ-β (result not shown) and although with a weaker reactivity, also interacted with the two half-peptides (Fig. 3C).

All bands seen in the lanes corresponding to each peptide were excised from the SDS-PAGE gels, digested with trypsin and submitted to MS/MS analysis. The identities of the peptides Jbtx, JbtxΔ-β, and Jbtx C-ter (and aggregated forms of the peptides) were confirmed by MS/MS analysis as shown in Fig. 3D. On the other hand, the peptide Jbtx N-ter was not identified in the MS/MS assay. The band corresponding to the dimer of the peptide Jbtx N-ter in the SDS-PAGE (Fig. 3B) reacted positively with the anti-Jbtx antibodies (Fig. 3C), thus confirming its identity. The tendency to form aggregates previously described for jaburetox-2Ec [19,46] persisted in Jbtx, as well as in all the mutated forms of this peptide, as confirmed by the MS/MS analysis. After a few days in aqueous solution, all the peptides formed insoluble precipitates. These aggregates did not revert to the monomeric state under a number of tested conditions [19]. High ionic strength accelerates the aggregation of Jbtx (data not shown), suggesting hydrophobic interactions as a driving force for the oligomerization process. Because it was not possible to ascertain the oligomeric state of each peptide in solution, their monomeric states were considered when expressing molar concentrations in the subsequent assays.

Since all mutated peptides retained considerable antigenicity towards anti-Jbtx-2Ec polyclonal antibodies, they probably kept their tridimensional structures, resembling the corresponding portions in Jbtx. The CD spectrum of Jbtx (not shown) indicated the presence mainly of irregular structures, with a minor contribution of β-sheets and helices. This type of CD spectrum has been observed for Chab I,

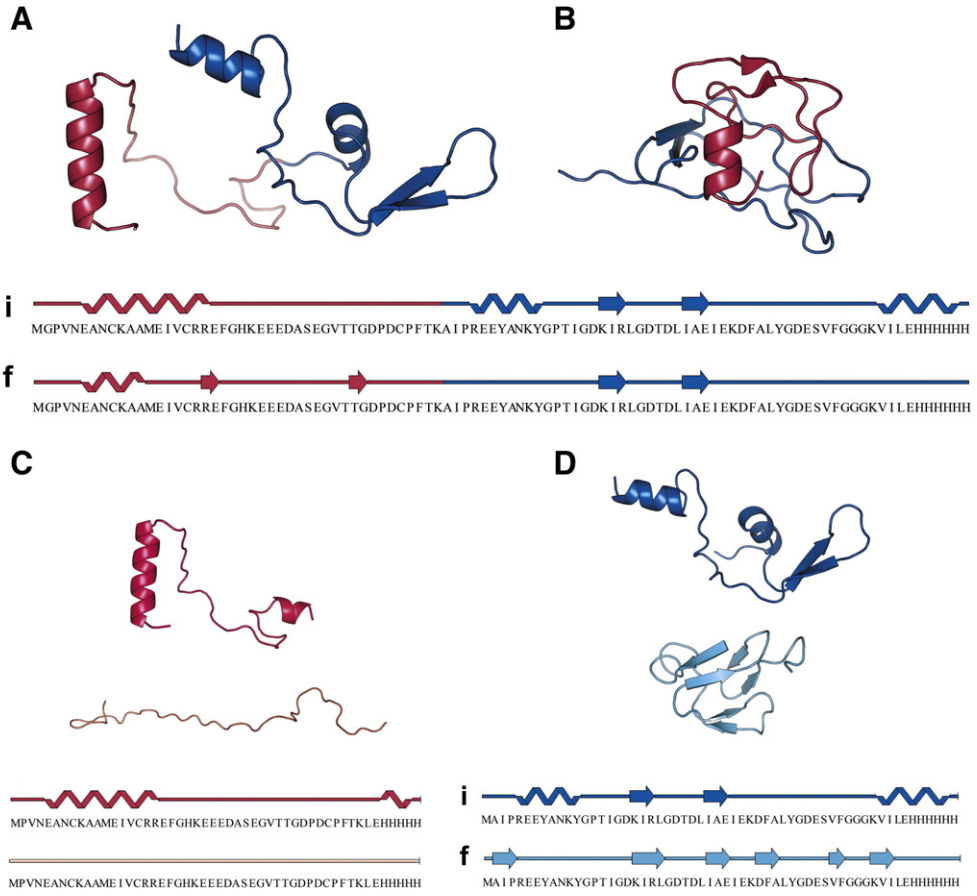

Fig. 2. Structural changes in jaburetox and its mutated versions after MD simulation of 500 ns. Three-dimensional representations of the full Jbtx peptide (A) initial and (B) final structures, with the N-terminal domain (residues 1–44) depicted in pink and the C-terminal domain in blue; (C) Jbtx N-ter (amino-terminal mutant): top, initial state; bottom, final state; (D) Jbtx C-ter (carboxy-terminal mutant): top, initial state; bottom, final state; Schematic representations of the secondary structure content of the (i) initial and (f) final structures are colored according to their three-dimensional counterparts. The corresponding amino acid sequences are also shown.

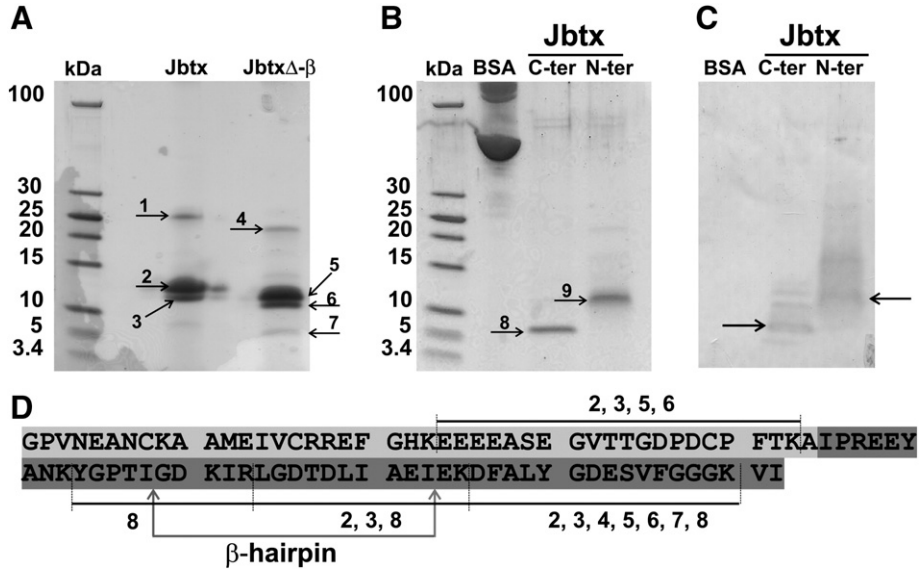

Fig. 3. (A and B) SDS-Tricine PAGE of jaburetox and their derived peptides. Numbered arrows indicate the bands that were excised and analyzed by mass spectrometry. *Lanes*: Jbtx, jaburetox; JbtxΔ-β, jaburetox with deleted β-hairpin motif; BSA, bovine serum albumin; C-ter, carboxy-terminal region of jaburetox; N-ter, amino-terminal region of jaburetox. (C) Western blot analysis with polyclonal anti-jaburetox antibodies. *Lanes*: BSA, bovine serum albumin as negative control; C-ter, carboxy-terminal region of jaburetox; N-ter, amino-terminal region of jaburetox; (D) amino acid sequence of jaburetox. The numbered lines above and below the sequence correspond to the arrows in panels A and B, showing parts of the jaburetox sequence identified by mass spectrometry. The sequence of Jbtx N-ter mutant is shown in light gray and that of the Jbtx C-ter in dark gray. The region corresponding to the β-hairpin is also indicated.

a charybdotoxin analog [47], and also for the acid unfolded state of equine β-lactoglobulin, which has residual helices and β-hairpins [48,49].

Simulations were carried out to establish the putative structures in solution of the mutated peptides representing the two half domains of Jbtx. The N-terminal mutant (residues 1 to 44) became completely unfolded after simulation (Fig. 2, panel C), while the C-terminal mutant (residues 45 to 93) showed propensity towards stabilization of a newly-formed β-sheet (Fig. 2, panel D).

3.3. Vesicle leakage promoted by Jbtx peptides

We employed LUVs composed by L-α-phosphatidic acid [19] as a membrane model to evaluate which part of the Jbtx molecule interacts with phospholipid membranes and induces vesicle leakage. Fig. 4 shows typical results. Vesicle leakage was more prominent when LUVs were treated with either Jbtx C-ter or Jbtx (5 μg/mL), although all peptides produced at least 80% of leakage at the end of the 10 min incubation period. Taken together, these findings showed that the β-hairpin is not essential for the membrane-disruptive activity of Jbtx. Moreover, the data indicated that all Jbtx-related peptides are able to induce LUV leakage, while the C-terminal region of the peptide seems to contribute the greatest effect. In fact, hydropathicity plots indicated the presence of prominent hydrophobic regions in both, the N-terminal and the C-terminal domains of Jbtx (Supplementary Fig. 2).

3.4. Insecticidal effect of Jbtx peptides

In order to compare the insecticidal activity of Jbtx to that previously described for Jbtx-2Ec [6,18], we tested the entomotoxic effect of Jbtx upon injection into *R. prolixus* nymphs. Employing a dose of 0.05 μg/mg of insect weight, 100% mortality was observed 48 h after injection (result not shown), indicating that the absence of the V5 epitope in Jbtx did not affect its insecticidal property. When the insecticidal activity of the β-hairpin deleted form (JbtxΔ-β) was assayed in *R. prolixus* nymphs, it produced an entomotoxic (mortality) effect equivalent to that of the original Jbtx, either by injection (Fig. 5A) or by feeding (Fig. 5B). Four days after injection into fifth instars *R. prolixus*, we have observed that the Jbtx N-term induced up to 60% mortality, while Jbtx C-ter caused less than 10% mortality

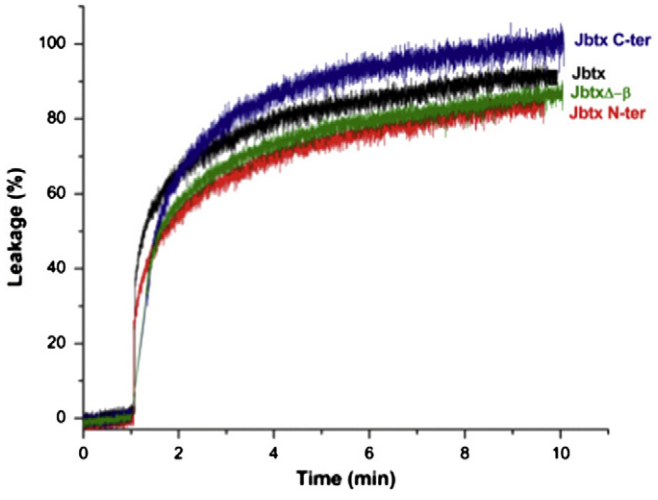

Fig. 4. Effect of jaburetox and derived mutants on LUVs composed by L-α-phospatidic acid. The carboxyfluorescein release assay was performed for each peptide at a final concentration of 5 μg/mL (Jbtx, 0.44 μM; JbtxΔ-β, 0.51 μM; Jbtx N-ter, 0.79 μM; and Jbtx C-ter, 0.73 μM) in 25 mM Tris, pH 7.0. The absence of leakage (0%) corresponds to the fluorescence of the vesicles at time zero; 100% leakage was taken as the value of fluorescence intensity obtained after addition of 1% (v/v) Triton X-100. The experiments were performed at 25 °C. The figure shows superimposed tracings of a typical result for each peptide to facilitate comparison.

(Fig. 5A). On the other hand, 24 h after feeding, both Jbtx N-ter and Jbtx C-ter had similar lethal effects on *R. prolixus* nymphs, ranging from 60 to 80% mortality (Fig. 5B).

Fifth instars *O. fasciatus* were also injected with Jbtx and its mutant variants. Similarly to what was observed for *R. prolixus* upon injections, Jbtx N-ter (Fig. 6A) and JbtxΔ-β (Fig. 6B) displayed lethal effects comparable to that of Jbtx, while Jbtx C-ter was near to inactive (Fig. 6A), suggesting that the N-terminal portion of the Jbtx carries its insecticidal domain.

3.5. Antidiuretic effect of Jbtx-related peptides on Malpighian tubules

We have previously described that, in the dose range of 10^{-16} to 10^{-15} M, Jbtx 2-Ec inhibited the serotonin-stimulated fluid secretion in *R. prolixus* Malpighian tubules [20]. Fig. 7 shows that Jbtx and all its variants, at a concentration of 1×10^{-15} M, were able to inhibit fluid secretion in the tubules producing similar antidiuretic effect.

3.6. In vivo neuromuscular blockade of cockroach nerve–muscle preparations induced by Jbtx-related peptides

The injection of Jbtx or its mutant versions (32 μg/g of animal weight) produced a time-dependent blockade of the cockroach nerve–muscle preparation (Fig. 8). Jbtx was the most effective and induced a complete neuromuscular paralysis at 35 ± 10 min followed by Jbtx N-ter at 80 ± 2 min (Fig. 8B). In contrast, the neuromuscular blockades induced by Jbtx Δ-β or Jbtx C-ter were only partial at the end of the 120 min recording time. The administration of insect saline alone did not interfere with normal neuromuscular responses during 120 min recordings (Fig. 8A). Thus, similar to what was observed in the case of the insecticidal activity (upon injection), these data suggest that the N-terminal half of Jbtx carries its entomotoxic domain. In this type of assay, however, there is a contribution of the β-hairpin to the effect.

4. Discussion

In this study we evaluated the jack bean urease-derived peptide Jbtx and three domain-deleted variants in order to identify the regions of the molecule that are critical for its entomotoxic activities. A previous version of Jbtx, harboring a large V5-antigen derived from the pET101/D-TOPO plasmid and called jaburetox-2Ec (Jbtx-2Ec), was shown to be lethal to *R. prolixus* by oral route and hemocoel injection [50,51] and to permeabilize vesicles composed of charged lipids [19]. Jbtx has the same 93 amino acid urease-derived sequence and the polyhistidine tail found in Jbtx-2Ec, but lacks the V5 epitope present in the later. Here we demonstrated that Jbtx displays insecticidal activity equivalent to that described for Jbtx-2Ec, evidencing that the epitope V5 is not implied in its entomotoxicity.

Comparing the structure obtained here for Jbtx with the model of jaburetox-2Ec generated by comparative modeling [19] (prior to the first description of the crystal structure of a plant urease [21]), important conformational similarities can be seen in the region correspondent to the short helix as well as in the large content of random coil conformation, even though jaburetox-2Ec exhibited a more well-defined β-hairpin than Jbtx. The differences in the models generated for these peptides might be attributed in part to the distinct initial structures used in the MD simulation, as *H. pylori* urease and jack bean urease served as template in the comparative modeling for jaburetox-2Ec [19] and Jbtx (this work), respectively.

Balasubramanian and Ponnuraj [21] were the first to report in 2010 the crystal structure of a plant (*C. ensiformis*, jack bean) urease at 2.05 Å of resolution. These authors confirmed the presence of an internal β-hairpin motif in the jack bean urease, previously suggested by our group to be present in the structure of jaburetox-2Ec [17,19], and proposed to be involved in the insecticidal activity of both urease and its derived entomotoxic peptide. The same group described insecticidal

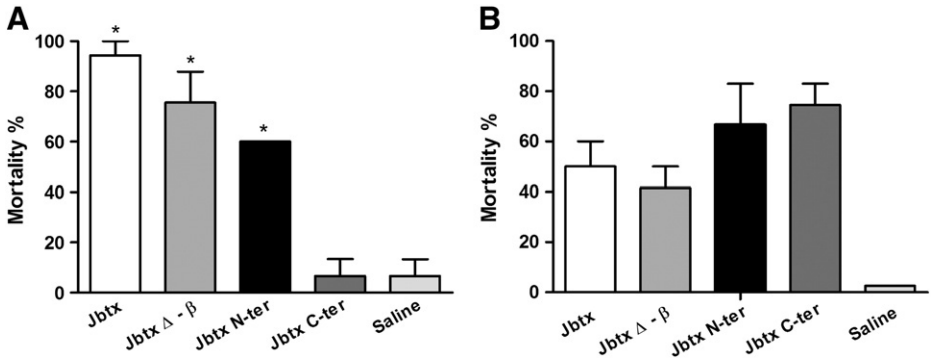

Fig. 5. Insecticidal effect of Jbtx and derived peptides on fifth instar *Rhodnius prolixus*. (A) Groups of 5 insects were injected with each peptide separately at final doses of 0.05 μg per mg of body weight. Control insects were injected with *Rhodnius* saline. The mortality was recorded after 96 h. Two independent bioassays were carried out for each peptide. Results shown are means and standard error. (B) Groups of 5 insects were fed on *R. prolixus* saline plus 1 mM ATP and the peptides separately at final doses of 0.1 μg per mg of body weight. Control insects were fed solely on *R. prolixus* saline plus 1 mM ATP. Mortality rate within each group was recorded after 24 h. Results shown are means and standard error.

and antifungal properties of the pigeon pea (*Cajanus cajan*) urease and reported the presence of a similar β-hairpin motif in the crystal structure of this urease [9]. Moreover, Balasubramanian and coworkers, using molecular modeling studies and short (5 ns) molecular dynamics simulations of Jbtx, suggested that its β-hairpin could self-associated into a β-barrel able to anchor into a membrane-like environment, and hypothesized an insecticidal mode of action of Jbtx based on pore formation [45].

Also present in bacterial ureases, the microbial β-hairpin motif is formed with contributions from the α- and the β urease chains while its counterpart in the single chain of plant ureases is formed exclusively by amino acids located in a region corresponding to the bacterial α-chain [21]. Our group reported that, contrasting to plant ureases, *Bacillus pasteurii* urease has no insecticidal activity against *Dysdercus peruvianus* [52]. Since the β-hairpin motif is present in the *B. pasteurii* urease as well [21], a plausible explanation for this could be the fact that part of the sequence corresponding to the N-terminal half of Jbtx is missing in bacterial ureases.

Here we demonstrated that Jbtx and JbtxΔ-β, its β-hairpin deleted version, behaved almost indistinguishably regarding LUV leakage, antidiuretic effect and insecticidal activity upon injection. These results strongly suggested that the β-hairpin motif is not involved in membrane-disturbing activity or in these biological properties of the peptide.

At that point we had no clues to any other possible motif in the Jbtx molecule that could be responsible for its biological properties, so we decided to produce two half-peptides, corresponding to the N-terminal and C-terminal half versions of Jbtx (Jbtx N-ter and Jbtx C-ter, respectively). The mutated peptides Jbtx N-ter and Jbtx C-ter were then tested for LUV leakage and for different types of entomotoxic activities. Two distinct groups of results were obtained depending on the assay: (i) Jbtx, JbtxΔ-β and Jbtx N-ter were equally active while and Jbtx C-ter was inactive or significantly less active; and (ii) all the peptides produced similar effects.

When tested for insecticidal activity upon injection into *R. prolixus* (Fig. 5A) or *O. fasciatus* (Fig. 6) nymphs, Jbtx, Jbtx Δ-β and Jbtx N-ter caused significant mortality after 96 h, while the survival rate of insects injected with Jbtx C-ter was equivalent to that of control group. It thus became clear from these experiments that the N-terminal half of Jbtx (Jbtx N-ter) has the insecticidal domain of Jbtx. This conclusion agrees with the fact that the deletion of the β-hairpin, which is present in the Jbtx C-ter, did not interfere on the entomotoxicity.

On the other hand, all the peptides were able to induce blockade of the cockroach neuromuscular junction *in vivo* (Fig. 8). The neuromuscular blockade induced by Jbtx resembles the effect of neurotoxins which act directly on receptor ion channels [53], among which are pore-forming neurotoxins [54]. In this work we did not attempt to elucidate the pharmacological interactions of Jbtx and related peptides at specific sites of insect neuromuscular junctions. The Jbtx N-ter peptide had an effect comparable to that of the intact peptide producing almost complete neuromuscular blockade after 40 min of recordings while JbtxΔ-β and Jbtx C-ter were clearly less active. The activity loss of JbtxΔ-β in this bioassay may reflect some critical alteration of the peptide 3D-structure affecting also its N-terminal domain, which alone is capable of producing full effect in the absence of the β-hairpin.

Upon feeding to *R. prolixus* (Fig. 5B) all the peptides were lethal, even Jbtx C-ter, contrasting with its lack of activity when injected into the hemolymph. This fact points to the presence of two active domains in the Jbtx molecule, with the amphipatic β-hairpin in the C-terminal domain probably interacting with insect's gut membranes as predicted,

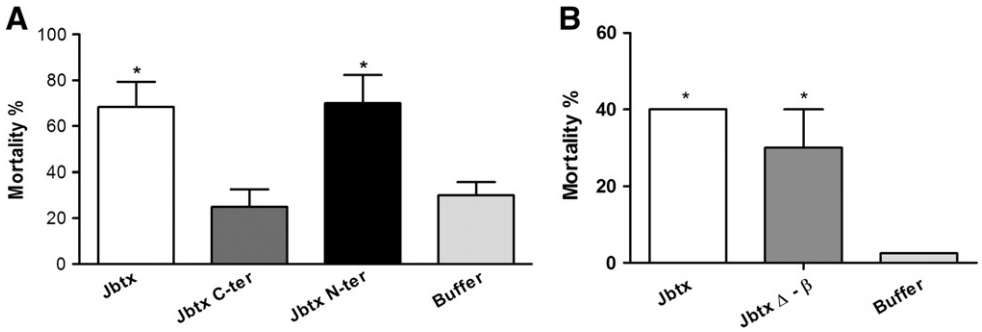

Fig. 6. Insecticidal effect of Jbtx and derived peptides on fifth instars *Oncopeltus fasciatus*. (A) Groups of 10 nymphs were injected with 1.5 μL of Jbtx, Jbtx N-ter or Jbtx C-ter into the hemocoel (dose of 0.015 μg/mg of insect body weight) or 20 mM phosphate buffer, pH 7.5 (control group). (B) Groups of 5 nymphs were injected with 1.5 μL of Jbtx or JbtxΔ-β peptides into the hemocoel (dose of 0.015 μg/mg of insect body weight) or 20 mM phosphate buffer, pH 7.5 (control group). The mortality rate was recorded after 96 h. Results are means ± standard error of triplicates of two independent experiments. (*) indicates statistically significant difference ($p \leq 0.05$) from the control group.

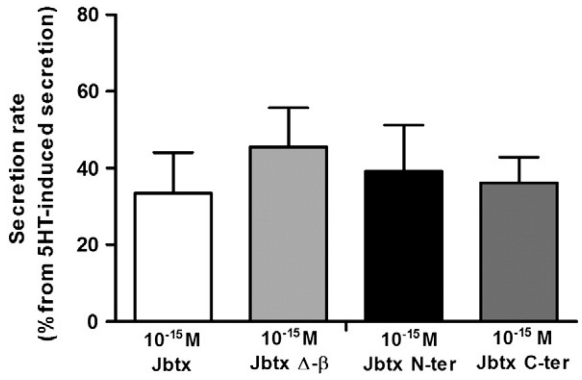

Fig. 7. Effect of jaburetox and mutants on secretion of *Rhodnius prolixus* Malpighian tubules. The assay was performed as described by Staniscuaski et al. [20]. Tubules were incubated with 2.5×10^{-8} M serotonin (5-hydroxy-tryptamine, 5-HT) for 20 min to record the maximal secretion. After washing, the tubules were incubated with the peptides (1×10^{-15} M) in the presence of serotonin for another 20 min. The secretion rate was expressed as a percentage from the control (serotonin without peptides). Results shown are means ± standard deviation of 5–6 replicates for each peptide.

when given by oral route. This conclusion could also be drawn from the facts that all the peptides had equivalent antidiuretic effects (Fig. 7) and that both terminal domains of Jbtx were able to induce leakage of vesicles (Fig. 4). The preliminary results using Planar Lipid Bilayers another artificial membrane composed only of lipids, also showed that all mutant versions of Jbtx form ion channels displaying membrane-disturbing properties (Piovesan A., unpublished data). On the other hand, Jbtx C-ter showed significantly lower activity than Jbtx or Jbtx N-ter, when its first contact within the insect was with the hemolymph probably due to a "saturating" effect of the lipid-rich medium on its membrane-disrupting ability.

All the peptides, including Jbtx C-ter, produced antidiuresis or were lethal given by oral route, circumstances where their first interaction happened with single cell layered tissues such as the Malpighian tubules [55] or the gut [56]. One hypothesis to explain the lack of specificity of these assays to discriminate the different Jbtx variants could be that biological multilayered tissue systems, such as the neuromuscular junction [57] and the whole insect (by injection, skipping the first contact with the gut), probably add additional levels of tissue- or cell specificity to the entomotoxic effects of Jbtx-related peptides. Altogether, our data indicate that the main entomotoxic domain of the urease-derived peptide Jbtx is located in its N-terminal half. However, depending on the bioassay, the C-terminal domain and/or its β-hairpin motif could also contribute part of the biological activity of Jbtx.

From the molecular dynamics simulation, it seems that the monomeric Jbtx peptide is mostly formed by coils (Fig. 2). Our simulation results confirm and expand previous theoretical observations [19], such as the compaction of the peptide in solution. Simulations of the half-peptides indicated that after 500 ns Jbtx N-ter adopts a random coil conformation while Jbtx C-ter acquires a newly-formed β-sheet (Fig. 2). These data may explain why Jbtx is highly prone to aggregation [19], and the instability of Jbtx N-ter in aqueous solution (unpublished results), possibly a consequence of the unfolding of the highly hydrophobic N-terminal of Jbtx that would require protein–protein (or protein–membrane) contact to stabilize.

Presently, to the best of our knowledge, it is not possible to compare the MD simulated structure of Jbtx to that of any other known insecticidal or membrane-disrupting peptide. The high level of coils, especially in the N-terminus, may be related to the peptide toxicity,

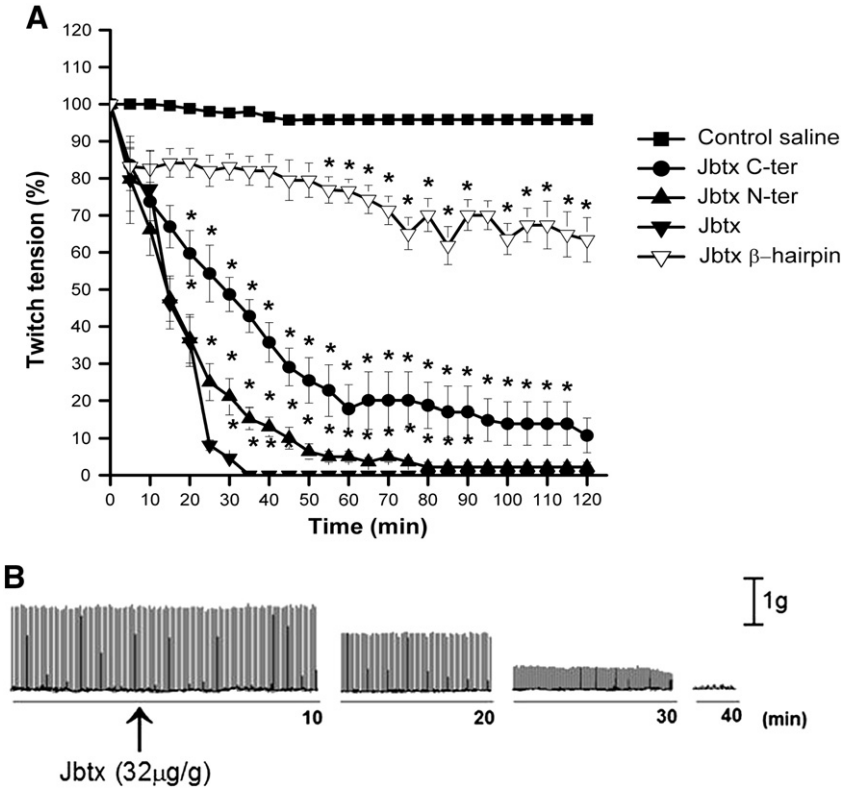

Fig. 8. Neuromuscular paralysis induced by Jbtx and peptides on *in vivo* cockroach coxal-adductor methatoracic nerve–muscle preparation. (A) Time course of the blockade of the neuromuscular activity in the presence of 32 μg/g of each version of Jbtx peptides against control insects treated only with saline (means ± standard error, n = 12). Note that Jbtx and Jbtx N-ter were able to induce complete paralysis. * indicates $p \leq 0.05$ in comparison to control saline, with ANOVA two way and Student *t* test. (B) Representative myographic 120 min recording of the coxal-adductor methatoracic nerve–muscle preparation of a Jbtx-treated cockroach.

since some toxins employ these unfolded states as recognition motifs. One example of such toxins is colicin, from *E. coli* [58]. These unfolded recognition domains may be advantageous for the toxins that carry them, since they allow these proteins to overcome steric restrictions while providing large average interaction surfaces per residue [58–60]. There are many reports in the literature of folding and oligomerization of proteins and peptides that acquire their biologically active state upon interaction with lipids or membranes. Examples are cecropin A, a 37-residue insect antimicrobial peptide [61,62], the Cyt1Aa toxin produced by *Bacillus thuringiensis* [63], anticancer β-hairpin peptides [64], antimicrobial, cell-penetrating peptides and fusion peptides such as the HIV fusion peptide FP23 [65], to cite a few.

The tendency to oligomerize and to interact with lipids exhibited by Jbtx brings the question whether the active form of the peptide (or its N-ter and C-ter versions) is an oligomer rather than a monomer. The oligomerization/aggregation phenomenon was also observed for Jbtx-2Ec, causing an enormous impact of the membrane-disruptive ability of the peptide [19].

Jbtx has promising biotechnological potential as a biopesticide. We are currently testing transgenic Jbtx expressing sugar cane (*Saccharum officinarum*) plants, and so far we have observed an increase of resistance to several species of lepidopterans in greenhouse conditions (Becker-Ritt et al., unpublished data). These data indicate the effectiveness of the peptide as an environment friendly insecticide with practical application, reducing crop losses while avoiding the use of chemical toxic agents.

We conclude that the urease-derived peptide Jbtx probably represents a new example of membrane-active peptide with insecticidal and fungitoxic activities. Its insecticidal activity was tracked down mostly to its N-terminal region and does not require the prominent β-hairpin present in the C-terminal region, although this part of the molecule probably contributes to its overall entomotoxic properties. Understanding the complex behavior of these peptides in solution as well as in the presence of lipids and biological membranes is a critical step towards unraveling their mechanisms of action and exploiting their potential as insecticidal agents.

Supplementary data to this article can be found online at http://dx.doi.org/10.1016/j.bbagen.2013.11.010.

Authors' contributions

A.H.S.M. and K.K. constructed the mutated peptides, M.S.D. helped in the insect bioassays, A.R.P. and C.F. carried out LUVs leakage assay, F.S. run the Malpighian tubules assay, D.R.D. performed MS assays, R.L-B. and H.V. conducted molecular modeling and simulations, C.A.D.B. and C.G.M.A. tested the peptides on the cockroach neuromuscular junction, C.R.C. wrote the paper and together with G.P., conceived and supervised all the work.

Acknowledgements

The authors wish to thank the Centro Nacional de Supercomputação at Universidade Federal do Rio Grande do Sul, for the assistance and access to the supercomputer; Dr. Yraima Cordeiro, Inst. Biophysiscs Carlos Chagas Filho, Universidade Federal do Rio Grande do Sul, for preliminary circular dichroism analyses of the peptides and B.Sc. Marinês de Avila Heberle, Unipampa, for helping collecting data on the cockroach preparation. This work was supported by grants from the Brazilian agencies: Coordenação de Aperfeiçoamento de Pessoal de Nível Superior (CAPES)—Edital de Toxinologia [proj 54/2011]; Conselho Nacional de Desenvolvimento Científico e Tecnológico (CNPq)—Edital Universal [proj. 47.0785/2011-47.5908/2012]; Fundação de Amparo à Pesquisa do Estado do Rio Grande do Sul (FAPERGS)—PRONEX [proj. 10/0014-2]. The authors declare no conflicts of interest related to this work.

References

[1] R. Ligabue-Braun, F.C. Andreis, H. Verli, C.R. Carlini, 3-to-1: unraveling structural transitions in ureases, Naturwissenschaften 100 (2013) 459–467.
[2] J.C. Polacco, M.A. Holland, Roles of urease in plant cells, Int. Rev. Cytol. 145 (1993) 65–103.
[3] C.R. Carlini, J.C. Polacco, Toxic properties of urease, Crop Sci. 48 (2008) 1665–1672.
[4] C.R. Carlini, M.F. Grossi-de-Sa, Plant toxic proteins with insecticidal properties. A review on their potentialities as bioinsecticides, Toxicon 40 (2002) 1515–1539.
[5] A.B. Becker-Ritt, C.R. Carlini, Fungitoxic and insecticidal plant polypeptides, Biopolymers 38 (2012) 367–384.
[6] F. Staniscuaski, C.R. Carlini, Plant ureases and related peptides: understanding their entomotoxic properties, Toxins 4 (2012) 55–67.
[7] A.B. Becker-Ritt, A.H. Martinelli, S. Mitidieri, V. Feder, G.E. Wassermann, L. Santi, M.H. Vainstein, J.T. Oliveira, L.M. Fiuza, G. Pasquali, C.R. Carlini, Antifungal activity of plant and bacterial ureases, Toxicon 50 (2007) 971–983.
[8] M. Postal, A.H.S. Martinelli, A.B. Becker-Ritt, R. Ligabue-Braun, D.R. Demartini, S.F.F. Ribeiro, G. Pasquali, V.M. Gomes, C.R. Carlini, Antifungal properties of Canavalia ensiformis urease and derived peptides, Peptides 38 (2012) 22–32.
[9] A. Balasubramanian, V. Durairajpandian, S. Elumalai, N. Mathivanan, A.K. Munirajan, K. Ponnuraj, Structural and functional studies on urease from pigeon pea (*Cajanus cajan*), Int. J. Biol. Macromol. 58 (2013) 301–309.
[10] C.R. Carlini, J.A. Guimaraes, Isolation and characterization of a toxic protein from *Canavalia ensiformis* (jack bean) seeds, distinct from concanavalin A, Toxicon 19 (1981) 667–675.
[11] C. Follmer, G.B. Barcellos, R.B. Zingali, O.L. Machado, E.W. Alves, C. Barja-Fidalgo, J.A. Guimaraes, C.R. Carlini, Canatoxin, a toxic protein from jack beans (*Canavalia ensiformis*), is a variant form of urease (EC 3.5.1.5): biological effects of urease independent of its ureolytic activity, Biochem. J. 360 (2001) 217–224.
[12] C.R. Carlini, A.E. Oliveira, P. Azambuja, J. Xavier-Filho, M.A. Wells, Biological effects of canatoxin in different insect models: evidence for a proteolytic activation of the toxin by insect cathepsinlike enzymes, J. Econ. Entomol. 90 (1997) 340–348.
[13] C.T. Ferreira-DaSilva, M.E. Gombarovits, H. Masuda, C.M. Oliveira, C.R. Carlini, Proteolytic activation of canatoxin, a plant toxic protein, by insect cathepsin-like enzymes, Arch. Insect Biochem. Physiol. 44 (2000) 162–171.
[14] A.R. Piovesan, F. Staniscuaski, J. Marco-Salvadori, R. Real-Guerra, M.S. Defferrari, C.R. Carlini, Stage-specific gut proteinases of the cotton stainer bug *Dysdercus peruvianus*: role in the release of entomotoxic peptides from *Canavalia ensiformis* urease, Insect Biochem. Mol. Biol. 38 (2008) 1023–1032.
[15] M.S. Defferrari, D.R. Demartini, T.B. Marcelino, P.M. Pinto, C.R. Carlini, Insecticidal effect of *Canavalia ensiformis* major urease on nymphs of the milkweed bug *Oncopeltus fasciatus* and characterization of digestive peptidases, Insect Biochem. Mol. Biol. 41 (2011) 388–399.
[16] R. Real-Guerra, C.R. Carlini, F. Staniscuaski, Role of lysine and acidic amino acid residues on the insecticidal activity of jackbean urease, Toxicon 71 (2013) 76–83.
[17] F. Mulinari, F. Staniscuaski, L.R. Bertholdo-Vargas, M. Postal, O.B. Oliveira-Neto, D.J. Rigden, M.F. Grossi-de-Sa, C.R. Carlini, Jaburetox-2Ec: an insecticidal peptide derived from an isoform of urease from the plant *Canavalia ensiformis*, Peptides 28 (2007) 2042–2050.
[18] F. Staniscuaski, C.T. Ferreira-Dasilva, F. Mulinari, M. Pires-Alves, C.R. Carlini, Insecticidal effects of canatoxin on the cotton stainer bug *Dysdercus peruvianus* (Hemiptera: Pyrrhocoridae), Toxicon 45 (2005) 753–760.
[19] P.R. Barros, H. Stassen, M.S. Freitas, C.R. Carlini, M.A.C. Nascimento, C. Follmer, Membrane-disruptive properties of the bioinsecticide Jaburetox-2Ec: implications to the mechanism of the action of insecticidal peptides derived from ureases, Biochim. Biophys. Acta, Proteins Proteomics 1794 (2009) 1848–1854.
[20] F. Staniscuaski, V.T. Brugge, C.R. Carlini, I. Orchard, In vitro effect of *Canavalia ensiformis* urease and the derived peptide Jaburetox-2Ec on *Rhodnius prolixus* Malpighian tubules, J. Insect Physiol. 55 (2009) 255–263.
[21] A. Balasubramanian, K. Ponnuraj, Crystal structure of the first plant urease from jack bean: 83 years of journey from its first crystal to molecular structure, J. Mol. Biol. 400 (2010) 274–283.
[22] A. Menez, Functional architectures of animal toxins: a clue to drug design? Toxicon 36 (1998) 1557–1572.
[23] A. Nikouee, M. Khabiri, S. Grissmer, R. Ettrich, Charybdotoxin and margatoxin acting on the human voltage-gated potassium channel hKv1.3 and its H399N mutant: an experimental and computational comparison, J. Phys. Chem. B 116 (2012) 5132–5140.
[24] X.D. Li, Y.F. Qiu, Y. Shen, C. Ding, P.H. Liu, J.P. Zhou, Z.Y. Ma, Splicing together different regions of a gene by modified polymerase chain reaction-based site-directed mutagenesis, Anal. Biochem. 373 (2008) 398–400.
[25] S.F. Altschul, D.J. Lipman, Protein database searches for multiple alignments, Proc. Natl. Acad. Sci. U. S. A. 87 (1990) 5509–5513.
[26] M.M. Bradford, A rapid and sensitive method for the quantitation of microgram quantities of protein utilizing the principle of protein-dye binding, Anal. Biochem. 72 (1976) 248–254.
[27] E. Gasteiger, C. Hoogland, A. Gattiker, S. Duvaud, M.R. Wilkins, R.D. Appel, A. Bairoch, Protein identification and analysis tools on the ExPASy server, in: J.M. Walker (Ed.), The Proteomics Protocols Handbook, Humana Press, 2005, pp. 571–607.
[28] J. Kyte, R.F. Doolittle, A simple method for displaying the hydropathic character of a protein, J. Mol. Biol. 157 (1982) 105–132.
[29] D.R. Demartini, C.R. Carlini, J.J. Thelen, Global and targeted proteomics in developing jack bean (*Canavalia ensiformis*) seedlings: an investigation of urease isoforms mobilization in early stages of development, Plant Mol. Biol. 75 (2011) 53–65.

[30] H. Schagger, G. Vonjagow, Tricine sodium dodecyl-sulfate polyacrylamide-gel electrophoresis for the separation of proteins in the range from 1-kDa to 100-kDa, Anal. Biochem. 166 (1987) 368–379.
[31] N. Dyballa, S. Metzger, Fast and sensitive colloidal Coomassie G-250 staining for proteins in polyacrylamide gels, J. Vis. Exp. 30 (2009).
[32] H. Towbin, T. Staehelin, J. Gordon, Electrophoretic transfer of proteins form polyacrylamide gels to nitrocellulose sheets. Procedure and some applications, Proc. Natl. Acad. Sci. U. S. A. 76 (1979) 4350–4354.
[33] R.J. Full, D.R. Stokes, A.N. Ahn, R.K. Josephson, Energy absorption during running by leg muscles in a cockroach, J. Exp. Biol. 201 (1998) 997–1012.
[34] K.A. Wafford, D.B. Sattelle, Effects of amino acid neurotransmitter candidates on an identified insect motoneurone, Neurosci. Lett. 63 (1986) 135–140.
[35] R. Sánchez, A. Šali, Comparative protein structure modeling: introduction and practical examples with Modeller, Methods Mol. Biol. 143 (2000) 97–129.
[36] R.A. Laskowski, M.W. Macarthur, D.S. Moss, J.M. Thornton, PROCHECK—a program to check the stereochemical quality of protein structures, J. Appl. Crystallogr. 26 (1993) 283–291.
[37] R. Luthy, J.U. Bowie, D. Eisenberg, Assessment of protein models with 3-dimensional profiles, Nature 356 (1992) 83–85.
[38] N. Guex, M.C. Peitsch, SWISS-MODEL and the Swiss-PdbViewer: an environment for comparative protein modeling, Electrophoresis 18 (1997) 2714–2723.
[39] B. Hess, C. Kutzner, D. van der Spoel, E. Lindahl, GROMACS 4: algorithms for highly efficient, load-balanced, and scalable molecular simulation, J. Chem. Theory Comput. 4 (2008) 435–447.
[40] C. Oostenbrink, A. Villa, A.E. Mark, W.F. Van Gunsteren, A biomolecular force field based on the free enthalpy of hydration and solvation: the GROMOS force-field parameter sets 53A5 and 53A6, J. Comput. Chem. 25 (2004) 1656–1676.
[41] H.J.C. Berendsen, J.R. Grigera, T.P. Straatsma, The missing term in effective pair potentials, J. Phys. Chem. 91 (1987) 6269–6271.
[42] B. Hess, H. Bekker, H.J.C. Berendsen, J. Fraaije, LINCS: a linear constraint solver for molecular simulations, J. Comput. Chem. 18 (1997) 1463–1472.
[43] T. Darden, D. York, L. Pedersen, Particle Mesh Ewald—an N. Log(N) method for Ewald sums in large systems, J. Chem. Phys. 98 (1993) 10089–10092.
[44] H.J.C. Berendsen, J.P.M. Postma, W.F. Vangunsteren, A. Dinola, J.R. Haak, Molecular dynamics coupling to an external bath, J. Chem. Phys. 81 (1984) 3684–3690.
[45] A. Balasubramanian, N. Balaji, N. Gautham, K. Ponnuraj, Molecular dynamics simulation and molecular modelling studies on the insecticidal domain from jack bean urease, Mol. Simul. 39 (2012) 357–366.
[46] K. Kappaun, Estudos com o Jaburetox: efeito tóxico de *E. coli* liofilizadas carregadas com o peptídeo e análise da influencia do epitopo V5 na formação de agregados, (M.Sc. dissertation) Cellular and Molecular Biology, Universidade Federal do Rio Grande do Sul, Porto Alegre, Brazil, 2012.
[47] E. Drakopoulou, J. Vizzavona, J. Neyton, V. Aniort, F. Bouet, H. Virelizier, A. Menez, C. Vita, Consequence of the removal of evolutionary conserved disulfide bridges on the structure and function of charybdotoxin and evidence that particular cysteine spacings govern specific disulfide bond formation, Biochemistry 37 (1998) 1292–1301.
[48] K. Nakagawa, A. Tokushima, K. Fujiwara, M. Ikeguchi, Proline scanning mutagenesis reveals non-native fold in the molten globule state of equine beta-lactoglobulin, Biochemistry 45 (2006) 15468–15473.
[49] M. Yamamoto, K. Nakagawa, M. Ikeguchi, Importance of polypeptide chain length for the correct local folding of a beta-sheet protein, Biophys. Chem. 168 (2012) 40–47.
[50] G. Tomazetto, F. Mulinari, F. Staniscuaski, B. Settembrini, C.R. Carlini, M.A.Z. Ayub, Expression kinetics and plasmid stability of recombinant *E-coli* encoding urease-derived peptide with bioinsecticide activity, Enzyme Microb. Technol. 41 (2007) 821–827.
[51] F. Staniscuaski, V.T. Brugge, C.R. Carlini, I. Orchard, Jack bean urease alters serotonin-induced effects on *Rhodnius prolixus* anterior midgut, J. Insect Physiol. 56 (2010) 1078–1086.
[52] C. Follmer, R. Real-Guerra, G.E. Wasserman, D. Olivera-Severo, C.R. Carlini, Jackbean, soybean and *Bacillus pasteurii* ureases: biological effects unrelated to ureolytic activity, Eur. J. Biochem. 271 (2004) 1357–1363.
[53] G. Corzo, E. Villegas, F. Gomez-Lagunas, L.D. Possani, O.S. Belokoneva, T. Nakajima, Oxyopinins, large amphipathic peptides isolated from the venom of the wolf spider Oxyopes kitabensis with cytolytic properties and positive insecticidal cooperativity with spider neurotoxins, J. Biol. Chem. 277 (2002) 23627–23637.
[54] Z. Andreeva-Kovalevskaya, A.S. Solonin, E.V. Sineva, V.I. Ternovsky, Pore-forming proteins and adaptation of living organisms to environmental conditions, Biochem. Mosc. 73 (2008) 1473–1492.
[55] S.H.P. Maddrell, Secretion by the Malpighian tubules of Rhodnius. The movements of ions and water, J. Exp. Biol. 51 (1969) 71–97.
[56] W.R. Terra, Evolution of digestive systems of insects, Annu. Rev. Entomol. 35 (1990) 181–200.
[57] G.A. Edwards, H. Ruska, E. de Harven, Neuromuscular junctions in flight and tymbal muscles of the Cicada, J. Biochem. Biophys. Cytol. 4 (1958) 251–256.
[58] G. Anderluh, Q. Hong, R. Boetzel, C. MacDonald, G.R. Moore, R. Virden, J.H. Lakey, Concerted folding and binding of a flexible colicin domain to its periplasmic receptor TolA, J. Biol. Chem. 278 (2003) 21860–21868.
[59] A.K. Dunker, J.D. Lawson, C.J. Brown, R.M. Williams, P. Romero, J.S. Oh, C.J. Oldfield, A.M. Campen, C.R. Ratliff, K.W. Hipps, J. Ausio, M.S. Nissen, R. Reeves, C.H. Kang, C.R. Kissinger, R.W. Bailey, M.D. Griswold, M. Chiu, E.C. Garner, Z. Obradovic, Intrinsically disordered protein, J. Mol. Graph. Model. 19 (2001) 26–59.
[60] V.N. Uversky, Natively unfolded proteins: a point where biology waits for physics, Protein Sci. 11 (2002) 739–756.
[61] L. Silvestro, P.H. Axelsen, Membrane-induced folding of cecropin A, Biophys. J. 79 (2000) 1465–1477.
[62] L. Otvos, Antibacterial peptides isolated from insects, J. Pept. Sci. 6 (2000) 497–511.
[63] C. Rodriguez-Almazan, I. Ruiz de Escudero, P. Emiliano Canton, C. Munoz-Garay, C. Perez, S.S. Gill, M. Soberon, A. Bravo, The amino- and carboxyl-terminal fragments of the Bacillus thuringensis Cyt1Aa toxin have differential roles in toxin oligomerization and pore formation, Biochemistry 50 (2011) 388–396.
[64] C. Sinthuvanich, A.S. Veiga, K. Gupta, D. Gaspar, R. Blumenthal, J.P. Schneider, Anticancer beta-hairpin peptides: membrane-induced folding triggers activity, J. Am. Chem. Soc. 134 (2012) 6210–6217.
[65] P. Wadhwani, J. Reichert, J. Bürck, A.S. Ulrich, Antimicrobial and cell-penetrating peptides induce lipid vesicle fusion by folding and aggregation, Eur. Biophys. J. 41 (2012) 177–187.

III. Artigo Publicado

Marco-Salvadori *et al*., 2012

● Participação no desenho e na execução dos experimentos relativos a presença de inibidores da atividade ureásica na hemolinfa de insetos. Item 3.5 (Figs. 7 e 8).

Biological Control 63 (2012) 253–263

Contents lists available at SciVerse ScienceDirect

Biological Control

journal homepage: www.elsevier.com/locate/ybcon

Characterization of entomopathogenic nematodes and symbiotic bacteria active against *Spodoptera frugiperda* (Lepidoptera: Noctuidae) and contribution of bacterial urease to the insecticidal effect

Juliana De Marco Salvadori [a,b], Marina Schumacher Defferrari [a,1], Rodrigo Ligabue-Braun [a,1], Elene Yamazaki Lau [c], José Roberto Salvadori [d], Celia Regina Carlini [a,e,*]

[a] Graduate Program in Cellular and Molecular Biology, Center of Biotechnology, Universidade Federal do Rio Grande do Sul, Porto Alegre, RS, Brazil
[b] Secretaria de Saúde, Prefeitura Municipal de Passo Fundo, RS, Brazil
[c] Empresa Brasileira de Pesquisa Agropecuária, Centro Nacional de Pesquisa de Trigo, Passo Fundo, RS, Brazil
[d] Faculdade de Agronomia e Medicina Veterinária, Universidade de Passo Fundo, RS, Brazil
[e] Dept. Biophysics and Center of Biotechnology, Universidade Federal do Rio Grande do Sul, Porto Alegre, RS, Brazil

HIGHLIGHTS

- Soil nematodes from the South of Brazil were screened for pathogenicity against *S. frugiperda.*
- Symbiotic bacteria associated to these nematodes were isolated and characterized.
- Urease production by symbiotic bacteria along infection in *S. frugiperda* was evaluated.
- A positive correlation was found between bacterial urease production and entomopathogenicity.

GRAPHICAL ABSTRACT

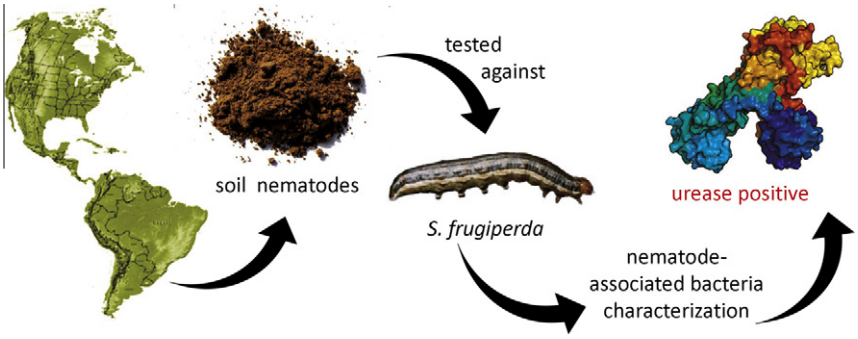

ARTICLE INFO

Article history:
Available online 24 August 2012

Keywords:
Photorhabdus
Xenorhabdus
Insecticidal activity
Virulence factor
Urease
Hemolymph

ABSTRACT

Entomopathogenic nematodes carrying symbiotic bacteria represent one of the best non-chemical strategies for insect control. Infective juveniles of *Heterorhabditidae* and *Steinernematidae* nematodes actively seek the host in the soil, penetrating through insect's openings to reach the hemocoel where symbiotic bacteria in the genera *Photorhabdus* or *Xenorhabdus*, respectively, are released. The bacteria replicate and produce virulence factors that rapidly kill the insect host, providing nutrients for the nematodes development and reproduction within the insect cadaver. More studies are necessary to better understand the factors implicated in the nematode-bacteria association, particularly focusing the bacterial symbionts, the final effectors of the insect death. Our group has shown that ureases are lethal to some groups of insects and may contribute to the entomopathogenic properties of the symbiotic bacteria.

The fall armyworm *Spodoptera frugiperda* (Lepidoptera: Noctuidae) is one of the major insect pests in corn (*Zea mays*) crops in Brazil, with infestations resulting in reduction up to 39% yield and losses amounting US$ 500 million annually. Native strains of entomopathogenic nematodes active against *S. frugiperda* represent a promising alternative to the intensive use of chemical insecticides to control fall armyworm population in corn plantations.

* Corresponding author at: Dept. Biophysics, Universidade Federal do Rio Grande do Sul, Av. Bento Gonçalves 9500, 91501-970 Porto Alegre, RS, Brazil. Fax: +55 51 3308 7003.
E-mail addresses: julianasalvadori@yahoo.com.br (J.D.M. Salvadori), msdeff@gmail.com (M.S. Defferrari), rodrigobraun@cbiot.ufrgs.br (R. Ligabue-Braun), yamazaki@cnpt.embrapa.br (E. Yamazaki Lau), salvadori@upf.br (J.R. Salvadori), celia.carlini@pq.cnpq.br, ccarlini@ufrgs.br (C.R. Carlini).
URL: http://www.ufrgs.br/laprotox (C.R. Carlini).
[1] These authors have contributed equally to this work.

1049-9644/$ - see front matter
http://dx.doi.org/10.1016/j.biocontrol.2012.08.002

In this study we screened soil nematodes collected in the south region of Brazil for pathogenicity against *S. frugiperda*. Symbiotic bacteria associated with these nematodes were isolated and characterized. We also evaluated urease production by the symbiotic bacteria *in vitro* and along the course of infection in *S. frugiperda* and demonstrated that urease production correlated positively to their entomopathogenicity.

1. Introduction

Entomopathogenic nematodes carrying symbiotic bacteria represent one of the best non-chemical strategies supporting insect control (Boemare et al., 1997; Forst et al., 1997; Lang et al., 2011; Zhu et al., 2011). In the soil, the infective juveniles of these nematodes (*Heterorhabditis* or *Steinernema* genera) actively seek the host in the soil, penetrate through insect's natural openings, travel to the hemocoel and release symbiotic bacterial cells (mostly species of *Photorhabdus* or *Xenorhabdus*, respectively). The bacteria multiply and release a number of virulence factors, including complexes of toxins, hydrolytic enzymes, hemolysins, and antimicrobial compounds, that kill the insect host usually within 48 h (Eleftherianos et al., 2010; ffrench-Constant and Bowen, 2000; ffrench-Constant et al., 2007), thus providing nutrients for the nematodes development and reproduction within the insect cadaver. More studies are still necessary to better understand the factors implicated in the nematode–bacteria association, particularly focusing the bacterial symbionts, which are final effectors of the insect death (Campos-Herrera et al., 2009).

Our group described for the first time the insecticidal properties of plant ureases and urease-derived peptides (Carlini et al., 1997; Follmer et al., 2004; Mulinari et al., 2007). The mode of entomotoxic action of these polypeptides is not yet completely elucidated (Carlini and Polacco, 2008), with distinct mechanisms and signaling pathways being triggered by the whole molecule or its derived peptide(s) (Staniscuaski et al., 2009, 2010). In the case of intact urease, several ureolysis-independent toxic effects are known and these can be cumulative or synergistic to the enzymatic release of highly toxic ammonia by the enzyme. Our initial studies have suggested that lepidopterans apparently are not susceptible to ureases (Carlini et al., 1997) and that bacterial ureases are devoid of insecticidal activity (Follmer et al., 2004). Contrasting with our observations, Martin et al. (2009) reported that urease-positive strains of *Bacillus thuringiensis* Berliner were better-fitted as biological control agents against the gypsy moth *Lymantria dispar* Linnaeus than urease-negative isolates. Thus a re-evaluation of the entomotoxicity of bacterial ureases and the susceptibility of lepidopterans to ureases is needed.

The fall armyworm *Spodoptera frugiperda* (J.E. Smith) (Lepidoptera: Noctuidae) is one of the major insect pests in corn (*Zea mays* Linnaeus) crops in Brazil, with infestations resulting in reduction up to 39% yield and losses amounting US$ 500 millions annually depending on climate conditions and stage of development of the attacked plants, among other factors (Cruz et al., 1999; Cruz and Turpin, 1983; Mendes et al., 2011). Native strains of entomopathogenic nematodes active against *S. frugiperda* represent a promising alternative to the intensive use of chemical insecticides to control fall armyworm populations in corn plantations.

In this study we screened soil nematodes collected in the south region of Brazil for pathogenicity against *S. frugiperda*. Symbiotic bacteria associated with these nematodes were isolated and characterized. We also evaluated urease production by the symbiotic bacteria and its potential contribution to entomopathogenicity.

2. Materials and methods

2.1. Insects and nematodes

S. frugiperda larvae were provided by the Entomology Laboratory, Embrapa Trigo, Passo Fundo, RS, Brazil. The insects were reared on artificial diets (Burton and Perkins, 1972) at 25 ± 2 °C, a relative humidity of 60 ± 10% and a 14/10 h light/dark cycle. The colony was managed as described by (Parra, 1998). Newly hatched larvae were transferred to glass vials containing the solidified diet and closed with cotton balls, and allowed to develop until pupation. The pupae were put in plates with vermiculite inside cages for the emergence of adults. One male and one female were then transferred to individual cages with the internal walls covered with filter paper (Whatmann n°1) and with free access to a 10% v/v honey solution.

Entomopathogenic nematodes (EPN) were from a collection kept by the Insect Pathology Laboratory from Embrapa Trigo, Passo Fundo, RS, Brazil. The EPNs were cultured in *Tenebrio molitor* Linnaeus (Coleoptera: Tenebrionidae). For that a suspension of 20 infective juvenile nematodes in 500 μL of distilled water was applied to *T. molitor* larvae, kept in 90 mm Petri dishes with filter paper-covered bottoms. The plates were maintained at 23 ± 2 °C, 60 ± 10% relative humidity during 4 days until death of the larvae. Dead insects were transferred to White traps in incubators at 23 ± 2 °C for emergence and capture of EPNs (White, 1927). Recovered infective juveniles were counted under a stereoscopic microscope and used for bioassays within 7 days.

2.2. Screening of nematode entomotoxicity

Eight EPN isolates (NEPETs 05, 06, 07, 12, 15, 30, 32 and 33) were evaluated for their pathogenicity toward *S. frugiperda* larvae. The bioassays were run in 12-well plates experimental units at 28 ± 2 °C, 60 ± 10% relative humidity, 14/10 h light/dark cycle, with the bottom of cells covered with filter paper (Whatmann n°1). *S. frugiperda* 5th instars starved for 24 h were placed inside the cells with small pieces of maize leaves and 100 infective juveniles (in 300 μL of distilled water) per insect larva were added to the center of the cells. Control groups received 300 μL distilled water instead. Mortality of insects and typical signs of EPN infection were registered daily during 5 days. Experiments in quadruplicates were totally randomized with 48 insects for each EPN isolate.

EPNs were identified taxonomically according to Adams and Nguyen (2002).

2.3. Bacteria isolation

Entomopathogenic bacteria (EB) were isolated from the insect's hemolymph according to the method of Poinar and Thomas, 1966. Each of the eight EPN isolates was incubated with *S. frugiperda* hemolymph in a BOD chamber at 23 ± 2 °C for 20 h and then the suspensions were plated in nutrient agar. After 24 h, bacterial colonies were plated in NBTA agar and the process was repeated every 24 h until isolated colonies were obtained. For the bioassays, the isolated bacterial colonies were inoculated in liquid LB medium and let multiply for 16 h at 28 ± 2 °C and then the cell concentra-

tion was adjusted to 10^4 cells per 10 μL after counting on a Neubauer chamber.

2.4. Virulence assay of bacteria in S. frugiperda

EB suspensions were injected in 25 insects per isolate and LB medium diluted in saline was used as control. Before injection, the surface of the larvae was disinfected by immersing the insects in 1% NaOH for 10 s and then rinsed with distilled water. For injections, one of the insect's prolegs was cut and 10 μL of the bacterial suspension containing 10^4 cells were inoculated into the abdominal cavity with a Hamilton syringe fitted with a 10 μL needle. The insects were kept at 28 ± 2 °C and mortality was registered daily. Experiments in quadruplicates were totally randomized with 25 insects for each bacterial isolate and tested dose.

2.5. Extraction of bacterial DNA and sequencing of the 16S gene

For extraction of DNA, isolated bacteria colonies were collected from the agar plates into 500 μL sterile 1.5 mL microtubes and 200 μL of sterile MilliQ water was added. Cells were disrupted by heating at 100 °C for 10 min and then centrifuged at 10,000*g* for 2 min. Supernatants were deproteinized by addition of 200 μL of chloroform:isoamylic acid (24:1 v/v) followed by centrifugation (10,000*g* for 10 min). The aqueous phases containing nucleic acids were transferred to new 1.5 mL microtubes and stored at −20 °C. Primers used to amplify the 16S rDNA region were: 5′-gAA gAg TTT gAT CAT ggC TC-3′ (sense) and 5′-Aag gAg gTg ATC Cag CCg CA-3′ (antisense) (Kim et al., 2009). Primers used for sequencing the amplified fragments were: 5′-GAA GAG TTT GAT CAT GGC TC-3′; 5′-AAG GAG GTG ATC CAG CCG CA-3′; 5′-CTC CTA CGG GAG GCA GCA GTG GGG-3′ (16S362f); 5′-CGA AAG CGT GGG GAG CAA ACA GG-3′ (16S786f); 5-TGC GCT CGT TGC GGG ACT TAA CC-3′ (16S760r) and 5′-GAC TAC CAG GGT ATC TAA TCC TG-3′ (16S455r) (Cruz et al., 2001; Kim et al., 2009).

PCR amplification was performed according to Saiki et al., 1988, with some modifications. The standard 50 μL PCR mixtures contained: 10 μL of 5× reaction buffer, 1 μL of dNTP mixture (2.5 mM each), 2 μL of 5 μM forward primer, 2 μL of 5 μM reverse primer, 0.25 μL of Taq polymerase (5 U/μL), 3 μL of template DNA and 31.75 μL of distilled water. The negative controls contained all components of the PCR except the DNA template. The mixtures were incubated in a DNA thermal cycler for a 35-cycle amplification series. After initial denaturation at 94 °C for 3 min, each cycle included denaturation at 94 °C for 45 s, annealing at 62 °C for 45 s, and extension at 72 °C for 2 min. The final extension was carried out at 72 °C for 7 min. The reaction products were separated in a 1% agarose gel containing 0.5 μg of ethidium bromide per mL and were visualized under UV light with an imager. PCR products were purified with illustra™ GFX™ PCR DNA and Gel Band Purification Kit (GE Healthcare, UK) according the manufacture's instructions.

Sequencing was carried out at the ACTGene Laboratory (Centro de Biotecnologia, UFRGS, Porto Alegre, RS, Brazil) using an ABI-PRISM 3100 Genetic Analyzer (Applied Biosystems). The genomic sequences were analyzed using the Phred/Phrap/Consed package.

2.6. Biochemical characterization of bacterial isolates

EB isolates grown in LB medium were submitted to biochemical characterization using the commercial kits BacTray I, II and III (Laborclin, Brazil) following the manufacter's instructions.

2.7. Bacterial growth curves

Entomopathogenic bacterial strains 30H-B, 33S-C, 5S-L and 15H-S were cultivated in 300 mL of LB broth under agitation at 150 rpm in an orbital shaker, at 28 °C. Bacterial growth was determined at time intervals by measuring the optical density (OD) at 600 nm. Aliquots of bacterial cultures were sampled for determination of urease content and protein concentration after 2, 8, 11 and 24 h of growth when OD ranged 0.16–0.19; 0.38–0.42; 0.52–0.66 and 0.9–1.18, respectively.

2.8. Urease production by bacterial isolates in culture

Production of urease during growth of the bacterial isolates was visualized as a reddish color around the colonies grown on urea agar plates (McGee et al., 1999).

Aliquots of bacterial cells grown in LB broth were lysed using an ultrasonic homogenizer, 10 pulses of 1 min in an ice bath and then centrifuged at 10 min, 10,000*g*, 4 °C. After discarding the pellets, the supernatants were collected, diluted in 20 mM sodium phosphate pH 7.5 to a protein concentration of 1 mg/mL and used for enzymatic determination of urease. Protein concentration of the cell lysates was determined by their absorbance at 280 nm.

Ammonia released by urease activity was determined colorimetrically at 570 nm using the phenol nitroprussiate method (Weatherburn, 1967). For the assays, triplicated points of 100 μg protein of bacterial cell lysates in multiwell plates were incubated with 5 mM urea, in 50 mM sodium acetate (pH 5–6); 50 mM sodium phosphate (pH 7–8) or 50 mM tris (hydroxylmethyl) aminomethane (pH 9.0), at 37 °C, for 12 h. Absorbance was measured in a plate reader and urease activity is expressed as units of absorbance at 570 nm generated under the conditions described.

2.9. Collection of hemolymph

Hemolymph samples of *Spodoptera* larvae were collected 24 h after inoculation into the hemocoel of 10^4 cells of 15 H-S, 30 H-B, 33 S-C and 5 S-L strains. For hemolymph collection, one proleg of ice-immobilized larvae was cut and the flowing hemolymph was collected with a pipette tip, and mixed with 10% of its volume of a chilled anticoagulant solution (0.01 M EDTA, 0.1 M glucose, 0.062 M NaCl, 0.026 M citric acid, pH 4.6). Typically 25–30 μL of hemolymph were collected from each larva. The pH of the hemolymph was measured immediately after collection, before mixing with the anticoagulant, using pH indicator strips (pH 0–14, Merck Chemicals, Germany). The hemolymph was then centrifuged for 1 min, 5000*g* at 4 °C and tested for urease activity immediately after. Alternatively, hemolymph aliquots were mixed with 5X-electrophoresis sample buffer and boiled for 5 min before electrophoretic analysis.

2.10. Urease detection in hemolymph

Hemolymph samples of control and infected larvae 24 h after inoculation were analyzed for ureolytic activity (Weatherburn, 1967), and 12% SDS–PAGE (Laemmli, 1970) followed by Western blot (Towbin et al., 1979) using a rabbit IgG raised against the *Helicobacter pylori* urease (1:20.000) (Santa Cruz Biotechnology, USA). An anti-rabbit IgG coupled to alkaline phosphatase (Sigma Chemical Co, USA) was used as the secondary antibody (1:25.000). The color reaction was developed with nitroblue tetrazolium chloride (NBT) and 5-bromo-4-chloro-3-indoyl phosphate (BCIP).

The urease-inhibitory activity of the hemolymph was tested by incubating aliquots of freshly collected hemolymph with 4 μg of highly purified *Canavalia ensiformis* DC Linnaeus urease (type III, Sigma Chem. Co., USA) or 0.4 μg *H. pylori* urease, purified according

to Wassermann et al., 2010, in the presence of 5 mM urea, 20 mM sodium phosphate buffer, 150 mM NaCl buffer, at pH 7.5, for 2 h at 37 °C.

2.11. Phylogenetic and homology analyses

Phylogenetic analyses were performed by the Neighbor-joining method (Saitou and Nei, 1987). Evolutionary distances were estimated using the Kimura-2 parameter (Kimura, 1980) using the MEGA version 5.0 software (Molecular Evolutionary Genetic Analysis) (Tamura et al., 2007). In total, 1000 repetitions were performed using the bootstrapping method (Felsenstein, 1985), to determine the reliability of each node of the tree. Sequences similar to those being inspected for identification were acquired by BLAST over the NCBI database (http://blast.ncbi.nlm.nih.gov/Blast.cgi) (Altschul and Lipman, 1990).

2.12. Statistical analysis

Data are expressed as mean ± standard error. Significance of differences between means was determined using one-way ANOVA. Results were considered statistically different when $p < 0.05$ (Tukey test).

3. Results

3.1. Entomopathogenic effect of nematodes and symbiotic bacteria in S. frugiperda

Table 1 shows the pathogenic effects of eight isolates of nematodes and their symbiotic bacteria on 5th instar *S. frugiperda*. The nematodes, classified into the *Steinernematidae* or *Heterorhabibditidae* families, produced mortality in the range of 28–56% with a dose of 100 infective juveniles per larva. EPN strains number 07 (*Steinernema*), 12 and 15 (*Heterorhabditis*) killed 70–80% of the tested insects. Isolated symbiotic bacteria injected into *S. frugiperda* (10^4 cells per larva) produced high levels of lethality (Table 1), particularly those from *Heterorhabditis* EPN 12, 15, 30 and 32.

Fig. 1 depicts the time course of mortality induced by injection of 10^4 cells of symbiotic bacteria into the hemocoel of *S. frugiperda*. The data show that bacteria isolated from *Heterorhabiditis* nematodes were more lethal than those from *Steinernema* nematodes, producing ca. 90% mortality after 3 days.

3.2. Identification of symbiotic bacteria isolates

Amplified rDNA sequences were submitted to the Ribosomal Database Project II server (http://rdp.cme.msu.edu). All sequences belong to Proteobacteria, Gammaproteobacteria class, Enterobacteriales order and Enterobacteriaceae family. At the genus level, the sequences were distributed (at 100% confidence level) into two taxa: 12H-A, 30H-B, 32H-E and 15H-S belong to the *Photorhabdus* genus while 33S-C, 6S-J, 5S-L and 7S-U, belong to *Xenorhabdus*. The sequences were submitted to BLAST against the NCBI nucleotide database for a similarity search. For *Xenorhabdus* bacteria, alignments with 99% identity were obtained for *Xenorhabdus szentirmaii* Lengyel et al. species. Bacterial isolates 33S-C, 6S-J, 5S-L matched sequence AJ810295.1, and 7S-U matched DQ211712. In the case of bacteria within the *Photorhabdus* genus, isolates 12H-A and 30H-B showed 98% and 99% identity with *Photorhabdus* sp. (AB355865), 15H-S matched *Photorhabdus luminescens* subsp. *laumondii* Fischer Le-Saux et al. (BX571863.1) with 98% identity and 32H-E was identified as *P. luminescens* subsp. *luminescens* (Thomas and Poinar) (AY278641.1) with 99% identity. Figs. 2 and 3 show the phylogenentic trees for the *Photorhabdus* and *Xenorhabdus* bacteria.

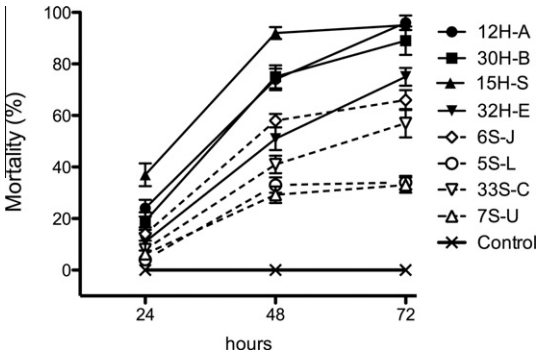

Fig. 1. Time course of the mortality of *S. frugiperda* (5th instars) injected into the hemocoel with 10,000 bacterial cells isolated from entomopathogenic nematodes. Data represent mean ± s.e.m. of quadruplicated points with 48 insects per point.

3.3. Biochemical characterization of symbiotic bacteria

All bacteria were positive for the activities of arginine decarboxylase, lysine decarboxylase, ornithine decarboxylase and production of acetyl methyl carbinol. They were all negative for phenylalanine desaminase, enzymatic hydrolysis of thiosulfate and utilization of acetamide and malonate as a carbon source.

Bacteria belonging to the *Photorhabdus* genus (12H-A, 30H-B, 32H-E and 15H-S) were negative for fermentation of rhamnose, adonitol, salycine, arabinose or sorbitol and positive for mannitol. All *Photorhabdus* bacteria hydrolyzed urea and esculin, were negative for oxidase and positive for indol and citrate. *Xenorhabdus* bacteria were more diverse in their biochemical profile. Except for 6S-J, the other isolates were negative for hydrolysis of esculin, positive

Table 1
Entomopathogenic effect of nematodes and symbiont bacteria in *Spodoptera frugiperda* 5th instars.

EPN strain	Source in Brazil* (State)	Nematode family	Bacterial isolate**	*S. frugiperda* mortality (%)***	
				100 infective juveniles per larva after 5 days	10^4 bacterial cells per larva after 3 days
05	RS	*Steinernematidae*	5S-L	54 ± 5.1^{c}	34 ± 2.6^{e}
06	RS	*Steinernematidae*	6S-J	28 ± 1.5^{d}	66 ± 3.8^{cd}
07	RS	*Steinernematidae*	7S-U	70 ± 2.5^{ab}	33 ± 3.0^{e}
12	PR	*Heterorhabditidae*	12H-A	77 ± 1.9^{a}	96 ± 2.8^{a}
15	RS	*Heterorhabditidae*	15H-S	69 ± 3.5^{ab}	95 ± 1.9^{a}
30	SC	*Heterorhabditidae*	30H-B	56 ± 2.7^{bc}	89 ± 5.5^{ab}
32	SC	*Heterorhabditidae*	32H-E	55 ± 2.7^{bc}	75 ± 3.4^{bc}
33	RS	*Steinernematidae*	33S-C	51 ± 4.0^{c}	57 ± 5.5^{d}

* States: RS – Rio Grande do Sul; SC – Santa Catarina; PR – Paraná.
** Bacterial isolates were identified by the number of the EPN source followed by H or S (referring to EPN genera) and a letter.
*** Accumulated mortality (mean ± standard error). Quadruplicate points with 48 (infective juveniles) or 25 (bacterial cells) insects per point. Means in the same column followed by a different letter are statistically different ($p < 0.05$).

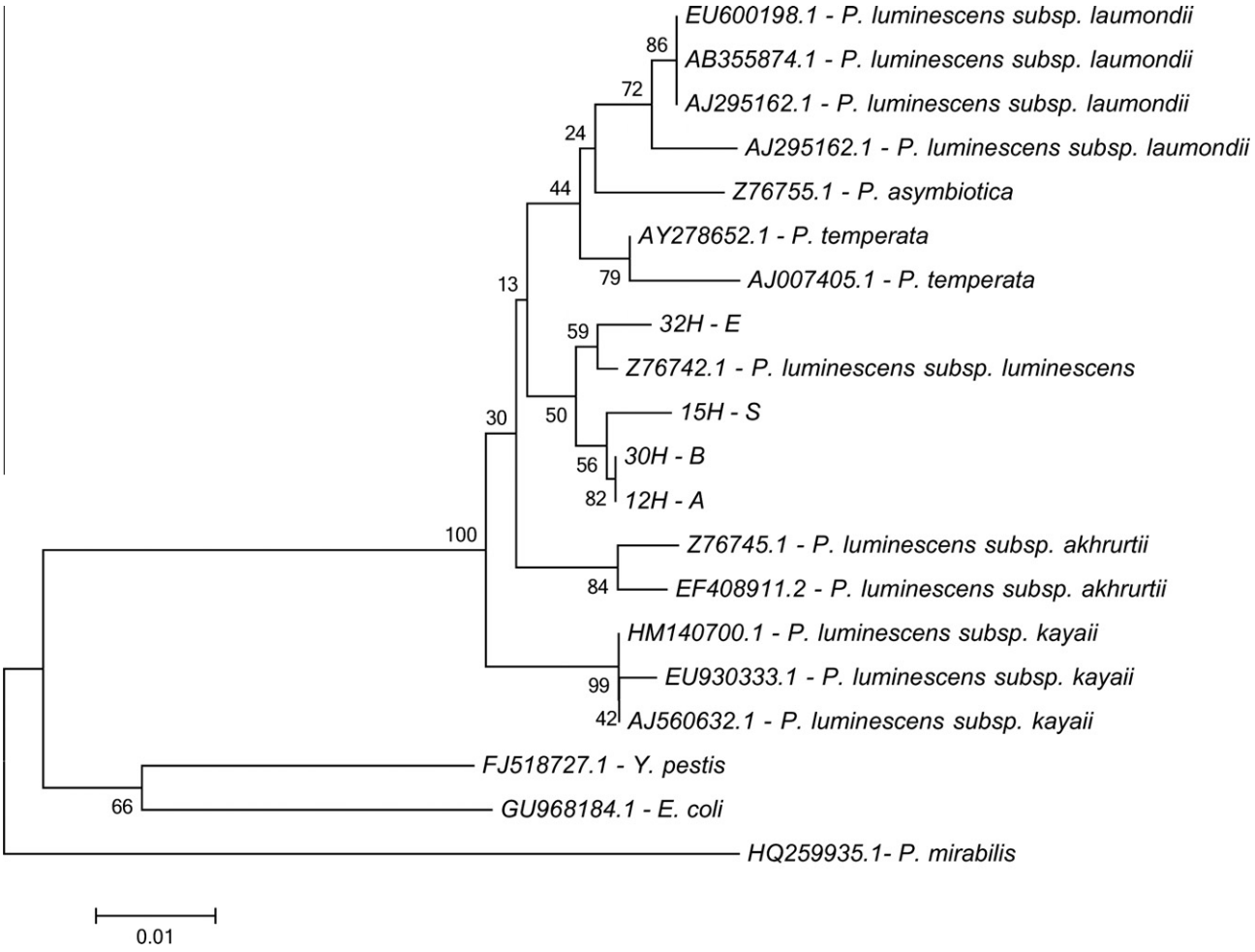

Fig. 2. Distance tree of *Photorhabdus* bacterial symbionts. The tree was constructed from 16S rDNA sequences ($n = 20$) by neighbor-joining using the Kimura 2-parameters model on MEGA 5.0 software. All positions containing gaps and missing data were eliminated.

for oxidase and for fermentation of arabinose. Only 5S-L and 7S-U were positive for indol reaction and tolerance to cetrimide. Isolate 33S-C was the only one among the *Xenorhabdus* bacteria able to hydrolyze urea, while unable to grow in the presence of citrate, rhamnose, adonitol and salycine. These characteristics, summarized in Table 2, are consistent with the taxonomical classification at the genus level (Boemare and Akhurst, 2006).

3.4. Production of urease by entomopathogenic bacteria

Urease production by *Photorhabdus* and *Xenorhabdus* entomopathogenic bacteria was assessed by the urea agar test and ureolytic activity. No urease activity was detected in the supernatants of cell cultures, even after 24 h.

To evaluate the production of urease along the growth curve, four aliquots of the cultures of strains 5S-L, 33S-C, 15H-S and 30H-B were collected at three time points corresponding to the exponential phase of multiplication and a fourth aliquot was taken at the stationary phase (Fig. 4). Urease content was determined by the hydrolysis of urea (Figs. 5 and 6) in the supernatant of bacterial cell lysates.

Fig. 5 shows the ureolytic activity at different pH of the cell lysates sampled during the growth curve of the strains 5S-L, 33S-C, 15H-S and 30H-B.

The patterns of urease production of strains 15H-S, 5S-L and 33S-C followed the growth curve approaching maximal levels at the stationary phase. In contrast, strain 30H-B apparently produces two urease isoenzymes, an acidic form with optimal pH ~5 at the beginning of the exponential phase and a basic one, with optimal pH 8, at the stationary phase. While the ureases produced by strains 15H-S and 5S-L showed similar levels of enzyme activities and optimal pH 6.0, strain 33S-C produced about 10-fold higher urease activity with optimal pH 8.0.

Fig. 6 illustrates the optimal pH of the ureases produced by the different bacterial isolates. While bacteria 30H-B (in the early exponential phase), 15H-S and 5S-L showed (near to) maximal urease activity at pH 5, urease produced by strain 33S-C had only 10% of its activity at this pH. Only the 33S-C urease had maximal activity at pH 8.0. All ureases were active in the pH range 7–8, while very low or no urease activity could be detected at pH 9.0 (not shown). Data in Tables 2 and 3 suggest a positive correlation between urease production by the bacteria and their entomopathogenic effect on *S. frugiperda* larvae. *Xenorhabdus* bacteria, except for 33S-C isolate, produced much less urease and were less effective in killing the larvae. Interestingly, we found a direct correlation between the specific activity of acidic ureases (optimal pH 5–6) produced in the stationary phase and mortality of *S. frugiperda* larvae injected with the bacteria (Fig. 6B).

3.5. Urease activity and pH of hemolymph in injected larvae

SDS–PAGE (Fig. 7) and Western blots (data not shown) of hemolymph collected 24 h after injection of 10^4 bacterial cells into the larvae hemocoel revealed the presence of the 60 kDa subunit typ-

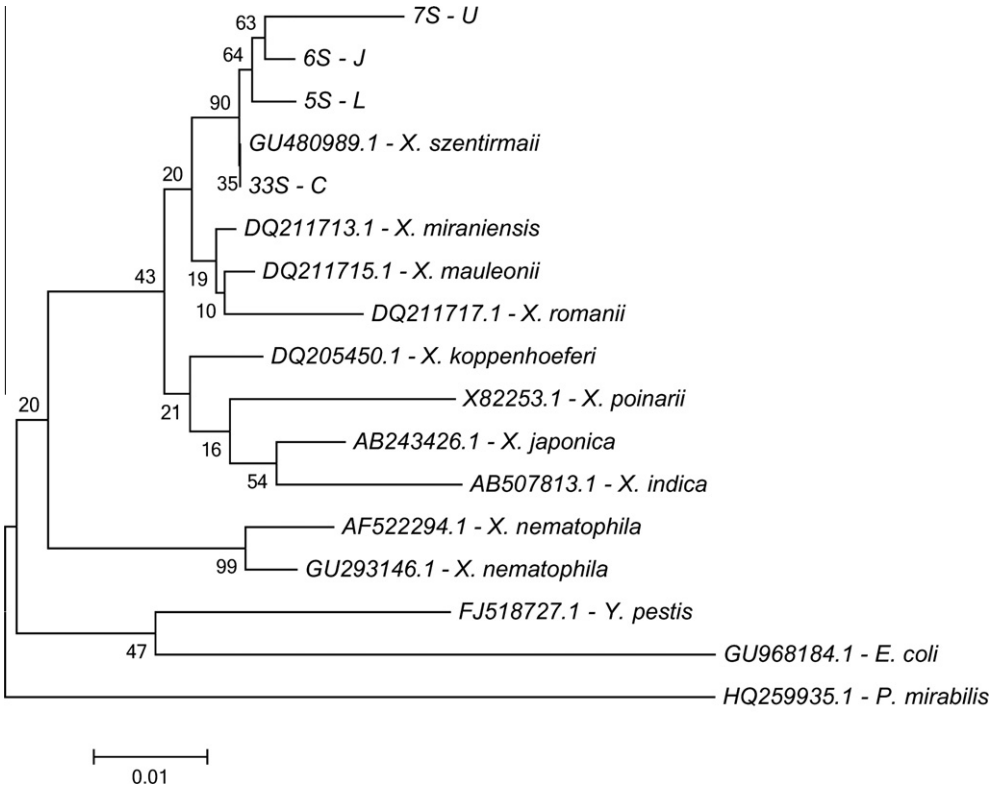

Fig. 3. Distance tree of *Xenorhabdus* bacterial symbionts. The tree was constructed from 16S rDNA sequences ($n = 17$) by neighbor-joining using the Kimura 2-parameters model on MEGA 5.0 software. All positions containing gaps and missing data were eliminated.

Table 2
Biochemical profiles of entomopathogenic *Photorhabdus* and *Xenorhabdus* bacteria.

	Photorhabdus				*Xenorhabdus*			
	12H-A	30H-B	32H-E	15H-S	33S-C	6S-J	5S-L	7S-U
Oxydase	–	–	–	–	+	–	+	+
β-Galactosidase	+	+	–	–	–	–	–	–
Arginine decarboxylase	+	+	+	+	+	+	+	+
Lysine decarboxylase	+	+	+	+	+	+	+	+
Ornithine decarboxylase	+	+	+	+	+	+	+	+
Hydrogen sulfate	–	–	–	–	–	–	–	–
Urease	+	+	+	+	+	–	–	–
Acetyl methyl carbinol	+	+	+	+	+	+	+	+
Phenylalanine desaminase	–	–	–	–	–	–	–	–
Tryptophan desaminase	+	+	+	+	+	+	–	–
Malonate	–	–	–	–	–	–	–	–
Rhamnose	–	–	–	–	+	–	–	–
Adonitol	–	–	–	–	+	–	–	–
Salycine	–	–	–	–	+	–	–	–
Arabinose	–	–	–	–	+	–	+	+
Inositol	+	+	–	+	+	–	–	–
Sorbitol	–	–	–	–	+	–	–	–
Sucrose	–	+	–	–	+	–	–	–
Mannitol	+	+	+	+	+	–	–	–
Rafinose	–	+	–	–	+	–	–	–
Cetrimide	–	–	–	–	–	–	+	+
Acylamidase	–	–	–	–	–	–	–	–
Citrate	+	+	+	+	–	+	+	+
Maltose	+	+	–	+	+	–	+	+
Esculetin	+	+	+	+	–	+	–	–

ical of bacterial urease in all samples. This result confirms the production of urease by the symbiotic bacteria within the host.

The pH of the hemolymph was in the range 7.0–7.5 either for control (non-injected or buffer-injected) larvae or for the larvae injected with any of the four bacterial strains, after 24 h. In all cases the hemolymph was transparent and slightly green except for the larvae injected with the 30H-B bacteria, for which it appeared melanized. Considering these pH values, it could be expected that bacterial urease would be active in the hemolymph along the entire course of infection.

The ureolytic activity of bacterial urease in the hemolymph of control and infected *S. frugiperda* was assayed using exogenous urea. Although the Western blots confirmed the presence of urease in the hemolymph of all larvae 24 h after injection of the bacterial

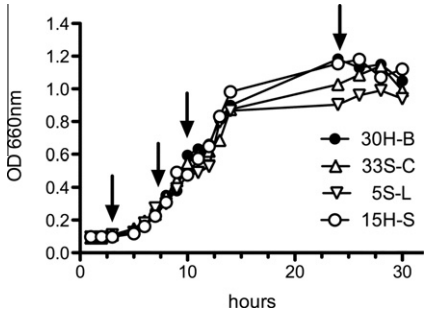

Fig. 4. Growth curve of bacterial strains 5S-L, 33S-C, 15H-S and 30 H-B in LB broth under agitation at 150 rpm in an orbital shaker at 28 °C. The arrows indicate the points when the four aliquots were taken for determination of urease content.

cells and its absence in non-infected ones, the enzyme activity of the bacterial urease could only be detected in the hemolymph of larvae injected with strain 30H-B (*ca.* 0.072 A570/12 h/μL). Surprisingly, a strong inhibitory effect of the *S. frugiperda* hemolymph upon the enzyme activity of jackbean and *H. pylori* urease was detected (Fig. 8). The urease-inhibitory property of *S. frugiperda* hemolymph was the same for control (non-injected) or bacteria-infected larvae. As shown in Fig. 5, except for bacteria 33S-C, the production of urease continues after the bacteria reached the stationary phase, suggesting that along the course of infection, increases in bacterial urease levels could eventually overcome this inhibition. Table 3 summarizes the results of urease production by entomopathogenic bacteria.

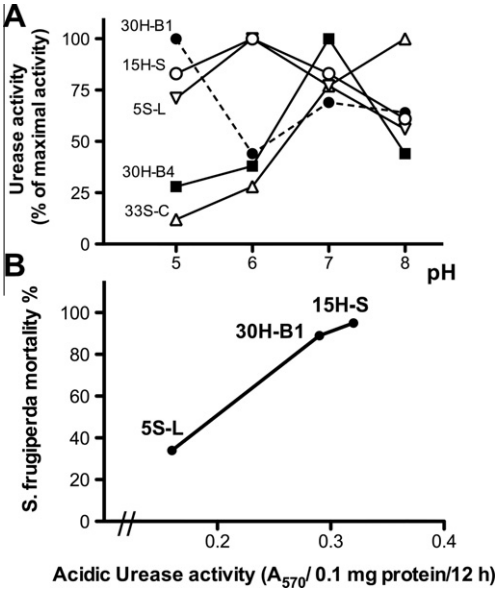

Fig. 6. Panel A: Effect of pH on urease activity in cell lysates of entomopathogenic bacteria. Ureolytic activity is expressed as percentage of the maximal activity taken as 100%. Bacterial cells of strains 15H-S, 33S-C and 5S-L were collected after 24 h of growth. Strain 30H-B was sampled after 2 (B1) and 24 h (B4) for comparison. Panel B: Correlation between the levels of acidic urease production by 5S-L 30H-B and 15H-S bacterial strains and the mortality of *S. frugiperda* larvae injected with 10^4 bacterial cells after 48 h.

3.6. Homology and sequence analysis of Photorhabdus sp. urease

The genome of two species of *Photorhabdus* are available at the NCBI genome data, the entomopathogen *P. luminescens* subsp. *laumondii* TTO1 and the human oportunistic pathogen *Photorhabdus asymbiotica* subsp. *asymbiotica* (Fischer Le-Saux et al.) ATCC 43949. Table 4 depicts values of a BLAST analysis of the similarity of *Photorhabdus* ureases deduced from the genome information compared to the single chain jackbean (*C. ensiformis*) urease, the di-chain urease of *H. pylori* and two bacterial tri-chain ureases

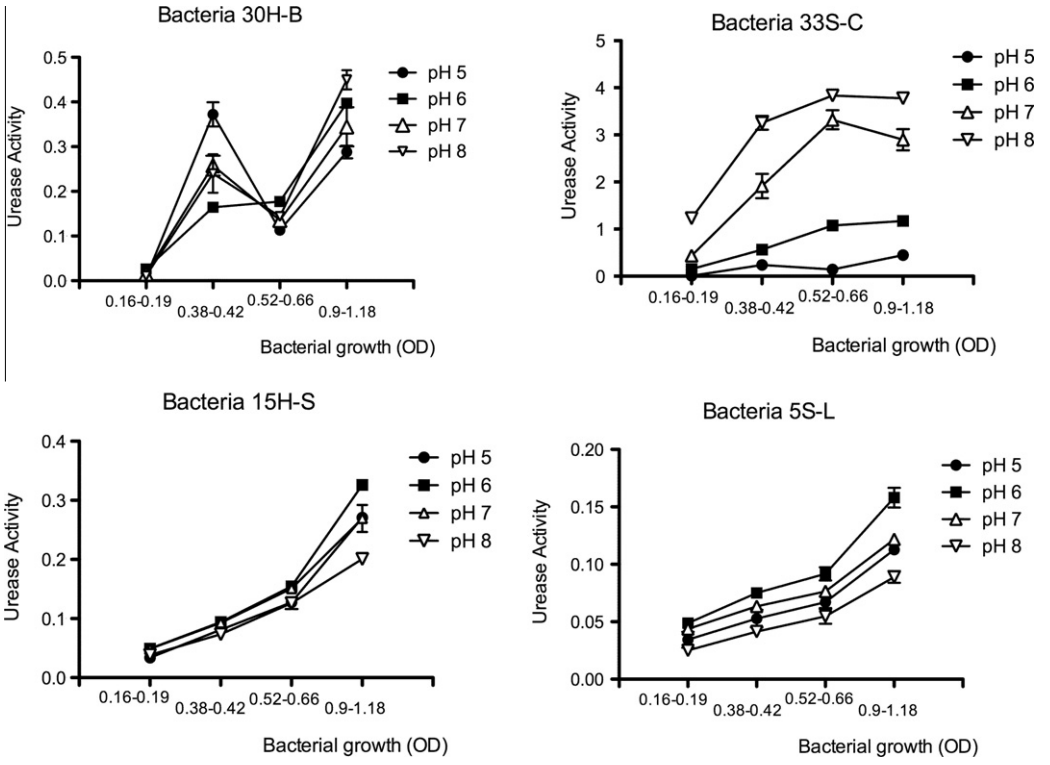

Fig. 5. Urease activity at different pH measured at four points of the growth curve of entomopathogenic bacteria 30H-B, 15H-S, 33S-C and 5S-L. Aliquots of bacterial culture were sampled at 2, 8, 12 and 24 h of growth. After centrifugation, the cell pellet was lysed and the supernatants were used for determination of urease activity. Data (mean ± s.e.m) are expressed as absorbance at 570 nm/100 μg protein/12 h at 37 °C of quadruplicated points.

Table 3
Production of urease by entomopathogenic bacteria.

Bacterial strain	Urease production			*S. frugiperda*	
	Urea agar	Cell lysates		Urease in hemolymph*	Mortality%**
		A_{570}/0.1 mg/h	pH optimum		
Xenorhabdus					
5 S-L	(−)	0.16	6	WB	34 ± 2.6^{e}
6 S-J	(−)	n.d.	n.d.	n.d.	66 ± 3.8^{cd}
7 S-U	(−)	n.d.	n.d.	n.d.	33 ± 3.0^{e}
33 S-C	(+)	3.77	8	WB	57 ± 5.5^{d}
Photorhabdus					
12 H-A	(+)	n.d.	n.d.	n.d.	96 ± 2.8^{a}
15 H-S	(+)	0.32	6	WB	95 ± 1.9^{a}
30 H-B***	(+)	0.45	8 (4)	WB +	89 ± 5.5^{ab}
		0.29	5 (1)	ureolysis	
32 H-E	(+)	n.d.	n.d.	n.d.	75 ± 3.4^{bc}

n.d. – not determined.
* The presence of bacterial ureases in the hemolymph of injected *S. frugiperda* larvae was detected by Western blot against anti-*H. pylori* urease and hydrolysis of urea (ureolysis).
** Mortality of *S. frugiperda* larvae 24 h after injection of 10^4 bacterial cells into the hemocoel. Means followed by a different letter are statistically different ($p < 0.05$).
*** Bacterial strain 30H-B was sampled at two time points of the growth curve (see Fig. 4), corresponding to 2 h (1), and 24 h (4) of growth, respectively.

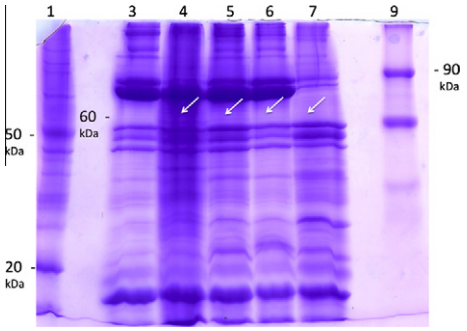

Fig. 7. Electrophoretic analysis of *S. frugiperda* hemolymph 24 h after bacterial infection. Aliquots (30 μL) of hemolymph were applied to 12% polyacrylamide gel containing 0.1% sodium dodecyl sulfate (SDS–PAGE). Lanes: (1) Mr. markers; (3) control (larvae injected with LB broth); (4) larvae injected with 30H-B; 5) larvae injected with 33S-C; (6) larvae injected 5S-L; (7) larvae injected with 15H-S; (9) jackbean urease (8 μg). The arrows indicate the position of 60 kDa bands revealed in Western blots against anti-*H. pylori* urease.

(the soil bacterium *Bacillus pasteurii* [Miquel] and the insect pathogen *Yersinia enterocolitica* [Schleifstein and Coleman]). The identity among all ureases irrespective of their source is around 55% (Mobley et al., 1995). In that context, it can be seen that *Photorhabdus* ureases follow the expected trend with at least 53–60% identity compared to the other ureases. Interestingly, *Y. enterocolitica* urease shares larger identity (70–83%) with *Photorhabdus* urease and both display optimal pH in acidic values (Bhagat and Virdi, 2009) (Supplementary Fig. 1).

4. Discussion

In this study we have identified eight isolates of entomopathogenic nematodes native to the south of Brazil that are potentially effective in controlling *S. frugiperda* populations in maize plantations. Among these isolates, two of *Heterorhabditis* genus and one of *Steinernema* killed about 70% of infected larvae after five days under laboratory conditions. Similar levels of mortality of *S. frugiperda* were observed when the nematodes were tested upon the larvae or pupae in the soil (Salvadori, unpublished data).

Other screenings of entomopathogenic nematodes active against *Spodoptera* species were reported (Abdel-Razek, 2006; Garcia et al., 2008; Glazar et al., 1991). Negrisoli et al. (2010) studied the efficacy of three Brazilian strains of entomopathogenic nematodes in association with commercial insecticides to control *S. frugiperda* in laboratory conditions and in corn fields. Campos-Herrera et al. (2009) reported eighteen isolates of *Xenorhabdus* species associated with *Steinernema* nematodes from Spain and studied

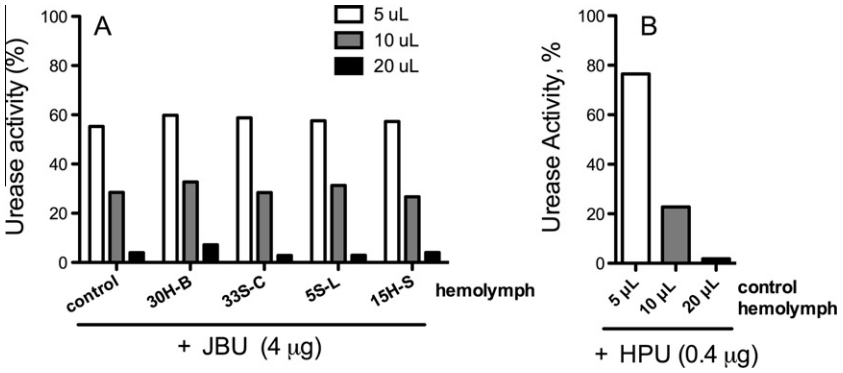

Fig. 8. Urease Inhibitory Activity of *S. frugiperda* hemolymph. Jackbean urease (4 μg; panel A) or *H. pylori* urease (0.4 μg; panel B) were incubated with hemolymph collected from larvae 24 h after injection of the bacterial strains, in the presence of 5 mM urea, in 20 mM sodium phosphate buffer, 150 mM NaCl pH 7.5, in a final volume of 100 μL, for 2 h at 37 °C. Hemolymph from non-injected larvae (control) was tested in the same conditions. The results (means of duplicated points) represent the residual urease activity as compared to the reaction carried out in the absence of hemolymph.

Table 4
BLAST hits for ureases from *Photorhabdus* genomes.

		Urease/urease chains*								
		JBU	HPU		BPU			YEU		
		A	A	B	A	B	C	A	B	C
P. asymbiotica	Query coverage (%)	90**	86	99	100	93	99	100	69	99
	E value	0.0	$2e^{-54}$	0.0	$7e^{-35}$	$5e^{-29}$	0.0	$7e^{-52}$	$2e^{-51}$	0.0
	Max ident. (%)	55	53	57	56	52	57	79	68	83
P. luminescens	Query coverage (%)	94	86	99	100	89	99	100	66	99
	E value	0.0	$6e^{-55}$	0.0	$6e^{-35}$	$4e^{-29}$	0.0	$3e^{-51}$	$4e^{-52}$	0.0
	Max ident. (%)	55	53	57	60	53	57	79	72	83

* JBU, jackbean (*C. ensiformis*) urease; HPU, *H. pylori* urease; BPU, *B. pasteurii* urease; YEU; *Y. enterocolitica* urease.
** Sequences analyzed (search translated nucleotide database using a protein query [tblastn]) were: JBU (gi 167228), BPU A(gi 157884143), BPU B (gi 6573658), BPU C (gi 6573659), HPU A(gi 16974910), HPU B (gi 16974911), YEU A (gi 431750), YEU B (gi 431751), YEU C (gi 431752).

the pathogenicity of four of these isolates towards *Spodoptera littoralis* (Boisduval).

Symbiotic bacteria associated to the entomopathogenic nematodes were successfully isolated and classified taxonomically both by phenotypic-biochemical criteria and sequencing of 16S rDNA (Liu et al., 2001). It is well-known that the relationship between the bacterium and the nematode is highly specific and nematodes only maintain mutual associations with their cognate bacteria or very closely related strains (Eleftherianos et al., 2010). As expected, phylogenetic analysis assigned the bacteria isolated from *Heterorhabditis* and *Steinernema* nematodes respectively into the *Photorhabdus* or *Xenorhadbus* genus. In the case of *Photorhabdus* bacteria, all isolates were close to the well-known entomopathogenic bacterium *P. luminescens* subsp. *luminenscens*. The isolates of *Xenorhabdus* bacteria clustered near to *X. szentirmaii*, which were recovered from nematodes occurring in Argentina, very close to the locations where the nematodes described here were collected (Lee and Stock, 2010).

The entomopathogenic potential of the isolated symbiotic bacteria was evaluated by injection into the hemocoel of 5th instars. All four *Photorhabdus* species produced 75–96% mortality of injected larvae after three days. On the other hand, *Xenorhabdus* bacteria were less active, with mortality rates in the range 33–57% after the same time. This higher lethality of *Photorhabdus* bacteria when injected into *S. frugiperda* larvae correlates with the better efficiency of *Heterorhabditis* nematodes to kill the insects.

A number of factors are implicated in the insecticidal properties of symbiotic bacteria associated with entomopathogenic nematodes. *P. luminescens* (Thomas and Poinar) produces several types of toxins, which are relevant in its trilateral symbiosis with nematodes and insects. A high molecular mass (~1 megaDa) insecticidal toxin (Tc) formed by three components (TcA-, TcB- and TcC-like proteins) complexes, is essential for symbiosis and insecticidal activity (ffrench-Constant and Bowen, 2000; ffrench-Constant et al., 2007; Forst et al., 1997; Silva et al., 2002). The biologically active components of the Tc toxins are ADP-ribosyltransferases (Fieldhouse and Merrill, 2008), which modifies actin and Rho GTPases (Lang et al., 2010, 2011). *Xenorhabdus* bacteria produce a similar toxin complex composed of three proteins (XptA2, XptB1 and XptC1) which *in vitro* can form hybrid complexes with its *Photorhabdus* counterparts (Sheets et al., 2011). The toxin "Makes caterpillars floppy 1" (Mcf1) is also implicated in the insecticidal property of *P. luminescens* (Daborn et al., 2002). Mcf1 induces apoptosis and has sequence similarity with a BH3 (Bcl2-homology 3 domain); it also inhibits hemocyte motility and function, apparently through the Rho subfamily protein Rac (Dowling et al., 2004, 2007).

Another factor that might contribute to the insecticidal properties of *Photorhabdus* and *Xenorhabdus* bacteria is the production of urease. In previous studies (Carlini et al., 1997; Ferreira-DaSilva et al., 2000) we have demonstrated that the entomotoxic activity of canatoxin (an isoform of *C. ensiformis* urease) (Follmer et al., 2001) relies mostly, but not exclusively, on the ability of insects to release an internal peptide from the ingested urease molecule upon the action of cathepsin-like digestive enzymes. Insects with trypsin-based digestion, as is the case of lepidopterans, were found to be insensitive to the lethal action of ingested urease, probably due to their inability to release the entomotoxic peptide(s) contained within the protein molecule (Carlini et al., 1997; Ferreira-DaSilva et al., 2000). We also reported previously that the urease of the soil bacterium *B. pasteurii* was innocuous when fed to the cotton stainer bug *Dysdercus peruvianus* Guérin-Menéville (Follmer et al., 2004). Due of their tri-chain structure, bacterial ureases lack part of the amino acid sequence of the entomotoxic peptide identified in the single chain *C. ensiformis* urease (Mulinari et al., 2007) and this might explain its inability to kill the bugs.

On the other hand, more recent studies have shown that picomolar concentrations of intact jackbean ureases, although not killing the kissing bug *Rhodnius prolixus* Stäl, exert a number of entomotoxic effects such as inhibition of diuresis (Carlini et al., 1997), directly affecting Malpighian tubules (Staniscuaski et al., 2009) and water transport in the crop, as well as increasing the frequency of crop contractions (Staniscuaski et al., 2010). These effects might contribute to the toxicity of urease given orally to insects, acting synergistically with the entomotoxic peptide formed upon hydrolysis of the protein in the hemipteran midgut.

The observations made by Martin et al., 2009, demonstrating that urease production correlated positively to the fitness of *B. thuringiensis* strains to control the gypsy moth *Lymantria dispar*, led us to re-evaluate the potential entomotoxic properties of bacterial ureases and the susceptibility of lepidopterans to entomotoxic effects of ureases. These authors described that among fifty *B. thuringiensis* isolates, only those producing urease activity had the ability to pass repeatedly from one gypsy moth larva to the next, without intervening growth on artificial media. The authors speculated that the role of *B. thuringiensis* urease could be related to biodegradation, improving the ability of the bacteria to replicate in the hemolymph (Martin et al., 2009).

In the present work we studied the urease production of four entomopathogenic bacteria, two *Photorhabdus* spp. and two *Xenorhabdus* spp., both *in vitro* and during the course of infection caused by injection of the bacteria into *S. frugiperda* hemocoel. The pattern of urease production *in vitro* followed the curve of bacteria growth, accumulating in high levels towards the stationary phase. In three of the studied bacterial strains, the results suggest the presence of a single type of urease with optimal activity at an acidic (15H-S and 5S-L) or basic (33S-C) pH range. In contrast, the *Photorhabdus* 30H-B isolate produced predominantly an acidic urease during the exponential phase while a second type, more basic urease, was detected in the stationary phase. The urease specific activity (expressed as A570/12 h/100 μg protein) in acidic media for all

bacteria at the stationary phase was in the range of 0.1–1.0, whereas the basic urease produced by *Xenorhabdus* 33S-C bacteria reached specific activity levels of 3.0–4.0.

The data summarized in Table 3 suggest a positive correlation between urease production by the bacteria and their entomopathogenic effect on *S. frugiperda* larvae. *Xenorhabdus* bacteria, except for 33S-C isolate, produced much less urease than *Photorhabdus* isolates and were less effective in killing the larvae. Interestingly, there is a direct correlation between the specific activity reached by acidic ureases (optimal pH 5–6) in cell lysates sampled at the stationary phase and mortality induced by injecting bacteria into *S. frugiperda* larvae (Fig. 6B).

Urease was produced by the bacteria *in vivo* during the course of infection in lepidopteran larvae and could be detected by SDS–PAGE/Western blot of hemolymph sampled 24 h after injection. Urease activity was detected in the hemolymph of *S. frugiperda* injected with the *Photorhabdus* isolate 30H-B. Considering the pH values of hemolymph in infected larvae, it is expected that bacterial urease could be active in the hemolymph along the entire course of infection. Although most insects are uricotelic, urea has been detected in the hemolymph and in the excreta of many insects and arginase is widely distributed in insects (Burrsell, 1967; Cochran, 1985; Klowden, 2007; Pant and Kumar, 1978). It is noteworthy that in some insects urea concentration in the hemolymph increases depending on the diet and under certain physiological conditions, such as metamorphosis (Hirayama et al., 1999; Pant and Kumar, 1978; Sumida et al., 1993). An increased amount of urea in the infected *S. frugiperda* may result from the release of mitochondrial arginase and arginine from injured tissues. Hydrolysis of this endogenous urea by the bacterial ureases and the release of toxic ammonia would contribute to the entomotoxic effect.

On the other hand our results (Fig. 8) showed the presence of urease inhibitor(s) in the hemolymph of control and bacterial-infected *S. frugiperda* implying that the enzyme's activity would be blocked. Thus, if urease contributes somehow to the entomopathogenic effect of the symbiotic bacteria, this is probably not related to its enzyme activity. Our previous data showed that the ureolytic activity of ureases is not relevant to their insecticidal properties in hemipterans and bruchid beetles (Carlini et al., 1997; Ferreira-DaSilva et al., 2000). Preliminary results indicated the presence of inhibitor(s) of urease activity in the hemolymph of the lepidopteran *Galleria melonella* Linnaeus and also in that of the hemipteran *D. peruvianus* (data not shown). As we previously reported, *D. peruvianus* is highly susceptible to ureolysis-independent entomotoxic effects of plant ureases (Follmer et al., 2004; Piovesan et al., 2008; Staniscuaski et al., 2005). Altogether, these facts raise the possibility that ureases also display ureolysis-independent entomotoxic effect in lepidopterans.

This is the first description of the presence of urease inhibitors in animals. The concentration of this(ese) inhibitor(s) apparently did not change in response to the bacterial infection. The same volume of hemolymph inhibited either 4 μg of jackbean urease or 0.4 μg of *H. pylori* urease, suggesting that this inhibitory activity is more adapted to counteract the action of dietary plant ureases than serving a defense role against infection by urease-producing bacteria.

The chemical nature of this(ese) inhibitor(s), apparently a ca. 10 kDa thermostable molecule (data not shown), was not investigated in the present work. The presence of inhibitors of metalloproteinases (Vilcinskas and Wedde, 2002; Wedde et al., 2007), cysteine proteinases (Miyaji et al., 2007) and serine proteinases (Zhen et al., 2009; Zou et al., 2006) in the hemolymph of insects of different orders has been described. As urease belongs to the superfamily of the amidohydrolases (Holm and Sander, 1997) which encompass some structurally related peptidases (Thoden et al., 2003), a possibility exists that the observed inhibition is due to a proteinase inhibitor.

Conclusion

In this work we have identified entomopathogenic nematodes native to the South region of Brazil, potentially effective for use in the biocontrol of *S. frugiperda*. Symbiotic bacteria associated to these nematodes were characterized biochemically and by their 16S rDNA as belonging to *Photorhabdus* and *Xenorhabdus* genera. Urease production by the symbiotic bacteria correlated positively to their entomopathogenicity. The presence of urease inhibitors in the insect's hemolymph, described here for the first time, suggested that ureases display ureolysis-independent entomotoxic effects in lepidopterans, contributing to the overall toxicity of the nematodes-bacteria complexes.

Authors contribution

J.D.M.S has conducted all experiments with EPNs and EB; M.S.D. carried out the studies on the presence of urease and inhibitors in hemolymph samples; R.L-B. analyzed urease sequences; E.Y.L. worked on taxonomy of EB; J.R.S. collaborated with helpful suggestions and discussing data; C.R.C. conceived this work and wrote the paper .

Acknowledgments

This work was financed by grants from the Brazilian agencies CAPES-MEC (Coordenação de Aperfeiçoamento de Pessoal de Nível Superior), CNPq-MCT (Conselho Nacional de Desenvolvimento Científico e Tecnológico) and FAPERGS (Fundação de Amparo a Pesquisa do Estado do Rio Grande do Sul). We are grateful to Dr. Lidia Fiuza (UNISINOS), Dr. Lucia Vargas (UCS) and Dr. Paulo Roberto Valle da Silva Pereira (EMBRAPA/Trigo) for supplying *S. frugiperda* larvae and granting access to laboratories facilities.

Appendix A. Supplementary data

Supplementary data associated with this article can be found, in the online version, at http://dx.doi.org/10.1016/j.biocontrol.2012.08.002.

References

Abdel-Razek, A., 2006. Infectivity prospects of both nematodes and bacterial symbionts against cotton leafworm, *Spodoptera littoralis* (Biosduval) (Lepidoptera : Noctuidae). J. Pest. Sci. 79, 11–15.
Adams, B.J., Nguyen, K.B., 2002. Taxonomy ans Systematics. In: Gaugler, R. (Ed.), Entomopathogenic Nematology. Rutgers University, New Jersey, pp. 1–28.
Altschul, S.F., Lipman, D.J., 1990. Protein database searches for multiple alignments. Proc. Natl. Acad. Sci. USA 87, 5509–5513.
Bhagat, N., Virdi, J.S., 2009. Molecular and biochemical characterization of urease and survival of *Yersinia enterocolitica* biovar 1A in acidic pH *in-vitro*. BMC Microbiol. 9, 262.
Boemare, N., Akhurst, R.J., 2006. The genera *Photorhabdus* and *Xenorhabdus*. Springer sicence+Business Media, New York.
Boemare, N., Thaler, J.O., Lanois, A., 1997. Simple bacteriological tests for phenotypic characterization of *Xenorhabdus* and *Photorhabdus* phase variants. Symbiosis 22, 167–175.
Burrsell, E., 1967. The excretion of nitrogen in insects. Adv. Insect Physiol. 4, 33–67.
Burton, R.L., Perkins, W.D., 1972. WSB, a new laboratory diet for corn earworm Lepidoptera-Noctuidae and fall armyworm Lepidoptera-Noctuidae. J. Econ. Entomol. 65, 385.
Campos-Herrera, R., Tailliez, P., Pages, S., Ginibre, N., Gutierrez, C., Boemare, N.E., 2009. Characterization of *Xenorhabdus* isolates from La Rioja (Northern Spain) and virulence with and without their symbiotic entomopathogenic nematodes (Nematoda: Steinernematidae). J. Invertebr. Pathol. 102, 173–181.
Carlini, C.R., Oliveira, A.E., Azambuja, P., Xavier-Filho, J., Wells, M.A., 1997. Biological effects of canatoxin in different insect models: evidence for a proteolytic activation of the toxin by insect cathepsinlike enzymes. J. Econ. Entomol. 90, 340–348.
Carlini, C.R., Polacco, J.C., 2008. Toxic properties of urease. Crop Sci. 48, 1665–1672.
Cochran, D.G., 1985. Nitrogen excretion. Pergamon Press, Oxford.

Cruz, I., Figueiredo, M.L.C., Oliveira, A.C., Vasconcelos, C.A., 1999. Damage of *Spodoptera frugiperda* (Smith) in different maize genotypes cultivated in soil under three levels of aluminium saturation. Int J Pest Manage 45, 293–296.

Cruz, I., Turpin, F.T., 1983. Yield impact of infestations of the fall armyworm (Lepidoptera-Noctuidae) to midwhorl growth stage of corn. J. Econ. Entomol. 76, 1052–1054.

Cruz, L.M., de Souza, E.M., Weber, O.B., Baldani, J.I., Dobereiner, J., Pedrosa, F.D., 2001. 16S ribosomal DNA characterization of nitrogen-fixing bacteria isolated from banana (*Musa* spp.) and pineapple (*Ananas comosus* (L.) Merril). Appl. Environ. Microbiol. 67, 2375–2379.

Daborn, P.J., Waterfield, N., Silva, C.P., Au, C.P.Y., Sharma, S., Ffrench-Constant, R.H., 2002. A single *Photorhabdus* gene, makes caterpillars floppy (mcf), allows *Escherichia coli* to persist within and kill insects. Proc. Natl. Acad. Sci. USA 99, 10742–10747.

Dowling, A.J., Daborn, P.J., Waterfield, N.R., Wang, P., Streuli, C.H., ffrench-Constant, R.H., 2004. The insecticidal toxin Makes caterpillars floppy (Mcf) promotes apoptosis in mammalian cells. Cell. Microbiol. 6, 345–353.

Dowling, A.J., Waterfield, N.R., Hares, M.C., Le Goff, G., Streuli, C.H., Ffrench-Constant, R.H., 2007. The Mcf1 toxin induces apoptosis via the mitochondrial pathway and apoptosis is attenuated by mutation of the BH3-like domain. Cell. Microbiol. 9, 2470–2484.

Eleftherianos, I., Joyce, S., Ffrench-Constant, R.H., Clarke, D.J., Reynolds, S.E., 2010. Probing the tri-trophic interaction between insects, nematodes and *Photorhabdus*. Parasitol 137, 1695–1706.

Felsenstein, J., 1985. Confidence-limits on phylogenies – an approach using the bootstrap. Evolution 39, 783–791.

Ferreira-DaSilva, C.T., Gombarovits, M.E., Masuda, H., Oliveira, C.M., Carlini, C.R., 2000. Proteolytic activation of canatoxin, a plant toxic protein, by insect cathepsin-like enzymes. Arch. Insect Biochem. Physiol. 44, 162–171.

ffrench-Constant, R.H., Bowen, D.J., 2000. Novel insecticidal toxins from nematode-symbiotic bacteria. Cell. Mol. Life Sci. 57, 828–833.

ffrench-Constant, R.H., Dowling, A., Waterfield, N.R., 2007. Insecticidal toxins from *Photorhabdus* bacteria and their potential use in agriculture. Toxicon 49, 436-451.

Fieldhouse, R.J., Merrill, A.R., 2008. Needle in the haystack: structure-based toxin discovery. Trends Biochem. Sci. 33, 546–556.

Follmer, C., Barcellos, G.B., Zingali, R.B., Machado, O.L., Alves, E.W., Barja-Fidalgo, C., Guimaraes, J.A., Carlini, C.R., 2001. Canatoxin, a toxic protein from jack beans (*Canavalia ensiformis*), is a variant form of urease (EC 3.5.1.5): biological effects of urease independent of its ureolytic activity. Biochem. J. 360, 217–224.

Follmer, C., Real-Guerra, R., Wasserman, G.E., Olivera-Severo, D., Carlini, C.R., 2004. Jackbean, soybean and *Bacillus pasteurii* ureases: biological effects unrelated to ureolytic activity. Eur. J. Biochem. 271, 1357–1363.

Forst, S., Dowds, B., Boemare, N., Stackebrandt, E., 1997. *Xenorhabdus* and *Photorhabdus* spp.: bugs that kill bugs. Ann. Rev. Microbiol. 51, 47–72.

Garcia, L.C., Raetano, C.G., Leite, L.G., 2008. Application technology for the entomopathogenic nematodes *Heterorhabditis indica* and *Steinernema* sp (Rhabditida : Heterorhabditidae and Steinernematidae) to control *Spodoptera frugiperda* (Smith) (Lepidoptera : Noctuidae) in corn. Neotrop. Entomol. 37, 305–311.

Glazar, I., Galper, S., Sharon, E., 1991. Virulence of the nematode (Steinernematidis and Heterorhabditis) bacteria (*Xenorhabdus* spp.) complex to the Egyptian cotton leafworm *Spodoptera littoralis* (Lepidoptera, Noctuidae). J. Invertebr. Pathol. 57, 94–100.

Hirayama, C., Sugimura, M., Shinbo, H., 1999. Recycling of urea associated with the host plant urease in the silkworm larvae, *Bombyx mori*. J. Insect Physiol. 45, 15–20.

Holm, L., Sander, C., 1997. An evolutionary treasure: unification of a broad set of amidohydrolases related to urease. Proteins: Struct. Funct. Genet. 28, 72–82.

Kim, Y., Kim, K., Seo, J., Shrestha, S., Kim, H.H., Nalini, M., Yi, Y.K., 2009. Identification of an entomopathogenic bacterium, *Serratia* sp ANU101, and its hemolytic activity. J. Microbiol. Biotech. 19, 314–322.

Kimura, M., 1980. A simple method for estimating evolutionary rate of base substitutions through comparative studies of nucleotide sequences. J. Mol. Evol. 16, 111–120.

Klowden, M.J., 2007. Physiological systems in insects. Elsevier Academic Press, London, p. 688.

Laemmli, U.K., 1970. Cleavage of structural proteins during the assembly of the head of bacteriophage T4. Nature 227, 680–685.

Lang, A.E., Schmidt, G., Schlosser, A., Hey, T.D., Larrinua, I.M., Sheets, J.J., Mannherz, H.G., Aktories, K., 2010. *Photorhabdus luminescens* toxins ADP-ribosylate actin and RhoA to force actin clustering. Science 327, 1139–1142.

Lang, A.E., Schmidt, G., Sheets, J.J., Aktories, K., 2011. Targeting of the actin cytoskeleton by insecticidal toxins from *Photorhabdus luminescens*. N-S Arch. Pharmacol. 383, 227–235.

Lee, M.M., Stock, S.P., 2010. A multigene approach for assessing evolutionary relationships of *Xenorhabdus* spp. (gamma-Proteobacteria), the bacterial symbionts of entomopathogenic *Steinernema* nematodes. J. Invertebr. Pathol. 104, 67–74.

Liu, J., Berry, R.E., Blouin, M.S., 2001. Identification of symbiotic bacteria (*Photorhabdus* and *Xenorhabdus*) from the entomopathogenic nematodes *Heterorhabditis marelatus* and *Steinernema oregonense* based on 16S rDNA sequence. J. Invertebr. Pathol. 77, 87–91.

Martin, P.A.W., Farrar, R.R., Blackburn, M.B., 2009. Survival of diverse *Bacillus thuringiensis* strains in gypsy moth (Lepidoptera: Lymantriidae) is correlated with urease production. Biol. Control 51, 147–151.

McGee, D.J., May, C.A., Garner, R.M., Himpsl, J.M., Mobley, H.L., 1999. Isolation of *Helicobacter pylori* genes that modulate urease activity. J. Bacteriol. 181, 2477–2484.

Mendes, S.M., Boregas, K.G.B., Lopes, M.E., Waquil, M.S., Waquil, J.M., 2011. Fall armyworm responses to genetically modified maize expressing the toxin Cry 1A(b). Pesqui. Agropecu. Bras. 46, 239–244.

Miyaji, T., Kouzuma, Y., Yaguchi, J., Matsumoto, R., Kanost, M.R., Kramer, K.J., Yonekura, M., 2007. Purification of a cysteine protease inhibitor from larval hemolymph of the tobacco hornworm (*Manduca sexta*) and functional expression of the recombinant protein. Insect Biochem. Mol. Biol. 37, 960–968.

Mobley, H.L.T., Island, M.D., Hausinger, R.P., 1995. Molecular biology of microbial ureases. Microbiol. Rev. 59, 451–480.

Mulinari, F., Staniscuaski, F., Bertholdo-Vargas, L.R., Postal, M., Oliveira-Neto, O.B., Rigden, D.J., Grossi-de-Sa, M.F., Carlini, C.R., 2007. Jaburetox-2Ec: an insecticidal peptide derived from an isoform of urease from the plant *Canavalia ensiformis*. Peptides 28, 2042–2050.

Negrisoli, A.S., Garcia, M.S., Negrisoli, C., Bernardi, D., da Silva, A., 2010. Efficacy of entomopathogenic nematodes (Nematoda: Rhabditida) and insecticide mixtures to control *Spodoptera frugiperda* (Smith, 1797) (Lepidoptera: Noctuidae) in corn crops. Crop. Prot. 29, 677–683.

Pant, R., Kumar, S., 1978. Is a urea cycle present in insects? Biochem. J. 174, 341–344.

Parra, J.R.P., 1998. Criação de insetos para estudos com patógenos. FEALQ, Piracicaba.

Piovesan, A.R., Staniscuaski, F., Marco-Salvadori, J., Real-Guerra, R., Defferrari, M.S., Carlini, C.R., 2008. Stage-specific gut proteinases of the cotton stainer bug *Dysdercus peruvianus*: role in the release of entomotoxic peptides from *Canavalia ensiformis* urease. Insect Biochem. Mol. Biol. 38, 1023–1032.

Poinar, G.G., Thomas, G.M., 1966. Significance of Achromobacter nematophilus Poinar and Thomas (Achromobacteraceae: Eubacteriales) in the development of the nematode, DD-136 (Neoaplectana sp., Steinernematidae). Parasitol 56.

Saiki, R.K., Gelfand, D.H., Stoffel, S., Scharf, S.J., Higuchi, R., Horn, G.T., Mullis, K.B., Erlich, H.A., 1988. Primer-directed enzymatic amplification of DNA with a thermostable DNA-polymerase. Science 239, 487–491.

Saitou, N., Nei, M., 1987. The neighbor-joining method – a new method for reconstructing phylogenetic trees. Mol. Biol. Evol. 4, 406–425.

Sheets, J.J., Hey, T.D., Fencil, K.J., Burton, S.L., Ni, W.T., Lang, A.E., Benz, R., Aktories, K., 2011. Insecticidal toxin complex proteins from *Xenorhabdus nematophilus*. Structure and pore formation. J. Biol. Chem. 286, 22742–22749.

Silva, C.P., Waterfield, N.R., Daborn, P.J., Dean, P., Chilver, T., Au, C.P.Y., Sharma, S., Potter, U., Reynolds, S.E., ffrench-Constant, R.H., 2002. Bacterial infection of a model insect: *Photorhabdus luminescens* and *Manduca sexta*. Cell. Microbiol. 4, 329–339.

Staniscuaski, F., Brugge, V.T., Carlini, C.R., Orchard, I., 2009. In-vitro effect of *Canavalia ensiformis* urease and the derived peptide Jaburetox-2Ec on *Rhodnius prolixus* Malpighian tubules. J. Insect Physiol. 55, 255–263.

Staniscuaski, F., Brugge, V.T., Carlini, C.R., Orchard, I., 2010. Jack bean urease alters serotonin-induced effects on *Rhodnius prolixus* anterior midgut. J. Insect Physiol. 56, 1078–1086.

Staniscuaski, F., Ferreira-Dasilva, C.T., Mulinari, F., Pires-Alves, M., Carlini, C.R., 2005. Insecticidal effects of canatoxin on the cotton stainer bug *Dysdercus peruvianus* (Hemiptera: Pyrrhocoridae). Toxicon 45, 753–760.

Sumida, M., Haga, K., Tanaka, Y., Shimabukuro, J., Ichida, M., Matsubara, F., 1993. Developmental changes in urea in the hemolymph (determined by a urease-indophenol method) in hybrid strains of the silkworm *Bombyx mori*, and the effect of starvation in the 5th instar larvae, fed an artificial diet, on urea level in subsequent development. Comp Biochem Physiology A-Physiol 105, 563–570.

Tamura, K., Dudley, J., Nei, M., Kumar, S., 2007. MEGA4: Molecular evolutionary genetics analysis (MEGA) software version 4.0. Mol. Biol. Evol. 24, 1596–1599.

Thoden, J.B., Marti-Arbona, R., Raushel, F.M., Holden, H.M., 2003. High-resolution X-ray structure of isoaspartyl dipeptidase from *Escherichia coli*. Biochemistry 42, 4874–4882.

Towbin, H., Staehelin, T., Gordon, J., 1979. Electrophoretic transfer of proteins form polyacrylamide gels to nitrocellulose sheets. Procedure and some applications. Proc. Natl. Acad. Sci. USA 76, 4350–4354.

Vilcinskas, A., Wedde, M., 2002. Insect inhibitors of metalloproteinases. IUBMB Life 54, 339–343.

Wassermann, G.E., Olivera-Severo, D., Uberti, A.F., Carlini, C.R., 2010. *Helicobacter pylori* urease activates blood platelets through a lipoxygenase-mediated pathway. J. Cell Mol. Med. 14, 2025–2034.

Weatherburn, M.W., 1967. Phenol-hypochlorite reaction for determination of ammonia. Anal. Chem. 39, 971–974.

Wedde, M., Weise, C., Nuck, R., Altincicek, B., Vilcinskas, A., 2007. The insect metalloproteinase inhibitor gene of the lepidopteran *Galleria mellonella* encodes two distinct inhibitors. Biol. Chem. 388, 119–127.

White, G.F., 1927. A method for obtaining infective nematode larvae from culture. Science 66, 302–303.

Zhen, Z., Zhao, P.C., Hua, W., Mita, K., Jiang, H.B., 2009. A comparative analysis of serpin genes in the silkworm genome. Genomics 93, 367–375.

Zhu, H., Grewal, P.S., Reding, M.E., 2011. Development of a dessicated cadaver delivery system to apply entomopathogenic nematodes for control of soil pests. Appl. Eng. Agric. 27, 317–324.

Zou, Z., Lopez, D.L., Kanost, M.R., Evans, J.D., Jiang, H.B., 2006. Comparative analysis of serine protease-related genes in the honey bee genome: possible involvement in embryonic development and innate immunity. Insect Mol. Biol. 15, 603–614.

IV. Artigo Publicado

Paluzzi *et al*., 2012

● Participação no desenho e na execução dos experimentos que avaliaram uma possível participação da JBU e do Jaburetox na ativação/inibição do receptor de CAPA de *Rhodnius prolixus* em ensaios funcionais. Item 3.4 (Fig. 6).

Peptides 34 (2012) 127–134

Contents lists available at SciVerse ScienceDirect

Peptides

journal homepage: www.elsevier.com/locate/peptides

Investigation of the potential involvement of eicosanoid metabolites in anti-diuretic hormone signaling in *Rhodnius prolixus*

Jean-Paul V. Paluzzi[a,*], Paul Young[a], Marina S. Defferrari[b], Ian Orchard[c], Célia R. Carlini[d], Michael J. O'Donnell[a]

[a] Department of Biology, McMaster University, Hamilton, ON L8S 4K1, Canada
[b] Graduate Program in Cellular and Molecular Biology, Center of Biotechnology, Universidade Federal do Rio Grande do Sul, Porto Alegre, RS 91501-970, Brazil
[c] Department of Biology, University of Toronto Mississauga, Mississauga, ON L5L 1C6, Canada
[d] Department of Biophysics and Center of Biotechnology, Universidade Federal do Rio Grande do Sul, Porto Alegre, RS 91501-970, Brazil

ARTICLE INFO

Article history:
Received 4 August 2011
Received in revised form 21 October 2011
Accepted 23 October 2011
Available online 3 November 2011

Keywords:
Urease
Anti-diuresis
Malpighian tubule
Chagas'
Neuroendocrinology
Second messengers

ABSTRACT

The use of naturally occurring plant-derived compounds for controlling insect pests remains an attractive alternative to potentially dangerous synthetic chemical compounds. One prospective plant-based compound, isoforms of the so-called jack bean urease (JBU) from the jack bean, *Canavalia ensiformis*, as well a derived peptide, Jaburetox-2Ec, have insecticidal effects on an array of insect species. In the Chagas' disease vector, *Rhodnius prolixus*, some of the physiological effects attributed to these urease isoforms include inhibition of serotonin (5-HT)-stimulated fluid secretion by the Malpighian tubules (MTs). Here, we investigated whether the effects of these exogenous urease isoforms were targeting the neuroendocrine network involved in the anti-diuretic hormone (RhoprCAPA-2) signaling cascade. We show that pharmacological agents known to interfere with eicosanoid metabolite biosynthesis do not affect RhoprCAPA-2 inhibition of 5-HT-stimulated fluid secretion by MTs. In addition, we demonstrate that RhoprCAPA-2 inhibition of MTs is independent of extracellular or intracellular calcium. Using a heterologous system for analysis of receptor activation, we show that neither JBU nor Jaburetox-2Ec are agonists of the anti-diuretic hormone receptor, RhoprCAPAr1. Finally, activation of the receptor using sub-maximal doses of the natural ligand, RhoprCAPA-2, was not influenced by the presence of either JBU or Jaburetox-2Ec indicating that the urease isoforms do not compete with RhoprCAPA-2 for binding and activation of RhoprCAPAr1. Taken together, these results suggest that at least two distinct mechanisms leading to inhibition of fluid secretion by MTs exist in *R. prolixus* and, unlike the urease-related effects, the eicosanoid metabolite pathway is not involved in RhoprCAPA-2 mediated anti-diuresis.

1. Introduction

Rhodnius prolixus is a haematophagous insect that has been identified as a principal vector of Chagas' disease in Central and South America [56]. Transmission of the protozoan parasite *Trypanosoma cruzi*, that causes Chagas' disease in humans, occurs in close association with the rapid diuresis in *R. prolixus* that facilitates excretion of excess fluid and ions from the blood meal [32]. *T. cruzi* trypomastigotes are transmitted through fecal contamination of the bite wound produced by blood feeding [29]. The enormous blood meal imbibed by *R. prolixus* during each post-embryonic stage is required for nymphal development and also contributes to increased egg production in adult females [15]. The rapid diuresis that follows engorgement of vertebrate blood has been studied in detail and involves rapid rates of transport of ions that are present in excess in the blood meal, mainly sodium and chloride, as well as osmotically obliged water. The excess water and salts associated mainly with the non-nutritive plasma portion of the blood meal is removed by absorption across the lumen of the anterior midgut that is matched with secretion of primary urine by the MTs so that salt and water homeostasis is maintained within the haemolymph [25].

Two diuretic hormones have now been identified in *R. prolixus*: the first hormone, a biogenic amine, is serotonin (5-hydroxytryptamine; 5-HT); and, the second is a peptide, related to the corticotropin-releasing factor family of vertebrate peptides, RhoprCRF/DH [50]. Both of these diuretic hormones lead to rapid increases in fluid and ion transport across the anterior midgut epithelium [4,14,18,48,50] and are responsible for

* Corresponding author at: Department of Biology, McMaster University, Life Science Building Room # 524, 1280 Main Street West, Hamilton, ON L8S4K1, Canada. Tel.: +1 905 525 9140x23343; fax: +1 905 522 6066.
E-mail addresses: paluzzi@mcmaster.ca, jeanpaul.paluzzi@gmail.com (J.-P.V. Paluzzi).

0196-9781/$ – see front matter © 2011 Elsevier Inc. All rights reserved.
doi:10.1016/j.peptides.2011.10.025

increasing secretion rates by MTs over a thousand-fold relative to unstimulated tubules [23,24,26,51,52]. Secretion rates of this magnitude would result in disruption of haemolymph homeostasis within a short period of time if diuresis were not stringently controlled, and *R. prolixus* must be capable of down regulating diuresis to counter this effect [25,39,40]. Interestingly, however, although members of other diuretic peptide families are known to exist in *R. prolixus* [49,50,53,59], only 5-HT and RhoprCRF/DH are diuretic hormones acting on the anterior midgut [48,50,54] and MTs [12]. In order to prevent excessive loss of water and salts, the rapid diuresis terminates around 3–4 h post-feeding. An anti-diuretic neurohormone, namely RhoprCAPA-2, has been shown to inhibit 5-HT-stimulated absorption by the anterior midgut as well as inhibit 5-HT-stimulated secretion by MTs [18,33,34,36]. RhoprCAPA-2 exerts its effects on the anterior midgut and MTs through activation of the anti-diuretic hormone receptor, RhoprCAPAr1 [35].

Interestingly, isoforms of the jack bean urease (JBU) from the jack bean plant, *Canavalia ensiformis*, as well as a peptide derived from JBU, Jaburetox-2Ec (JBX), have been shown to have inhibitory actions on 5HT-stimulated secretion by MTs [46]. More specifically, the JBU effects were shown to be dependent on eicosanoid metabolites and calcium ions, whereas the effects of JBX may involve cyclic GMP [46].

Given that the primary targets eliciting the JBU and JBX effects in *R. prolixus* are unknown, we sought to elucidate if these exogenous plant-derived factors were acting on cellular targets of the native anti-diuretic peptide, RhoprCAPA-2. First, we determined whether the eicosanoid metabolite pathway inhibitors could block RhoprCAPA-2 inhibition of 5-HT-stimulated tubule fluid secretion. We next studied the involvement of intracellular and extracellular calcium in RhoprCAPA-2 inhibition of tubule fluid secretion stimulated by 5-HT. Lastly, we investigated if the anti-diuretic hormone receptor, RhoprCAPAr1, could be activated by either JBU or JBX, and furthermore we tested if RhoprCAPA-2-induced receptor activation could be modulated in the presence of either JBU or JBX. Our findings suggest that the JBU and JBX mediated inhibition of tubule fluid secretion is independent of the native anti-diuretic peptide signaling mechanism leading to the cessation of diuresis.

2. Methods

2.1. Animals

R. prolixus Stål were obtained from a laboratory colony at the Department of Biology, University of Toronto Mississauga. Insects were maintained at 25 °C and high relative humidity and were routinely fed on defibrinated rabbit blood (Cedarlane, Burlington, ON) using an artificial feeding membrane. Unfed fifth-instar insects were used in all experiments, approximately 6–8 weeks post-feeding as fourth instars.

2.2. Malpighian tubule (MT) fluid secretion assays

Insects were dissected under physiological saline as described previously [36]. Malpighian tubules were excised whole and transferred on glass probes to 20 μl drops of saline submerged in water-saturated paraffin oil in Sylgard-coated Petri dishes. The entire upper/distal (secretory) segment of the tubule was placed in the saline droplet and the lower/proximal end of each tubule was wrapped around a minuten pin. The length of the lower (reabsorptive) tubule section for each tubule that was excised was not standardized, as fluid secretion rates were found to be unaffected by the length of the lower tubule [27,39]. Tubule secretion was monitored after rupturing the lower tubule segment between the saline droplet and the minuten pin with fine forceps. Transfer of secreted droplets following set intervals was accomplished using a micro-aspirator. The diameter of the secreted droplet was used to calculate volume (V) and determined by use of an ocular micrometer and calculated using the formula $V = (\Pi/6)d^3$, where d represents the diameter of the droplet measured by an ocular micrometer.

Stimulation of fluid secretion by MTs with 5-HT was carried out using either 100 nM or 1 μM. The lower dose was used to produce sub-maximal rates of fluid secretion [54] that could be challenged with the anti-diuretic peptide, RhoprCAPA-2, while the higher dose of 5-HT was used to achieve maximal secretion rates. To ensure functionality of the excised MTs and exclusion of damaged preparations, the first treatment involved sub-maximal concentrations of 5-HT over 30 min and were used to determine control secretion rates. Subsequently, the tubules were washed with saline and incubated for 30 min with sub-maximal 5-HT in combination with an experimental compound (endogenous anti-diuretic peptide alone or in presence of pharmacological agent). Following a saline wash, tubules were treated with a high dose of 5-HT for 30 min in order to determine maximal secretion rates which were used for normalization of data if required. In order to determine if extracellular calcium was required for anti-diuretic peptide signaling, fluid secretion assays were carried out in calcium-free saline containing the calcium chelator, ethylene glycol-bis(2-aminoethylether)-N,N,N′,N′-tetraacetic acid (EGTA; 1 mM) and supplementing with $MgCl_2$ to maintain saline osmolarity. The involvement of intracellular calcium stores in anti-diuretic peptide signaling was tested using the intracellular calcium antagonist, 8-(diethylamino)octyl-3,4,5-trimethoxybenzoate hydrochloride (TMB-8) [11]. Serotonin hydrochloride (5-hydroxytryptamine hydrochloride; 5-HT), TMB-8, dexamethasone and indomethacin were purchased from Sigma (Oakville, Ontario, Canada). RhoprCAPA-2 was obtained as described previously [36].

2.3. Jack bean urease and recombinant peptide, Jaburetox-2Ec

Jack bean urease (JBU) was purchased (Sigma, Oakville, ON) and prepared as a 1 mM stock solution as described previously [46]. The V5-His6 tagged recombinant peptide, Jaburetox-2Ec (JBX), was purified as described previously [30]. In brief, *Escherichia coli* BL21(DE3)-strain bacteria (NEB, Pickering, ON) were transformed with pET101-JBX recombinant vector and cells were grown overnight on LB plates containing ampicillin. Colonies containing recombinant vector were confirmed following standard plasmid minipreparation (BioBasic, Markam, ON) and DNA sequencing (Center for Applied Genomics at the Hospital for Sick Children, Toronto, ON). An aliquot of recombinant bacteria liquid culture grown overnight was taken and added to fresh media (250 mL) containing ampicillin. Cells were grown at 37 °C with shaking (~300 rpm) until an OD_{600} = 0.6–0.8 at which point isopropyl β-D-thiogalactopyranoside (IPTG) was added to a final titer of 0.5 mM. Following a 3 h induction, cells were harvested, resuspended in lysis buffer (50 mM sodium phosphate buffer, pH 7.0, 400 mM NaCl, 100 mM KCl, 10% glycerol, 0.5% Triton X-100 and 10 mM imidazole), sonicated and centrifuged (14,000 × *g* for 20 min). The supernatant was processed on a nickel affinity column (Ni-NTA-agarose; Qiagen, Mississauga, ON), which was previously equilibrated with buffer (50 mM sodium phosphate buffer pH 8.0, 300 mM NaCl, 10 mM imidazole). After 30 min, the column was washed with 20 mL of the same buffer, containing 20 mM imidazole. The protein was eluted with the equilibration buffer containing 200 mM imidazole and quantified following the Bradford assay [5]. The samples were dialyzed against 20 mM sodium phosphate, 1 mM ethylenediaminetetraacetic acid (EDTA), 5 mM β-mercaptoethanol, pH 7.5, 0.02% sodium azide.

2.4. CAPA receptor assay

In order to test the possible interaction or activation of the anti-diuretic hormone receptor by JBU or JBX, we transiently transfected Chinese hamster ovary (CHO) cells with the functional CAPA receptor variant, RhoprCAPAr1. Initially, recombinant CHO cells were prepared by stably expressing the bioluminescent reporter protein aequorin from the jellyfish, *Aequorea victoria*. The codon-optimized aequorin encoding full-length open reading frame within the mammalian expression vector, pcDNA3.1+ (Invitrogen, Burlington, ON), was a kind gift from Dr. Yoonseong Park (Entomology, Kansas State University) [21]. The recombinant-vector containing aequorin was linearized using BglII (Invitrogen, Burlington, ON) in order to reduce the likelihood of vector integration into the CHO cell genome in a way that would impede optimal expression [58]. CHO cells were transfected at 80–90% confluency in basal Dulbecco's Modified Eagle's Medium (DMEM)/F12 (1×, 1:1) media containing 4-(2-hydroxyethyl)piperazine-1-ethanesulfonic acid (HEPES) (Invitrogen, Burlington, ON) and were then subjected to Geneticin selection 48 h later. After two weeks of Geneticin selection (400 μg/mL), individual recombinant colonies were seeded into separate wells of a 96 well cell-culture dish (Fisher Scientific, Ottawa, ON). Colonies were grown to confluence and seeded in duplicate plates maintained under Geneticin selection. In order to identify colonies with optimal aequorin expression and yielding the greatest signal-to-noise ratio, individual monoclonal recombinant lines were assayed in the calcium reporter assay as described previously [35] in response to 25 μM ATP, which acts on endogenous P_{2U}-purinoceptor leading to calcium mobilization [19]. The line showing the greatest luminescent response to ATP treatment, called *CHOK1-aeq* for future reference, was expanded for preparation of cryo-stocks and CAPA receptor analysis.

CHOK1-aeq cells were grown to 90% confluency in complete media containing Geneticin (200 μg/mL) and transfected in basal media (without serum or anti-biotic) with RhoprCAPAr1 (in pcDNA3.1+) using FuGENE HD (Roche Applied Science, Laval, QC) transfection reagent following manufacturer instructions. The receptor assay was carried out 48–60 h after transfection as previously described [35].

2.5. Statistics

Figures were prepared in GraphPad Prism 4.0 and data analyzed accordingly using either unpaired *t*-test or one-way ANOVA and appropriate post-test. Differences between treatments were considered significant if $p < 0.05$.

3. Results

3.1. Investigation of eicosanoid signaling in 5-HT stimulated secretion by MTs

In order to assess if eicosanoid metabolites are involved in 5-HT-stimulated fluid secretion by MTs, we challenged tubules with 100 nM 5-HT alone or in the presence of either 25 nM dexamethasone (Fig. 1A), a phospholipase A2 inhibitor, or 1 μM indomethacin (Fig. 1B), a cyclooxygenase inhibitor. The results demonstrate that neither pharmacological agent could inhibit 5-HT stimulated fluid secretion by MTs. Therefore, it does not appear that eicosanoid metabolites are involved in 5-HT stimulated secretion by *R. prolixus* MTs.

3.2. Investigation of eicosanoid signaling in RhoprCAPA-2 inhibition of MTs

To evaluate the association of the arachidonic acid pathway in the anti-diuretic function of RhoprCAPA-2 on MTs, we tested the effect of dexamethasone. Firstly, MTs were stimulated with 100 nM 5-HT alone for 30 min. At the end of this first interval, secreted droplets were measured and MTs were washed with saline and treated with 100 nM 5-HT and 1 μM RhoprCAPA-2 in the presence or absence of 2.5 nM dexamethasone. Following this second interval, secreted droplets were measured and MTs were again washed with saline and treated with 1 μM 5-HT for 30 min to determine maximum secretion rates (data not shown), which was recorded in the event it was necessary to normalize the data due to differences in 5-HT stock efficacy. Malpighian tubules treated with 100 nM 5-HT and 1 μM RhoprCAPA-2, in the presence or absence of dexamethasone, showed secretion rates significantly lower (over two-fold) than treatments receiving 100 nM 5-HT alone. Importantly, there was no significant change in the inhibition of fluid secretion by RhoprCAPA-2 in the presence of dexamethasone (Fig. 2). The effect of a higher dose of dexamethasone (25 nM) was also tested; however, this also had no significant effect on RhoprCAPA-2 inhibition of tubule fluid secretion stimulated by 5-HT (data not shown).

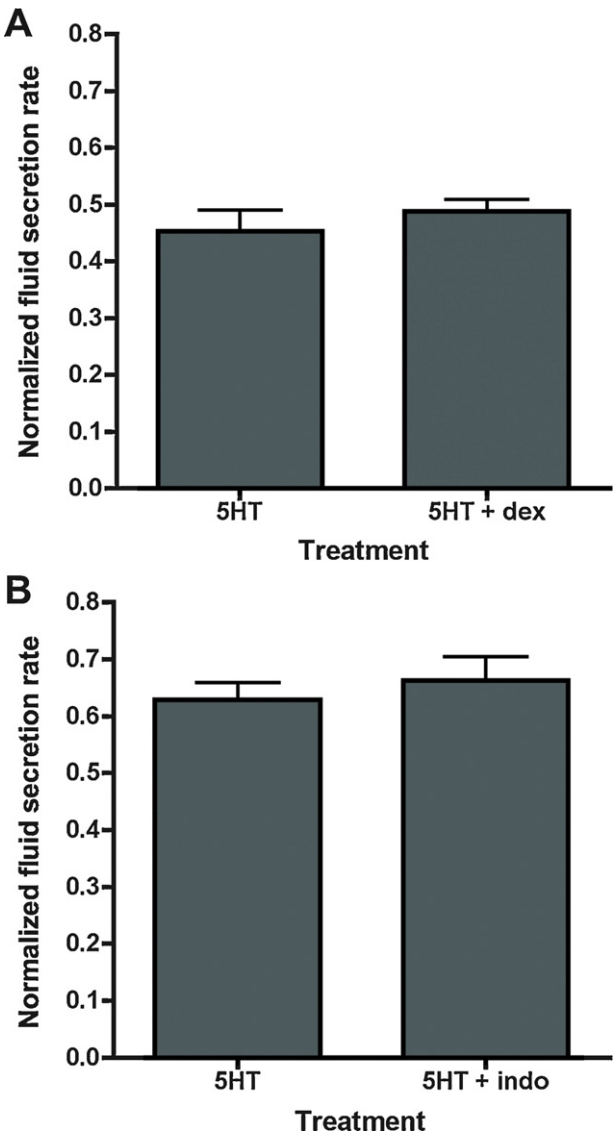

Fig. 1. Stimulation of Malpighian tubule fluid secretion by 5-HT is independent of eicosanoid metabolites. Tubules were treated with 100 nM 5HT alone or together with either 25 nM dexamethasone (A) or 1 μM indomethacin (B). Data is plotted as normalized values relative to maximum secretion rates obtained following treatment with 1 μM 5-HT. Data were arcsin transformed prior to statistical analysis. Values are mean ± S.E.M.; $n = 8–10$ per treatment.

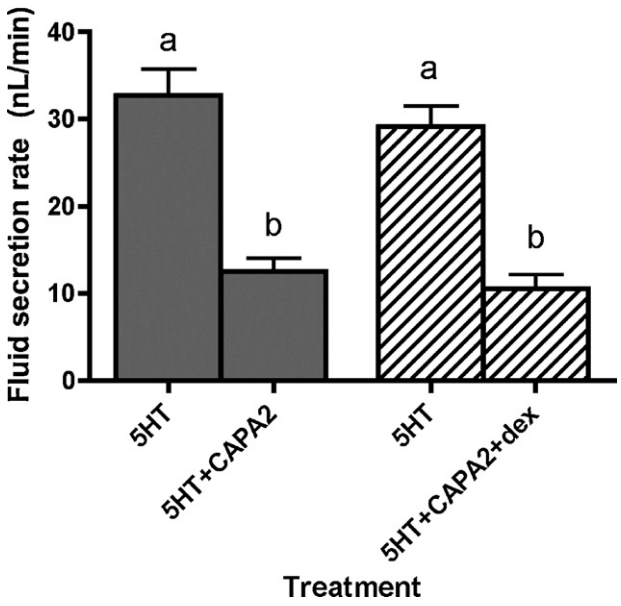

Fig. 2. Lack of effect by dexamethasone (dex) on the inhibitory actions of the anti-diuretic peptide, RhoprCAPA-2, on tubule fluid secretion stimulated by 5-HT. Tubules were challenged with 100 nM 5-HT alone over the first 30 min. Over the next 30 min, tubules were treated with 100 nM 5HT + 1 μM RhoprCAPA-2 or 100 nM 5HT + 1 μM RhoprCAPA-2 + 2.5 nM dexamethasone. Values are mean ± S.E.M. Columns denoted with different letters are significantly different ($p < 0.01$, One-way ANOVA, Tukey post-test).

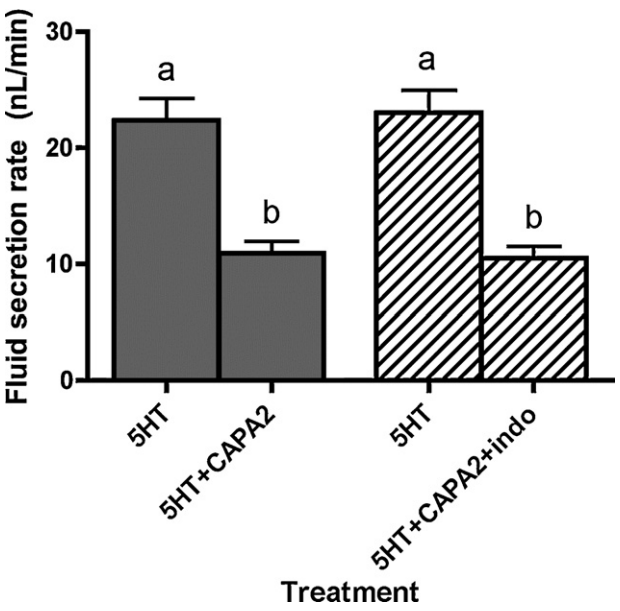

Fig. 3. Lack of effect by indomethacin (indo) on the inhibitory actions of the anti-diuretic peptide, RhoprCAPA-2, on tubule fluid secretion stimulated by 5-HT. Tubules were challenged with 100 nM 5-HT alone over first 30 min. Over the next 30 min, tubules were treated with 100 nM 5-HT + 1 μM RhoprCAPA-2 or 100 nM 5HT + 1 μM RhoprCAPA-2 + 1 μM indomethacin. Values are mean ± S.E.M. Columns denoted with different letters are significantly different ($p < 0.01$, One-way ANOVA, Tukey post-test).

In order to ascertain the lack of involvement of eicosanoids in RhoprCAPA-2 elicited anti-diuresis, we investigated the effect of another inhibitor of the eicosanoid pathway, indomethacin. This anti-inflammatory drug has been shown to be a potent inhibitor of cyclooxygenase activity [1,41], thus inhibiting the production of prostaglandins. Experiments were carried out as discussed above for dexamethasone treatment; however, indomethacin was used at a dose of 1 μM. Both treatments involving RhoprCAPA-2 showed fluid secretion rates that were significantly lower (over two-fold) than tubules receiving 100 nM 5-HT alone (Fig. 3). However, there was no change in the ability of RhoprCAPA-2 to inhibit fluid secretion in tubules stimulated by 5-HT in the presence or absence of indomethacin.

3.3. Examining the role of calcium in regulation of secretion by MTs

The subsequent experiments were carried out to investigate the potential involvement of calcium ions in anti-diuretic hormone signaling. In calcium-free saline, RhoprCAPA-2 maintained the ability to inhibit fluid secretion of MTs stimulated with 5-HT (Fig. 4). Also, there was no significant change in rates of secretion by MTs stimulated with 5-HT in the presence or absence of extracellular calcium. In order to investigate the role of intracellular calcium stores on the inhibitory action of RhoprCAPA-2, we utilized calcium-free saline containing the calcium antagonist, TMB-8. In the absence of extracellular calcium and presence of TMB-8, RhoprCAPA-2 maintains its ability to inhibit 5-HT stimulated fluid secretion by MTs (Fig. 5). In addition, it appears that 5-HT is also unaffected since there is no significant change in fluid secretion in calcium-free saline containing calcium antagonist, TMB-8.

3.4. Investigation of CAPA receptor activation by urease isoforms

Given the possibility that the anti-diuretic effect of JBU on MTs is mediated via a membrane bound receptor, we investigated whether the CAPA receptor could be activated by JBU, or its derived peptide, JBX. Using a heterologous expression system, we transiently expressed the RhoprCAPA receptor (RhoprCAPAr1) and tested a series of doses of JBU and JBX (between 12.5 fM and 1.25 μM). As a control, we tested the natural ligand of the CAPA receptor, RhoprCAPA-2 at several doses (between 25 pM and 2.5 μM). Neither JBU nor JBX were capable of eliciting activation of the CAPA receptor over the series of doses tested (Fig. 6). As expected, RhoprCAPA-2 demonstrated activation of the receptor

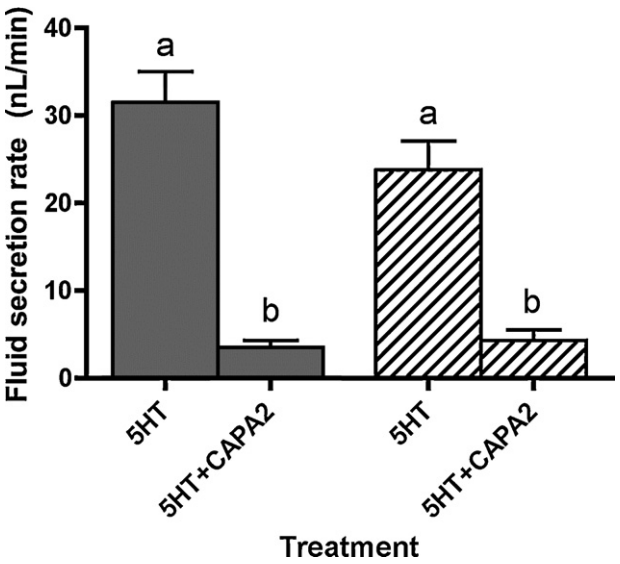

Fig. 4. The inhibitory action of RhoprCAPA-2 on fluid secretion of MTs is independent of extracellular calcium. Tubules were challenged with 100 nM 5-HT alone over the first 30 min and then received 100 nM 5-HT + 1 μM RhoprCAPA-2 over a second 30 min treatment in normal saline (filled columns) or calcium-free saline containing 1 mM EGTA (hatched columns). Values are mean ± S.E.M. Columns denoted with different letters are significantly different ($p < 0.01$, One-way ANOVA, Tukey post-test).

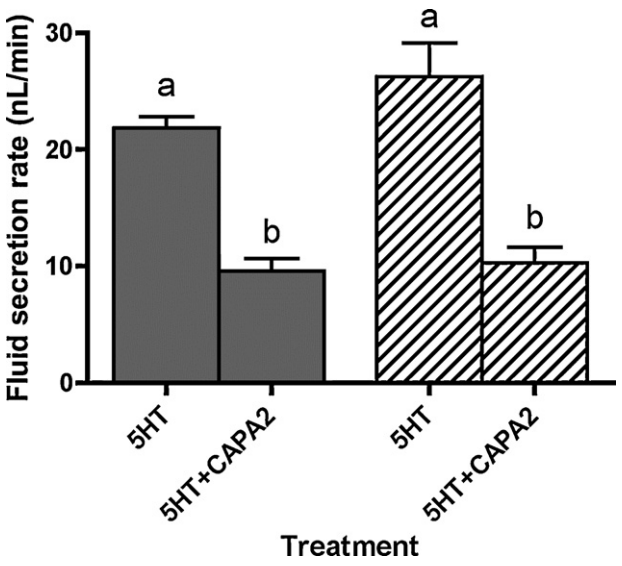

Fig. 5. The inhibitory action of RhoprCAPA-2 on fluid secretion of MTs is not affected by the calcium antagonist, TMB-8. Tubules were challenged with 100 nM 5-HT alone over the first 30 min and then received 100 nM 5-HT + 1 μM RhoprCAPA-2 over a second 30 min treatment in calcium-free saline containing 1 mM EGTA (filled columns) or calcium-free saline containing EGTA and 1 nM TMB-8 (hatched columns). Values are mean ± S.E.M. Columns denoted with different letters are significantly different ($p < 0.01$, One-way ANOVA, Tukey post-test).

(EC_{50} = 612 nM), validating functionality of the receptor assay system.

One final possibility warranting investigation was the potential interaction of JBU or JBX with the native anti-diuretic hormone, RhoprCAPA-2. This could potentially lead to interference with neuroendocrine signaling within the insect, which could lead to disruption in water and/or ion balance. To test this possibility, we again utilized the receptor assay system and used a dose of the native anti-diuretic hormone yielding approximately 50% activation of the receptor. In this way, we could investigate if activation of

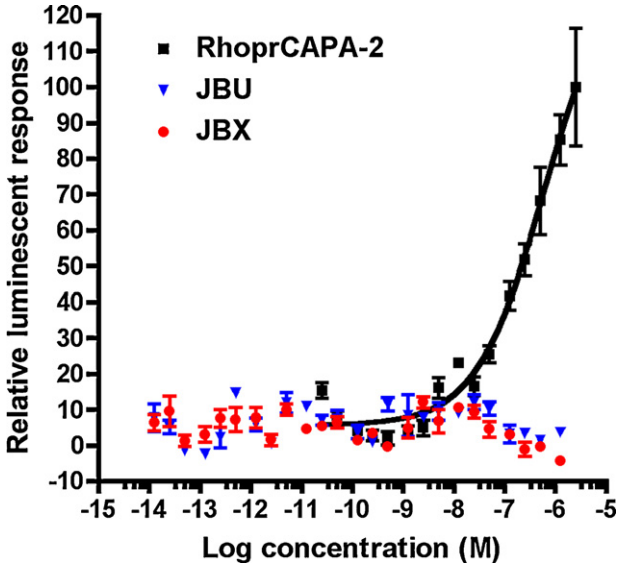

Fig. 6. Heterologous expression assay of the *R. prolixus* CAPA receptor (RhoprCAPAr1) in CHO-K1 cells. Activity of the natural ligand, RhoprCAPA-2, as well as Jack Bean Urease (JBU) and the urease-derived recombinant peptide, Jaburetox-2Ec (JBX) from *Canavalia ensiformis*. CAPA receptor was transiently expressed in CHO-K1 cells stably expressing cytoplasmic aequorin (see Section 2). For each data point, vertical bars denote S.E.M. and all values are plotted relative to the average maximum luminescent response obtained by RhoprCAPA-2 (EC_{50} = 612 nM).

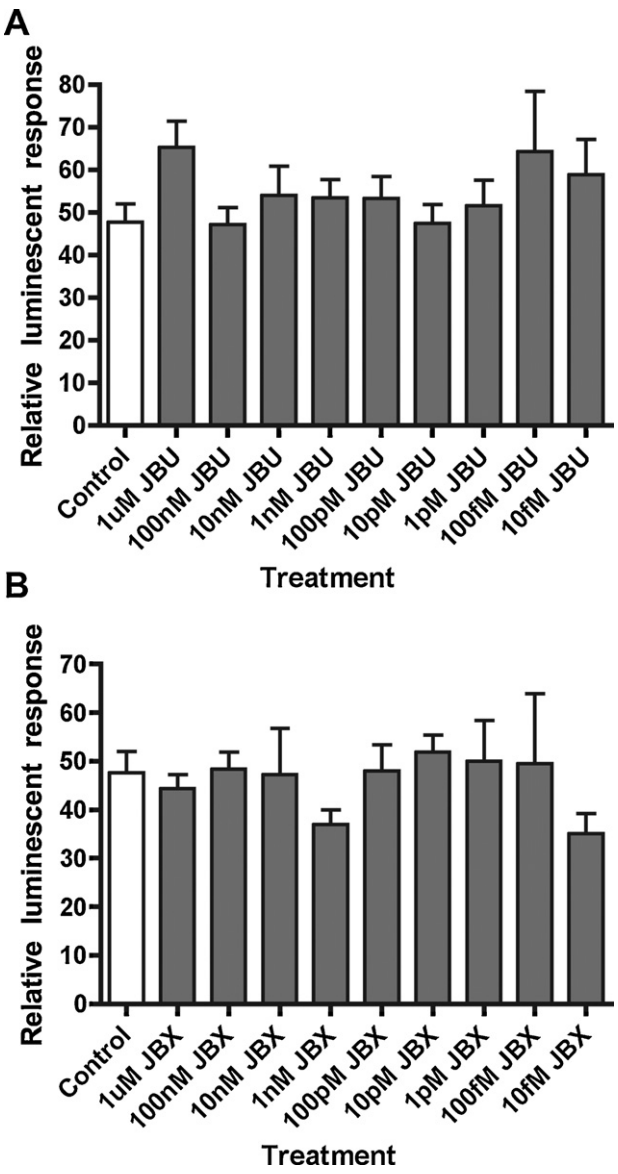

Fig. 7. Heterologous expression assay of the *R. prolixus* CAPA receptor (RhoprCAPAr1) in CHO-K1 cells. Activity of the natural ligand, RhoprCAPA-2, at a dosage of 500 nM in the absence (control open-column) or presence of various doses of (A) Jack Bean Urease (JBU) or (B) urease-derived recombinant peptide, Jaburetox-2Ec (JBX) from *Canavalia ensiformis*. CAPA receptor was transiently expressed in CHO-K1 cells stably expressing cytoplasmic aequorin (see Section 2). For each data point, vertical bars denote S.E.M. and all values are plotted relative to the average maximum luminescent response obtained by application of RhoprCAPA-2 alone at a dosage of 2.5 μM. No significant difference was observed between control and treatments with different doses of either JBU or JBX ($p > 0.05$, One-way ANOVA, Dunnett's post-test).

the receptor was potentiated or attenuated in the presence of various doses of either JBU or JBX. CAPA receptor activation by 500 nM RhoprCAPA-2 in the presence of JBU tested at doses between 10 fM and 1 μM did not produce any significant change in receptor activation compared to controls with RhoprCAPA-2 alone (Fig. 7A). Similarly, 500 nM RhoprCAPA-2 in the presence of JBX tested at doses between 10 fM and 1 μM did not generate receptor activation significantly different from 500 nM RhoprCAPA-2 alone (Fig. 7B).

4. Discussion

The search for environmentally benign and species-specific agents to control insect pests remains an attractive alternative to non-specific and potentially dangerous synthetic chemical

compounds. Peptidomimetics, or non-peptide small molecules that act as mimics for neuropeptides, may have great potential for application in pest control owing to their biostability as well as the vast array of physiological processes they regulate [43]. Prospective agents that may be suitable in pest control strategies must be carefully studied in order to determine the physiological effects in both the target pest species as well as in unintended target species, that could come in to contact with these compounds. Urease isoforms and their derived peptides, from the jack bean plant, *C. ensiformis*, have emerged as potentially effective compounds in control of insect pests [7]. For example, the recombinant peptide JBX, which is equivalent to the urease-derived peptide following cleavage by insect cathepsin-like enzymes, has been shown to have potent insecticidal effects [30,45,55]. The presence of, and activation by, cathepsin-like digestive enzymes was shown to be necessary for cleavage and release of the insecticidal compound, pepcanatoxin [30]. As a result, insects with trypsin-like digestive enzyme are not sensitive to oral administration of JBU [9], but are nonetheless sensitive to injection of the recombinant peptide JBX, equivalent to the insecticidal peptide from JBU [30]. Considering the various effects in mammalian cells, including exocytosis in an array of cell types [2,8,16,31], more research is needed to determine the suitability of these compounds as insecticides.

Until recently, the mode of action of the urease isoforms in insects was unresolved. In mammalian models, effects of urease isoforms were shown to be calcium-dependant and also shown to involve eicosanoids derived from the lipoxygenase pathway of arachidonic acid metabolism [3,8]. Recent studies have shown that urease-related biological effects also involve arachidonic acid metabolites in insects. For example, in *R. prolixus*, fluid secretion of MTs stimulated by the diuretic hormone, 5-HT, can be inhibited by JBU or JBX [46]. Specifically, the effects of JBU are blocked by applying dexamethasone [46], which interferes with eicosanoid metabolite signaling by inhibiting phospholipase A2 activity [28]. In addition, the inhibitory action of JBU on MTs was shown to be calcium-dependent since removing extracellular and intracellular sources of this ion abolishes the activity of JBU [46]. In the anterior midgut of *R. prolixus*, indomethacin has been shown to abolish the potentiation of 5-HT induced gut contractions by JBU [44]. Our studies utilizing inhibitors of arachidonic acid signaling indicate that RhoprCAPA-2 inhibition of fluid secretion in tubules stimulated with 5-HT is independent of eicosanoid metabolites. Specifically, neither dexamethasone nor indomethacin were capable of blocking the inhibitory activity of RhoprCAPA-2 on MTs. Interestingly, JBX activity on the MTs is thought to involve a signaling cascade that is also independent of eicosanoid metabolites, but may involve cGMP [46]. Earlier, it was believed that cGMP may also be a second messenger for the endogenous anti-diuretic peptide [39] since this molecule antagonizes the effects of cAMP (the second messenger of diuretic hormones). However, with the identification of the endogenous anti-diuretic peptide, treatment of tubules with RhoprCAPA-2 in the absence of 5-HT did not yield levels of cGMP significantly higher than saline controls [34,36]. Nonetheless, the decrease in cGMP levels that occurs following treatment of MTs with 5-HT is abolished when RhoprCAPA-2 is co-applied, likely indicating inhibition of a cGMP-hydrolyzing phosphodiesterase rather than increased guanylate cyclase activity. More recently, studies investigating the effects of RhoprCAPA-2 on fluid absorption and ion transport across the anterior midgut of *R. prolixus* also demonstrated a cGMP-independent pathway, since cGMP is stimulatory at this tissue [18].

The involvement of calcium ions in eliciting the anti-diuretic activity of RhoprCAPA-2 was investigated since urease effects in insects and mammals have been shown to be calcium dependent. For example, canatoxin (a urease isoform), promotes the influx of calcium required for phospholipase activation in platelets [16]. In *R. prolixus*, JBU inhibition of MTs requires calcium since interference with extracellular or intracellular pools abolishes JBU effects [46]. Here, we show that RhoprCAPA-2 can effectively inhibit fluid secretion of MTs in the absence of extracellular calcium sources and presence of the calcium antagonist, TMB-8. In comparison to other insects, this is a rather surprising result since CAPA peptides are known to require extracellular calcium for stimulation of fluid secretion by MTs of *Drosophila melanogaster* [42]. Thus, it is evident that the pathway leading to stimulation of fluid secretion in some dipteran insects [38] is not responsible for the anti-diuretic effect associated with CAPA peptides in *R. prolixus* [34,36]. Interestingly, studies involving dexamethasone in other systems have shown that it can also inhibit inducible nitric oxide synthase expression [22]. Therefore, this suggests another key component of the CAPA signaling cascade in *D. melanogaster* [6,13] is not involved in the anti-diuretic effects of CAPA peptides in *R. prolixus*. To support this conclusion, studies on MTs of *R. prolixus* using a nitric oxide donor, sodium nitroprusside (SNP), failed to elicit any significant effect on fluid secretion [40]. In contrast to this finding, a similar dose of SNP was previously utilized in *D. melanogaster* and demonstrated stimulatory action on fluid secretion by MTs [13].

Receptor activation experiments revealed that the anti-diuretic hormone receptor, RhoprCAPAr1, is not the cellular target leading to inhibition of tubule fluid secretion by ureases. Neither JBU nor JBX can elicit activation of the CAPA receptor, and in addition, neither urease isoform modulated the activation of the receptor by sub-maximal doses of the natural ligand, RhoprCAPA-2. Importantly, we must note that the heterologous system utilized for this receptor assay is dependent on calcium mobilization, and thus, this would appear to contradict the above-mentioned *in vitro* experiments demonstrating the lack of calcium involvement. However, studies have shown that differences in post-translational processing or receptor promiscuity often occurs when utilizing heterologous systems [20,47], which in some cases can be advantageous in determining receptor–ligand pairing when downstream signaling partners are unknown. This is also supported by the sizeable disparity in RhoprCAPA-2 potency (~100-fold) observed between physiological assays involving inhibition of tubule fluid secretion (IC_{50} = 4 nM) [36] and heterologous receptor assays (EC_{50} = 385 nM) [35]. Attempts at expressing and functionally characterizing the *R. prolixus* CAPA receptor in other heterologous cell-based systems, such as *Drosophila* S2 cells, HEK-293 cells, CHO-K1 recombinant lines containing promiscuous G proteins, all failed to yield quantifiable data for receptor–ligand interaction (Paluzzi, unpublished observations); while native CHO-K1 cells successfully facilitated receptor characterization [35]. This demonstrates the importance of identifying a suitable expression system by testing an array of systems, if readily available, for receptor subtypes that are difficult to characterize.

In conclusion, inhibition of Malpighian tubule fluid secretion by RhoprCAPA-2 is independent of eicosanoid metabolites and calcium. In addition, results from pharmacological studies and receptor functional assays suggest that the inhibitory actions of urease isoforms on *R. prolixus* MTs are likely independent of the signaling cascade involving RhorpCAPA-2 and its cognate receptor, RhoprCAPAr1. These findings suggest the existence of an alternative eicosanoid metabolite-dependent inhibitory pathway leading to inhibition of 5-HT-stimulated secretion by MTs in *R. prolixus*. Eicosanoid metabolite-dependent inhibition of basal fluid secretion by MTs has been documented previously in insects. Specifically, in both *Aedes aegypti* and *Formica polyctena*, inhibition of eicosanoid biosynthesis reduced basal fluid secretion rates [37,57]. Therefore, future research will investigate this apparent eicosanoid metabolite-involvement in inhibition of diuretic hormone-stimulated fluid secretion in *R. prolixus*.

The rapid post-gorging diuresis occurring in *R. prolixus*, and in related Triatominae species, is of great importance for the transmission of *T. cruzi* leading to Chagas' disease. While chemotherapeutic agents are available for treating infected individuals during the acute stage of infection, these drugs have serious side effects and are not as effective in the chronic stages of infection [10,17]. Thus, improving our understanding of how endogenous and exogenous factors regulate homeostasis in insects of medical importance can play a significant role in the development of agents to control or eradicate these important disease vectors.

Acknowledgements

This work was supported through a NSERC postdoctoral fellowship to J.P.P., NSERC Discovery Grants to M.J.O, and I.O and graduate research exchange funding to M.S.D. through the Emerging Leaders in the Americas Program (ELAP) of the Canadian Bureau for International Education.

References

[1] Banik NL, Matzelle D, Terry E, Gantt-Wilford G, Hogan EL. Inhibition of proteolysis by a cyclooxygenase inhibitor, indomethacin. Neurochem Res 2000;25:1509–15.
[2] Barja-Fidalgo C, Guimaraes JA, Carlini CR. Canatoxin, a plant protein, induces insulin release from isolated pancreatic islets. Endocrinology 1991;128:675–9.
[3] Barja-Fidalgo C, Guimaraes JA, Carlini CR. Lipoxygenase-mediated secretory effect of canatoxin the toxic protein from *Canavalia ensiformis* seeds. Toxicon 1991;29:453–9.
[4] Barrett FM. Absorption of Fluid from the anterior midgut in Rhodnius. J Insect Physiol 1982;28:335–41.
[5] Bradford MM. A rapid and sensitive method for the quantitation of microgram quantities of protein utilizing the principle of protein–dye binding. Anal Biochem 1976;72:248–54.
[6] Broderick KE, MacPherson MR, Regulski M, Tully T, Dow JAT, Davies SA. Interactions between epithelial nitric oxide signaling and phosphodiesterase activity in Drosophila. Am J Physiol: Cell Physiol 2003;285:C1207–18.
[7] Carlini ClR, Polacco JC. Toxic properties of urease. Crop Sci 2008;48:1665–72.
[8] Carlini CR, Guimaraes JA, Ribeiro JM. Platelet release reaction and aggregation induced by canatoxin, a convulsant protein: evidence for the involvement of the platelet lipoxygenase pathway. Br J Pharmacol 1985;84:551–60.
[9] Carlini CR, Oliveira AEA, Azambuja P, Xavier-Filjo J, Wells MA. Biological effects of canatoxin in different insect models: evidence for a proteolytic activation of the toxin by insect cathepsinlike enzymes. Anglais 1997;90:340–8.
[10] Castro JA, de Mecca MM, Bartel LC. Toxic side effects of drugs used to treat Chagas' disease (American trypanosomiasis). Hum Exp Toxicol 2006;25:471–9.
[11] Charo IF, Feinman RD, Detwiler TC. Inhibition of platelet secretion by an antagonist of intracellular calcium. Biochem Biophys Res Commun 1976;72:1462–7.
[12] Donini A, O'Donnell MJ, Orchard I. Differential actions of diuretic factors on the Malpighian tubules of *Rhodnius prolixus*. J Exp Biol 2008;211:42–8.
[13] Dow JA, Maddrell SH, Davies SA, Skaer NJ, Kaiser K. A novel role for the nitric oxide-cGMP signaling pathway: the control of epithelial function in Drosophila. Am J Physiol 1994;266:R1716–9.
[14] Farmer J, Maddrell SHP, Spring JH. Absorption of fluid by the midgut of Rhodnius. J Exp Biol 1981;94:301–16.
[15] Friend WG, Choy CT, Cartwright E. The effect of nutrient intake on the development and the egg production of *Rhodnius prolixus* Stahl (Hemiptera: Reduviidae). Can J Zool 1965;43:891–904.
[16] Ghazaleh FA, Francischetti IM, Gombarovits ME, Carlini CR. Stimulation of calcium influx and platelet activation by canatoxin: methoxyverapamil inhibition and downregulation by cGMP. Arch Biochem Biophys 1997;339:362–7.
[17] Guedes PM, Silva GK, Gutierrez FR, Silva JS. Current status of Chagas disease chemotherapy. Expert Rev Anti Infect Ther 2011;9:609–20.
[18] Ianowski JP, Paluzzi JP, Te Brugge VA, Orchard I. The antidiuretic neurohormone RhoprCAPA-2 downregulates fluid transport across the anterior midgut in the blood-feeding insect *Rhodnius prolixus*. Am J Physiol Regul Integr Comp Physiol 2010;298:R548–57.
[19] Iredale PA, Hill SJ. Increases in intracellular calcium via activation of an endogenous P2-purinoceptor in cultured CHO-K1 cells. Br J Pharmacol 1993;110:1305–10.
[20] Kenakin T. Agonist-receptor efficacy. I. Mechanisms of efficacy and receptor promiscuity. Trends Pharmacol Sci 1995;16:188–92.
[21] Kim YJ, Spalovska-Valachova I, Cho KH, Zitnanova I, Park Y, Adams ME, et al. Corazonin receptor signaling in ecdysis initiation. Proc Natl Acad Sci U S A 2004;101:6704–9.
[22] Kunz D, Walker G, Eberhardt W, Pfeilschifter J. Molecular mechanisms of dexamethasone inhibition of nitric oxide synthase expression in interleukin 1 beta-stimulated mesangial cells: evidence for the involvement of transcriptional and posttranscriptional regulation. Proc Natl Acad Sci U S A 1996;93:255–9.
[23] Maddrell SH. Excretion in the blood-sucking bug, *Rhodnius Prolixus* Stal. II. The normal course of diuresis and the effect of temperature. J Exp Biol 1964;41:163–76.
[24] Maddrell SH, Herman WS, Mooney RL, Overton JA. 5-Hydroxytryptamine: a second diuretic hormone in *Rhodnius prolixus*. J Exp Biol 1991;156:557–66.
[25] Maddrell SH, O'Donnell MJ, Caffrey R. The regulation of haemolymph potassium activity during initiation and maintenance of diuresis in fed *Rhodnius prolixus*. J Exp Biol 1993;177:273–85.
[26] Maddrell SHP. Excretion in the blood-sucking bug, *Rhodnius prolixus* Stal. I. The control of diuresis. J Exp Biol 1963;40:247–56.
[27] Maddrell SHP, Phillips JE. Secretion of hypo-osmotic fluid by the lower Malpighian tubules of *Rhodnius prolixus*. J Exp Biol 1975;62:671–83.
[28] Miller JS, Nguyen T, Stanley-Samuelson DW. Eicosanoids mediate insect nodulation responses to bacterial infections. Proc Natl Acad Sci U S A 1994;91:12418–22.
[29] Mortara RA, Andreoli WK, Fernandes MC, da Silva CV, Fernandes AB, L'Abbate C, et al. Host cell actin remodeling in response to Trypanosoma cruzi: trypomastigote versus amastigote entry. Subcell Biochem 2008;47:101–9.
[30] Mulinari F, Staniscuaski F, Bertholdo-Vargas LR, Postal M, Oliveira-Neto OB, Rigden DJ, et al. Jaburetox-2Ec: an insecticidal peptide derived from an isoform of urease from the plant *Canavalia ensiformis*. Peptides 2007;28:2042–50.
[31] Olivera-Severo D, Wassermann GE, Carlini CR. Ureases display biological effects independent of enzymatic activity: is there a connection to diseases caused by urease-producing bacteria? Braz J Med Biol Res 2006;39:851–61.
[32] Orchard I. Serotonin: a coordinator of feeding-related physiological events in the blood-gorging bug, *Rhodnius prolixus*. Comp Biochem Physiol A: Mol Integr Physiol 2006;144:316–24.
[33] Orchard I, Paluzzi JP. Diuretic and antidiuretic hormones in the blood-gorging bug *Rhodnius prolixus*. Ann N Y Acad Sci 2009;1163:501–3.
[34] Paluzzi JP, Orchard I. Distribution, activity and evidence for the release of an anti-diuretic peptide in the kissing bug *Rhodnius prolixus*. J Exp Biol 2006;209:907–15.
[35] Paluzzi JP, Park Y, Nachman RJ, Orchard I. Isolation, expression analysis, and functional characterization of the first antidiuretic hormone receptor in insects. Proc Natl Acad Sci U S A 2010;107:10290–5.
[36] Paluzzi JP, Russell WK, Nachman RJ, Orchard I. Isolation, cloning, and expression mapping of a gene encoding an antidiuretic hormone and other CAPA-related peptides in the disease vector, *Rhodnius prolixus*. Endocrinology 2008;149:4638–46.
[37] Petzel DH, Stanley-Samuelson DW. Inhibition of eicosanoid biosynthesis modulates basal fluid secretion in the malpighian tubules of the yellow-fever mosquito (Aedes-Aegypti). J Insect Physiol 1992;38:1–8.
[38] Pollock VP, McGettigan J, Cabrero P, Maudlin IM, Dow JAT, Davies SA. Conservation of capa peptide-induced nitric oxide signalling in Diptera. J Exp Biol 2004;207:4135–45.
[39] Quinlan MC, O'Donnell MJ. Anti-diuresis in the blood-feeding insect *Rhodnius prolixus* Stal: antagonistic actions of cAMP and cGMP and the role of organic acid transport. J Insect Physiol 1998;44:561–8.
[40] Quinlan MC, Tublitz NJ, O'Donnell MJ. Anti-diuresis in the blood-feeding insect *Rhodnius prolixus* Stal: the peptide CAP2b and cyclic GMP inhibit Malpighian tubule fluid secretion. J Exp Biol 1997;200:2363–7.
[41] Rainsford KD. Inhibitors of eicosanoids. In: Curtis-Prior P, editor. The Eicosanoids. Chichester, UK: John Wiley & Sons, Ltd.; 2004. p. 189–210.
[42] Rosay P, Davies SA, Yu Y, Sozen MA, Kaiser K, Dow JA. Cell-type specific calcium signalling in a Drosophila epithelium. J Cell Sci 1997;110(Pt 15):1683–92.
[43] Scherkenbeck J, Zdobinsky T. Insect neuropeptides: structures, chemical modifications and potential for insect control. Bioorg Med Chem 2009;17:4071–84.
[44] Staniscuaski F, Te Brugge V, Carlini CR, Orchard I. Jack bean urease alters serotonin-induced effects on *Rhodnius prolixus* anterior midgut. J Insect Physiol 2010;56:1078–86.
[45] Staniscuaski F, Ferreira-Dasilva CT, Mulinari F, Pires-Alves M, Carlini CR. Insecticidal effects of canatoxin on the cotton stainer bug *Dysdercus peruvianus* (Hemiptera: Pyrrhocoridae). Toxicon 2005;45:753–60.
[46] Staniscuaski F, Te Brugge V, Carlini CR, Orchard I. In vitro effect of *Canavalia ensiformis* urease and the derived peptide Jaburetox-2Ec on *Rhodnius prolixus* Malpighian tubules. J Insect Physiol 2009;55:255–63.
[47] Tate CG, Grisshammer R. Heterologous expression of G-protein-coupled receptors. Trends Biotechnol 1996;14:426–30.
[48] Te Brugge V, Ianowski JP, Orchard I. Biological activity of diuretic factors on the anterior midgut of the blood-feeding bug, *Rhodnius prolixus*. Gen Comp Endocrinol 2009;162:105–12.
[49] Te Brugge V, Paluzzi JP, Neupert S, Nachman RJ, Orchard I. Identification of kinin-related peptides in the disease vector, *Rhodnius prolixus*. Peptides 2011;32:469–74.
[50] Te Brugge V, Paluzzi JP, Schooley DA, Orchard I. Identification of the elusive peptidergic diuretic hormone in the blood-feeding bug *Rhodnius prolixus*: a CRF-related peptide. J Exp Biol 2011;214:371–81.
[51] Te Brugge VA, Miksys SM, Coast GM, Schooley DA, Orchard I. The distribution of a CRF-like diuretic peptide in the blood-feeding bug *Rhodnius prolixus*. J Exp Biol 1999;202:2017–27.
[52] Te Brugge VA, Nassel DR, Coast GM, Schooley DA, Orchard I. The distribution of a kinin-like peptide and its co-localization with a CRF-like peptide in the blood-feeding bug, *Rhodnius prolixus*. Peptides 2001;22:161–73.
[53] Te Brugge VA, Schooley DA, Orchard I. Amino acid sequence and biological activity of a calcitonin-like diuretic hormone (DH31) from *Rhodnius prolixus*. J Exp Biol 2008;211:382–90.

[54] Te Brugge VA, Schooley DA, Orchard I. The biological activity of diuretic factors in *Rhodnius prolixus*. Peptides 2002;23:671–81.
[55] Tomazetto G, Mulinari F, Staniscuaski F, Settembrini B, Carlini CR, Ayub MAZ. Expression kinetics and plasmid stability of recombinant E-coli encoding urease-derived peptide with bioinsecticide activity. Enzyme Microb Technol 2007;41:821–7.
[56] Vallejo GA, Guhl F, Schaub GA. Triatominae-Trypanosoma cruzi/*T. rangeli*: vector–parasite interactions. Acta Trop 2009;110:137–47.
[57] Van Kerkhove E, Pirotte P, Petzel DH, Stanley-Samuelson DW. Eicosanoid Biosynthesis inhibitors modulate basal fluid secretion rates in the malpighian tubules of the ant, Formica-Polyctena. J Insect Physiol 1995;41:435–41.
[58] Wurm FM. Production of recombinant protein therapeutics in cultivated mammalian cells. Nat Biotechnol 2004;22:1393–8.
[59] Zandawala M, Paluzzi JP, Orchard I. Isolation and characterization of the cDNA encoding DH(31) in the kissing bug, *Rhodnius prolixus*. Mol Cell Endocrinol 2010;331:79–88.

V. Artigo Publicado

Aguirre *et al*., 2011

● Participação no desenho e na execução dos experimentos que identificaram e caracterizaram a atividade de peptidases envolvidas na vitelogênese do inseto hematófago *Dipetalogaster maxima*. Item 3.4 (Figs. 6 e 7).

Insect Biochemistry and Molecular Biology 41 (2011) 832–841

Contents lists available at ScienceDirect

Insect Biochemistry and Molecular Biology

journal homepage: www.elsevier.com/locate/ibmb

Biochemical changes in the transition from vitellogenesis to follicular atresia in the hematophagous *Dipetalogaster maxima* (Hemiptera: Reduviidae)

Silvina A. Aguirre [a,1,2], Leonardo L. Fruttero [a,1,2], Jimena Leyria [a,3], Marina S. Defferrari [b], Paulo M. Pinto [b,5], Beatriz P. Settembrini [c,4], Edilberto R. Rubiolo [a], Célia R. Carlini [d], Lilián E. Canavoso [a,*,4]

[a] Departamento de Bioquímica Clínica, Centro de Investigaciones en Bioquímica Clínica e Inmunología (CIBICI-CONICET). Facultad de Ciencias Químicas-Universidad Nacional de Córdoba. Córdoba, CP 5000, Argentina
[b] Graduate Program in Cellular and Molecular Biology, Center of Biotechnology, Universidade Federal do Rio Grande do Sul, Porto Alegre, Brazil
[c] Museo Argentino de Ciencias Naturales-CONICET, Buenos Aires, Argentina
[d] Department of Biophysics and Center of Biotechnology, Universidade Federal do Rio Grande do Sul, Porto Alegre, Brazil

ARTICLE INFO

Article history:
Received 8 May 2011
Received in revised form
23 June 2011
Accepted 30 June 2011

Keywords:
Triatominae
Vitellogenesis
Follicular atresia
Cathepsin D-like peptidase
Vitellogenin
Vitellin

ABSTRACT

In this work, we have explored the biochemical changes characterizing the transition from vitellogenesis to follicular atresia, employing the hematophagous insect vector *Dipetalogaster maxima* as a model. Standardized insect rearing conditions were established to induce a gradual follicular degeneration stage by depriving females of blood meal during post-vitellogenesis. For the studies, hemolymph and ovaries were sampled at representative days of pre-vitellogenesis, vitellogenesis and early and late follicular atresia. When examined by scanning electron microscopy, ovarioles at the initial stage of atresia were small but still showed some degree of asynchronism, a feature that was lost in an advanced degeneration state. At late follicular atresia, *in vivo* uptake assays of fluorescently labeled vitellogenin (Vg-FITC) showed loss of competitiveness of oocytes to uptake vitellogenin. Circulating vitellogenin levels in atresia were significantly higher than those registered at pre-vitellogenesis, most likely to maintain appropriate conditions for another gonotrophic cycle if a second blood meal is available. Follicular atresia was also characterized by partial proteolysis of vitellin, which was evidenced in ovarian homogenates by western blot. When the activity of ovarian peptidases upon hemoglobin (a non-specific substrate) was tested, higher activities were detected at early and late atresia whereas the lowest activity was found at vitellogenesis. The activity upon hemoglobin was significantly inhibited by pepstatin A (an aspartic peptidase inhibitor), and was not affected by E64 (a cysteine peptidase inhibitor) at any tested conditions. The use of specific fluorogenic substrates demonstrated that ovarian homogenates at early follicular atresia displayed high cathepsin D-like activity, whereas no activity of either, cathepsin B or L was detected. Mass spectrometry analysis of the digestion products of the substrate Abz-AIAFFSRQ-EDDnp further confirmed the presence of a cathepsin D-like peptidase in ovarian tissue. In the context of our findings, the early activation of cathepsin D-like peptidase could be relevant in promoting yolk protein recycling and/or enhancing follicle removal.

1. Introduction

In insects, vitellogenesis is the central event of reproduction. Depending on the species analyzed, vitellogenesis is under regulatory control of 20-hydroxyecdysone (20E) or juvenile hormone (JH), although the involvement of neuropeptides in the control of oogenesis was also demonstrated (Swevers et al., 2005).

In hematophagous insects, vitellogenesis is elicited by a blood meal, which in turn drives a massive synthesis of yolk protein precursors in the fat body, mainly vitellogenin. This phospholipoglycoprotein is taken up by developing oocytes by receptor mediated endocytosis and stored as vitellin in yolk bodies (Snigirevskaya and Raikhel, 2005). Vitellin, together with lipids, constitutes the major metabolic resource to sustain embryogenesis. In some species, vitellin also sustains the development of the first larval instar (Postlethwait and Giorgi, 1985; Oliveira et al., 1989; Giorgi and Nordin, 2005).

* Corresponding author. Tel.: +54 351 434 4974; fax: + 54 351 433 3048.
E-mail address: lcanavo@mail.fcq.unc.edu.ar (L. E. Canavoso).
[1] These authors contributed equally to this work.
[2] Research Fellows from CONICET-Argentina.
[3] Research Fellow from FONCyT-Argentina.
[4] Members of the CIC-CONICET-Argentina.
[5] Present address: Universidade Federal do Pampa, Campus de São Gabriel, RS, Brazil.

0965-1748/$ – see front matter © 2011 Elsevier Ltd. All rights reserved.
doi:10.1016/j.ibmb.2011.06.005

When physiological, behavioral or environmental factors are unfavorable to promote reproduction, the ovarian tissue experiences changes and some follicles degenerate to an atretic stage. During this process, termed follicular atresia, oocytes undergo resorption (oosorption) instead of being laid as eggs. In most instances, oosorption is a reproductive strategy directed to conserve metabolic resources to ensure future reproductive success (Bell and Bohm, 1975). In *Culex pipiens pallens* follicular atresia is common in developing ovaries which must adjust a batch of eggs to available nutrients (Uchida et al., 2001). Oosorption may increase female lifespan by nutrient recycling (Wang and Horng, 2004). In some species of predatory lady beetles, females engage in oosorption under limited prey availability (Kajita and Evans, 2009).

Starvation and shortage of food are the main causes of oosorption (Bell and Bohm, 1975). Food deprivation in females of *Periplaneta americana* promoted oosorption, and vitellin stored in developing oocytes is released into the hemolymph without any proteolysis (Bell, 1971). Loss of yolk bodies and other cellular structures observed in the mosquito *C. p. pallens* indicate that follicular atresia and oosorption are more complex than a combination of cessation of vitellogenesis and death of the oocyte. Thus, an early activation of cathepsin-like peptidases presumably enhances oosorption (Uchida et al., 2001). In the stink bug *Plautia crossota stali*, results suggested that once oosorption begins, stored vitellin is degraded and released into the hemolymph as either, small peptides or aminoacids (Kotaki, 2003). Although the enzymatic breakdown of yolk protein occurs throughout embryogenesis (Fialho et al., 2002; Yamahama et al., 2005; Oliveira et al., 2008), some peptidases could activate early during atresia favoring nutrient recycling. However, no conclusive evidences linking nutrient recycling and oosorption are available until present. Although follicular atresia and oosorption are integral parts of the operating system controlling ovarian function, they have received scarce exploration.

Triatomines are hematophagous insects of importance in public health since they are vectors of Chagas' disease. Triatomine females must surpass a threshold level in both, the amount and quality of a blood meal in order to achieve oogenesis (Stoka et al., 1987). Recently, we have characterized the changes related to vitellogenesis of anautogenous *Dipetalogaster maxima*. We have shown at biochemical and cellular level that the gonotrophic cycle is coupled with the intake of blood meal (Aguirre et al., 2008). Under standardized rearing conditions the first oviposition period of *D. maxima* lasts 25–28 days after blood intake. Thereafter, ovaries enter into a post-vitellogenic stage during which, some terminal oocytes will undergo resorption. In triatomines, at least for the second batch of eggs, the blood meal is needed to resume vitellogenesis (Stoka et al., 1987). If another blood meal is ingested, oosorption may cease and the ovary becomes productive. Whereas in mosquitoes follicular atresia and oosorption occur very fast (Clements and Boocock, 1984; Uchida et al., 2001), in *D. maxima* the onset of follicular atresia takes several days because ovarioles are asynchronous with each other. Although atresia has been reported in *Rhodnius prolixus* (Huebner and Anderson, 1972) no further characterization has been performed in any triatomine species.

In this work, we took advantage of standardized laboratory conditions that allow us to explore morphological and biochemical changes that take place in the transition from vitellogenesis to follicular atresia in *D. maxima*. The atretic process induced by unfavorable nutritional conditions was characterized by loss of competitiveness of oocytes to vitellogenin uptake, partial vitellin proteolysis and activation of cathepsin D-like peptidases. Furthermore, circulating levels of vitellogenin were significantly higher than those registered at pre-vitellogenesis. Taken together, the results suggest a complex interaction of events involved in the establishment of atresia, being its exploration relevant to improve our understanding of biology of reproduction of Triatominae.

2. Materials and methods

2.1. Chemicals

Microtiter plates (Delta Lab, Barcelona, Spain), enhanced chemiluminescence (ECL) detection kit (PerkinElmer, Waltham, MA, USA), osmium tetroxide (Polysciences INC, Warringthon, PA, USA), Fluorsave (Calbiochem, Darmstadt, Germany), Tissue-Tek embedding medium (OCT) (Miles, Elkhart, IN, USA), and electrophoresis protein standards (Biorad, Hercules, CA, USA) were from indicated commercial sources. Bovine hemoglobin, pepstatin-A, trans-epoxysuccinyl-L-leucylamido (4-guanidino)-butane (E64), horseradish peroxidase (HRP)-conjugated goat anti-rabbit IgG, bovine serum albumin (BSA), *o*-phenylenediamine, methyl-coumarin amide (MCA)-coupled substrates, dimethyl sulfoxide (DMSO), fluorescein isothiocyanate (FITC) and all the remaining chemicals were from Sigma-Aldrich (St. Louis, MO, USA). The fluorogenic peptide substrate Abz-AIAFFSRQ-EDDnp (Abz, ortho-aminobenzoic acid; EDDnp, ethylenediamine-2,4-dinitrophenyl) was a kind gift from Dr. Maria Aparecida Juliano (Dept. Biophysics, Universidade Federal de São Paulo, Brazil).

2.2. Insects

Insects were taken from a colony of anautogenous *D. maxima*, which is maintained under standardized conditions (28 °C, 70% humidity, 8:16 h light:dark photoperiod) and fed every two weeks on hen blood (Canavoso and Rubiolo, 1993).

For the experiments, males and females were separated before feeding at the last nymphal instar. Newly-emerged females were segregated individually and placed together with two recently fed males for a period of 48 h and checked for mating by observation of the spermatophore. Mated females were maintained in individual containers until they were able to feed a blood meal (day 10–12 post-ecdysis), which represented between 3.0 and 5.5 fold the body weight of the insect. Under these conditions, females were daily monitored and both, the beginning and the end of the oviposition period, which was confirmed if females did not lay eggs during five consecutive days, were recorded. Females were also monitored during 30 days after the end of the oviposition (post-vitellogenesis) without receiving any blood meal. For the studies, hemolymph and ovaries were sampled from females at representative days of the reproductive cycle as indicated in Fig. 1: (a) pre-vitellogenesis (day 2 post-ecdysis, unfed period), (b) vitellogenesis (days 4–6 post-blood feeding); (c) post-vitellogenesis (days 10–12 and days 30–32 after the end of oviposition for early and late atresia, respectively). To explore the dynamics between circulating vitellogenin and its storage in oocytes, additional time points during pre-vitellogenesis (day 4 post-ecdysis) and vitellogenesis (days 8–10 post-blood feeding) were tested.

2.3. Scanning electron microscopy (SEM)

The cuticle of the abdomen was dissected out and ovaries were flushed with cold fixative (2% glutaraldehyde in 0.1 M cacodylate buffer, pH 7.3). The samples were kept in the same fixative at 4 °C overnight. Following several rinses in the same buffer, samples were postfixed in 1% osmium tetroxide in 0.1 M cacodylate buffer, pH 7.3 for 24 h at 4 °C. The tissues were washed thoroughly in distilled water and dehydrated in graded ethanol series (20, 40, 60 and 80%) to absolute ethanol. Special care was taken in handling the samples to prevent the distortion of the ovarian morphology.

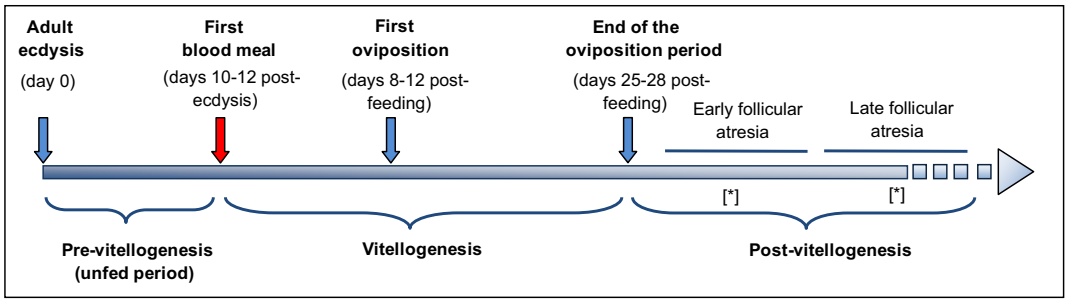

Fig. 1. The reproductive cycle of anautogenous *D. maxima*. Under standardized rearing conditions pre-vitellogenesis comprises the period from the ecdysis of the female adult stage (day 0) until the first blood-meal (days 10–12 post-ecdysis). Thereafter, females enter in vitellogenesis and the first egg is laid around days 8–12 post-feeding. Vitellogenesis usually extends 25–28 days post-feeding. At the end of the oviposition cycle and without a second blood meal, follicles enter in post-vitellogenesis and degenerate (follicular atresia). In *D. maxima*, morphological changes allow to distinguish an early follicular atresia (approximately the first fifteen days of post-vitellogenesis) and a late atretic stage, which extends until a female receives a second blood meal. In our experimental conditions, days 10–12 and 30–32 post-vitellogenesis were sampled as representative time points of early and late follicular atresia, respectively (shown as asterisks).

Minimal collapse of soft tissues was achieved by air drying the specimens. Samples were mounted on the stubs, coated in gold palladium and examined in a Philips XL30 SEM microscope.

2.4. Vitellogenin and vitellin quantification

The levels of vitellogenin in the hemolymph and the amount of vitellin in ovaries at different stages of the reproductive cycle were assessed by indirect enzyme-linked immunosorbent assay (ELISA), employing a polyclonal anti-vitellin antibody (anti-Vt), which cross-reacted with vitellogenin. Standardized conditions for ELISA were recently reported (Aguirre et al., 2008).

For the assays, the hemolymph was individually collected from immobilized insects with a Hamilton syringe, from cut legs while gently pressing the abdomen. Hemolymph was collected in ice-cold microtubes, in the presence of 10 mM Na_2EDTA, 5 mM dithiotreitol and protease inhibitors. Samples were centrifuged at 10,000 × *g* for 5 min at 4 °C to remove hemocytes and then stored for one week at −70 °C for vitellogenin quantification.

After hemolymph collection, ovaries were carefully dissected out under cold phosphate buffered saline (PBS, 66 mM Na_2HPO_4/KH_2PO_4, 150 mM NaCl, pH 7.4) using a standard stereoscope with an optic fiber light source. The excess of PBS from ovaries was gently removed using filter paper to avoid tissue disruption. Wet ovaries were individually weighed and then homogenized in buffer Tris–NaCl (20 mM Tris, 150 mM NaCl, pH 7.4) containing a mixture of protease inhibitors: 0.3 μM pepstatin, 1 μM aprotinin, 0.5 μM N-α-p-tosyl-L-lysine chloromethyl ketone (TLCK) and 1 mM benzamidine, using disposable homogenizers. The homogenates were first centrifuged at 2500 × *g* for 10 min at 4 °C and the floating fat cake and pellet were discarded. The resulting material was centrifuged at 15,000 × *g* for 30 min at 4 °C and the supernatants collected and used for ELISA as previously reported (Fruttero et al., 2011). Protein concentration was determined according to Bradford (1976), using bovine serum albumin as standard.

2.5. In vivo vitellogenin uptake by oocytes

In vivo uptake assays were assessed by using purified vitellogenin from hemolymph of vitellogenic females obtained by a combination of KBr gradient ultracentrifugation followed by ion-exchange chromatography on DEAE-Trisacryl-M (Fruttero et al., 2011). Purified vitellogenin was labeled with FITC (Vg-FITC, 1 mg/ml) in DMSO as described elsewhere (Hermanson, 1996). For the experiments, females at different stages of the reproductive cycle were injected with 10 μl of Vg-FITC (20 μg/insect) into the hemolymph. Insects were kept at 28 °C or 4 °C (controls) and 3 h post-injection, the ovaries were carefully dissected out and the outer sheaths were removed. Ovarioles were individually rinsed with PBS and placed in the same buffer into borosilicate chambers (Lab-Tek chambered cover glass system) to be examined *in toto* with a confocal laser microscope Olympus FV300, equipped with appropriate filters (excitation 488 nm/emission 519 nm). Digital images were processed using Olympus Fluoview 1.7.1.0 Viewer software (Japan).

Supplementary video related to this article can be found at 10.1016/j.ibmb.2011.06.005.

2.6. Western blot

The proteolysis of vitellin during follicular atresia was evidenced by western blot, after fractionation of ovarian homogenates in 7.5% polyacrylamide gel electrophoresis (SDS-PAGE). Conditions for western blot were reported previously (Aguirre et al., 2008). The main subunits of vitellin (Mr ~170 and 174 kDa, detected as a single inmunoreactive band) and its proteolytic fragments were probed with anti-Vt antibody (1:5000), followed by incubation with HRP-conjugated goat anti-rabbit IgG (1:5000). Bands were visualized by enhanced chemiluminescence.

2.7. Enzymatic assays

Pools of 2–3 ovaries from females at different stages of the reproductive cycle were homogenized in cold sodium phosphate buffer (NaPB, 20 mM, pH 7.0). Homogenates were then centrifuged at 10,000 × *g* for 20 min at 4 °C and the resulting supernatants were analyzed for protein quantification (Bradford, 1976) and immediately employed for the enzymatic assays.

The profile of acid peptidases was assessed using bovine hemoglobin as substrate (final concentration 0.2%) in a reaction mixture of 50 μl containing 40–200 μg of protein homogenate and sodium acetate 100 mM, pH 4.0 (Stanisçuaski et al., 2005). Incubations were carried out for 1 h at 37 °C and were stopped by the addition of 40 μl of 10% trichloroacetic acid (TCA). The material was centrifuged at 8000 × *g* (20 min, 4 °C) and acid-soluble peptides in the supernatants were read at 280 nm.

To identify the classes of peptidases present in ovarian homogenates, aliquots of homogenates were pre-incubated with specific inhibitors of aspartic peptidases (pepstatin A) and cysteine peptidases (E64), at a final concentration of 10 μM each (30 min, room temperature). Thereafter, assays were carried out as previously stated. For all conditions assayed, reaction blanks were performed by addition of substrate after the TCA step. In all cases,

specific hemoglobinolytic activity was expressed as A_{280}/μg protein homogenate/h.

The activity of cathepsin D-like peptidase(s) was assayed using the specific synthetic fluorogenic substrate Abz-AIAFFSRQ-EDDnp (Sorgine et al., 2000; Piovesan et al., 2008; Defferrari et al., 2011). Aliquots of homogenates (10–30 μg of proteins) were incubated in 96 wells microplates at 37 °C with 20 μM of substrate and 20 mM citrate–phosphate buffer (pH 3.5), in 100 μl final volume. Reactions were monitored every 11 s for 30 min in an F-Max fluorometer (Molecular Devices Inc.) with 320/430 nm excitation/emission filters. The effect of pH on specific activity was tested with 20 mM citrate–phosphate buffer (pH 2.0–5.0). Additionally, the activity of cathepsin B and L cysteine peptidases was assayed with specific MCA-coupled substrates (Z-RR-7-amido-MCA and Z-FR-7-amido-MCA, respectively) at a final concentration of 2 μM, with 370/460 nm excitation/emission filters. Results were expressed as relative fluorescence units (RFU)/μg protein/min.

2.8. Determination of cleavage site by mass spectrometry (LC-MS)

Digestion products of the fluorogenic substrate Abz-AIAFFSRQ-EDDnp after the enzymatic reaction were analyzed by liquid chromatography (LC) separation (reverse phase HPLC) coupled to mass spectrometry at the UNIPROTE-MS facility, Center of Biotechnology, Universidade Federal do Rio Grande do Sul, Porto Alegre, RS, Brazil. Five microliters of the reaction standardized as stated in 2.7 were applied on an electrospray ionization (ESI) quadrupole-time of flight (Q-TOF) Q-TOF Micro™ mass spectrometer (Waters Corporation) coupled to a nanoAcquity Ultra Performance LC (UPLC, Waters Corporation). A nanoflow ESI probe, calibrated in the *m*/*z* region 50–20000 using phosphoric acid, was used for lockmass measurement during all chromatographic runs. The samples were separated a Symmetry C18 and BEH 130-C18 capillary columns (Waters Corporation) eluted with a linear gradient of 0–90% acetonitrile in 0.1% formic acid. The mass spectrometric data were collected in a full scan mode from *m*/*z* 50 to 1400 in positive mode. Typical LC and ESI conditions were: flow of 600 nL/min, nanoflow capillary voltage at 3.5 kV and a cone voltage of 100 V. Data were processed and analyzed using MassLynx™ v. 4.1 software.

2.9. Statistical analysis

For the biochemical parameters, three to four independent experiments were performed and data for each point were registered by triplicate. Graphs and statistical tests were performed using GraphPad Prism and GraphPad Instat 3.0 computer programs. Results were expressed as mean ± SEM. Student's *t*-test was used for comparisons and a P value <0.05 was considered statistically significant.

3. Results

3.1. Morphological characterization of the reproductive cycle of D. maxima

The two ovaries of anautogenous *D. maxima*, the largest of all triatomines, contain seven ovarioles of the telotrophic type. The ovarioles have an apical lanceolate-shaped tropharium containing the nurse cells, followed by a vitellarium with oocytes in various stages of development. After appropriate stimulus, the terminal oocytes, which are distant of the nurse cells, are surrounded by a follicular epithelium to constitute a follicle (Huebner and Anderson, 1972; Aguirre et al., 2008).

The ovarian tissue of *D. maxima* undergoes remarkable changes through the reproductive cycle of the insect, which are triggered by the access to a blood meal. During the unfed period (pre-vitellogenic stage), which under standardized rearing conditions lasts 10–12 days, ovarioles are of small size (1.2–1.5 mm, unfixed condition), show a prominent tropharium and a disc-shaped vitellarium at their base (Fig. 2A). After blood feeding, terminal oocytes (α position) are stimulated to undergo yolk deposition, entering into the vitellogenic phase. At this time, ovarioles start to display a typical asynchronous development characterized by the presence of terminal oocytes of different sizes. Each ovariole contains only one vitellogenic oocyte at a time, but smaller oocytes in β-γ position are also present (Fig. 2B). As shown in Fig. 1, the time elapsed from the first blood meal until the first egg is detected comprises 8–12 days, which in turn indicates the time needed for the first oocyte to complete its development.

Although the reproductive cycle of *D. maxima* exhibits some expected heterogeneity, the vitellogenesis usually extends 25–28 days, a period during which females lay a whole batch of 30–35 eggs. Under standardized conditions, females take a second blood meal 5–7 days after the oviposition period has ceased to resume vitellogenesis successfully. However, at the end of oviposition and without a second blood meal, some terminal follicles degenerate and oocytes are resorbed. Degeneration of follicles, also termed follicular atresia, occurs gradually in ovarian tissue. Thus, in an early atretic stage, ovarioles maintain some degree of asynchronism, but oocytes undergoing incipient and advanced resorption can be simultaneously observed (Fig. 2C). During late atresia, ovarioles lose asynchronism, become small (2.1–2.4 mm, unfixed condition) and all of them exhibit resorbed oocytes (Fig. 2D). In our experimental conditions, monitoring individual follicles by a long period of time is not possible; thus the days needed to complete oosorption cannot be determined.

3.2. Changes in circulating vitellogenin and its uptake and storage by oocytes

We have analyzed the dynamics relative to the levels of circulating vitellogenin, the main yolk protein precursor, and its storage as vitellin in ovarian tissue throughout the reproductive cycle of *D. maxima* females (Fig. 3). As can be seen in this figure, the smallest amounts of both proteins were found at pre-vitellogenesis (days 2 and 4 post-ecdysis). As expected, vitellogenesis was characterized by high levels of vitellogenin in the hemolymph and vitellin in the ovary, reaching averages at the onset of vitellogenesis of 15 μg/μl and 1200 μg/ovary, respectively (days 4–6 post-blood feeding). In contrast, at representative days of early and late atresia, circulating vitellogenin and vitellin in the ovaries were significantly lower than those found during vitellogenesis. These parameters were higher in comparison to those registered at pre-vitellogenesis. There were no significant differences in the amounts of vitellogenin between early and late atresia (days 10–12 and 30–32 after the end of oviposition period, respectively), but the amounts of vitellin at early atretic stage were higher than in late atresia (Fig. 3).

At a cellular level, results on vitellogenin uptake *in vivo* as analyzed by confocal laser microscopy during the reproductive cycle of *D. maxima* were in agreement with the biochemical findings reported above (Fig. 4). Thus, females at pre-vitellogenesis, injected with labeled Vg-FITC showed a very weak fluorescent signal inside some pre-vitellogenic terminal oocytes (Fig. 4A). Active uptake and deposition of Vg-FITC was observed in vitellogenic oocytes at 3 h post-injection, with a strong fluorescent signal localized in yolk bodies (Fig. 4B). An integration of multiple confocal planes (Z axis) corresponding to a terminal oocyte showed that a homogeneous distribution of fluorescent vitellin occurs over

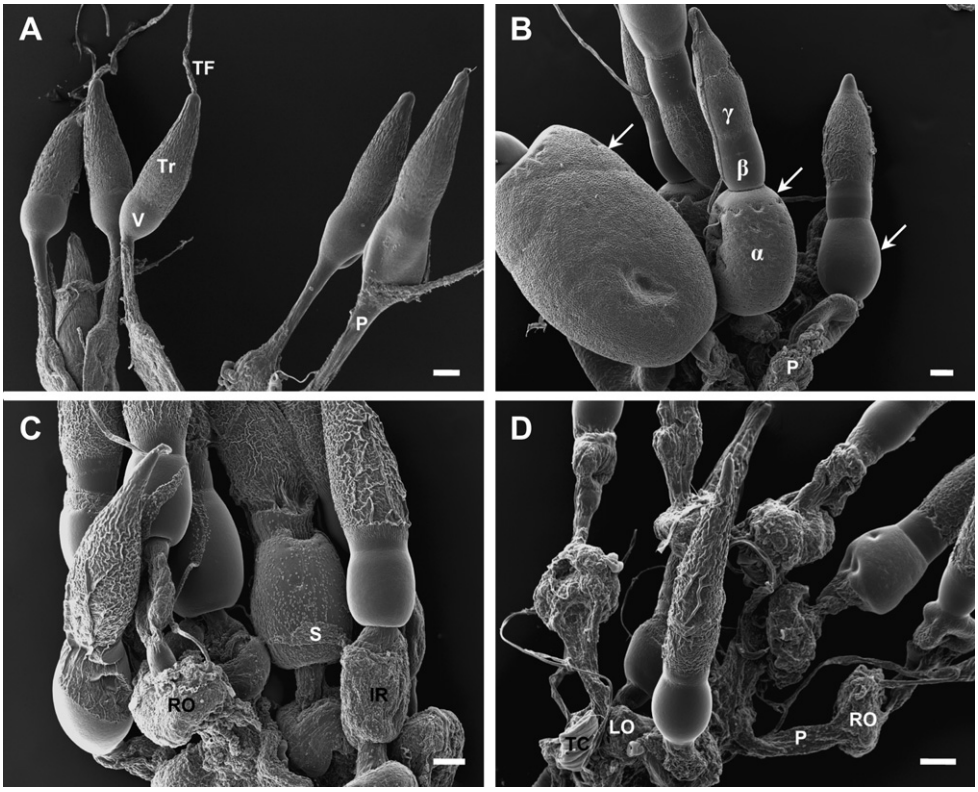

Fig. 2. Scanning electron micrographs of ovarian tissue during the reproductive cycle of *D. maxima*. (A), Ovarioles in pre-vitellogenesis (day 2 post-ecdysis, unfed period). (B), Ovary during vitellogenic stage. Ovarioles show the typical asynchronous development characterized by vitellogenic terminal oocytes of different sizes. Arrows point to positions of developing oocytes. α, β and γ indicate the positions of alpha, beta and gamma oocytes, respectively. (C), Early follicular atresia, the ovarioles maintain some degree of asynchronism, but oocytes undergoing incipient and advanced resorption are present. (D), Ovary in the late stage of atresia with all ovarioles exhibiting resorbed oocytes. V, vitellarium; Tr, tropharium; TF, terminal filament; P, pedicel; IR, oocyte undergoing incipient resorption; RO, resorbed oocyte; S, outer sheath; Tc, tracheolae; LO, lateral oviduct. Bars: 100 μm.

a short period of time (supplementary video). As expected, insects kept at 4 °C after the injection (control of endocytosis) evidenced no Vg-FITC uptake. In addition, when tissues such as the midgut and the fat body were examined, no fluorescence associated with Vg was observed (results not shown).

During early follicular atresia, the process of vitellogenin uptake was poor, and a faint fluorescent label located mainly at the cortical zone of terminal oocytes was observed (Fig. 4C). This pattern did not change even if ovarioles were observed at a longer time post-injection (results not shown). At late atresia, no fluorescence was detected in terminal oocytes, consistent with the end of the active vitellogenin uptake and deposition (results not shown).

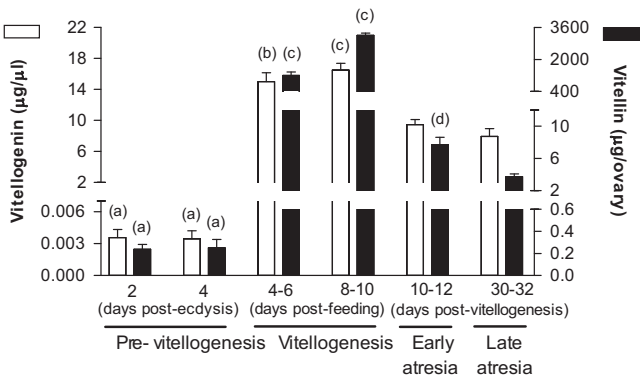

Fig. 3. Changes of vitellogenin (Vg) levels in the hemolymph and vitellin (Vt) deposits in the ovary during the reproductive cycle of *D. maxima*. Measurements were performed by indirect ELISA using a polyclonal anti-Vt antibody. Results are expressed as mean ± SEM ($n = 4$). (a) $P < 0.001$ vs. 4–6 days and 8–10 days post-feeding, early and late atresia; (b) $P < 0.01$ vs. early atresia and $P < 0.001$ vs. late atresia; (c) $P < 0.001$ vs. early and late atresia; (d) $P < 0.01$ vs. late atresia.

3.3. Proteolysis of vitellin during follicular atresia

Because follicular atresia is associated with degradation of nutritional resources, being vitellin the main yolk protein stored in oocytes, we decided to evidence the proteolysis of this protein throughout the reproductive cycle of *D. maxima*. Whereas at vitellogenesis only the major vitellin subunits were detected by anti-Vt antibody (Fig. 5, lane 2), several minor proteolytic fragments were visualized in homogenates of ovaries sampled at early and late follicular atresia. Moreover, vitellin proteolysis showed similar profiles in both stages (Fig. 5, lanes 3–4).

3.4. Enzymatic assays

In order to investigate the biochemical factors involved in yolk protein degradation during follicular atresia, we first measured the activity of ovarian peptidases by using hemoglobin, a non-specific substrate, at acid pH (4.0). Results in Fig. 6 showed that all homogenates obtained from ovaries at different stages of reproduction displayed activity upon hemoglobin. However, significantly higher activities were detected at early and late atresia whereas the lowest activity was found at vitellogenesis. The high activity upon hemoglobin was almost completely inhibited by pepstatin A, an aspartic peptidase inhibitor, in homogenates of atretic stages (~96% and 97% of inhibition in early and late follicular atresia, respectively), and strongly inhibited in homogenates of pre-

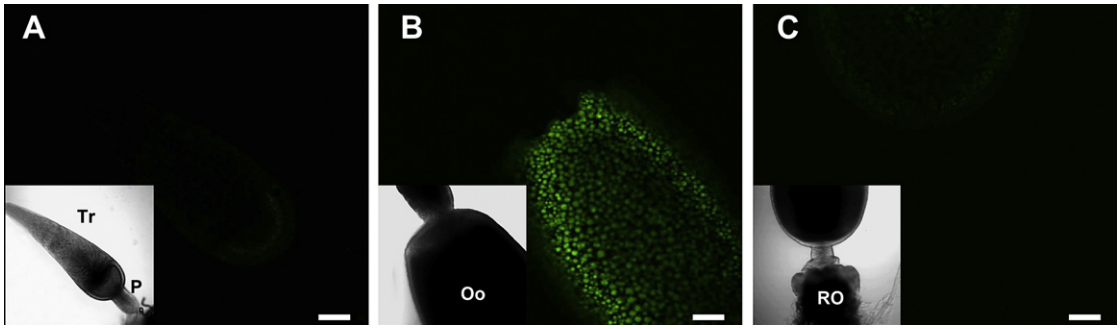

Fig. 4. *In vivo* uptake of vitellogenin-FITC (Vg-FITC) by oocytes of *D. maxima* at different stages of the reproductive cycle. Vg-FITC was injected into the hemocoel of females. Ovaries were dissected out and visualized *in toto* by laser scanning confocal microscopy. (A) Pre-vitellogenic follicle (day 2 post-ecdysis) showing a faint fluorescent signal inside the terminal oocyte; (B) Terminal follicle (α oocyte, day 5 post-blood meal) undergoing active Vg uptake and exhibiting intense fluorescence in yolk bodies; (C) Terminal follicle at early follicular atresia (day 12 post-vitellogenesis) displaying a weak fluorescent pattern at the cortical area of oocyte. In the same ovariole, no fluorescence was observed in a resorbed oocyte. Inserts correspond to DIC images. Tr, tropharium; P, pedicel; Oo, oocyte; RO, resorbed oocyte. Bars: 100 μm.

vitellogenic ovaries (~64% inhibition). In addition, inhibition of the low enzymatic activity found at vitellogenesis reached ~86%. No inhibition by E64 (a cysteine peptidase inhibitor) was observed in any condition analyzed.

Taken into account that proteolytic activity upon hemoglobin found in ovaries at atretic stages was susceptible to pepstatin A, we performed the partial characterization of cathepsin D-like activity, an aspartic peptidase, using the specific fluorogenic substrate Abz-AIAFFSRQ-EDDnp (Sorgine et al., 2000). Additionally, homogenates were also tested for cathepsin B and L-like activities employing specific MCA-coupled substrates (Z-RR-7-amido-MCA and Z-FR-7-amido-MCA, respectively). The profile of proteolytic activity upon specific substrates found in ovarian homogenates at early follicular atresia showed a high activity level of cathepsin D-like peptidase, whereas no activity of either, cathepsin B or L was detected (Fig. 7A). The activity of cathepsin D-like enzyme upon its fluorogenic substrate was pH-dependent, being optimal at pH 3.5 (Fig. 7B). Therefore, all remaining assays were performed at this acidic pH. As it was shown in hemoglobinolytic assays, homogenates of ovarian tissue at both atretic stages displayed the highest activities upon fluorogenic substrate for cathepsin D (Fig. 7C). This proteolytic activity was completely inhibited by pepstatin A (98.7% inhibition), as shown in assays performed with homogenates at early atresia (Fig. 7D).

3.5. Determination of cleavage site by LC-MS

To confirm that cathepsin D-like peptidase is responsible for the high peptidase activity found in homogenates of ovarian tissue at follicular atresia, the digestion products of the specific substrate, Abz-AIAFFSRQ-EDDnp, by homogenates were analyzed by LC-MS. The hydrolysis of the substrate at optimum pH of the enzymatic reaction (3.5) resulted in two major chromatographic peaks, corresponding to the fragments FSRQ-EDDnp (peak 1, retention time 10.94 min) and Abz-AIAF (peak 2, retention time 16.55 min). Minor impurities not characterized were also detected (Fig. 8A). As shown by mass spectrum profiles (Fig. 8B–C), the observed masses of two fragments were coincident with the predicted masses of the digestion products of the substrate as performed by cathepsin D (Fig. 8D). Similar results were obtained by MALDI-TOF-MS (data not shown). Taken together, these results demonstrated that ovarian

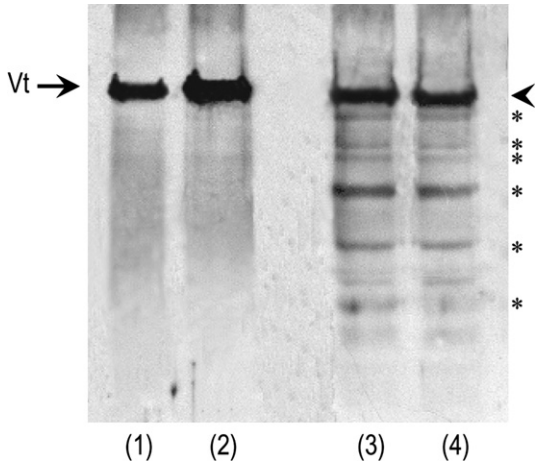

Fig. 5. Vitellin (Vt) proteolysis *in vivo* during follicular atresia of *D. maxima*. Homogenates of ovaries obtained at vitellogenesis, early and late follicular atresia (lanes 2–4 respectively, 8 μg each) were probed with a polyclonal anti-Vt antibody. In lane 1, arrow indicates immunoreactive band recognizing the main subunits of purified Vt (0.2 μg/lane to avoid overexposition). Arrowhead and asterisks indicate intact Vt and the main proteolytic fragments, respectively, detected in early and late atretic ovarian homogenates (lanes 3–4).

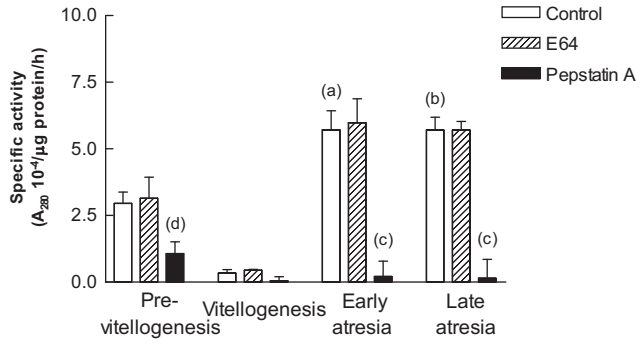

Fig. 6. Proteolytic profile upon hemoglobin of ovarian tissue homogenates throughout reproductive cycle of *D. maxima*. For controls, the activity of peptidases was assessed using 0.2% bovine hemoglobin in a reaction mixture containing 40–200 μg of protein homogenates and sodium acetate 100 mM, pH 4.0 as stated in Materials and Methods. Incubations were stopped by addition of TCA and soluble fragments of substrate present in the supernatants were read at 280 nm. The effect of inhibitors was analyzed by pre-incubating aliquots of homogenates with either, 10 μM E64 or pepstatin A, inhibitors of cysteine or aspartic peptidases, respectively. In all cases, specific hemoglobinolytic activity is expressed as A_{280}/μg protein homogenate/h. Results are expressed as mean ± SEM ($n = 4$). (a) $P < 0.05$ vs. pre-vitellogenesis (control condition) and $P < 0.01$ vs. vitellogenesis (control condition); (b) $P < 0.05$ vs. pre-vitellogenesis (control condition) and $P < 0.001$ vs. vitellogenesis (control condition); (c) $P < 0.01$ vs. early and late atresia (control condition); (d) $P < 0.05$ vs. pre-vitellogenesis (control condition).

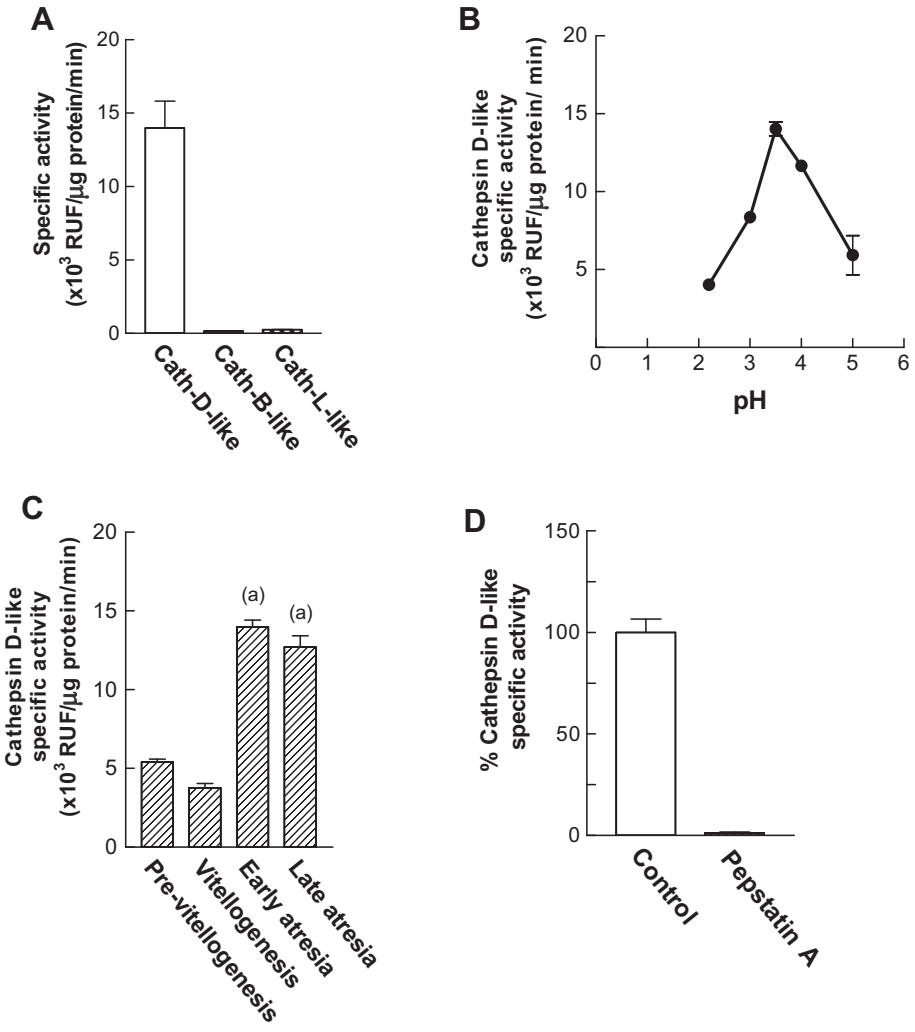

Fig. 7. Partial characterization of cathepsin-like peptidases in ovarian homogenates of *D. maxima*. (A), Activity profile of cathepsin D, B and L at early atresia using specific fluorogenic substrates (Abz-AlAFFSRQ-EDDnp for cathepsin D-like peptidase; Z-RR-7-amido-MCA and Z-FR-7-amido-MCA for cathepsin B and L-like peptidases, respectively); (B), Effect of pH on cathepsin D-like activity upon Abz-AlAFFSRQ-EDDnp substrate; (C), Specific activity of cathepsin D-like peptidase throughout reproductive cycle of *D. maxima*; (D), inhibition of cathepsin D-like activity at early atresia by pepstatin A. Except for (C), all the assays were performed with homogenates at early follicular atresia. Reactions were carried out by incubating 10–30 µg of protein with specific substrates (20 µM or 2 µM for Abz-EDDnp and MCA-coupled substrates, respectively) according to conditions detailed in Materials and Methods. The effect of pepstatin A was analyzed by pre-incubating 10 µM of inhibitor with the reaction mixture. Reactions were monitored in a fluorometer for 30 min with 320/430 nm excitation/emission filters (cathepsin D-like peptidase) or 370/460 nm excitation/emission filters (cathepsin B and L-like peptidases). Results are expressed as relative fluorescence units (RFU)/µg protein/min and are the mean ± SEM ($n = 3$). (a) $P < 0.001$ vs. pre-vitellogenesis and vitellogenesis.

homogenates preferentially cleave the specific substrate between two phenylalanine residues, consistent with the expected cleavage site for cathepsin D-like enzymes (Sorgine et al., 2000).

4. Discussion

When insect females face unfavorable nutritional and/or environmental conditions, the ovarian follicles undergo atresia and oocytes are resorbed (Bell and Bohm, 1975; Uchida et al., 2004). Some species exploit oosorption to preserve metabolic resources, ensuring the success of additional gonotrophic cycles when the individual finds food or its environmental circumstances are improved (Bell and Bohm, 1975).

In insects, the mechanisms that promote and regulate follicular atresia and oosorption are poorly understood. Current knowledge is supported by work on Blattodea, Diptera and Heteroptera (Bell, 1971; Uchida et al., 2001, 2004; Kotaki, 2003). In Triatominae, atresia has received little attention and there are few studies confined to *R. prolixus* (Wigglesworth, 1936; Huebner and Anderson, 1972). In this context, *D. maxima* constitutes an attractive model to explore the events related to follicular atresia since the female ingest a large blood meal, and its slow metabolism elicits physiological changes in a gradual mode. This fact enables the characterization of the early events that lead to follicular degeneration, in opposition to most species previously analyzed, in which the onset of atresia occurs very fast.

In *D. maxima*, the transition from vitellogenesis to follicular atresia was characterized by the shrinking of the oocytes, a typical finding already described in the stink bug *P. c. stali* (Kotaki, 2003), in the cockroaches *P. americana* and *Nauphoeta cinerea* (Bell, 1971; Barrett et al., 2008) and in the mosquito *C. p. pallens* (Uchida et al., 2004).

The biochemical parameters evaluated throughout the reproductive cycle of *D. maxima* showed correlation with the morphological changes found in the ovarian tissue. As was previously reported in *D. maxima* (Aguirre et al., 2008) as well as in other species (Kotaki, 2003; Fruttero et al., 2011), the high levels of hemolymphatic vitellogenin after a blood meal were consistent with the pronounced remodeling of ovarioles observed during

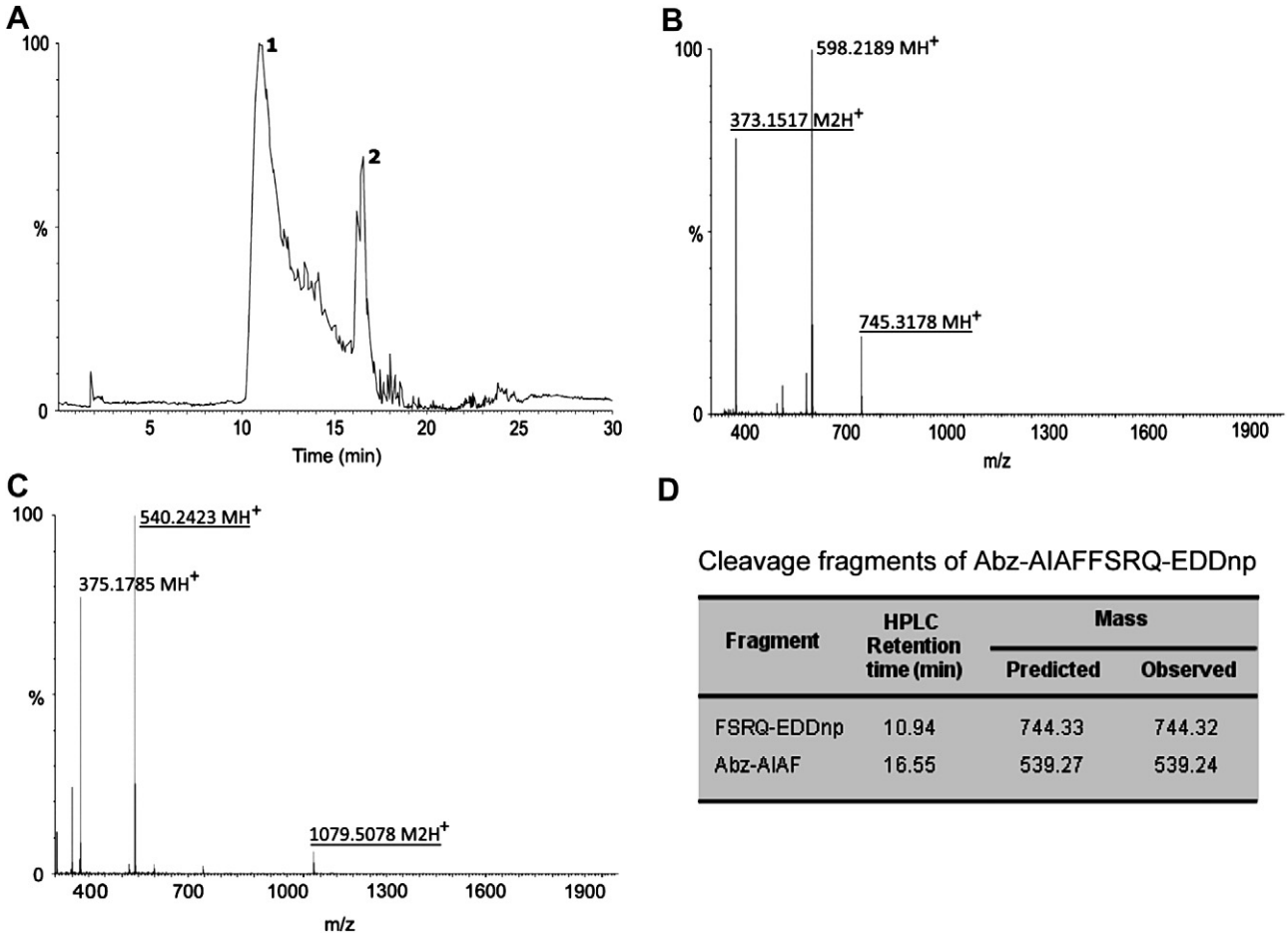

Fragment	HPLC Retention time (min)	Mass	
		Predicted	Observed
FSRQ-EDDnp	10.94	744.33	744.32
Abz-AIAF	16.55	539.27	539.24

Fig. 8. Determination of cleavage site of fluorogenic substrate Abz-AIAFFSRQ-EDDnp by liquid chromatography-mass spectrometry (LC-MS). (A), Total ion chromatogram of the enzymatic reaction products showing two major peaks (1 and 2); (B–C), Mass spectrum profiles of the substrate fragments corresponding to FSRQ-EDDnp (peak 1) and Abz-AIAF (peak 2), respectively. Ions corresponding to digestion products are underlined. Ions detected at *m*/*z* 580–600 in (B) and *m*/*z* 350–380 in (C) represent impurities not characterized. (D), Summary of results shown in (A–C) and comparison between the observed mass and the predicted mass for each substrate fragment. Figure shows results of a representative experiment. Experimental details are stated in materials and methods.

vitellogenesis, and with the increasing amounts of vitellin found at the ovarian tissue. However, two remarkable findings need a special consideration. The first one is concerned with the fact that at early and late follicular atretic stages, the amount of both, vitellogenin and vitellin, were significantly higher than those registered at pre-vitellogenesis. The second one is in relationship with the partial proteolysis of vitellin evidenced in homogenates of atretic ovarian tissues (Fig. 5). There are several physiological factors accounting for the circulating levels of vitellogenin and among them, the rate of its synthesis at the fat body, the capacity of oocytes to uptake vitellogenin and the half-life of this yolk protein precursor are of significant importance. Besides, considering that oosorption allows the females to adjust their reproductive physiology to conditions such as starvation (Bell and Bohm, 1975), it is also possible that yolk proteins may be recycled back to the hemolymph to conserve metabolic resources. In *P. americana*, intact vitellin was released from the oocytes to the hemolymph in females experiencing starvation-induced oosorption, thus contributing to increase vitellogenin levels in the hemolymph (Bell, 1971). In the hemipteran *P. c. stali,* once oosorption was induced, the aminoacids and peptides arising from vitellin degradation would return back to the hemolymph (Kotaki, 2003). More recently, yolk digestion within the ooplasm in the hymenopteran *Eretmocerus eremicus* was demonstrated by ultrastructural analysis (Asplen and Byrne, 2006). In *D. maxima*, expression of vitellogenin protein in the fat body was detected even at late atresia (results not shown), but in a lesser extent than in vitellogenesis (Aguirre et al., 2008). In addition, we demonstrated that during atresia, vitellogenin uptake by oocytes was minimal (Fig. 4C). We cannot rule out that in *D. maxima*, the levels of vitellogenin measured in the hemolymph could also result from the capacity of anti-Vt antibody to recognize proteolytic fragments of vitellin recycling back to the hemolymph. Taken together, it seems that several pathways could account for the circulating levels of vitellogenin detected in the atretic stages, most likely to maintain appropriate conditions that allow a fast resuming of vitellogenesis if females take a second blood meal.

The capacity of the oocytes for taking up vitellogenin depends on several factors, being the acquisition of patency and the expression of vitellogenin receptors at the surface of the oocytes critical issues (Wyatt and Davey, 1996; Snigirevskaya and Raikhel, 2005; Tufail and Takeda, 2009). As expected, vitellogenic ovaries of *D. maxima* were able to perform active uptake and deposition of yolk proteins (Supplementary video). A remarkable level of vitellogenin endocytosis during vitellogenesis was also described in *R. prolixus* (Oliveira et al., 1986) and more recently, in *Panstrogylus megistus* (Fruttero et al., 2011). In contrast, uptake of vitellogenin by terminal oocytes was minimal at early follicular atresia (Fig. 4C), being completely abolished if degeneration proceeds (late atresia, data not shown). In *R. prolixus,* the oostatic hormone inhibits the action of JH on vitellogenic follicles, thus preventing the oocyte

from yolk deposition (Davey and Kuster, 1981). More recently, it was proposed that oostatic hormone and 20E could play key roles in the atretic process (Uchida et al., 2004). On the basis of the standardized conditions presented in this work, *D. maxima* might represent a useful model to further explore the potential endocrine regulation of oosorption, which at present is not understood.

It is known that some insect proteolytic enzymes stored in oocytes are progressively activated to promote yolk protein degradation during embryogenesis (Izumi et al., 1994; Giorgi and Nordin, 2005). In this regard, two acid peptidases, a serine carboxypeptidase and a cathepsin B-like endopeptidase were reported in *Aedes aegypti* (Cho et al., 1991, 1999). On the other hand, a cysteine peptidase purified from *Bombyx mori* oocytes showed preferential activity against vitellin (Yamamoto and Takahashi, 1993). Moreover, interplay between acid phosphatase and cysteine peptidase in mediating vitellin breakdown during early embryogenesis of *P. americana* has been suggested (Oliveira et al., 2008). Uchida et al. (2001) proposed that in the mosquito *C. p. pallens,* preoviposition activation of cathepsin B and L-like peptidase in degenerating ovarian follicles could be responsible for the early proteolysis of yolk proteins.

In *D. maxima*, we have also found a significant acid peptidase activity at early and late atresia (Fig. 6). Furthermore, the use of specific fluorogenic substrates allowed us to demonstrate that such activity was attributed to a cathepsin D-like peptidase (Sorgine et al., 2000), which in turn was completely inhibited by pepstatin A, in agreement with other aspartic peptidases (Gacko et al., 2007). When the cleavage site upon the synthetic substrate (Abz-AIAFFSRQ-EDDnp) was determined by LC-MS (Fig. 8), we found a preference of the enzyme for acting on hydrophobic residues around the scissile bond, as was described for cathepsin D (Athaudaa and Takahashia, 2002; Piovesan et al., 2008). Taken together, our results suggest that cathepsin D-like peptidase is involved in the process of follicle degeneration, probably by promoting early yolk protein degradation. Preliminary tandem mass spectrometry data from a partial vitellin sequence of *D. maxima* indicate several possible cleavage sites for cathepsin D in its primary structure. However, further studies will be necessary to assess a more precise function of the enzyme. In the triatomine *R. prolixus*, cathepsin D and acid phosphatase are involved in a programmed proteolysis of yolk protein throughout embryogenesis (Nussenzveig et al., 1992; Fialho et al., 2002, 2005; Gomes et al., 2010). Therefore, it is plausible that in *D. maxima* the same enzymatic system would be operative during atresia. At a cellular level, cathepsin D would also be involved in the removal of atretic follicles. In mammals, the activity of cathepsin D is linked to authophagy (Koike et al., 2005) and its modulating action on apoptosis is also recognized (Benes et al., 2008). In *Drosophila virilis*, apoptosis and autophagy act synergistically to achieve a more efficient elimination of the degenerated nurse cells and abnormal egg chambers (Velentzas et al., 2007). Preliminary results suggest that progressive establishment of follicular atresia in *D. maxima* is accomplished by the confluence of more than one mechanism of programmed cell death.

Altogether, results in *D. maxima* suggest that once follicular atresia is induced, biochemical and cellular mechanisms operate in concert, being difficult to establish the magnitude of their individual contributions. Whether early activation of cathepsin D-like peptidase could mediate yolk protein recycling to either, increase female lifespan or maintain younger oocytes until improvement of nutritional conditions is still unknown. Further studies are needed to determine to what extent this aspartic peptidase is involved in cell death mechanisms executed during removal of degenerating follicles. In Chagas' disease vectors, these aspects which have a clear impact in the life cycle of females and on the epidemiology of the disease, deserve further exploration.

Acknowledgments

This work was supported by grants from FONCyT (PICT 2007-01333, ANPCyT-Argentina), CONICET and SECyT-UNC (L.E.C.). C.R.C. acknowledges financial support from the Brazilian agencies Conselho Nacional de Desenvolvimento Científico e Tecnologico (CNPq—Ed. CABBIO and PROSUL); Coordenadoria de Aperfeiçoamento de Pessoal de Nível Superior (CAPES—CAPG-BA 05/2005) and Fundação de Amparo a pesquisa do Estado do Rio Grande do Sul (FAPERGS). The authors are grateful to M.Sc. Jeferson Segalin for technical assistance in the mass spectrometry assays. Technical support of R. Stariolo (Coordinación Nacional de Control de Vectores, Córdoba, Argentina) and F. Tricarico (Servicio de Microscopía Electrónica, Museo Argentino de Ciencias Naturales-CONICET, Bs. Aires) is greatly appreciated. L.E.C. and E.R.R. dedicate this work to Dr. Silvia Frede.

References

Aguirre, S.A., Frede, S., Rubiolo, E.R., Canavoso, L.E., 2008. Vitellogenesis in the hematophagous *Dipetalogaster maxima* (Hemiptera: Reduviidae), a vector of Chagas' disease. J. Insect Physiol. 54, 393–402.

Asplen, M.K., Byrne, D.N., 2006. Quantification and ultrastructure of oosorption in *Eretmocerus eremicus* (Hymenoptera: Aphelinidae). J. Morphol. 267, 1066–1074.

Athaudaa, S.B., Takahashia, K., 2002. Cleavage specificities of aspartic proteinases toward oxidized insulin B chain at different pH values. Protein Pept. Lett. 9, 289–294.

Barrett, E.L.B., Preziosi, R.F., Moore, A.J., Moore, P.J., 2008. Effects of mating delay and nutritional signals on resource recycling in a cyclically breeding cockroach. J. Insect Physiol. 54, 25–31.

Bell, W.J., 1971. Starvation-induced oöcyte resorption and yolk protein salvage in *Periplaneta americana*. J. Insect Physiol. 17, 1099–1111.

Bell, W.J., Bohm, M.K., 1975. Oosorption in insects. Biol. Rev. Camb. Philos. Soc. 50, 373–396.

Benes, P., Vetvicka, V., Fusek, M., 2008. Cathepsin D – many functions of one aspartic protease. Crit. Rev. Oncol. Hematol. 68, 12–28.

Bradford, M.M., 1976. A rapid and sensitive method for the quantitation of micrograms quantities of protein utilizing the principle of protein-dye binding. Anal. Biochem. 72, 248–254.

Canavoso, L.E., Rubiolo, E.R., 1993. Hemolymphatic components in vectors of *Trypanosoma cruzi*: study in several species of the Subfamily Triatominae (Hemiptera: Reduviidae). Rev. Inst. Med. Trop. São Paulo 35, 123–128.

Cho, W.L., Deitsch, K.W., Raikhel, A.S., 1991. An extraovarian protein accumulated in mosquito oocytes is a carboxypeptidase activated in embryos. Proc. Natl. Acad. Sci. U. S. A. 88, 10821–10824.

Cho, W.L., Tsao, S.M., Hays, A.R., Walter, R., Chen, J.S., Snigirevskaya, E.S., Raikhel, A.S., 1999. Mosquito cathepsin B-like protease involved in embryonic degradation of vitellin is produced as a latent extraovarian precursor. J. Biol. Chem. 274, 13311–13321.

Clements, A.N., Boocock, M.R., 1984. Ovarian development in mosquitoes: stages of growth and arrest, and follicular resorption. Physiol. Entomol. 9, 1–8.

Davey, K.G., Kuster, J.E., 1981. The source of an antigonadotropin in the female of *Rhodnius prolixus* Stal. Can. J. Zool. 59, 761–764.

Defferrari, M.S., Demartini, D.R., Marcelino, T.B., Pinto, P.M., Carlini, C.R., 2011. Insecticidal effect of *Canavalia ensiformis* major urease on nymphs of the milkweed bug *Oncopeltus fasciatus* and characterization of digestive peptidases. Insect Biochem. Mol. Biol. 41, 388–399.

Fialho, E., Silveira, A.B., Masuda, H., Silva-Neto, M.A., 2002. Oocyte fertilization triggers acid phosphatase activity during *Rhodnius prolixus* embryogenesis. Insect Biochem. Mol. Biol. 32, 871–880.

Fialho, E., Nakamura, A., Juliano, L., Masuda, H., Silva-Neto, M.A., 2005. Cathepsin D-mediated yolk protein degradation is blocked by acid phosphatase inhibitors. Arch. Biochem. Biophys. 436, 246–253.

Fruttero, L.L., Frede, S., Rubiolo, E.R., Canavoso, L.E., 2011. The storage of nutritional resources during vitellogenesis of *Panstrogylus megistus* (Hemiptera: Reduviidae): the pathways of lipophorin in lipid delivery to developing oocytes. J. Insect Physiol. 57, 475–486.

Gacko, M., Minarowska, A., Karwowska, A., Minarowski, L., 2007. Cathepsin D inhibitors. Folia Histochem. Cytobiol. 45, 291–313.

Giorgi, F., Nordin, J.H., 2005. Biochemical and ultrastructural aspects of vitellin utilization during embryogenesis. Part B. Adiyodi, A.G., Adiyodi, R.G. (Eds.). In: Raikhel, A.S. (Ed.), Reproductive Biology of Invertebrates, vol. 12. Science Publishers Inc., Enfield, NH, USA, pp. 355–391.

Gomes, F.M., Oliveira, D.M., Motta, L.S., Ramos, I.B., Miranda, K.M., Machado, E.A., 2010. Inorganic polyphosphate inhibits an aspartic protease-like activity in the eggs of *Rhodnius prolixus* (Stahl) and impairs yolk mobilization in vitro. J. Cell Physiol. 222, 606–611.

Hermanson, G., 1996. Antibody modification and conjugation. In: Bioconjugate Techniques. Academic Press, San Diego, pp. 456–493.

Huebner, E., Anderson, E., 1972. A Cytological study of the ovary of *Rhodnius prolixus*. J. Morphol. 137, 385–416.
Izumi, S., Yano, K., Yamamoto, Y., Takahashi, S.Y., 1994. Yolk proteins from insect eggs: structure, biosynthesis and programmed degradation during embryogenesis. J. Insect Physiol. 40, 735–746.
Kajita, Y., Evans, E.W., 2009. Ovarian dynamics and oosorption in two species of predatory lady beetles (Coleoptera: Coccinellidae). Physiol. Entomol. 34, 185–194.
Koike, M., Shibata, M., Waguri, S., Yoshimura, K., Tanida, I., Kominami, E., Gotow, T., Peters, C., von Figura, K., Mizushima, N., Saftig, P., Uchiyama, Y., 2005. Participation of autophagy in storage of lysosomes in neurons from mouse models of neuronal ceroid-lipofuscinoses (Batten disease). Am. J. Pathol. 167, 1713–1728.
Kotaki, T., 2003. Oosorption in the stink bug, *Plautia crossota stali*: induction and vitellogenin dynamics. J. Insect Physiol. 49, 105–113.
Nussenzveig, R.H., Oliveira, P.L., Masuda, H., 1992. Identification of yolk platelet-associated hidrolases in the oocytes of *Rhodnius prolixus*. Arch. Insect Biochem. Physiol. 21, 253–262.
Oliveira, P.L., Gondim, K.C., Guedes, D.M., Masuda, H., 1986. Uptake of yolk protein in *Rhodnius prolixus*. J. Insect Physiol. 32, 859–866.
Oliveira, P.L., Petretski, M.D.A., Masuda, H., 1989. VT processing and degradation during embryogenesis in *R. prolixus*. Insect Biochem. 19, 489–498.
Oliveira, D.M.P., Ramos, I.B., Reis, F.C.G., Lima, A.P.C.A., Machado, E.A., 2008. Interplay between acid phosphatase and cysteine proteases in mediating vitellin degradation during early embryogenesis of *Periplaneta americana*. J. Insect Physiol. 54, 883–891.
Piovesan, A.R., Stanisçuaski, F., Marco-Salvadori, J., Real-Guerra, R., Defferrari, M.S., Carlini, C.R., 2008. Stage-specific gut proteinases of the cotton stainer bug *Dysdercus peruvianus*: role in the release of entomotoxic peptides from *Canavalia ensiformis* urease. Insect Biochem. Mol. Biol. 38, 1023–1032.
Postlethwait, J.H., Giorgi, F., 1985. Vitellogenesis in insects. In: Browder, L.W. (Ed.), Developmental Biology: A Comprehensive Synthesis, vol. 1. Plenum Press, New York, pp. 85–136.
Snigirevskaya, E.S., Raikhel, A.S., 2005. Receptor-mediated endocytosis of yolk proteins in insect oocytes. Part B. Adiyodi, A.G., Adiyodi, R.G. (Eds.). In: Raikhel, A.S. (Ed.), Reproductive Biology of Invertebrates, vol. 12. Science Publishers Inc., Enfield, NH, USA, pp. 198–227.
Sorgine, M.H., Logullo, C., Zingali, R.B., Paiva-Silva, G.O., Juliano, L., Oliveira, P.L., 2000. A heme-binding aspartic proteinase from the eggs of the hard tick *Boophilus microplus*. J. Biol. Chem. 275, 28659–28665.
Stanisçuaski, F., Ferreira-Dasilva, C.T., Mulinari, F., Pires-Alves, M., Carlini, C.R., 2005. Insecticidal effects of canatoxin on the cotton stainer bug *Dysdercus peruvianus* (Hemiptera: Pyrrhocoridae). Toxicon 45, 753–760.
Stoka, A.M., Salomón, O.D., Noriega, F.G., 1987. Physiology of Triatominae's reproduction. In: Brenner, R.B., Stoka, A.M. (Eds.), Chagas' Disease Vectors, vol. 2. CRC Press, Florida, pp. 109–129.
Swevers, L., Raikhel, A.S., Sappington, T.W., Shirk, P., Iatrou, K., 2005. Vitellogenesis and post-vitellogenic maturation of the insect ovarian follicle. In: Gilbert, L.I., Iatrou, K., Gill, S.S. (Eds.), Comprehensive Molecular Insect Science, vol. 1. Elsevier, Oxford, UK, pp. 87–155.
Tufail, M., Takeda, M., 2009. Insect vitellogenin/lipophorin receptors: molecular structures, role in oogenesis, and regulatory mechanisms. J. Insect Physiol. 55, 87–103.
Uchida, K., Ohmori, D., Ueno, T., Nishizuka, M., Eshita, Y., Fukunaga, A., Kominami, E., 2001. Preoviposition activation of cathepsin-like proteinases in degenerating ovarian follicles of the mosquito *Culex pipiens pallens*. Dev. Biol. 237, 68–78.
Uchida, K., Nishizuka, M., Ohmori, D., Ueno, T., Eshita, Y., Fukunaga, A., 2004. Follicular epithelial cell apoptosis of atretic follicles within developing ovaries of the mosquito *Culex pipiens pallens*. J. Insect Physiol. 50, 903–912.
Velentzas, A.D., Nezis, I.P., Stravopodis, D.J., Papassideri, I.S., Margaritis, L.H., 2007. Mechanisms of programmed cell death during oogenesis in *Drosophila virilis*. Cell Tissue Res. 327, 399–414.
Wang, M.H., Horng, S.B., 2004. Egg dumping and life history strategy of *Callosobruchus maculatus*. Physiol. Entomol. 29, 26–31.
Wigglesworth, V.B., 1936. The function of the corpus allatum in growth and reproduction of *Rhodnius prolixus* (Hemiptera). Quart. J. Micr. Sci. 79, 91–121.
Wyatt, G.R., Davey, K.G., 1996. Cellular and molecular actions of juvenile hormone. II, roles of juvenile hormone in adult insects. Adv. Insect Physiol. 26, 1–155.
Yamahama, Y., Yamamoto, Y., Watabe, S., Takahashi, S.Y., 2005. Regulation of yolk protein degradation during insect embryogenesis. Part B. Adiyodi, A.G., Adiyodi, R.G. (Eds.). In: Raikhel, A.S. (Ed.), Reproductive Biology of Invertebrates, vol. 12. Science Publishers Inc., Enfield, NH, USA, pp. 315–354.
Yamamoto, Y., Takahashi, S.Y., 1993. Cysteine proteinase from *Bombyx* eggs: role in programmed degradation of yolk proteins during embryogenesis. Comp. Biochem. Physiol. B. 106, 35–45.

VI. Marina Schumacher Defferrari

Curriculum Vitae 2014

Marina Schumacher Defferrari

Curriculum Vitae

marina.defferrari@ufrgs.br

Rua Frederico Etzberger, 412 - Porto Alegre, RS

91720-510 **Brasil**

+55 51 99035506 | +55 51 33986090

Formação

2010 - 2014 **Doutorado em Biologia Celular e Molecular**

Universidade Federal do Rio Grande do Sul, Brasil

Tese: Efeitos da urease majoritária de *Canavalia ensiformis* sobre o sistema imunitário do hemíptero *Rhodnius prolixus*

Orientação: Dra. Célia R. Carlini

com períodos de intercâmbio na

Universidade de Toronto em Mississauga, Canadá (de Janeiro, 2011 a Julho, 2011 e de Março 2012 a Março 2013)

Orientação: Dr. Ian Orchard

2008 - 2010 **Mestrado em Biologia Celular e Molecular**

Universidade Federal do Rio Grande do Sul, Brasil

Dissertação: Efeitos tóxicos da urease majoritária de *Canavalia ensiformis* e do peptídeo recombinante Jaburetox-2Ec sobre o hemíptero *Oncopeltus fasciatus*

Orientação: Dra. Célia R. Carlini

com períodos de intercâmbio na

Universidade de Toronto em Mississauga, Canadá (de Agosto, 2008 a Fevereiro, 2009)

Orientação: Dr. Ian Orchard

e na

Universidade Austral, Argentina (de Outubro, 2009 a Dezembro, 2009)

Orientação: Dra. Beatriz Settembrini

2003 - 2008 **Bacharelado em Biologia Molecular, Celular e Funcional**
Universidade Federal do Rio Grande do Sul, Brasil

Publicações

8. Defferrari, M.S., da Silva, R., Orchard, I., Carlini, C.R. **2014.** Jack bean (*Canavalia ensiformis*) urease induces eicosanoid-modulated hemocyte aggregation in the Chagas' disease vector *Rhodnius prolixus*. Toxicon. DOI

7. Martinelli, A.H., Kappaun, K., Ligabue-Braun, R., **Defferrari, M.S.**, Piovesan, A.R., Stanisçuaski, F., Demartini, R.D., Verli, H., Dal Belo, C.A., Almeida, C.G., Follmer, C., Carlini, C.R., Pasquali, G. **2014**. Structure-function studies on Jaburetox, a recombinant insecticidal and antifungal peptide derived from jack bean (Canavalia ensiformis) urease. Biochimica et Biophysica Acta - General Subjects. DOI

6. Defferrari, M.S., Lee, D.H., Fernandes, C.L., Orchard, I., Carlini, C.R. **2014**. A phospholipase A2 gene is linked to jack bean urease toxicity in the Chagas' disease vector *Rhodnius prolixus*. Biochimica et Biophysica Acta - General Subjects. DOI

5. Marco-Salvadori, J., **Defferrari, M. S.**, Ligabue-Braun, R., Yamazaki-Lau, E., Salvadori, J. R., Carlini, C.R. **2012**. Characterization of entomopathogenic nematodes and symbiotic bacteria active against *Spodoptera frugiperda* (Lepidoptera: Noctuidae) and contribution of bacterial urease to the insecticidal effect. Biological Control, 63, 253- 263. DOI

4. Paluzzi, J.V., Young, P., **Defferrari, M.S.**, Orchard, I., Carlini, C.R., O'Donnell, M.J. **2012**. Investigation of the potential involvement of eicosanoid metabolites in anti-diuretic hormone signaling in *Rhodnius prolixus.* Peptides, 34, 127-134. DOI

3. Aguirre, S.A., Fruttero, L.L., Leyria, J., **Defferrari, M. S.**, Pinto, P.M., Settembrini, B.P., Rubiolo, E.R., Carlini, C.R., Canavoso, L.E. **2011**. Biochemical changes in the transition from vitellogenesis to follicular atresia in the hematophagous *Dipetalogaster maxima* (Hemiptera: Reduviidae). Insect Biochemistry and Molecular Biology, 41, 832-841. DOI

2. Defferrari, M.S., Demartini, D.R., Marcelino, T.B., Pinto, P.M., Carlini, C.R. **2011**. Insecticidal effect of *Canavalia ensiformis* major urease on nymphs of the milkweed bug *Oncopeltus fasciatus* and characterization of digestive peptidases. Insect Biochemistry and Molecular Biology, 41, 388-399. DOI

1. Piovesan, A., Staniscuaski, F., Marco-Salvadori, J., Real-Guerra, R., **Defferrari, M.S.** Carlini, C.R. **2008**. Stage-specific gut proteinases of the cotton stainer bug *Dysdercus peruvianus*: Role in the release of entomotoxic peptides from *Canavalia ensiformis* urease. Insect Biochemistry and Molecular Biology, 38, 1023-1032. DOI

Idiomas

Português	Nativo
Inglês	Fluente
Espanhol	Intermediário

Co-cupervisão de estudantes de graduação

2. Samantha Diane Dyer. *Canavalia ensiformis* urease effects on *Dysdercus peruvianus*' hemocytes. Bacharelado em Ciências Biológicas. Universidade Federal do Rio Grande do Sul, Porto Alegre, Brasil. **2011**.

1. Thiago Beltram Marcelino. Characterization of digestive proteinases of *Oncopeltus fasciatus* (Hemiptera: Lygaeidae) adults and their role on urease hydrolysis and toxicity. Bacharelado em Ciências Biológicas. Universidade Federal do Rio Grande do Sul, Porto Alegre, Brasil. **2009.**

Apresentações em conferências e simpósios

5. **Defferrari, M.S.**, Carlini, C.R., Orchard, I. Identification and cloning of a phospholipase A2 transcript in *Rhodnius prolixus*. Insect Biotech Conference, St. Catherine's, Canada. **2012**.

4. **Defferrari, M.S.**, Zandawala, M., Carlini, C.R., Orchard, I. Cloning of the phospholipase A2 and cyclooxygenase transcripts in *Rhodnius prolixus* and influence of a jack bean urease diet. Insect Biotech Conference, St. Catherine's, Canada. **2011**.

3. **Defferrari, M.S.**, TeBrugge, V.A., Orchard, I., Carlini, C.R. Toxic effects of *Canavalia ensiformis* urease and recombinant peptide Jaburetox-2Ec on *Oncopeltus fasciatus* nymphs. Mini-simpósio: "Multi-funcionalidade de ureases", Porto Alegre, Brasil. **2010**.

2. **Defferrari, M.S.**, Salvadori, J.M., Carlini, C.R. Caracterização e purificação de proteinases digestivas de *Oncopeltus fasciatus*: papel no processamento da urease de *Canavalia ensiformis*. XIX Salão de Iniciação Científica, Porto Alegre, Brasil. **2007**.

1. **Defferrari, M.S.**, Silva, F.B., Waldow, V.A., Baz, F.C., Bonatto, S.L. Filogenia molecular de planárias terrestres neotropicais utilizando-se o gene ribossomal 18S e o gene mitocondrial citocromo oxidase I. VXIII Salão de Iniciação Científica, Porto Alegre, Brasil. **2006**.

Posters

6. Marcelino, T.B., **Defferrari, M.S.**, Carlini, C.R. Characterization of digestive proteinases of *Oncopeltus fasciatus* (Hemiptera: Lygaeidae) adults and the entomotoxic effect of urease. XXXIX Reunião Anual da Sociedade Brasileira de Bioquímica e Biologia Molecular - SBBq, Foz do Iguaçu, Brasil. **2010**.

5. **Defferrari, M.S.**, TeBrugge, V.A., Orchard, I., Carlini, C.R. Toxic effects of

Canavalia ensiformis urease and recombinant peptide Jaburetox-2Ec on *Oncopeltus fasciatus* nymphs. XXXIX Reunião Anual da Sociedade Brasileira de Bioquímica e Biologia Molecular - SBBq, Foz do Iguaçu, Brasil. **2010**.

4. **Defferrari, M.S.**, TeBrugge, V.A., Orchard, I., Carlini, C.R. Toxic effects of *Canavalia ensiformis* urease on *Oncopeltus fasciatus*. XVI World Congress of the International Society on Toxinology, Recife, Brasil. **2009**.

3. **Defferrari, M.S.**, Carlini, C.R. Characterization of digestive proteinases from *Oncopeltus fasciatus*: role on *Canavalia ensiformis* urease processing. XXXVII Reunião Anual da Sociedade Brasileira de Bioquímica e Biologia Molecular - SBBq, Águas de Lindóia, Brasil. **2008**.

2. **Defferrari, M.S.**, Salvadori, J.M., Carlini, C.R. Caracterização e purificação de proteinases digestivas de *Oncopeltus fasciatus*. XXII Reunião Anual da Federação de Sociedades de Biologia Experimental - Fesbe, Águas de Lindóia, Brasil. **2007**.

1. **Defferrari, M.S.**, Waldow, V.A., Baz, F.C., Bonatto, S.L. Análise filogenética molecular de planárias terrestres neotropicais utilizando-se o gene ribossomal 18S. 50° Congresso Brasileiro de Genética, Águas de Lindóia, Brasil. **2005**.